Studies on horizontal cells of the carp retina with special reference to temperature and calcium

Cunningham, Jonathan R.C.

Studies on Horizontal Cells of the Carp Retina with Special Reference to Temperature and Calcium

by

Jonathan R. C. Cunningham

A Thesis submitted in partial fulfilment of the requirements for the degree of Doctor of Philosophy

Biological Sciences

The University of Durham
1995

Declaration

This thesis is entirely the result of my own work. It has not been accepted for any other degree and is not being submitted for any other degree.

J. Cunningham
Jan. 1995

Acknowledgements

The following are acknowledged for their contributions.

My supervisor Dr. D. Hyde for guidance and encouragement. Also other members of the academic staff of the Biological Sciences Department for their constructive comments.

The technical staff of the Biological Sciences Department of Durham University for their assistance (in particular Jack Warner, Judith Chambers, Dave Hutchinson and Eric Henderson).

The Department of Education for Northern Ireland for financial support.

My parents, for financial and moral support.

Hayley, for her constant support and encouragement throughout the last three years.

Glossary

AM	Acetoxymethyl ester
4–AP	4–Aminopyridine
BAPTA	1,2–bis(2–aminophenoxy)ethane–N,N,N′,N′–tetraacetic acid
BSA	Bovine Serum Albumen (Fraction V, Sigma)
cAMP	Cyclic adenosine 3′,5′–monophosphate
cGMP	Cyclic guanosine 3′,5′–monophosphate
CNS	Central Nervous System
DMSO	Dimethyl Sulfoxide
EGTA	Ethylene glycol–bis(β–aminoethylether) N,N,N′,N′–tetraacetic acid
GABA	γ–amino–n–butyric acid
HEPES	N–[2–hydroxyethyl]piperazine–N′–[2–ethanesulphonic acid]
I–V	Current–voltage
MOPS	(3–[N–Morpholino]propanesulphonic acid)
MW	Molecular Weight
NMDA	N–methyl–D–aspartic acid
R	Gas constant ($8.315 JK^{-1}mol^{-1}$)
RMS	Root Mean Squared
S.E.M.	Standared Error of Mean
T	Absolute temperature
TEA	Tetraethylammonium chloride
TTX	Tetrodotoxin
UV	Ultra–violet
$[X]_i$	Intracellular concentration of ion X
$[X]_o$	Extracellular concentration of ion X

Abstract

Carp (*Cyprinus carpio*) were acclimated to 8±1°C, 16±1.5°C and 26±1°C. Dark adapted retinas were isolated and light induced responses of H1 horizontal cells recorded. The dynamic range of these cells was affected by temperature, showing a decrease on heating or cooling from an optimum temperature. The effect of acclimation was to shift this optimum in an adaptive manner. A move from 16°C to 8°C resulted in ~44% acclimation, while a move from 16°C to 26°C resulted in ~67% acclimation. The rates of change of membrane potential and latency of the response also showed adaptive changes on acclimation.

Isolated horizontal cells were voltage clamped using the whole cell patch clamp technique. The current–voltage (I–V) relationship of the prominent anomalous rectifier current was displaced by changes in the extracellular potassium concentration and was blocked by Ba^{2+} or Rb^{+}. Its amplitude did not appear to be affected by thermal acclimation. A pharmacologically isolated sustained Ca^{2+} current, with an I–V relationship characteristic of an L–type current, also showed no apparent thermal acclimation.

The ratiometric calcium indicator Fura-2 was used to measure the intracellular calcium concentration in isolated horizontal cells. The intracellular calcium concentration rose on depolarization of the cells, in an extracellular calcium concentration dependent manner. This increase was blocked by various metal ions with varying sensitivities: $La^{3+}>Cd^{2+}>Cu^{2+}>Co^{2+}\geq Ni^{2+}$. The rate of change of intracellular calcium concentration was increased by increased temperature, but did not appear to be affected by thermal acclimation. Sustained depolarizations (up to 15 minutes) resulted in sustained elevations in intracellular calcium concentration proportional to the degree of depolarization.

Possible mechanisms underlying the long and short term effects of temperature on the horizontal cell responses are discussed. The sustained calcium current and the intracellular calcium concentration changes are disscused in terms of the potential roles of this current and the significance of the subsequent intracellular calcium concentration changes.

Contents

Chapter I

Introduction

1.1 The Retina — Why?

Dowling (1987) commented that

> 'the retina is an approachable part of the brain
> that can provide significant insights into central
> nervous system mechanisms in higher animals.'

Although physically isolated from the rest of the brain the vertebrate retina is part of the central nervous system with the same origin, the neural tube, and has many similar features. For instance it is isolated from the vascular system by a blood–retinal barrier similar to the blood–brain barrier and most of the spaces between the retinal neurones are taken up by glial cells (called Müller cells) to leave small extracellular spaces, as in the brain.

The approachabilty of the retina is largely due to its isolation from the rest of the central nervous system. Its position at the back of the eye is largely maintained by the pressure exerted on it by the vitreous humor, being attached only at the periphery (the *ora serrata*) and around the optic nerve. It can consequently be quite simply removed and maintained in a suitable environment for a number of hours, during which time it appears to continue to function. In this way it becomes 'an intact slice of the CNS' (Kato *et al.*, 1991).

The histology of the retina has been studied for many years using both the light microscope, initially by Ramón y Cajal in the late 19^{th} century, and more recently the electron microscope. By the application of intracellular recording techniques and more recently by studying the electrical properties of isolated retinal neurones our knowledge of the relationship between the retinal structure, the electrical properties of retinal neurones and their function is continually improving (see for example Dowling and Werblin, 1969; Werblin and Dowling, 1969).

Carp retinas, like all vertebrate retinas, have six main classes of cell arranged in a layered structure (Fig. 1.1). Intracellular recordings have been made from all the different cell classes (e.g. Werblin and Dowling, 1969, in *Necturus*) and from a wide variety of species including examples from elasmobranchs, teleosts, amphibians, reptiles and mammals (Dowling, 1987). Generally the responses recorded from across this species diversity are similar. One important aspect of the responses recorded from distal retinal neurones is that they are graded membrane potential changes. The ganglion cells, which form the axons of the optic nerve, regularly fire action potentials, and some classes of amacrine cells show transient responses. However, the graded potential changes of the photoreceptors, horizontal cells and bipolar cells transmit information in an analogue way, as opposed to the digital nature of all–or–nothing action potentials. The sensitivity of the retina is such that Barlow (1953), before intracellular recordings had even been made, suggested that it was 'unlikely that [retinal integration] could be done by the transmission of all–or–nothing impulses.' The graded nature of their responses makes retinal neurones ideal subjects to study the mechanisms of signal integration and modification.

The carp retina is particularly suited to electrophysiological studies for a number of reasons (Kato *et al.*, 1991). As in other ectothermic species the retinal neurones are larger than in endotherms. Cyprinid retinas are tetra/trichromatic with three separate cone types maximally sensitive to short ($\sim 460nm$), medium ($\sim 525nm$) and long ($\sim 620nm$) wavelengths, usually called blue, green and red responsive cones respectively, (Marks, 1965; Kaneko and Tachibana, 1985). A further ultra–violet photoreceptor is also thought to exist (Neumeyer and Arnold, 1987). The horizontal cells are particularly prominent in the carp retina and form distinct layers immediately adjacent to the photoreceptor layer.

1.2 Phototransduction

In order to understand the responses of horizontal cells in the intact retina to light stimuli (Chapter 2) and consequently to be able to relate the properties of isolated horizontal cells (Chapters 3 and 4) to the *in vitro* function some knowledge of how the incoming stimuli (light) are converted to electrical signals in the photoreceptors is required. Most of the work on phototransduction has been carried out on rods, but the basic mechanisms appear to be similar in both rods and cones,

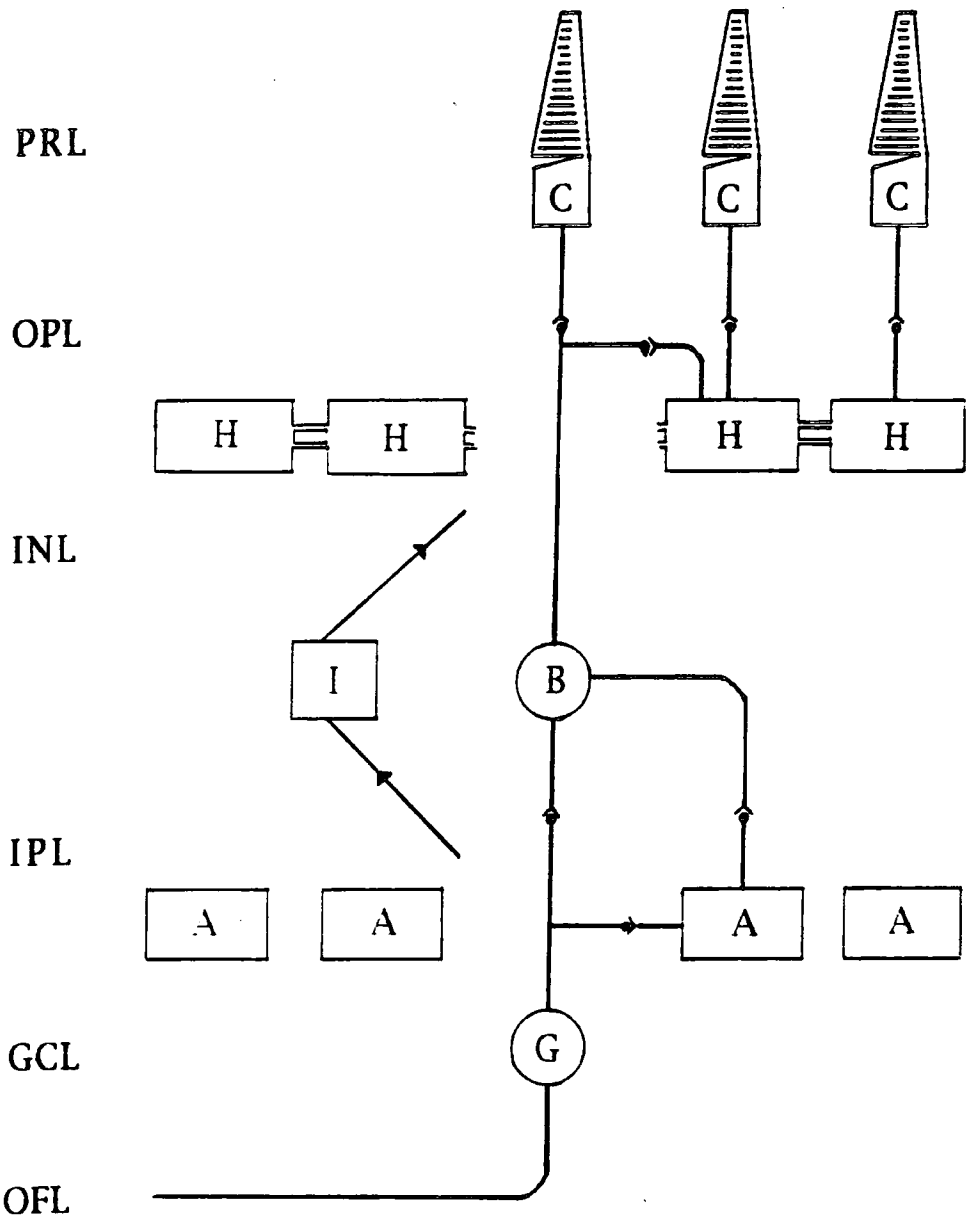
PRL
OPL
INL
IPL
GCL
OFL
C
C
C
H
H
H
H
I
B
A
A
A
A
G

the main differences being in the kinetics of the biochemical reactions (Watanabe and Murakami, 1992; Yau, 1994). It appears that all the various proteins involved in rod phototransduction have different isoforms expressed in cones (Yau, 1994).

Tomita (1970) demonstrated by intracellular recording that photoreceptor responses to illumination are graded hyperpolarizations. He showed that this was mediated by the closure of 'light–sensitive' cation (primarily Na^+) permeable channels and a reduction of the so called 'dark–current' (Hagins, 1970; Baylor *et al.*, 1979). The phototransduction mechanism is capable of amplifying the effect of a single photon to a change in the photoreceptor membrane potential. This response can be measured in the photoreceptors and is capable of detection, as was shown by the psychophysical studies of Hecht *et al.* (1942). The photoreceptor biochemical cascade responsible for converting the energy of a single photon to a membrane potential change of about a millivolt demonstrates a power gain of about 10^5 (Chabre and Vuong, 1992). Understanding of the mechanisms responsible for this amplification and the second messengers involved is constantly improving and is comprehensively covered by a number of recent reviews (Pugh and Lamb, 1990; 1993; McNaughton, 1990; Stryer, 1991; Kaupp and Koch, 1992; Yau, 1994).

The light sensitive photopigment consists of a large protein (opsin) with an attached chromophore. The chromophore is either retinal or 3–dehydroretinal which, when combined with the opsin, forms a rhodopsin or a porphyropsin respectively, the latter being the dominant photopigment in carp (Bowmaker, 1990). The absorption of a photon by the chromophore molecule results in a high probability of the isomerization of the molecule from the *11–cis* form to the *all–trans* form. The probability of spontaneous isomerization is very low (about once in a thousand years) which results in the exceptionally low signal–to–noise ratio in photoreceptors (Stryer, 1991). Isomerisation of the chromophore results in a series of conformational changes in the protein opsin. One of the intermediates, metarhodopsin II, is thought to be the active form and is often represented by R^*. The presence of R^* then triggers the first of a number of amplifying steps which result in the appropriate change in second messenger concentration:-

1 The light activated opsin activates a G–protein, called Transducin (T), by catalyzing the exchange of transducin bound GDP with GTP resulting in dis-

sociation of transducin, releasing the T_α–GTP subunit. By lateral diffusion in the photoreceptor membranes R^* can activate many transducin molecules, which are also bound in the membrane.

2 The T_α–GTP subunit activates a phosphodiesterase (PDE), also in the disk membranes, by removing the inhibitory effect of the bound γ subunits. By removing both the γ subunits ($\alpha\beta\gamma\gamma \rightarrow \alpha\beta\gamma \rightarrow \alpha\beta$) PDE is stimulated more than 1500 fold.

3 The activated PDE molecule catalyses the hydrolysis of cGMP and it is this reduction in cGMP concentation which reduces the number of open membrane channels.

The 'light–sensitive' membrane channels are in fact cGMP sensitive (Fesenko *et al.*, 1985). They have multiple binding sites (at least 3) for cGMP and are opened by the binding of this second messenger, although whether all the cGMP binding sites have to be filled is not known. The nature of the multiple binding sites means that the steepest part of the cGMP concentration conductance curve is at low cGMP concentrations and consequently in the dark state, even though the dark–current is at its maximum, <5% of the channels are open (Pugh and Lamb, 1993; Yau, 1994). The reduction in free cGMP concentration results in the closure of a proportion of the open channels and the consequent hyperpolarization of the photoreceptor.

The recovery phase of the response to illumination requires the termination of the biochemical cascade described above and an increase in the cGMP concentration. These are mediated by the following steps, a number of which are influenced by the intracellular calcium concentration which drops on the closure of the cGMP sensitive channels which are partially permeable to calcium. This is because of the continued activity of a sodium–calcium–potassium exchanger in the inner segment, which together with a sodium–potassium ATPase completes the circuit required by the dark–current. The termination steps (Pugh and Lamb, 1990; 1993; McNaughton, 1990; Stryer, 1991; Kaupp and Koch, 1992; Yau, 1994) are:

1 The light activated opsin is inactivated by phosphorylation and the binding of a protein called arrestin. The phosphorylation is inhibited by calcium.

2 Hydrolysis of the terminal phosphate of the T_α–GTP molecule appears to be the normal mechanism of inactivation of the G–protein.

3 The mechanism of PDE inactivation is not fully understood, although it probably requires the recombination of PDE_γ subunits with the $PDE_{\alpha\beta}$ subunit.

4 The drop in intracellular calcium concentration results in the removal of inhibition on guanylate cyclase which is mediated by a calcium sensitive protein, possibly recoverin (Dizhoor *et al.*, 1991; Lambrecht and Koch, 1991, though see Gray–Keller *et al.*, 1993). This results in an increase in the cGMP concentration and consequently in the opening of the membrane channels and the repolarization of the membrane.

5 The cGMP sensitive membrane channel also seems to be affected by the drop in intracellular calcium concentration. The sensitivity to cGMP is reduced when a calcium–calmodulin complex is bound to the channel so that on reduction of the calcium concentration this effect is removed and the channel is more likely to open.

The effect of the drop in intracellular calcium on reduction of the dark current is to influence not only the speed of the recovery of the membrane potential on the offset of a light stimulus, but also to allow the photoreceptor to adapt to the light stimulus. Under constant illumination the drop in intracellular calcium concentration will result in the repolarization of the membrane for the reasons described above, providing the photoreceptor with an increased range of membrane potentials to which it can hyperpolarize on further increases in illumination intensity.

1.3 Horizontal Cell Responses

1.3.1 Horizontal Cell Classes

The horizontal cells are second order neurones postsynaptic to the photoreceptors (Fig. 1.1). In the cyprinid retina there appear to be four different types of

horizontal cell which are postsynaptic to different photoreceptor types (Stell and Lightfoot, 1975). The horizontal cells postsynaptic to the cones were referred to as H1, H2 and H3. They appeared to form connections with the red, green and blue (H1), green and blue (H2) and blue (H3) cones respectively (Stell and Lightfoot, 1975; Downing and Djamgoz, 1989).

These different classes of cone driven horizontal cells appear to be distributed in reasonably distinct layers in the cyprinid retina with H1 cells more distal, H3 cells more proximal and H2 cells intermediate (Stell and Lightfoot, 1975). Members of the same class are connected by gap junctions (Dowling, 1987) which allow the passage of reasonably large molecules between cells, as demonstrated by the movement of dye molecules such as lucifer yellow with a molecular weight of over 400 (Kaneko, 1971; Kaneko and Stuart, 1984).

Horizontal cells in fish retinas are either axonless (rod driven) or have long thin axons leading to a tubular structure in the inner nuclear layer (Stell, 1975). Unlike in higher vertebrates these axon terminals do not appear to form synapses with photoreceptors (Stell, 1975; Dowling, 1987) but respond to illumination with similar responses to the horizontal cell bodies (Yagi, 1986).

1.3.2 A Hyperpolarizing Response

H1 cells in the isolated but intact fish retina respond to illumination by graded hyperpolarizations of their membrane potential as was first recorded by Svaetichin (1953), though he did not attribute the responses to horizontal cells (see Section 2.1.2). They are referred to as luminosity cells as they respond to all visible wavelengths with hyperpolarizing responses unlike the H2 and H3 cells (see below).

As described in Section 1.2 photoreceptors respond to illumination with a hyperpolarizing response. Soon after this was electrophysiologically established (Kaneko and Hashimoto, 1967) the Russians Byzov and Trifonov proposed that photoreceptors released an excitatory neurotransmitter continuously in the dark, which was reduced on illumination–induced hyperpolarization (Byzov and Trifonov, 1968; Trifonov, 1968). The presence of the transmitter in the dark, and its reduction on illumination, results in the horizontal cells being depolarized in the dark and hyperpolarizing in response to illumination — a sign–conserving synapse.

This is now the generally accepted mechanism by which the hyperpolarizing horizontal cell response is generated (Kaneko, 1987; Dowling, 1987).

L–glutamate has for some time been the prime candidate for the photoreceptor transmitter. Glutamate has been shown to depolarize horizontal cells in both the intact retina (Cervetto and MacNichol, 1972; Wu and Dowling, 1978; Lasater and Dowling, 1982; Ariel *et al.*, 1984) and after isolation (Lasater and Dowling, 1982; Dowling *et al.*, 1983; Ariel *et al.*, 1984; Perlman *et al.*, 1989) by opening membrane channels with a reversal potential of around $0mV$ (Hals *et al.*, 1986; Murase *et al.*, 1987; O,Dell and Christensen, 1989; Perlman *et al.*, 1989) and possibly by closing potassium channels (Lasater and Dowling, 1982; Tachibana, 1985) although it has been suggested that this latter effect is attributable to the method of application of the drug causing localized changes in the potassium concentration in the boundry layer around the cell (Perlman *et al.*, 1988, and see Section 3.4.2). Copenhagen and Jahr (1989) have shown that isolated turtle photoreceptors release excitatory amino acids which can increase the opening probability of glutamate channels in patch clamp outside out membrane patches.

The effect of the gap junctions between horizontal cells of the same class described above is that the receptive fields of the cells far exceeds the dendritic area of individual cells. Electrical signals can travel over distances of more than $2mm$ (Naka and Rushton, 1967) whereas the dendritic spread of the cells is usually 30–150μm (Stell and Lightfoot, 1975). It has been suggested that the function of the axon terminals is to increase the lateral spread of the signal (Yagi, 1986) due to the high electrical resistance of the axon and axon terminal membrane and the extensive gap junctional coupling between both axon terminals and the axons themselves (Yagi and Kaneko, 1988).

1.3.3 The Feedback Hypothesis

The discovery by Baylor *et al.* (1971) that cones could respond to diffuse or annular illumination by depolarizing led them to suggest that the hyperpolarizing responses of horizontal cells, generated by the illumination of many cones, was causing depolarization of the single cone through negative feedback. Since then further direct evidence of negative feedback from horizontal cells onto cones is

primarily based on intracellular recordings of cone responses (e.g. in carp Wu and Dowling, 1980; Murakami *et al.*, 1982).

The polarity of H2 and H3 horizontal cell responses to illumination of the retina by various wavelengths of light is often explained in terms of a negative feedback pathway from horizontal cells to cones (Baylor *et al.*, 1971; Fuortes and Simon, 1974; Stell and Lightfoot, 1975; Kaneko, 1987; Kato *et al.*, 1991; Wagner and Djamgoz, 1993; Wu, 1992, 1994). The H2 cell hyperpolarizes to medium wavelength (green) stimuli, but depolarizes to long wavelength (red) stimuli and is referred to as a red–depolarizing/green–hyperpolarizing (or biphasic) chromaticity cell. The H3 cell is referred to as a blue–hyperpolarizing/green–depolarizing/red–hyperpolarizing (or triphasic) chromaticity cell. It is proposed that the red cone dominated H1 cells provide negative feedback onto the green cones, causing depolarization on illumination with long wavelengths. The sign–conserving synapse between the green cones and the H2 cells consequently results in depolarization of this cell at these wavelengths. The same basic mechanism of negative feedback from the H2 cells to the blue cones results in the triphasic response of the H3 cells.

The mechanism of this feedback from horizontal cells to photoreceptors is thought to be mediated by chemical synapses, with GABA as the transmitter (Lam *et al.*, 1978; Murakami *et al.*, 1982; Yazulla and Kleinschmidt, 1983; Yazulla, 1986; Wu, 1991), at least for H1 cells (Marc *et al.*, 1978). Like photoreceptors, the horizontal cells are thought to release transmitter tonically in the dark, with reductions on hyperpolarization of the cell. Cones have been shown to be sensitive to GABA (Kaneko and Tachibana, 1986) and the feedback response is inhibited by the $GABA_A$ receptor blocker bicuculline (Lam *et al.*, 1978; Kaneko and Tachibana, 1986; Wu, 1991). Conventional vesicle containing synapses that might mediate this feedback pathway have been seen only very rarely (Dowling, 1987). However transmitter release by 'non–conventional' intracellular calcium independent membrane transport (Bernath, 1992; Levi and Raiteri, 1993) has been cited as the main mechanism for GABA release from these cells (Schwartz, 1982, 1987; Yazulla and Kleinschmidt, 1983; Ayoub and Lam, 1984). However this mechanism has only been shown to occur at H1 cells, and the sensitivity of cone photoreceptors to GABA does not appear to include blue cones (Murakami *et al.*, 1982; Tachibana and Kaneko, 1984; Kaneko and Tachibana, 1986).

Although this mechanism would provide the biphasic and triphasic responses of the H2 and H3 cells there remains some doubt that the pathway described could be responsible for the degree of colour–opponency observed (Burkhardt, 1993) due to the size of the depolarizing responses in the horizontal cells compared to those in the cones. This does not mean that the feedback pathway from the horizontal cells to the photoreceptors described does not exist, only that some other mechanism(s) may also be also required to generate these responses. Various hypotheses have been suggested to explain the differences in strength of the colour–opponency observed in the cones and horizontal cells such as nonlinearity of the cone–photoreceptor sign conserving synapse or the feedback is not mediated by a chemical synapse, but is electrotonic (see Djamgoz and Yamada, 1990; Burkhardt, 1993).

1.3.4 Horizontal Cell Feedforward Synapses

As well as feedback synapses to photoreceptors horizontal cells also appear to form synapses with the other second order retinal neurones; the bipolar cells (Dowling, 1987). There are two basic types of bipolar cell; ON–centre and OFF–centre, with the response to illumination in the receptive field centre being depolarization and hyperpolarization respectively (Werblin and Dowling, 1969; Kaneko, 1970; Saito, 1987). The response to the centre of the receptive field is mediated by the photoreceptors with their small receptive field, while the antagonistic response to the surround area is mediated by the horizontal cells with their large receptive field (Dowling, 1987; Djamgoz and Yamada, 1990; Kolb and Lipetz, 1991).

Bipolar cells are the first neurones of the visual path to demonstrate clear center–surround antagonistic receptive field organisation. Some bipolar cells in the carp retina are colour coded with the most complex receptive field patterns being the double–opponent fields. For example when the centre of the receptive field is stimulated with red light the cell depolarizes (R+), and hyperpolarizes on illumination with blue-green light (G–), whereas illumination of the surround by red light results in hyperpolarization (R–), and by blue–green light in depolarization (G+): Centre R+/G– Surround R–/G+ (Kaneko and Tachibana, 1985). A second double opponent cell type was also recorded from, with the opposite colour responses: Centre R–/G+ Surround R+/G–.

These responses require both sign conserving and sign inverting pathways between the photoreceptors and the bipolar cells and between the horizontal cells and the bipolar cells. The glutamate receptors on ON–centre bipolar cells are probably different from those on OFF–centre and horizontal cells (Dowling, 1987; Saito, 1987). They can be distinguished pharmacologically (Slaughter and Miller, 1981, 1983) and the action of glutamate on ON–bipolar cells is to close ionic channels as opposed to opening them as is the case for OFF–bipolar and horizontal cells (Dowling, 1987). It has been suggested that horizontal cells may mediate the surround antagonism of the bipolar cell via the cones (Kolb and Lipetz, 1991), but horizontal cell–bipolar cell synapses have been observed in most species (Dowling, 1987) and direct feedforward mechanisms seem probable too (Djamgoz and Yamada, 1990).

1.3.5 Plasticity of Horizontal Cell Properties

Dopamine, released by interplexiform cells processes radiating centrifugally to the outer plexiform layer (Dowling and Ehinger, 1978), has a number of neuromodulatory effects on various teleost retinal cells, including cone driven horizontal cells (Dowling, 1987, pages 153–163; Witkovsky and Dearry, 1991; Besharse and Iuvone, 1992; Djamgoz and Wagner, 1992).

Retinal homogenates and isolated horizontal cells demonstrate dopamine dependent accumulation of the intracellular second messenger cyclic AMP (cAMP) (Watling and Dowling, 1981; Van Buskirk and Dowling, 1981; Dowling *et al.*, 1983). The effects of dopamine described below are thought to be mediated by intracellular cAMP.

The spatial coupling of horizontal cells is decreased by dopamine, as has been demonstrated by decreased electrotonic spread of light induced signals (Negishi and Drujan, 1979), decreased spread of intracellular dyes (Teranishi *et al.*, 1983, 1984) and decreased coupling between attached pairs of isolated cells (Lasater and Dowling, 1985; Devries and Schwartz, 1989). In isolated cells dopamine has also been shown to increase glutamate conductances, by affecting the gating kinetics of the channels (Knapp and Dowling, 1987; Knapp *et al.*, 1990; Schmidt *et al.*, 1994). Dopamine also affects the GABA mediated feeedback between horizontal cells and photoreeceptors. The release of GABA from horizontal cells is reduced by

dopamine (Yazulla and Kleinschmidt, 1982) while horizontal cell spinules in the photoreceptor pedicles increase in size in a dopamine dependent manner. This, it is suggested, increases the area of contact between the horizontal cell and the photoreceptor responsible for the negative feedback and can explain the changes in colour opponency observed in the horizontal cells on the application of dopamine (Kirsh *et al.*, 1991; Wagner and Djamgoz, 1993). A further effect of dopamine has recently been demonstrated by Pfeiffer-Linn and Lasater (1993) who found that calcium conductances in bass horizontal cells resembling L–type and T–type current were significantly potentiated and inhibited respectively by dopamine and a membrane permeable version of cAMP.

1.4 The Effects of Temperature

1.4.1 The Thermal Environment

The thermal environment has a profound effect on all life forms. Most vertebrates are able to live only with body temperatures ranging from the freezing point of their tissues to about 40°C, although no individual species are able to survive such diverse temperatures. Generally the animal kingdom is, over simplistically, divided into two groups by the source of the thermal energy they utilise; *endotherms*, who maintain their core temperature by cellular metabolism and *ectotherms*, who derive their thermal energy primarily from the environment around them (Cowles, 1962). While many species can be accurately described by one or other of these terms there are also many exceptions (Cossins and Bowler, 1987 Chapter 3; Prosser and Heath, 1991). Some large insects are able to generate enough heat using their thoracic flight muscles to maintain their thorax temperature well above the air temperature during flight, and are sometimes referred to as temporal endotherms. Fish as a rule are ectotherms but some species, especially tuna and some sharks, are able to maintain the temperature of some of their organs considerably above the environmental temperature, by conserving heat generated by metabolism in these organs, and can be referred to as spatial endotherms.

Most fish however are true ectotherms. Their gills, as well as permitting the exchange of dissolved gases, act as heat exchangers so that the blood temperature takes on the temperature of the environment. Fish, such as carp, which live in a thermal environment which fluctuates, can be referred to as *poikilotherms*, as their body temperature tends to fluctuate with the environmental temperature.

1.4.2 Short Term Effects of Temperature

Temperature affects almost all biological processes. Generally, increasing temperature results in an increase in rate processes up to a maximum, after which further temperature increases result in decreases in the rate. The increasing effect of temperature, on many different processes, up to the 'optimum' (or maximum) rate has been described empirically in various ways (Cossins and Bowler, 1987 Chapter 2).

One of the most commonly used parameters is the Q_{10} which is the ratio of the rates of a process over a 10°C interval. If the rate increases in a semi-logarithmic manner with respect to temperature then the Q_{10} will be constant over this range. However it is more usual for the Q_{10} value to vary with temperature for most biological processes, often decreasing with increasing temperature. Consequently it is usual to quote the temperature range over which the Q_{10} was calculated.

The most frequent use of values such as the Q_{10} is for comparative purposes, although some attempts are made to derive biologically significant conclusions from Q_{10} values. Physical processes such as diffussion tend to have very low Q_{10} values while chemical processes have higher Q_{10} values. However conclusions as to the nature of rate limiting steps derived from the Q_{10} value (e.g. <2 is physical, >2 is chemical) are not reliable (Cossins and Bowler, 1987).

1.4.3 Long Term Effects of Temperature

1.4.3.1 Mechanisms of Acclimation

The thermal range experienced by many animals varies both diurnally and annually. For most aquatic animals, due to the thermal inertia of their environment, the main change is over the longer time period. There is a great deal of evidence that most organisms are not passive in their responses to such changes, but instead show varying adaptive mechanisms to offset the direct effects of longer term temperature changes. These acclimatizations to environmental changes, when studied in controlled conditions where all variables except the temperature are constant, are referred to as *acclimations* (Prosser, 1973).

Changes induced by acclimation can affect various levels of the organism. Whole organs can be affected, for example the relative ventricle size of carp increases when the fish are acclimated to lower temperatures (Goolish, 1987), or the cellular morphology can be affected, as is the case in carp intestinal mucosa which shows an increase in villi on acclimation to low temperatures (Lee, 1987). The changes can be very specific, as is the case in *Aplysia* where specific identifiable neurones increase in size on cold acclimation (Treistman and Grant, 1993). Much of the work on the effects of thermal acclimation is aimed at understanding the changes at the subcellular level. Such changes include alterations of densities of

enzymes and organelles (Sidel, 1983), the expression of different protein isoforms (Baldwin and Hochachka, 1970; Johnston, 1983) and homeoviscous adaptation (Sinensky, 1974) of cell and organelle membranes to compenste for thermal effects on the membrane viscosity (Hazel and Williams, 1990). Any adaptive changes must take place in such a way as to maintain the balance between, for example, membrane bound pumps, ion exchangers and membrane channels, all of which are likely to be differently affected by temperature (Hochachka, 1988). The functional role of these changes is to compensate for the detrimental effects of the changes of temperature experienced, and should improve the 'fitness' of the organism, for example improved swimming speed at lower temperatures (Rome *et al.*, 1985), although see Leroi *et al.* (1994) for an apparent exception.

1.4.3.2 Types of Acclimation

The usual method when studying acclimation is to compare the rates of the process under question over a range of temperatures from specimens acclimated to different temperatures. Comparisons of different rate–temperature relationships from different acclimation temperatures have resulted in the introduction of various different terms to describe them (see Cossins and Bowler, 1987, Chapter 5).

Precht (1958) devised a nomenclature to describe the degree of acclimation when comparing the rate of a particular process at two temperatures from different specimens which are acclimated to these temperatures. If specimen A is acclimated to temperature a and specimen B is acclimated to temperature b then

1 If the rate process is the same in specimen A at temperature a as in specimen B at temperature b then the acclimation is described as 'complete'.

2 If the rate process is the same in specimen A at temperature a as in specimen B at temperature a then the acclimation is described as 'none'.

Intermediate to these two can be described as 'partial' acclimation, with 'inverse' and 'supraoptimal' acclimation describing the rare occurrences where the rate–temperature relationship has shifted in a nonadaptive way in response to acclimation and has shifted to overcompensate for the temperature change respectively. These definitions were described as types 1–5 by Precht (1958) as shown in

Table 1.1 Types of acclimation as defined by Precht (1958).

Supraoptimal	Type 1
Complete	Type 2
Partial	Type 3
None	Type 4
Inverse	Type 5

Table 1.1.

These terms are based on comparisons of the rates at two temperatures. The classification of Prosser (1973) involves the comparison of the rate–temperature relationship over a range of temperatures. The lateral displacement and orientation of the rate–temperature curves plotted on a log–linear plot are combined to give the definitions shown in Table 1.2 (see Cossins and Bowler, 1987, Fig. 5.2).

Table 1.2 Types of acclimation as defined by Prosser (1973).

No Compensation	Type I
Translation	Type II
Rotation	Type III
Translation with Rotation	Type IV

The most common types of acclimation seen are partial (Type 3 as defined by Precht) and translational with some rotation (Type IV as defined by Prosser), with the different effects predominating over different temperature ranges (Cossins and Bowler, 1987).

1.4.3.3 Acclimation in the CNS

There is considerable evidence that the central nervous system is the vertebrate 'organ' which is most adversely affected by changes in temperature (Roots and Prosser, 1962; Lagerspetz, 1974; Prosser and Nelson, 1981; Montgomery and MacDonald, 1990) and therefore would be expected to show acclimation in those species capable of tolerating a wide thermal range (eurythermal species). Various aspects of the nervous system do show adaptive changes on acclimation such as the conduction velocity of action potentials (Harper *et al.*, 1990). However the origin of the breakdown of neural function on thermal extremes is probably located in the synaptic mechanism (Friedlander *et al.*, 1976; Prosser and Nelson, 1981; Cossins and Bowler, 1987). Prosser and Heath (1991) suggest that 'integrated systems are more temperature sensitive than their component parts' and that the detrimental effects of high and low temperature can be due to 'synaptic failure in the CNS'. For effective acclimation to thermal changes it would be expected that the sensitive integrating region of the CNS, the synapse, would play a dominant role (MacDonald, 1988, 1990).

The work on the effect of temperature on vertebrate synaptic transmission has largely been limited to the neuromuscular junction due to its accesibility and the body of knowledge on it. The lack of information on the effects of temperature on synaptic transmission in the vertebrate central nervous system is largely due to the difficulty in directly studying these synapses (Montgomery and McDonald, 1990). Much of the work has been on the time–course and frequency of neuromuscular miniature end plate potentials. Both of these variables are affected by temperature (Fatt and Katz, 1952; Duncan and Statham; 1977; Barrett *et al.*, 1978; Robertson and Wann, 1984; Harper *et al.*, 1989; Tiiska and Lagerspetz, 1994). Harper *et al.* (1989) reported a degree of acclimation of the time course of the rise phase of the miniature end plate currents, but not the fall phase, in carp extraocular muscle, and Tiiska and Lagerspetz (1994) also found no change in the temperature sensitivity of the fall phase of frog sartorious muscle on acclimation. The effect of temperature acclimation on the magnitude or time–course of evoked transmitter release (by stimulating the nerve) was not reported by any of these workers, although both are clearly affected by temperature (Barrett *et al.*, 1978). However

Tiiska and Lagerspetz (1994) did show that the synaptic delay of the frog sartorious neuromusclar junction did not show any significant compensatory changes on acclimation to 4°C and 20°C.

These clearly inconclusive results on the peripheral synapse are not necessarily of particular relevance to the CNS synapses as the vertebrate neuromuscular junction is specialised for one to one transmission of action potentials with a high saftey factor. A system more analogous to the vertebrate CNS is the crustacean neuromuscular junction which demonstrates integration of excitatory and inhibitory inputs from a number of axons (Kuffler *et al.*, 1984, Chapter 16). A considerable body of work has accumulated on the effects of thermal acclimation on this system in eurythermal crabs and crayfish (reviewed by Stephens, 1990). Both the end plate potential amplitude and facilitation at a eurythermal crab neuromuscular junction show ability to acclimate (Stephens and Atwood, 1982), with the former showing a maximum and the latter a minimum at around the acclimation temperature. It has been suggested that one of the mechanisms involved in the shift in temperature dependence of the responses is alterations in the membrane lipid composition which have been shown to occur during acclimation in crustaceans (Chapelle *et al.*, 1979). Vertebrate CNS synaptosomal membrane lipid compositions have also been shown to change on thermal acclimation, although they do not appear to demonstrate complete homeoviscous adaptation (Cossins, 1977; Cossins and Prosser, 1982). The significance of these homeoviscous adaptive mechanisms on the functional adaptation of synapses is questioned by MacDonald (1988, 1990), particularly with regard to the electrical properties of the cells. He suggests that the potential influence of the membrane constituents on the inexcitable properties of cells may be of more importance, such as exocytosis (and therefore transmitter release at vesicular synapses) and metabolic cascades involving membrane lipids.

The lack of direct electrophysiological recordings of vertebrate CNS synaptic responses and consequent lack of information on the effects of temperature acclimation means that it is not known if the effects observed in crustacean neuromuscular synapses are paralleled in vertebrate synapses. The analogue responses of the distal retinal neurons, including the horizontal cells, are more akin to the graded responses of CNS synapses than all–or–nothing action potentials and are therefore a favourable location for investigating the effects of temperature on the

CNS. As well as showing the characteristics of large post–synaptic potentials horizontal cells represent one of the earliest stages of visual integration and as such changes in their responses as a result of short and long term changes in temperature may have direct effects on the visual behaviour of the animals.

Chapter II

Microelectrode Measurements of Horizontal Cells in the Intact Retina.

2.1 INTRODUCTION

2.1.1 Early Microelectrode Recordings

Early (i.e. before 1940) recordings from neurones were limited to extracellular methods which provide information on the output of the neurones by recording action potentials. However extracellular recordings cannot directly measure the graded synaptic potentials involved in the integration of the information transmitted by the action potentials. Intracellular electrodes, using glass tubing drawn out to a fine tip and filled with an ionic solution, were developed over a number of years (1939–1949). Two of the most prominent workers in the field were Ling and Gerard (e.g. Ling and Gerard, 1949) though others were also involved, using similar approaches (see Edwards, 1983 for a brief review).

Initially intracellular recordings were from large cells, such as the squid giant axon, or muscle fibres. The first recordings of retinal neurones were reported by Svaetichin (1953) who attributed large, sustained, graded hyperpolarizations recorded on light stimuli in isolated teleost retinal preparations as being membrane potential changes in cone photoreceptors. It is now generally accepted that he was recording from horizontal cells and, in conjunction with MacNichol, used marker dyes in the microelectrode to concluded that the purely hyperpolarizing responses to a range of illumination wavelengths which they recorded (termed luminosity responses) were from horizontal cells (Svaetichin and MacNichol, 1958).

2.1.2 Microelectrode Recordings from Horizontal Cells

It was not until Kaneko (1970) used microelectrodes with the intracellular dye procion yellow to record from cells in the trichromatic goldfish retina that the issue of the origin of luminosity and chromaticity responses was finally resolved (Section

1.3). Since then microelectrode recordings from horizontal cells in the isolated intact retina (and in the eyecup preparation) have been of major use in increasing the understanding of the horizontal cell. The accessability and relative ease of recording from the horizontal cell, the use of graded potential changes rather than action potentials (Section 1.3.2) and the plasticity of the horizontal cells responses (Section 1.3.5) have frequently resulted in the responses recorded requiring 'some broadening or even revision of classical concepts of neuronal physiology' (Piccolino, 1986).

2.2 METHODS

2.2.1 Thermal Acclimation of the Fish

Carp were obtained from a commercial fish farm and varied in length from 15–25*cm*. They were kept in a ~1500 litre tank of dechlorinated tap water with a temperature range of 16±1.5°C with a through flow of water so that the tank volume was replaced approximatly every 24 hours. They remained here for some weeks before being transferred to ~250 litre tanks with temperature ranges of 8±1°C (a maximum of four fish per tank) or 26±1°C (a maximum of two fish per tank). These temperature changes were gradual, over a minimum of 36 hours, to reduce stress on the fish. In the smaller tanks there was also a through flow of water which replaced the tank volume in about 24 hours. The fish were fed a diet of pellets (Omega Pond Fish Food, medium pellet) approximately three times a week. The fish at higher temperatures ate most, though those at 8°C did usually continue to eat. The fish were kept at the new acclimation temperature for three weeks before recordings were made from their retinas. In those studies where the time course of thermal acclimation has been studied the effects are usually almost if not totally complete within this time span (e.g. in carp ATPase activities from the brain and kidney (Tirri *et al.*, 1978), in goldfish synaptosomal membrane composition (Cossins, 1983), in carp myofibrillar ATPase (Heap *et al.*, 1985) and in adaptive changes in phospholipid saturation (Hazel, 1989)).

2.2.2 Retinal Isolation

The retina was isolated and maintained as frequently described (e.g. Teranishi *et al.* 1984). Fish, taken during the light phase of the diurnal cycle, were kept for 40–60 minutes in the dark which facilitated the removal of the pigment epithelium from the retina. Subsequently the ambient light level was a very dim red light which was almost totally excluded from the experimental chamber to maintain the retina in as scotopic conditions as possible.

Fish were sacrificed by decapitation followed by pithing rostrally and caudally. One eye was then enucleated and placed on filter paper where extraneous muscle was removed. The optic nerve was cut as close to the sclera as possible, to enable the retina to come away from the back of the eye. The eye was then hemisected

posterior to the *ora serrata* to ensure that this point of attachment of the retina to the eye was severed. This eyecup preparation was then placed in chilled (~4°C) oxygen saturated saline (in millimolar): NaCl, 119; KCl, 4; $MgSO_4$, 1; $CaCl_2$, 1; Glucose, 10; HEPES, 10 bufferred to pH 7.5 (1 Molar NaOH).

Fine forceps were then used to dissect the retina and pigment epithelium from the sclera. Once in the saline the pigment epithelium could be easily lifted off the retina. This whole process was carried out in under three minutes to prevent anoxia of the tissue.

The retina was then placed on moist filter paper (Watman No.1) receptor side up. The vitreous humour caused the retina to form a dome on the paper. Gradually, as the filter paper absorbed the vitreous humour, the retina would flatten, sometimes over a period of hours. This would make it impossible to record from individual cells as they would be moving, so the absorption process was accelerated. A vacuum pump was used for 30–60 seconds to draw the vitreous into the filter paper, during which time the retina was in a constant stream of 100% oxygen, and saline was dripped onto it at a rate fast enough to prevent it from drying. Once the retina was seen to be visibly flatter it was transferred, still on the filter paper, to the experimental chamber.

The experimental chamber (see Fig. 2.1) was a rectangular plastic box of volume $27.3cm^3$. 100% oxygen, saturated with water, was passed very slowly over the retina, leaving the chamber by a $4mm$ square hole in the top which allowed the entry of the microelectrode. The top of the recording chamber was a single thickness of coverslip glass which let the light stimulus through with little attenuation, but helped to reduce evaporation from the retina surface and maintain a high oxygen partial pressure around the retina. To allow easy insertion and removal of the retina this top could be easily removed and replaced. The retina was stable in this high humidity and high O_2 partial pressure for at least four hours, with no observable difference in the horizontal cell recordings taken over this time scale.

2.2.3 Intracellular Recording

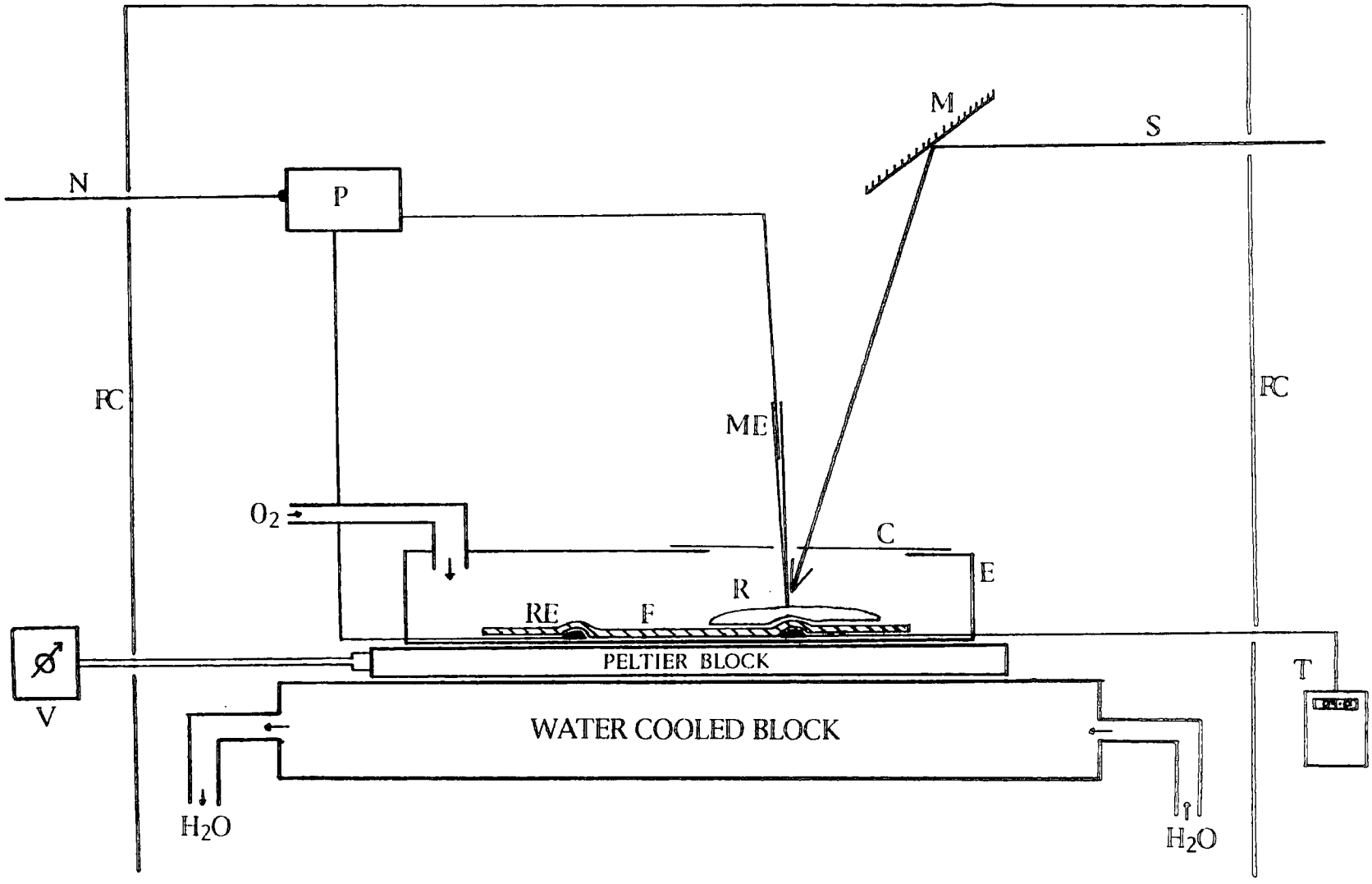
M
S
N
P
RC
RC
ME
O_2
C
E
R
RE
F
PELTIER BLOCK
V
T
WATER COOLED BLOCK
H_2O
H_2O

2.2.3.1 Microelectrodes and Electrical Apparatus

Microelectrodes were made from borosilicate tubing with an external diameter of $1mm$ and an internal diameter of $0.5mm$, with a rod of $0.1mm$ diameter attached to the inside of the barrel. They were pulled on a single stage puller (Clark Electromedical Instruments — LPP-2) and back filled with 3 Molar potassium acetate. The inner rod acted like a wick drawing the microelectrode solution into the tip. The microelectrodes had resistances of $200\text{–}400M\Omega$ when measured in saline by passing a small current ($\leq 1nA$) through them and measuring the potential change. The electrical connections to the microelectrode electrolyte and the retina were made by silver/silver chloride wires (Ag/AgCl).

The responses to light stimuli were recorded through a high input impedence preamplifier (the configuration of which was as in Colburn and Schwartz (1972)) and displayed on an oscilloscope (Tektronix 5113 Dual Beam Storage Oscilloscope). They were simultaneously recorded on magnetic tape (AR Vetter Co. Tape Recording Machine Model A) from which they could be played back to a chart recorder (Servoscribe 15) and digitized (Tektronix 5D10 Waveform Digitizer). Hard copy could then be produced using an X–Y plotter (Farnell).

2.2.3.2 Light Stimuli

The experimental chamber, microelectrode and micromanipulator were all situated in a Faraday cage made of sheet metal, the inside of which was painted matt black so as to absorb any scattered light. The light source and associated filters were outside this structure and the light beam passed through a $3cm$ diameter hole in the metal before being reflected onto the retina (Fig. 2.1). The room was also blacked out, to reduce any background light, although there was a low intensity red light source.

The stimulus light source used was a 70Watt/24Volt tungsten–halogen bulb run at 23.5 Volts, which produced a $\sim$2800°C light source. The light was focused and passed through two neutral density wedges which could be used to regulate the intensity of illumination falling on the retina, from 6.3 to $1.2 \times 10^4 \mu W cm^2$, as measured using a calibrated United Detector Technology PIN 10DP photodiode in conjunction with a Pacific Photometric Instruments Laboratory Photometer 110.

It was then passed through an aperture to control the area which was illuminated, before entering the Faraday cage and falling on the retina. The area of light could be switched between a circle of $4.5mm$ in diameter (covering >50% of the retina) and a bar of width $135\mu m$. Both of these stimuli could be moved over the retina, although the circle was always positioned so that the microelectrode was near the centre of the illuminated area. There was also a series of 15 interference filters (Blazers) which could be inserted into the light pathway, to give different wavelength stimuli. The duration of illumination stimuli was controlled by a motorised shutter. The stimuli were usually $500ms$ in duration and were interspersed by a $\sim$6 second period of darkness.

2.2.3.3 Technique

After filling the microelectrode and inserting the Ag/AgCl wire so that it was touching the electrolyte, the microelectrode was placed in a holder attached to the micromanipulator (Huxley design). The electrode was positioned so that it was in the centre of the area illuminated by the stimulus and very slowly lowered until the microelectrode tip touched the surface of the retina. This was easily recognised because the electrical circuit was completed by the microelectrode making contact with the upper surface of the retina.

The microelectrode resistance was then measured as described above to ensure suitability for cell penetration. An electrode with a resistance of less than $\sim 150M\Omega$ was disgarded as probably being broken at the tip. The junction potentials in the recording circuit result in a constant potential recorded at this stage. An equal but opposite potential was applied to the circuit to compensate for the junction potentials. Slowly varying junction potentials (limited to a few mV over the duration of any single recording) were not a problem when recording the fast (in comparison) potential changes elicited by the light stimuli, although it was not possible to tell if there were any variations in the resting potentials of cells with time because of these varying junction potentials.

Once in contact with the retina the microelectrode was advanced in $\sim 2\mu m$ steps. Over–adjustment of the capacitance compensation circuit (Halliwell and Whitaker, 1987) resulted in oscillations of potential difference across the microelectrode tip and this aided entry of the microelectrode into small cells (possibly

by physically vibrating the tip, although the mechanism is not known). When, on advancing the microelectrode, a hyperpolarizing jump of $\sim$15–30mV to a new sustained potential was recorded, the retina was illuminated with a test flash of white light. If a horizontal cell had been sucessfully penetrated a sustained hyperpolarization was recorded (as in Figs. 2.2, 2.5 and 2.9). In order to establish that a luminosity (H1) cell was being recorded from the retina was illuminated with a series of different spectral stimuli ($\sim$500–700nm) using the interference filters in the light pathway. In the majority of cases only hyperpolarizing responses were observed for all the wavelengths used. In a number of cases further advances of the recording electrode were carried out on completion of experiments when chromatic responses were recorded demonstrating that the H1 cell soma was being recorded from as opposed to the axon terminal. The retina was then exposed to a series of increasing intensities of illumination with no interference filters in the light pathway, as described in the results section (Section 2.3.1).

2.2.3.4 Control of Experimental Temperature

The experimental chamber containing the retina was placed on a peltier block so that the temperature could be varied by altering the current through the block (Fig. 2.1). This block also had a water cooled block beneath it to increase and improve the cooling range which could be achieved, by cooling the warm side of the peltier block. The base of the experimental chamber was about 1.5mm thick and the thermal contact between this and the peltier block was improved by a layer of heat sink compound. The retinal temperature was monitored using a thermocouple placed between the moist filter paper and the base of the chamber (RS Components Digital Thermometer – Thermocouple Type K).

2.3 RESULTS

2.3.1 Responses to Varying Light Intensities

On penetrating a luminosity horizontal cell its responses to a series of light intensities was recorded. The light intensity was increased stepwise until the response, viewed on the oscilloscope, was seen to be approaching a maximum (V_{max}), when the light intensity was reduced at intermediate values to those already used. The light stimuli were of $500ms$ duration with a dark interval of $\sim$6 seconds between them.

The changes in membrane potential recorded for increasing light stimuli from a single cell at a single temperature are shown superimposed in Fig. 2.2. The most obvious change is the increase in amplitude of response with increasing light stimulus. Fig. 2.3 shows the relationship between the amplitude of the response and the light intensity. The results can be fitted to the Michaelis Menten equation (Naka and Rushton, 1966; Dowling, 1987). The equation can be written as follows:–

$$V = V_{max}.\frac{I^h}{I^h + \sigma^h}$$

where V is the response amplitude at light intensity I, V_{max} is the maximum response amplitude, σ is the light intensity at which $V=\frac{1}{2}V_{max}$ and h is a constant.

The results were fitted to this equation by calculating V_{max}, σ, and h using a least squares minimization computer program. This was based on a method produced by Wilkinson (1961) which calculated V_{max} and σ, for a particular value of h and a Fibonacci search which converged on an estimate for h, as described by Atkins (1973). Fig. 2.3 shows that the results from the increasing light intensity stimuli fit the same equation as those from the decreasing light intensity stimuli.

Fig. 2.4 shows how three other features of the response vary as the response amplitude increases. Using the Waveform Digitizer (Section 2.2.3.1) the rate of change of the membrane potential during both the rise and fall phases of the responses was measured. The time taken for the initial change in membrane potential, from the onset of the light stimulus, was also measured. As would be expected

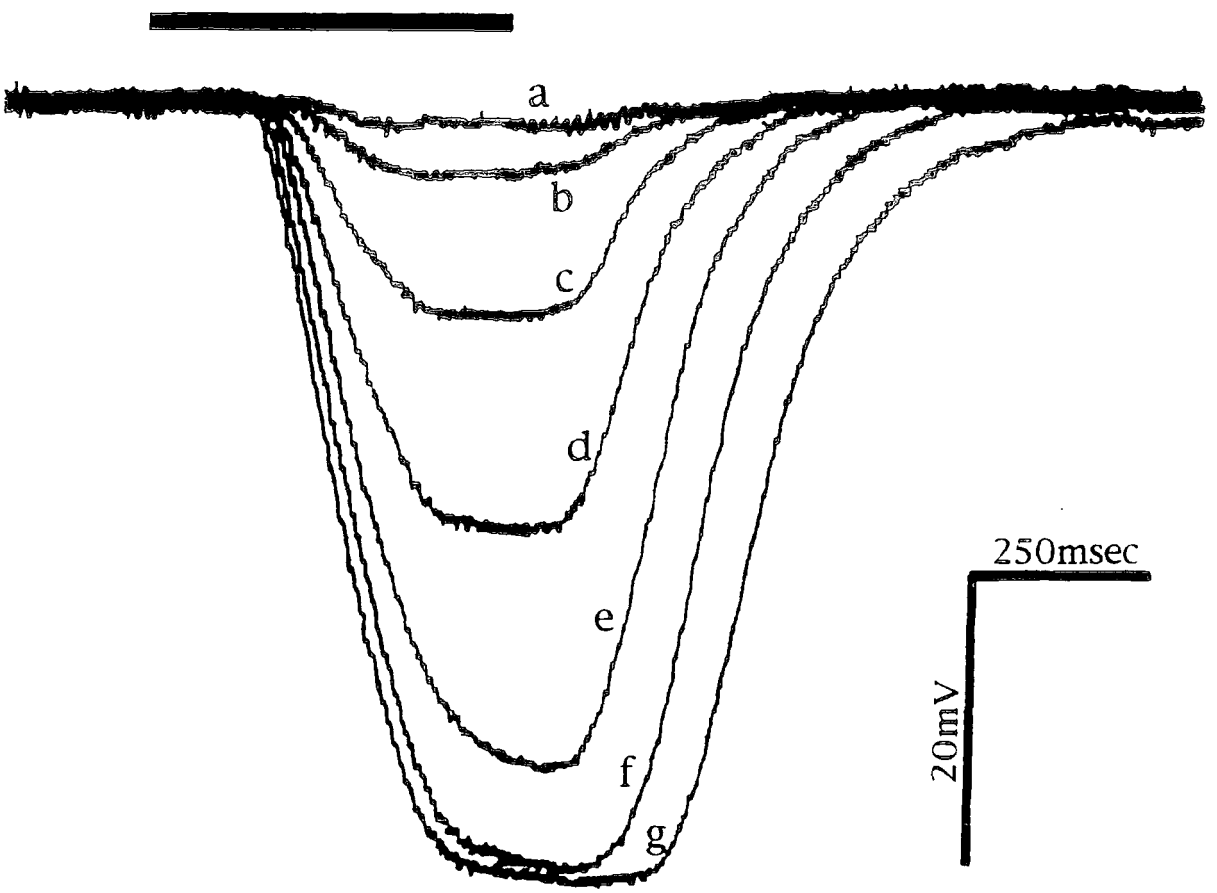
a
b
c
d
e
f
g
250msec
20mV

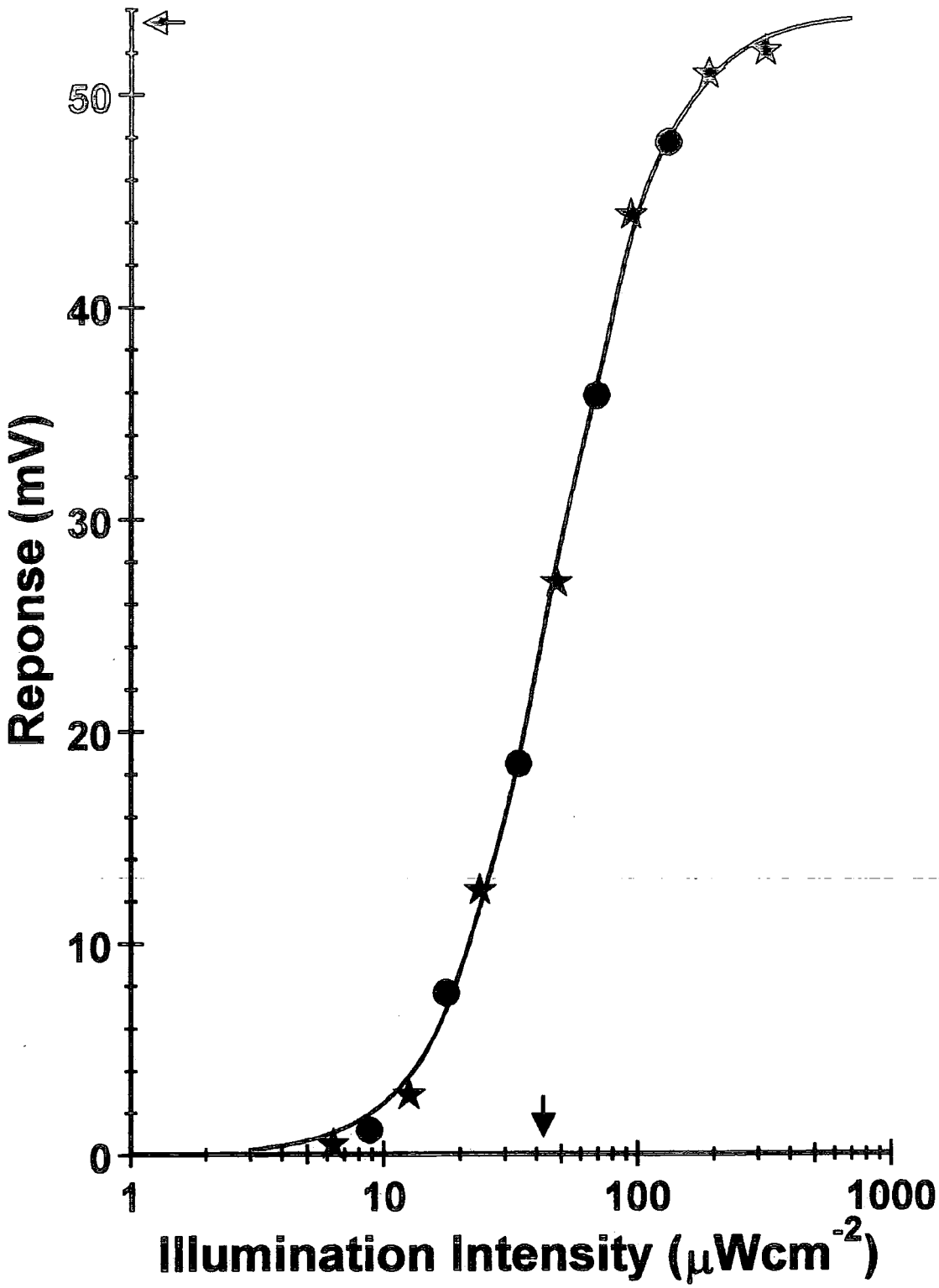
Reponse (mV)
0
10
20
30
40
50
1
10
100
1000
Illumination Intensity (μWcm-2)

the rate of change of the membrane potential (in volts per second) increases as the response amplitude increases (Fig 2.4). The time between the onset of the light stimulus and the first detectable change in the membrane potential (or response latency) decreases as the response amplitude increases. These variables are plotted against the response amplitude so that their values at half the maximum response ($\frac{1}{2}V_{max}$) could be calculated.

2.3.2 The Effect of Experimental Temperature

The effect of increasing temperature on a horizontal cell's responses to increasing light stimuli is shown in Fig. 2.5. The responses of a horizontal cell to a series of light intensities (from a fish acclimated to 16°C) was recorded at four different temperatures (7.9°C to 14.2°C). The changes in temperature had a number of pronounced effects on the response waveform. An obvious effect is a change in the response amplitude at the same stimulus intensity at the different temperatures. It can be clearly seen that V_{max} increases in these records as the temperature increases. However, it should also be noted that at the lower stimulus intensities the response amplitude increases with decreasing temperature. Both these effects of temperature can be more clearly seen in Fig. 2.6 where the response amplitudes are plotted against the stimulus intensity at the different temperatures. While in this example V_{max} increases from $\sim 26mV$ to $\sim 42mV$ on the increased experimental temperature the responses to the same low stimulus intensities (i.e. at the lowest four stimulus intensities shown) at 7.9°C and 9.5°C are larger than those at 12.2°C and 14.2°C. This effect of temperature on the sensitivity of the cell can be more easily demonstrated by comparing the light intensity required for half the maximum response (i.e. σ). This shows an increase from $17\mu W cm^{-2}$ to $36\mu W cm^{-2}$ on the increase in experimental temperature.

Although the effect of increasing temperature on V_{max} shown in Figs. 2.5 and 2.6 is an increase, this relationship does not continue at higher temperatures. The results from 56 horizontal cell recordings at different temperatures (all from fish acclimated to 16°C) are shown in Fig. 2.7. As can be seen V_{max} increases with temperature up to about 15°C. Further increases up to about 18°C do not result in large changes in V_{max} but temperatures above about 20°C result in a decrease in V_{max}.

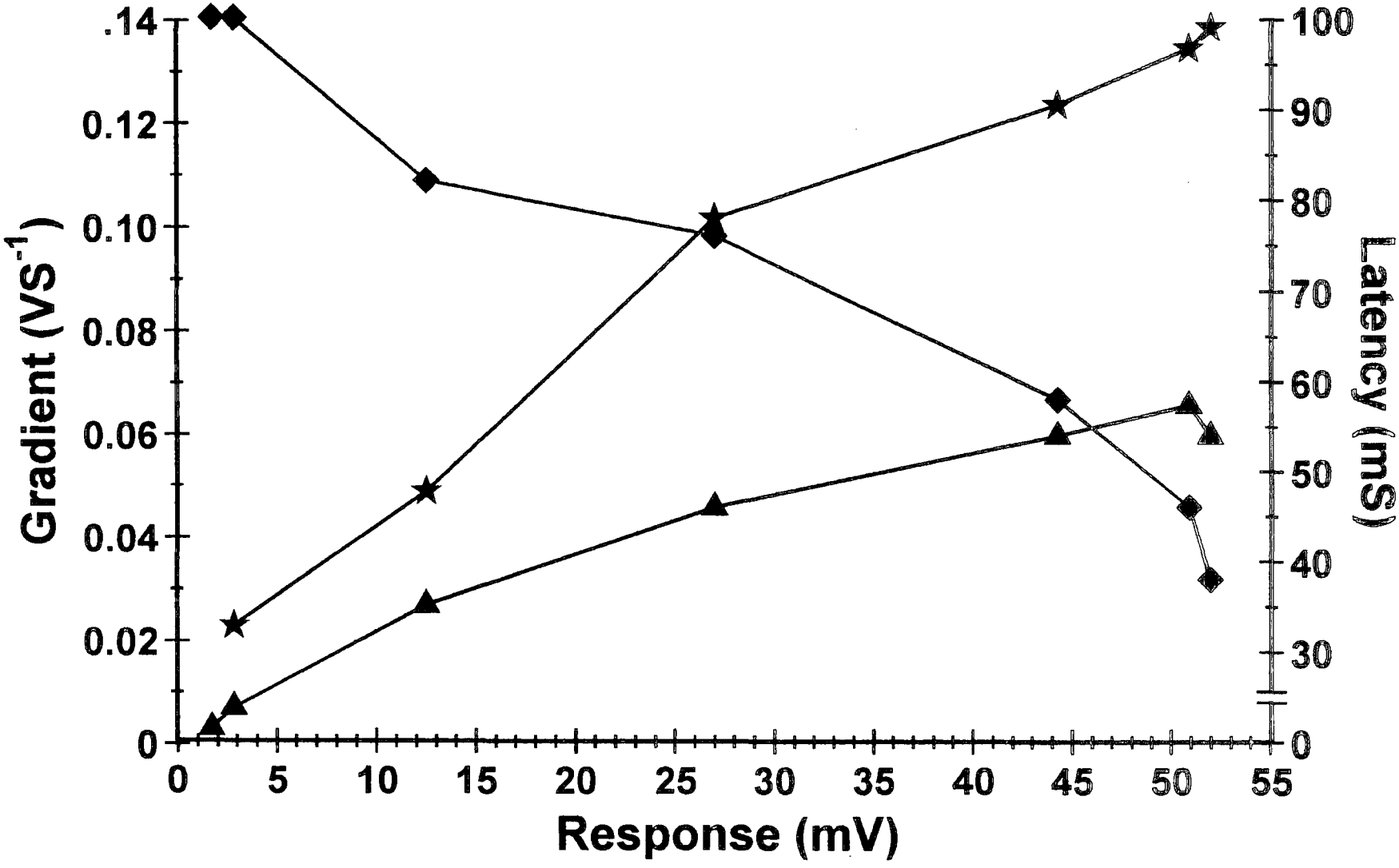
.14
0.12
0.10
0.08
0.06
0.04
0.02
0
Gradient (VS^{-1})
100
90
80
70
60
50
40
30
0
Latency (mS)
0
5
10
15
20
25
30
35
40
45
50
55
Response (mV)

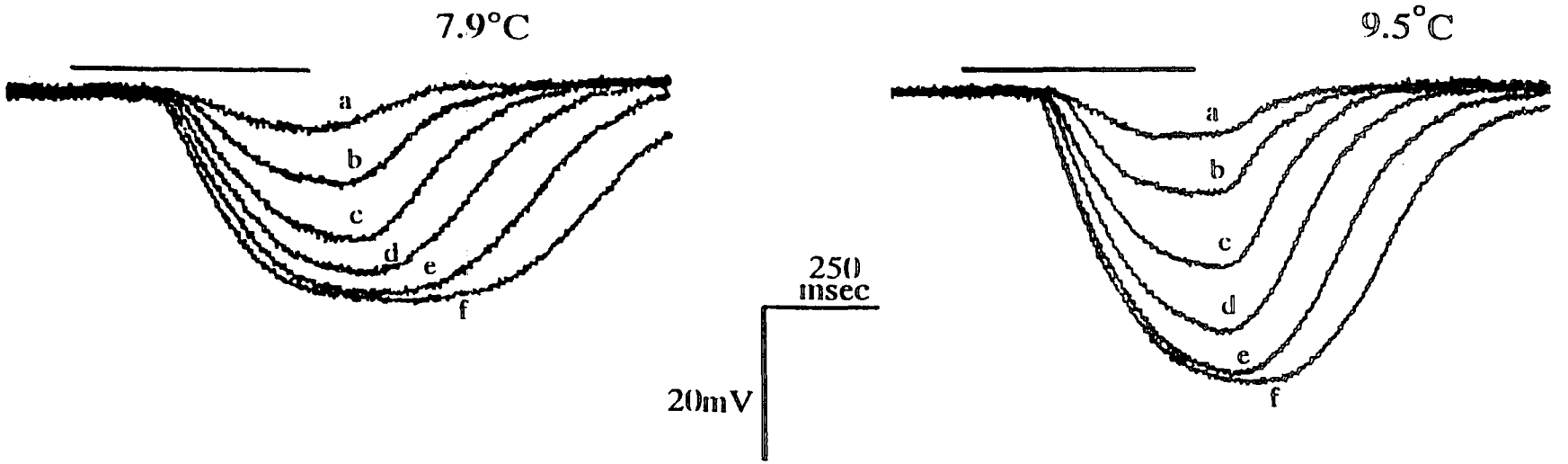
7.9°C
9.5°C
12.2°C
14.2°C
a
b
c
d
e
f
250
msec
20mV

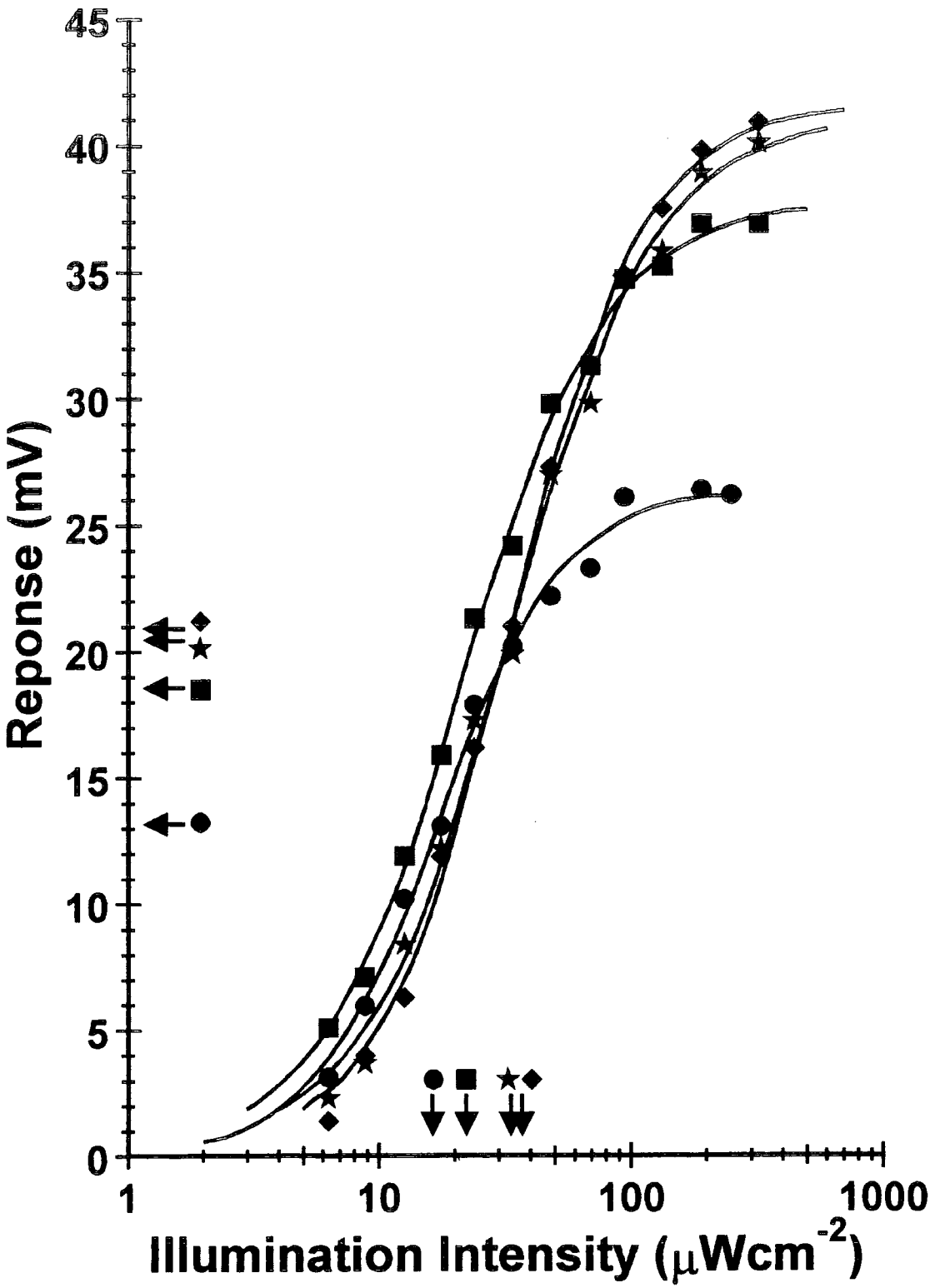
45
40
35
30
25
20
15
10
5
0
Reponse (mV)
1
10
100
1000
Illumination Intensity (μWcm-2)

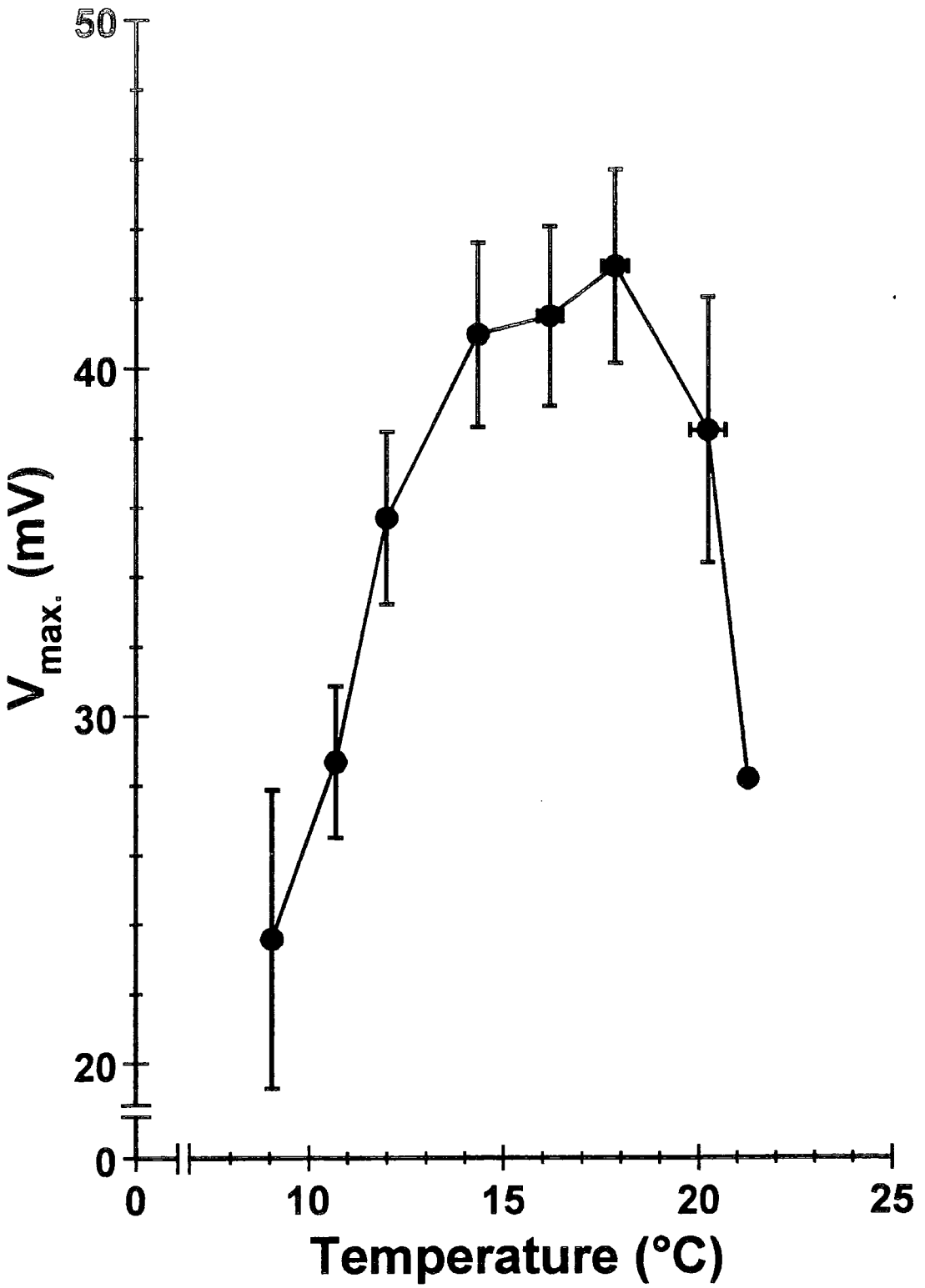
50
40
30
20
0
$V_{max.}$ (mV)
0
10
15
20
25
Temperature (°C)

The effect of temperature on the horizontal cells' sensitivity to the illumination stimuli does not show a comparable maximum. Fig. 2.8 shows how temperature effects σ from horizontal cells from two fish (both acclimated to 16°C). Differences in light adaptation of the two retinas causes the displacement of the results from the different fish on the graph. However, in both cases the value of σ increases with temperature with similar Q_{10} values measured between 10°C and 20 °C of 2.7 and 2.4 for the more and less light adapted retinas respectively.

The stability of recording was reduced if large temperature changes were attempted e.g. >10°C, possibly due to evaporation and condensation on the retina. Consequently the results in Fig. 2.5 only cover a ~6.5°C range. Fig. 2.9 shows the responses of two different cells at 9°C and 19°C which demonstrate the magnitude of the effects of temperature on the kinetics of the responses. As can be seen the shape of the responses to increasing light stimuli are very different at the two temperatures. Not only are the rates of change of the membrane potential much faster at the higher temperature but the latency is considerably reduced too. By measuring these variables at $\frac{1}{2}V_{max}$ the effects of temperature can be compared between cells. The rates of change of the membrane potential of both the rise and fall phases of the response and the response latency at $\frac{1}{2}V_{max}$ from 56 horizontal cells (all from fish acclimated to 16°C) at different temperatures are shown in Fig. 2.10. Over the temperature range of 10°C to 16°C the rate of change of the membrane potential with time of both the rise and fall phases of the response increased with increasing temperature, with Q_{10} values for both in the region of 4.0–4.4. The response latency decreased with increasing temperature with a Q_{10} over the same temperature range of ~2.1.

2.3.3 The Effect of Acclimation Temperature

The horizontal cell responses from fish acclimated to 8°C and 26°C (for three weeks) at various experimental temperatures were recorded in order to compare them with the responses from cells from fish acclimated to 16°C. The most pronounced effect of acclimation to both higher and lower temperatures was on the values of V_{max} (Fig. 2.11). Although there was no significant difference between the largest values of V_{max} from the different acclimation groups ($p > 0.05$ Students t–Test) these values occurred at different experimental temperatures — around

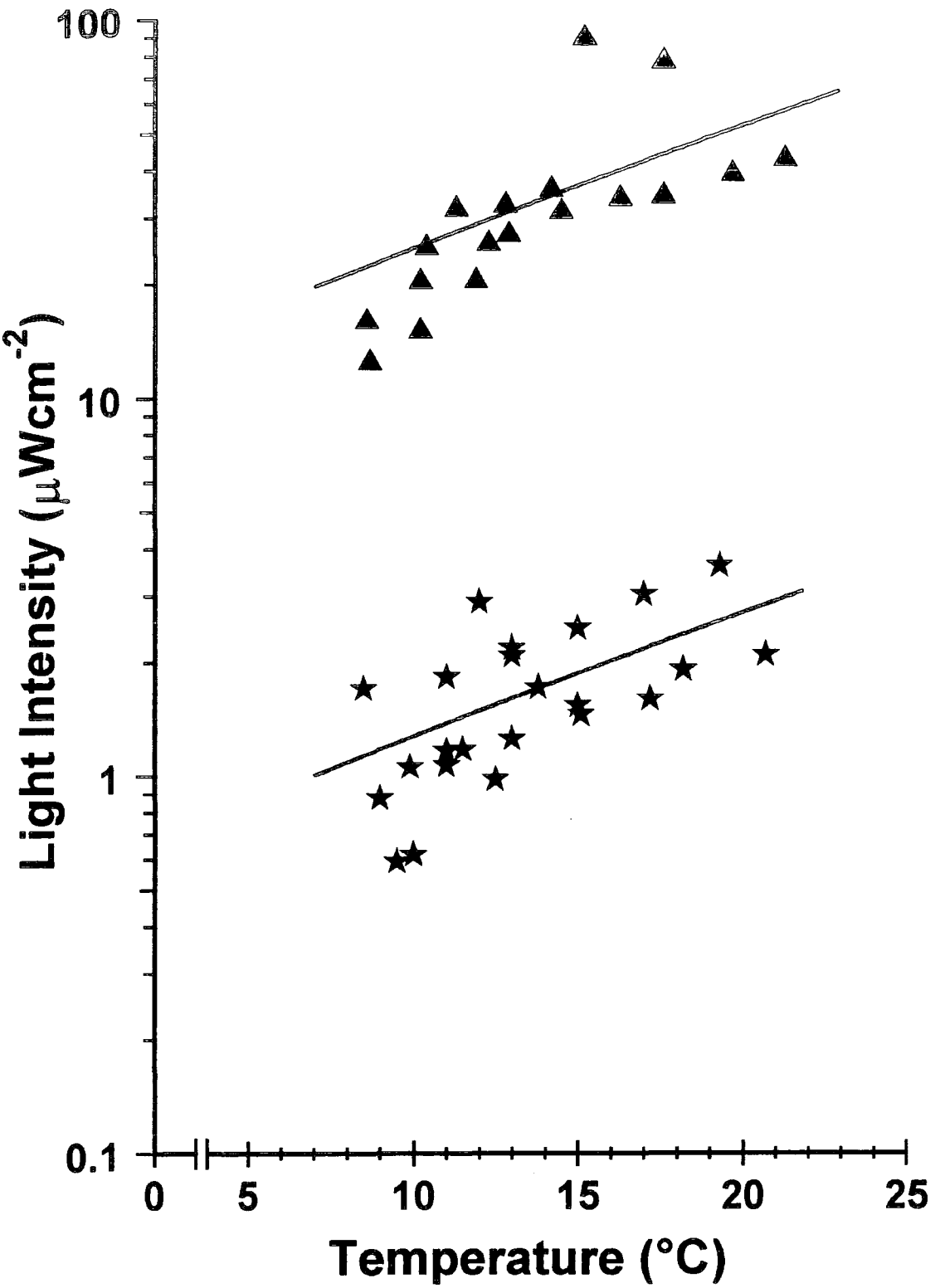
100
10
1
0.1
Light Intensity (μWcm-2)
0
5
10
15
20
25
Temperature (°C)

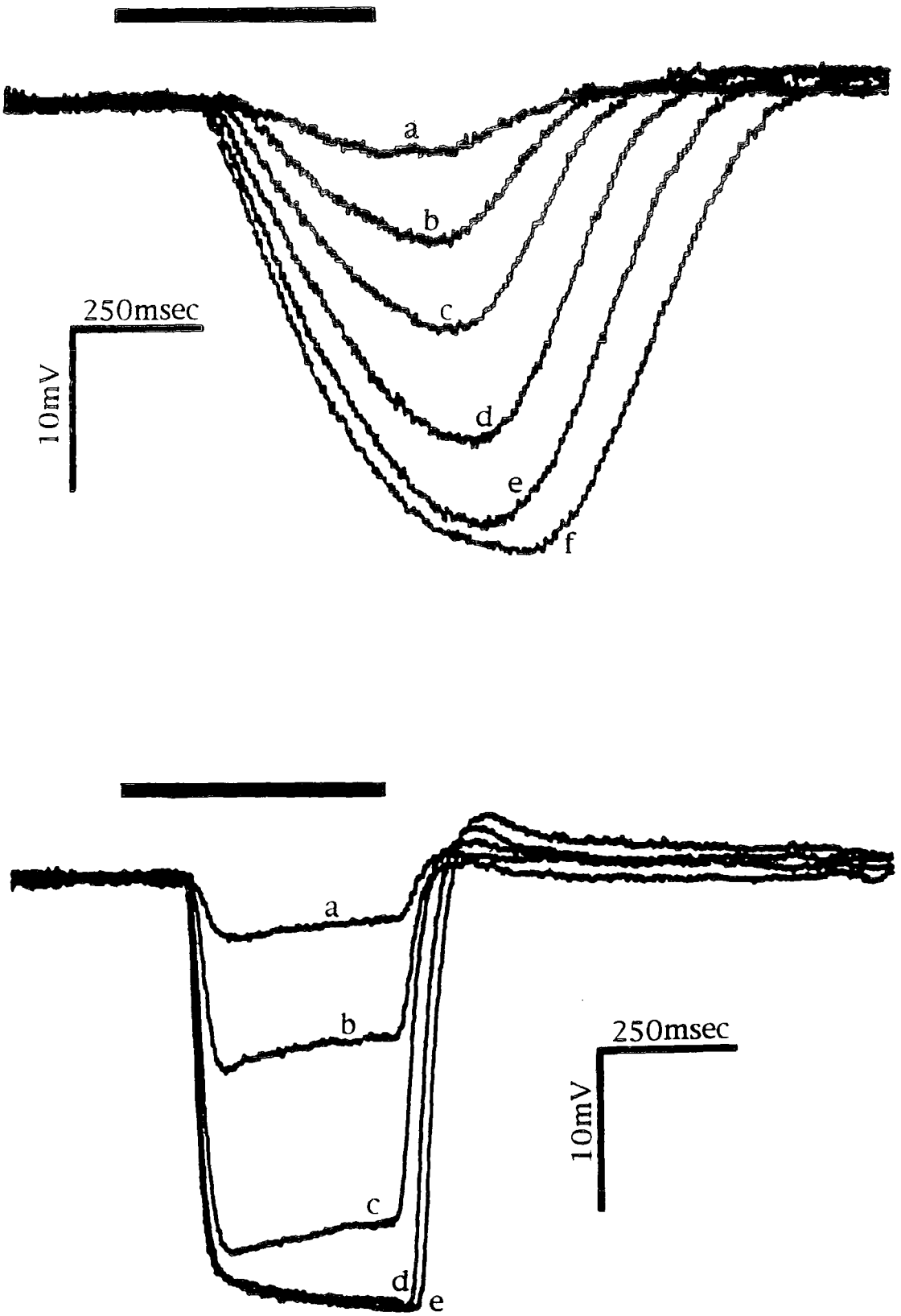
a
b
c
d
e
f
250msec
10mV
a
b
c
d
e
250msec
10mV

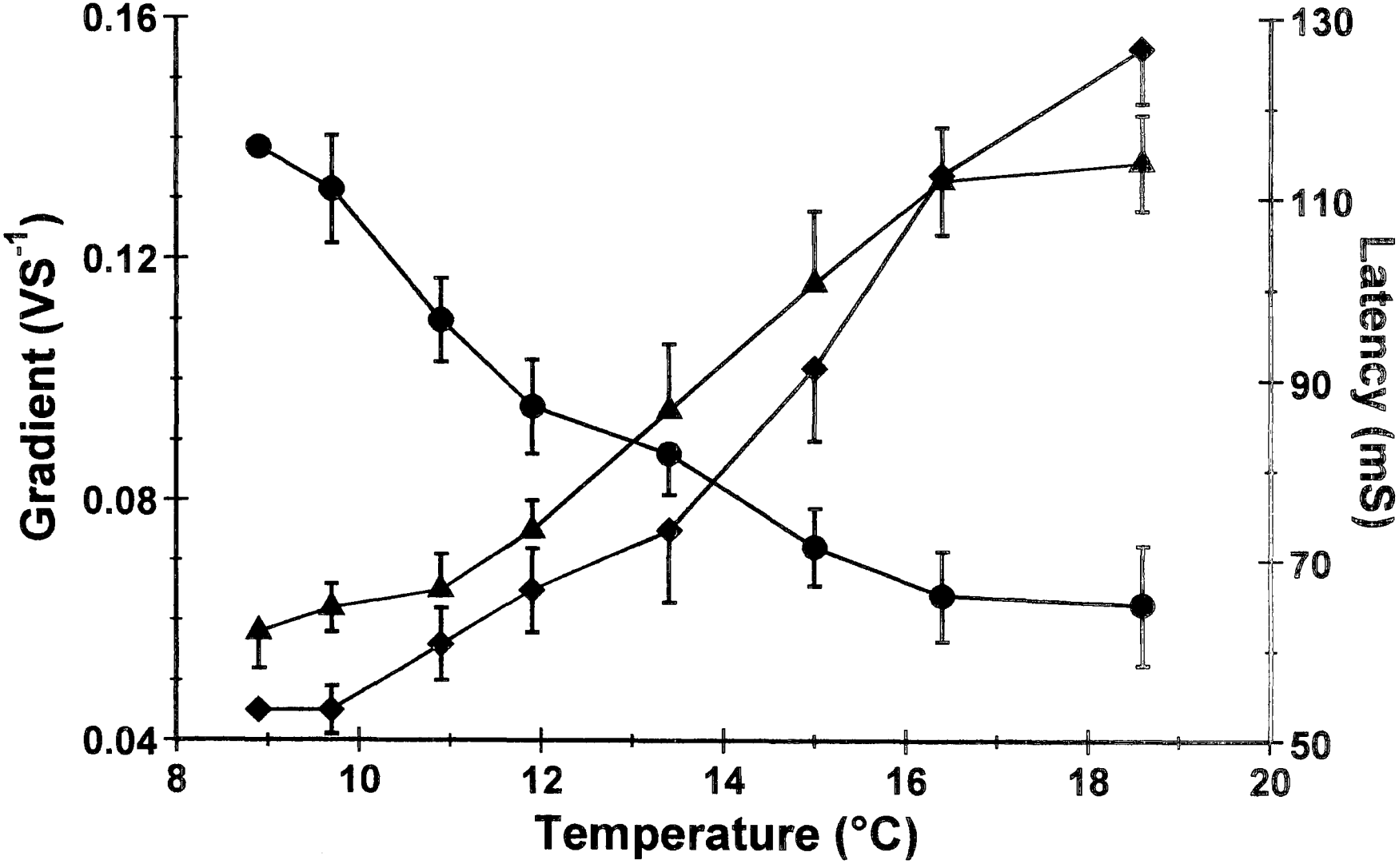
0.16
0.12
0.08
0.04
Gradient (VS^{-1})
130
110
90
70
50
Latency (ms)
8
10
12
14
16
18
20
Temperature (°C)

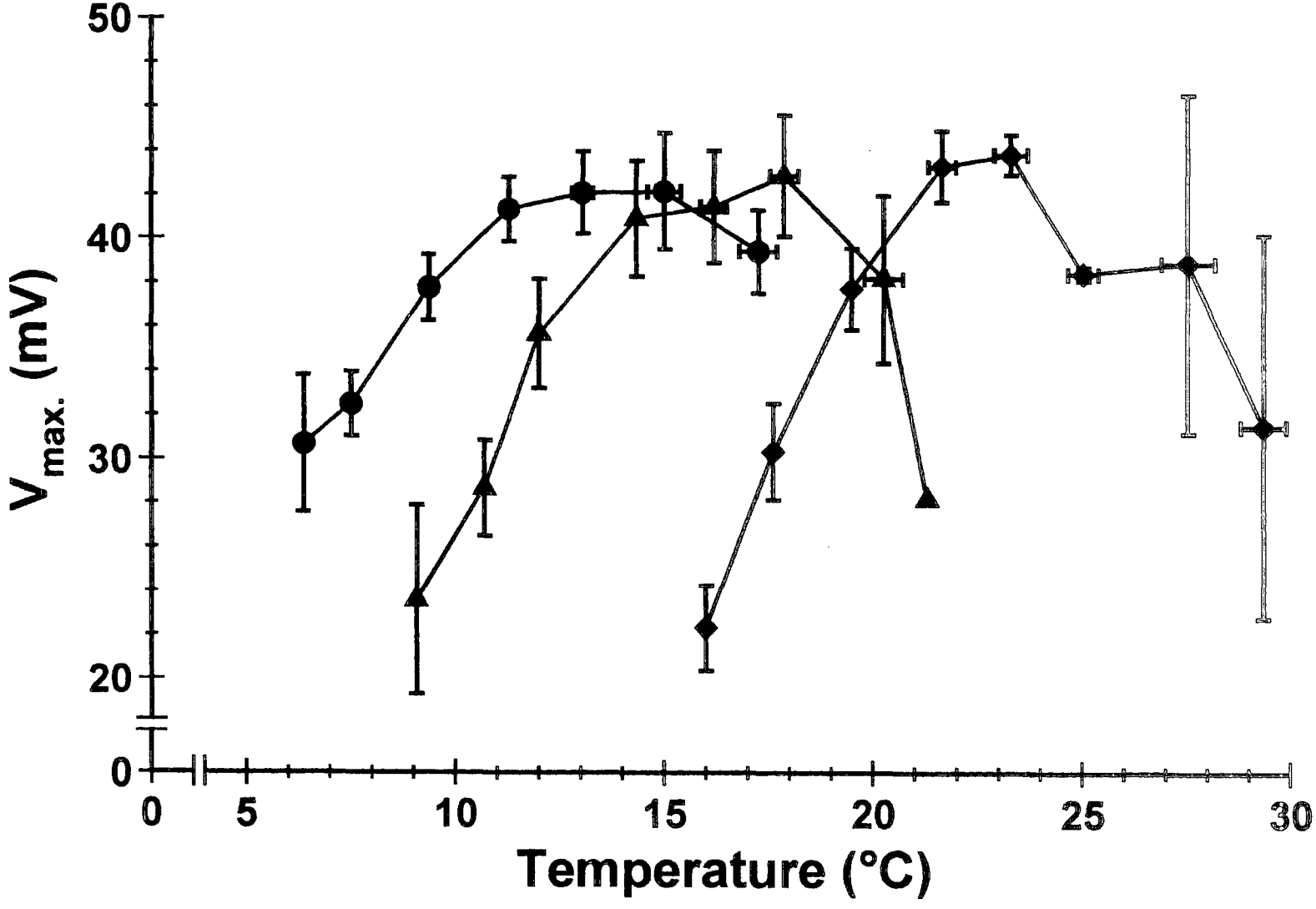
50
40
30
20
0
$V_{max.}$ (mV)
0
5
10
15
20
25
30
Temperature (°C)

13°C, 18°C and 23.5°C for cells from fish acclimated to 8°C, 16°C and 26°C respectively. The shape of the temperature–V_{max} relationship for each acclimation temperature is quite similar, especially comparing the decrease in V_{max} at lower temperatures. The effect of temperature acclimation appears to be a displacement of the temperature dependence of V_{max} along the temperature axis. This displacement is towards the acclimation temperature and is consequently clearly adaptive, although not enough to totally compensate for the temperature changes experienced by the fish. The values for V_{max} at experimental temperatures the same as the acclimation temperature are given in Table 2.1. According to the definition of Precht (1958) this is therefore an example of partial or Type 3 compensation.

Table 2.1. V_{max} values at experimental temperatures equal to the acclimation temperatures are presented as means ± S.E.M.

Acclimation and Experimental Temp.	V_{max}	n
8 ± 1°C	$33.3 \pm 1.5mV$	8
16 ± 1.5°C	$41.4 \pm 2.5mV$	9
26 ± 1°C	$38.4 \pm 3.1mV$	7

It is not possible to directly compare the sensitivity of the horizontal cell responses to light stimuli from fish acclimated to different temperatures because the main factor influencing the sensitivity was the degree of light adaptation of the retina. Although the retinas were dissected free in the same low light level and as far as possible treated the same before recordings were taken there were differences in the degree of light adaptation, probably due to differences in the length of time taken in the dissection and locating suitable cells (see Fig. 2.8 which demonstrates the extremes of light and dark adaptation observed). Consequently it was not possible to make a comparison of effects of temperature on sensitivity between cells from different fish.

The effects of acclimation on the rate of change of the membrane potential during the rise and fall phase of the horizontal cell response are shown in Figs. 2.12

and 2.13 respectively. For both the rise and fall phases of the response the rates of change of the membrane potential increase with increased temperature for all three acclimation temperatures. As for V_{max} the effect of temperature acclimation is a shift in the rate–temperature relationship along the temperarture axis, in such a way as to reduce the effect of the long term temperature change on the speed of the response. As was the case for V_{max} the adaptive change shown here is not complete. The response latency, however, decreases with experimental temperature for all three acclimation groups, but as for the previous variables the effect of acclimation is to displace the latency–temperature relationship along the temperature axis towards the acclimation temperaure (Fig 2.14).

2.3.4 The Length Constant

The retina was exposed to a slit of light of width $135\mu m$ and length $\sim 1.5cm$. By moving the position of the slit of light between stimuli across the retina the amplitude of the horizontal cell response rose to a peak and then decreased again as the stimulus position was moved over the recording electrode (Fig. 2.15). When these results were plotted on a log–linear plot they could be fitted with two straight lines (Fig. 2.16). The length constant λ which quantifies the degree of lateral spread of the signal in the horizontal cell syncitium is defined as

$$\lambda^2 = \frac{R_{\mathrm{m}}}{R_{\mathrm{s}}}$$

where R_{m} is the resistance of the horizontal cell membrane and R_{s} is the resistance of the horizontal cell syncitium. The length constant could be calculated from the gradient of these two lines using the equation

$$\ln V(x) = \frac{1}{\lambda}|x| + c$$

where $V(x)$ is the response amplitude a distance of x from the centre of the illumination slit and c is a constant. See Naka and Rushton (1967), Lamb (1976) and Fig. 2.16 for details.

The length constants of cells from fish acclimated to 8°C, 16°C and 26°C were measured at various temperatures. The results varied from $250\mu m$ to $1100\mu m$, with

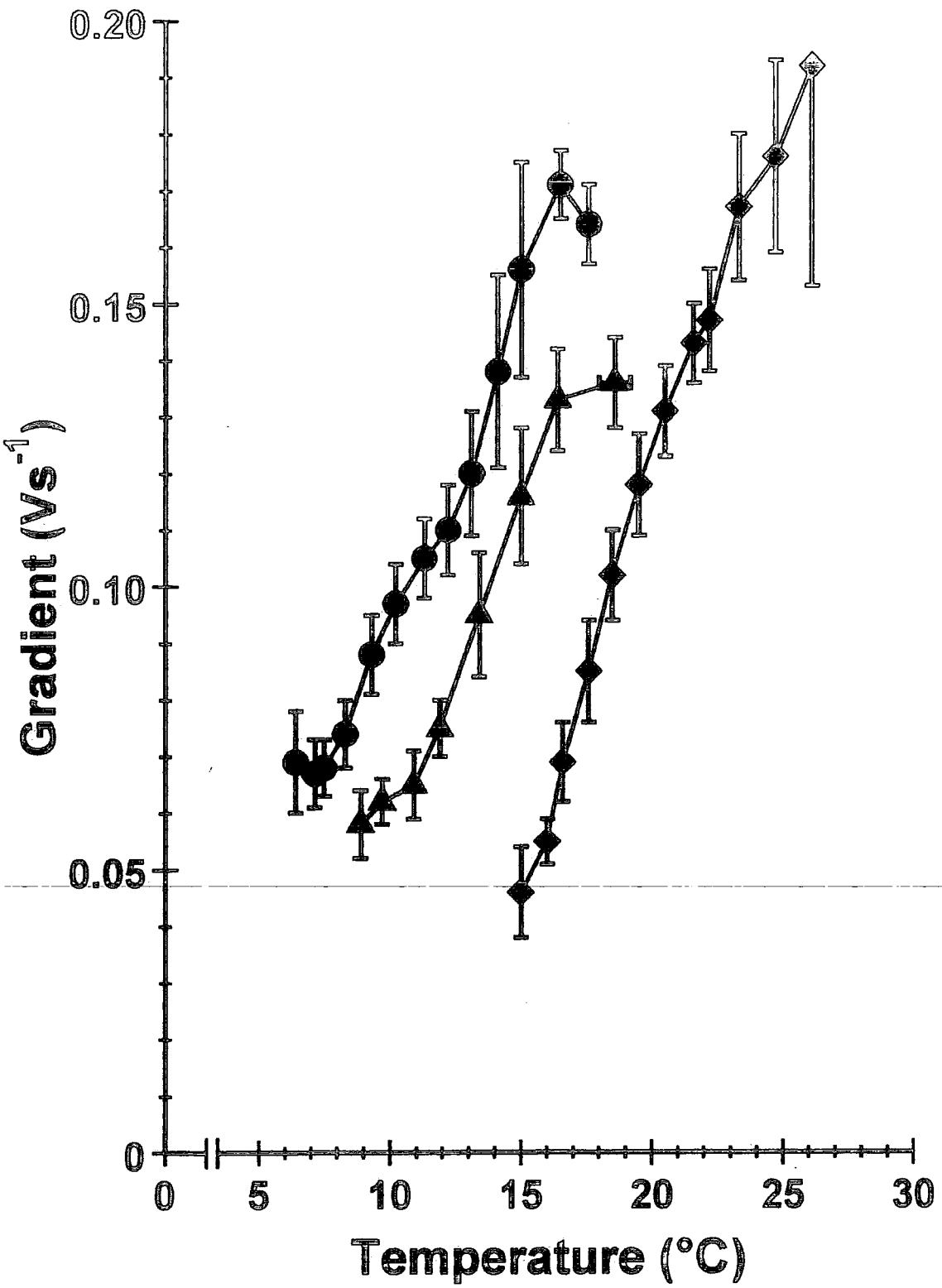
0.20
0.15
0.10
0.05
0
Gradient (Vs-1)
0
5
10
15
20
25
30
Temperature (°C)

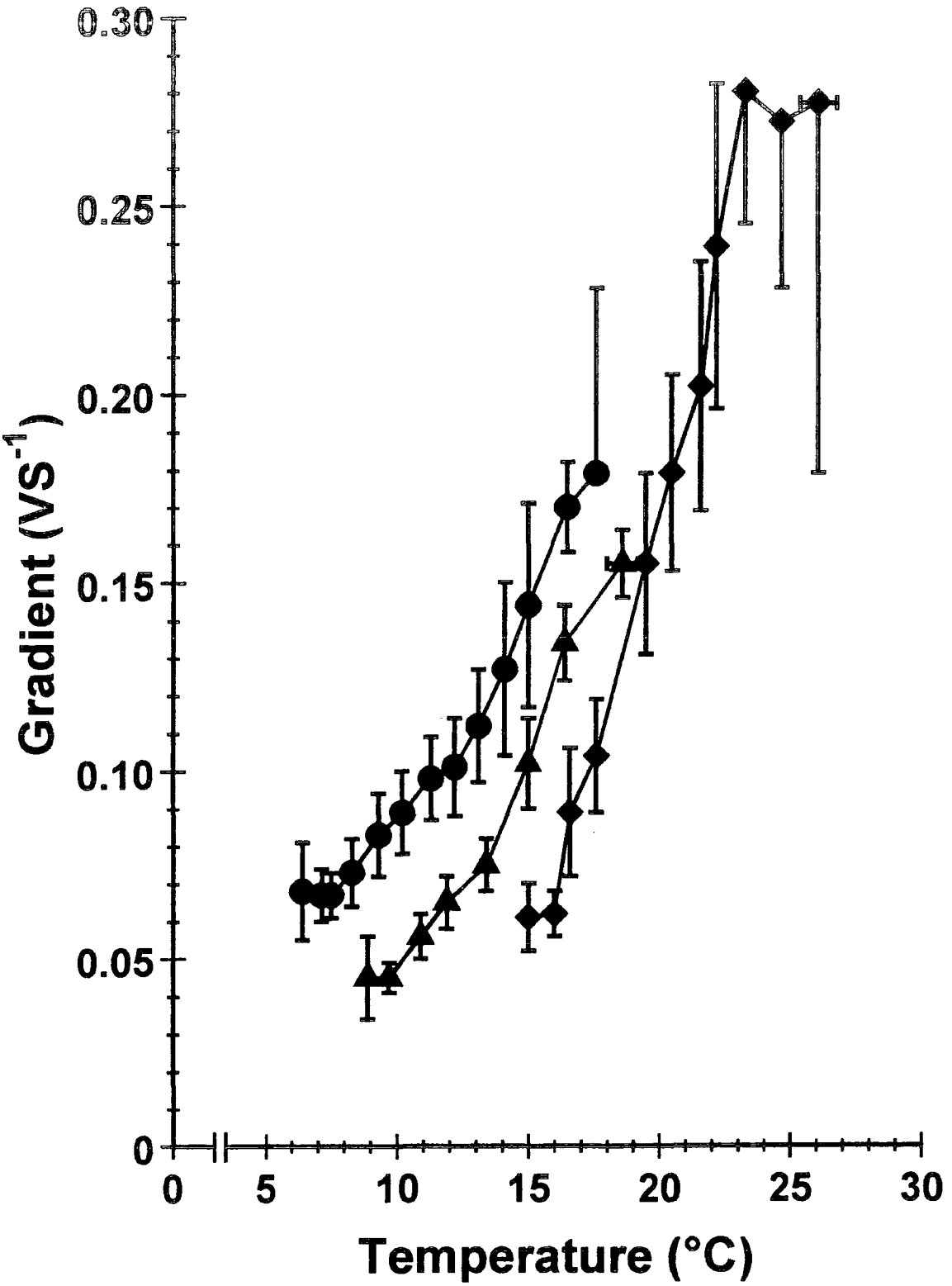
0.30
0.25
0.20
0.15
0.10
0.05
0
Gradient (VS-1)
0
5
10
15
20
25
30
Temperature (°C)

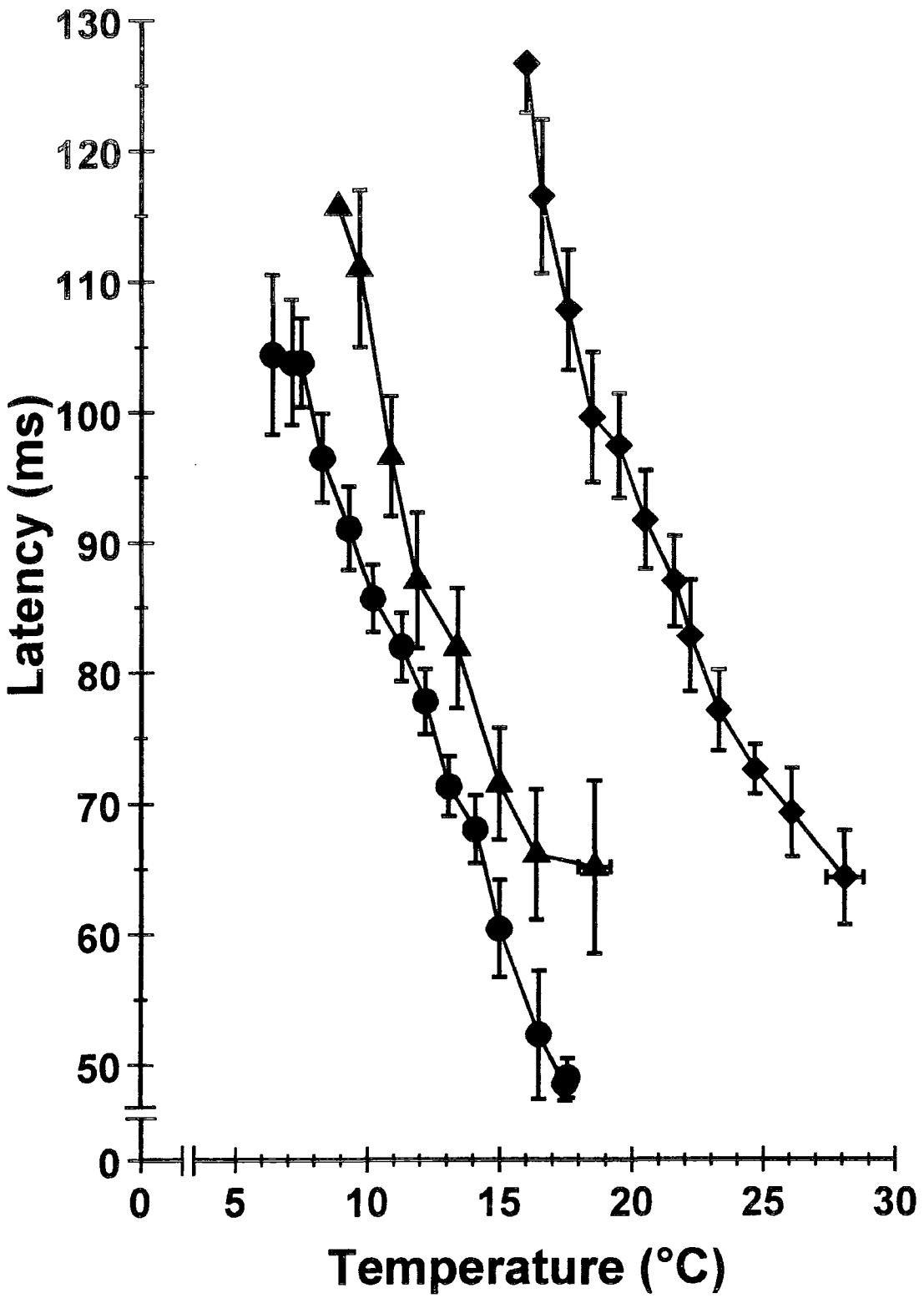
130
120
110
100
90
80
70
60
50
0
Latency (ms)
0
5
10
15
20
25
30
Temperature (°C)

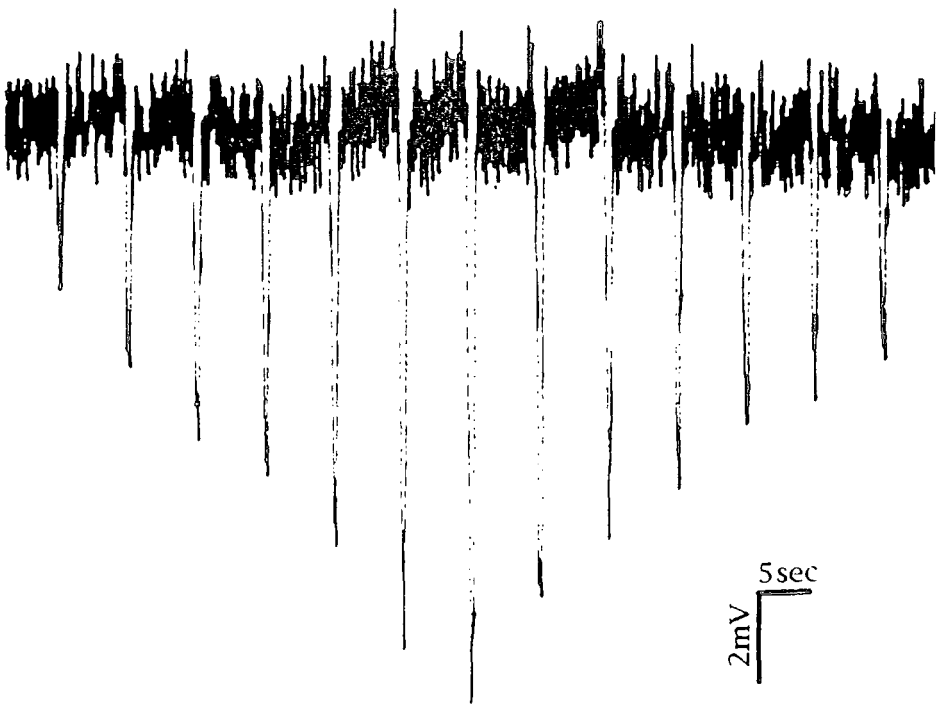

Figure 2.15. The retina was repeatedly illuminated with a slit of light ($135\mu m$ wide, $410\mu W cm^{-2}$) with a stimulus duration of $500ms$ interspersed by ~6 seconds darkness. Between each stimulus the slit of light was moved $225\mu m$ resulting in a progressive increase in response amplitude until the slit of light was above the microelectrode after which the response amplitude decreased again.

a reduction in length constant with temperature when the results from all three acclimation groups are included (Fig. 2.17). The mean length constant of cells from fish acclimated to 8°C was $806\pm181\mu m$ (n=26) while from fish acclimated to 16°C and 26°C it was $470\pm67\mu m$ (n=14) and $374\pm92\mu m$ (n=9) respectively. The results at 8°C are significantly different from those at 16°C ($p < 0.05$ Students t–Test) while there is no significant difference between those from 16°C and 26°C ($p > 0.05$ Students t–Test). The data from 8°C acclimated fish show a strong temperature dependence (correlation coefficient of 0.449; $p < 0.02$ Students t–Test) while those from fish acclimated to the higher temperatures do not (correlation coefficients of .006 and .177 for the data from fish acclimated to 16°C and 26°C respectively).

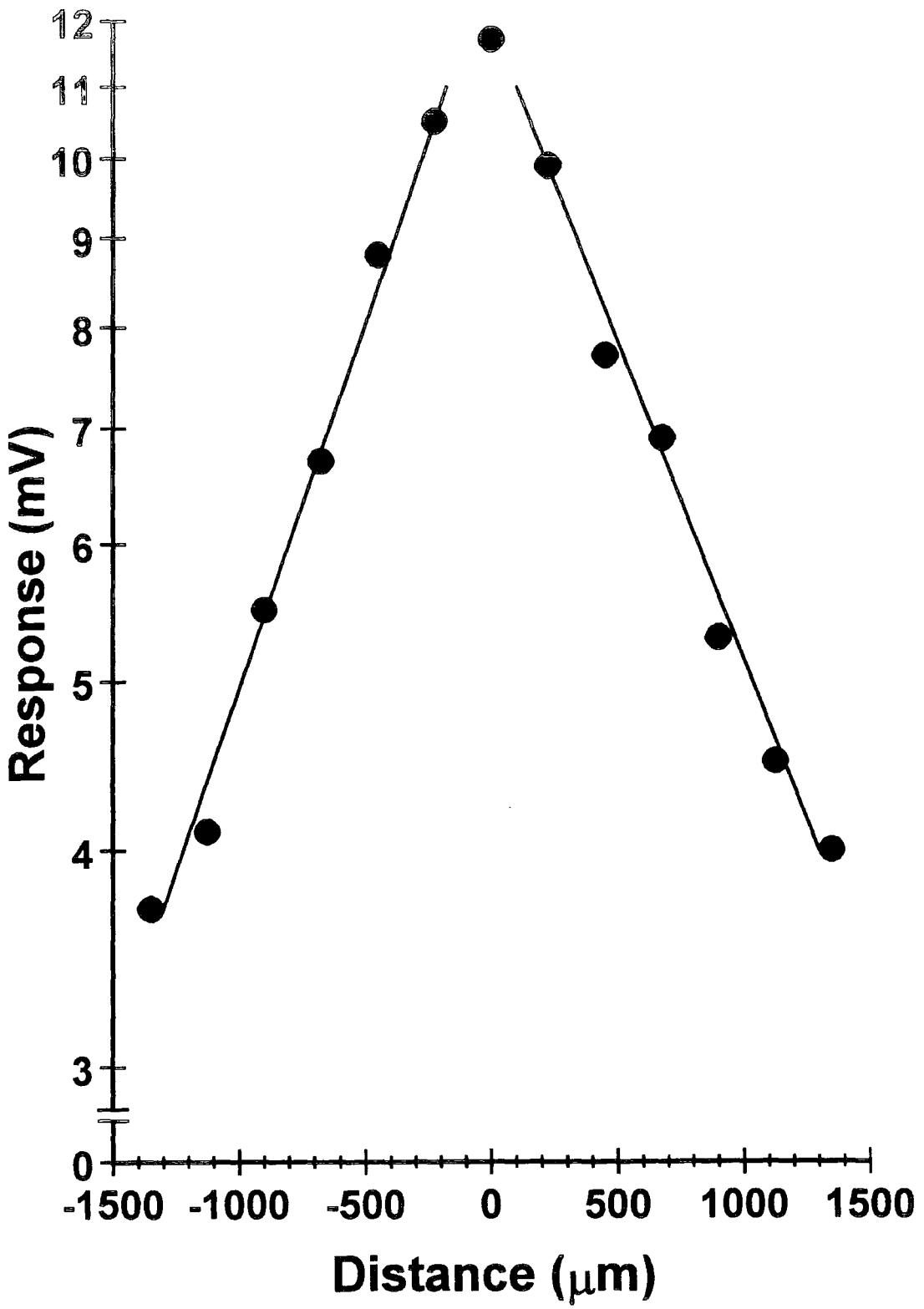
12
11
10
9
8
7
6
5
4
3
0
Response (mV)
-1500
-1000
-500
0
500
1000
1500
Distance (μm)

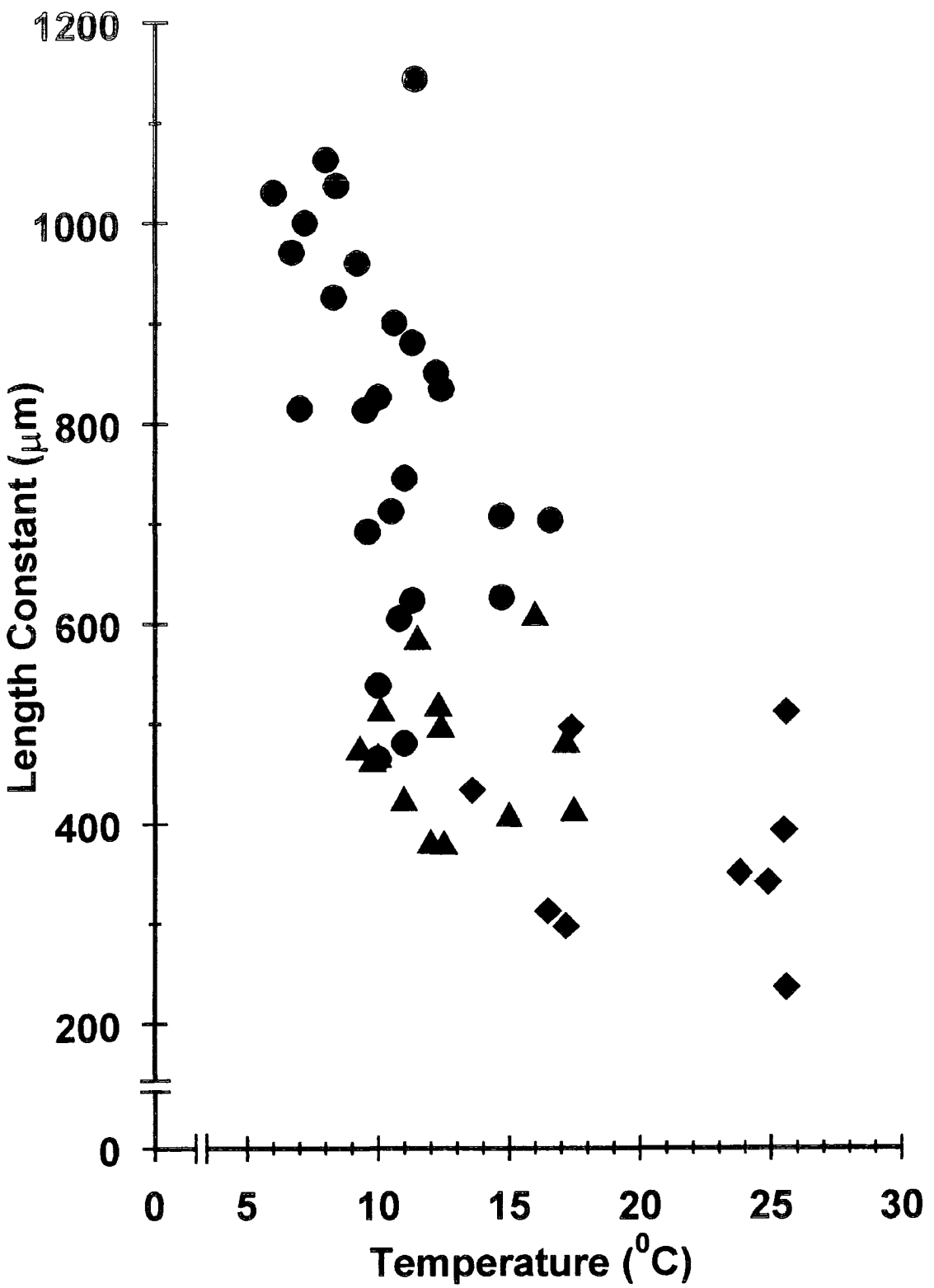
1200
1000
800
600
400
200
0
Length Constant (μm)
0
5
10
15
20
25
30
Temperature (0C)

2.4 DISCUSSION

2.4.1 General Effects of Temperature on the Retina

The effects of temperature on visual processes of various ectotherms have been studied at different levels of the visual pathway including photoreceptors (Baylor *et al.*, 1983; Lamb, 1984) second order neurones (Svaetichin *et al.*, 1965; Negishi and Svaetichin, 1966; Charlton and Naka, 1970) and ganglion cells (Schellart *et al.*, 1974; Aho *et al.*, 1993b) as well as the electroretinogram (Thorpe, 1973; Hanyu and Ali, 1963, 1964; Schellart *et al.*, 1974) and behavioural studies (Yager *et al.*, 1971; Thorpe, 1971, 1973; Aho *et al.*, 1988, 1993b).

The effects of temperature, as elucidated from the latter three experimental approaches, were on the sensitivity and the dynamic characteristics of the retina. The experiments of Aho and her collegues (Aho *et al.*, 1988, 1993b) demonstrate that the absolute sensitivity of amphibians, measured by behavioural experiments and from ganglion cell recordings, increases with decreasing temperature. This, it is suggested, is as a result of a reduction in spontaneous isomerizations of the chromophore at the lower temperatures. A low intensity background illumination largely abolished this temperature relationship (Aho *et al.*, 1993b), although Thorpe (1973) found that goldfish at 15°C demonstrated an overall increase in sensitivity across the visual spectrum compared to fish at 25°C using psychophysical studies. However these fish were acclimated to these experimental temperatures so the increased sensitivity may have been an adaptive mechanism to the reduced temperature (but see below). However Thorpe (1971) also found that the spectral sensitivity of goldfish, in psychophysical experiments, appeared to be affected by temperature with a relative reduction of sensitivity for wavelengths in the green region of the spectrum with lower temperatures, although ERG recordings (Thorpe, 1973; Schellart *et al.*, 1974) and ganglion cell responses (Schellart *et al.*, 1974) did not corroborate this.

The increase in maximum flicker fusion frequency on both increasing stimulus intensity and temperature in goldfish and salmon ERG (Hanyu and Ali, 1963 and 1964 respectively) and the decrease in latency of goldfish ganglion cell responses with increasing temperature (Schellart *et al.*, 1974) are less variable. Moreover they are reinforced by the reports on the effects of temperature on single units in the

retina, including the results of this study on the kinetics of horizontal cell responses. A further finding of Schellart *et al.* (1974) was that the maximum amplitude of the ERG occured at higher frequencies on increasing temperature, although the absolute amplitude was not affected. Shifting the amplitude–frequency relationships from different experimental temperatures on the frequncy axis demonstrated that the effects of temperature on high and low stimulus frequencies appeared to be the same (Schellart *et al.*, 1974; Fig. 3). This was cited as suggesting that either the dynamics of the individual steps of retinal integration were dependent on temperature in a similar way, or that a single temperature–dependent stage dominates, but these interesting alternatives were not explored further.

The effects of temperature on isolated photoreceptor responses were investigated by Baylor *et al.* (1983) and Lamb (1984) on rods from toads (*Bufo marinus*). Increasing temperature to 25°C and 30°C by these experimenters respectively resulted in increased maximum current changes on saturating stimuli due to increased dark current amplitudes. This increasing temperature–amplitude relationship did not appear to reach an upper limit over these temperature ranges. The kinetics of the responses also showed reasonably consistent changes over these temperature ranges with the time to peak decreasing with increasing temperature, with Q_{10} values of 2.7 and 2.2 respectively. The effects of temperature on the sensitivity of the rod responses to illumination presented in these two papers were contradictory, but see below. Robinson *et al.* (1993) showed a similar increase in dark current with temperature in isolated rat rods which showed no sign of reaching a maximum at temperatures of up to 40°C.

The effects of temperature on luminosity horizontal cells were investigated by Svaetichin *et al.* (1965), Negishi and Svaetichin (1966) and Charlton and Naka (1970). There are several distinct contrasts in the results presented by these different groups. One of the most extreme is the differing effects of temperature changes on the membrane potential of the horizontal cells in the unilluminated retina. In the studies of Svaetichin and his co–workers on fish from the families *Centropomidae* and *Gerridae* (Svaetichin *et al.*, 1965 and Negishi and Svaetichin, 1966 respectively) they found that the membrane potential hyperpolarized with increasing temperature where as Charlton and Naka (1970), working on the catfish *Ictarus punctatus*, found that temperature had no effect on the membrane

potential in the unilluminated state. The rates of temperature change used in these different experiments (e.g. $>1°Cs^{-1}$ in Svaetichin *et al.*, 1965 as opposed to changes over periods of minutes in Charlton and Naka, 1970) and the degree of light adaption (strongly light adapted in the Svaetichin experiments as opposed to reasonably dark adapted in the Charlton/Naka experiments) may have influenced the temperature responses.

Variations between these reports on the effects temperature on the illumination induced responses are also obvious. Svaetichin *et al.* (1965) found that the increase in temperature decreased the size of the responses over the temperature range examined whereas Charlton and Naka (1970) found the opposite — an increase in temperature resulted in an increase in maximum response amplitude up to a maximum, which then remained stable for further increases in temperature of over 10°C. The response amplitudes recorded by Negishi and Svaetichin (1966) showed a maximum, decreasing on either increasing or decreasing the temperature away from this optimal value which contradicts the results of Svaetichin *et al.* (1965), although this was attributed to species differences.

2.4.2 Temperature and Carp Horizontal Cell Responses

The dynamic range of horizontal cells (i.e. the range of membrane potentials from the resting potential in the dark to the saturated response) from fish acclimated to 16°C shown in Fig. 2.11 responds to increasing temperature by increasing to a maximum which is reasonably constant for a range of temperatures before falling rapidly on further increases (which is a typical pattern of thermal sensitivity, see Section 1.4.2). This is similar to the results of Negishi and Svaetichin (1966), which showed a reduction on response amplitude on increasing or decreasing temperature from an 'optimal' value. The lack of a reduction in response amplitude reported by Charlton and Naka (1970) in catfish may demonstrate a greater tolerance for high temperatures in this species, although the results in their Figure 3 appear to show some reduction in V_{max} at temperatures above ~26°C. The reduction in response amplitude reported by Svaetichin *et al.* (1965) was for temperatures increased above ~23°C. As no information on the thermal history of the animal was given this might represent the effects of temperature above the 'optimal', below which the response amplitude could also fall.

The temperature relationship of V_{max} shown for carp horizontal cells (Fig. 2.11) could be due to changes in the dynamic range of the photoreceptors or an effect on photoreceptor–horizontal cell synaptic transmission. The dynamic range of the toad rods recorded by Baylor *et al.* (1983) and Lamb (1984) increased over a wide range of tempertures (from 5°C to 30°C for animals maintained at 22–25°C) and of rods from rats over the temperature range of 17°C to 40°C (Robinson *et al.*, 1993). However it is possible that cones are more sensitive to high temperature. Alternatively the photoreceptor–horizontal synapse could be adversely affected by the elevated temperature and the illumination induced hyperpolarization of the photoreceptor transmitted with progressively reduced amplitude. This is in agreement with the suggestion that the breakdown in neural function on elevated temperature is due to the detrimental effects on synaptic transmission (Friedlander *et al.*, 1976; Prosser and Nelson, 1981; Cossins and Bowler, 1987). If this is the case then the thermal environment might be expected to have an influence on the dark resting potential. However the lack of data on the effect of temperature on the dark resting potential, primarily due to the slow electrode drift during experiments and consequently during temperature changes, means that no information on the tonic synaptic transmission in the dark is availiable.

The effects of temperature on the kinetics of carp horizontal cell responses (Fig. 2.10), as measured by the latency and the maximum rates of change of the rise and fall phase of the response at $\frac{1}{2}V_{max}$, show a reasonable degree of agreement with the results from catfish luminosity horizontal cells (Charlton and Naka 1970). Although the Q_{10} values for these variables are not constant over the temperature ranges used the rates of change of the membrane potential from cells from fish acclimated to 16°C have Q_{10} values of around 4–4.4 and the latency of $\sim$2.1. Charlton and Naka (1970) reported that the Q_{10} of the latency of catfish horizontal cells, over a similar temperature range, was 2.5 and of the rise phase of the response was as high as 5.3, although this was reduced at higher temperatures. The Q_{10} values reported by Baylor *et al.* (1983) and Lamb (1984) for the rise phase of the rod response (2.7 and 2.2 respectively) are considerably lower. If cones show similar temperature sensitivities to rods then the greater sensitivity of the horizontal cell responses may be due to additional effects at the photoreceptor–horizontal cell synaptic level.

The results in Fig. 2.6 show that the responses to the same low stimulus intensities (i.e. at the lowest four intensities shown) at 7.9°C and 9.5°C are clearly larger than those at 12.2°C and 14.2°C. The results of Charlton and Naka (1970) showed no systematic change in the stimulus intensity required for a response of $\frac{1}{2}V_{max}$ (i.e. σ) in response to temperature. The results presented in Fig. 2.8 are clearly contrary to this where the Q_{10} values for the light and dark adapted retinas respectively are 2.7 and 2.4. While the results of Robinson *et al.* (1993) on rat rods and of Baylor *et al.* (1983) on toad rods showed a similar temperature sensitivity of the half saturating response amplitude (Q_{10} values of 1.9 and 2.3 respectively), Lamb (1984), also working on toad rods, reported a maximum sensitivity at ~22°C. However this was based on the absolute response size on stimulation with 'dim' light as opposed to the stimulus required for a half maximum response, which was used in this work and that of Baylor *et al.* (1983) and Robinson *et al.* (1993). In fact the normalised stimulus intensity–response curves in Figure 2 of Lamb (1984) show the results at 6.7°C displaced significantly to the left compared to the those at 30.5°C demonstrating that if the same criteria had been used (i.e. temperature dependence of σ) then these results could have aggreed with those of this study too.

The improvements in abolute visual sensitivity with decreasing temperature observed in behavioural studies (Aho *et al.*, 1988; 1993b) are attributed to reduced rate of thermal isomerizations of the chromophore as opposed to increases in the actual individual photon induced signals at these low light levels. While such improved signal–to–noise characteristics could improve the visual threshold of an animal they would not generate the larger response amplitudes observed at low light intensities on reduced temperature. While changes in the amplification of the signal at the photoreceptor–horizontal cell synapse could be responsible, Robinson *et al.* (1993) suggest two mechanisms whereby the photoreceptor response could increase in amplitude on illumination at low temperatures, both of which, they suggested, contributed to the increased sensitivity of the rat rods. The efficiency with which photons were captured and converted into a signal by the chromophore increased with decreasing temperature. Also the amplitude of the membrane potential change on isomerization of a single chromophore molecule increased, possibly due to differential changes in the effect of temperature on the 'on' cascade of reactions as opposed to the 'off' reactions. A further potential

mechanism is that reductions in temperature reduce the rates of change of the membrane potential response. Consequently longer duration membrane potential changes are induced in response to single photons. These could therefore summate to a greater degree to produce a larger response on a supra–threshold stumulus.

The increased sensitivity in psychophysical studies at lower temperatures reported by Thorpe (1973) may therefore be an effect of temperature on the response amplitude, as well as an improved signal–to–noise ratio, since these animals were not fully dark adapted. The differences in sensitivity of cells from different retinas, because of the variations in the degree of light adaptation, meant that no direct comparison between retinas from fish acclimated to different temperatures could be made.

The effect of temperature on the length constant (Fig. 2.17) was to decrease the spread of the signal with increasing temperature when the data from all three acclimation groups is considered. However the different acclimation groups show different temperature sensitivities, with the 8°C acclimation group showing significant temperature dependance (the results have a correlation coefficient of 0.449, $p < 0.02$ Students t–Test), while the two higher acclimation temperature groups, albeit with fewer data points, do not (correlation coefficients of 0.006 and 0.117 respectively; $p > 0.05$ Students t–Test). These results suggest that the effect of temperature on the gap junctions, which dictate the length constant, is different between the low and higher two acclimation groups. The incease in conductivity between the cells at lower temperatures which results in the increased length constants is likely to be due to increased numbers of gap junctions or increased conductivity through the gap junctions. This is discussed further in Chapter 5.

2.4.3 The Effect of Acclimation Temperature

The effect of acclimation on the maximum response amplitude and the kinetics of the response are shown in Figs. 2.11 to 2.14. In each case there is a shift in the temperature sensitivity on acclimation, in the such a way as to compensate for the temperature change. The changes are almost always a simple translation of the temperature–response curve (Type II after Precht, 1958) and partial in that the displacement of the curve is not great enough to completely offset the long term temperature change (Type 3 after Prosser, 1976). An exception is the

gradient of the fall phase from cells from fish acclimated to 26°C which appears to show both displacement and rotation compared to the results from the acclimation temperature of 16°C (Type IV after Precht, 1958). Estimates of the completeness of the acclimation of these different characteristics of the response are given in Table 2.2.

Table 2.2. The completeness of the acclimation process estimated by various criteria. The displacement on the temperature axis of the curves was estimated, and the completeness of the acclimation calculated as a percentage.

	Acclimation Temperatures 16°C⇒8°C 8°C Acclimation Shift	Acclimation Temperatures 16°C⇒26°C 10°C Acclimation Shift
V_{max}	3.5°C — 44%	6.7°C — 67%
Latency	2.3°C — 29%	9.1°C — 91%
Gradient of Rise Phase	3.3°C — 41%	5.1°C — 51%
Gradient of Fall Phase	3.1°C — 39%	2.7°C* — 27%

* There appeared to be rotation as well as displacement of the Gradient–Temperature relationship when acclimated to 26°C compared to 16°C, so the value given is an estimate of the mean displacement from the 16°C curve.

They show that the acclimation to 26°C and 8°C from 16°C affects these different aspects of the horizotal cell response differently. The degree of acclimation is generally more complete for a change of temperature from 16°C to 26°C than it is on acclimation to the lower temperature. This is not surprising as the final thermal preference of carp is about 32°C (Fry, 1964; Neill *et al.*, 1972), although this is at the upper limit of their normal thermal range. Temperatures of 8–10°C are approaching the lower limits at which carp can maintain sustained activity and feeding. It is common to observe complete or almost complete acclimation occuring over a range of temperatures at the centre of the thermal range tolerated by an animal, and progressively less complete acclimation as the temperature approaches the thermal limits of the animal (Cossins and Bowler, 1987).

The mechanisms by which the various components of the horizontal cell responses may acclimate are numerous. The voltage dependent conductances of both the photoreceptors and the horizontal cells may contribute, but the most likely sites of acclimation would be the rate limiting steps in the phototransduction processes and the photoreceptor–horizontal cell synapse which might be expected to be thermally sensitive.

The sensitivity of the kinetics of the toad rod responses described by Baylor *et al.* (1983) and Lamb (1984) to temperature show that in these cells the phototransduction process is temperature sensitive. If cone phototransduction, which appears to proceed along very similar lines to rod phototransduction (Watanabe and Murakami, 1992; Yau, 1994), shows qualitatively similar temperature sensitivity then it might be expected that the kinetics of the horizontal cell responses and their ability to acclimate may stem, at least in part, from the phototransduction process.

One important aspect of the phototransduction mechanism is the properties of the disk membranes associated with the photopigment, G–protein Transducin and the phosphodiesterase (PDE). These membranes are known to have a very high 'fluidity' which allows the rapid diffusion of the membrane bound protein molecules, possibly as a mechanism to maintain rapid phototransduction kinetics (Liebman *et al.*, 1982; Pugh and Lamb, 1993). Nevertheless the rate of lateral diffusion of the activated rhodopsin and transducin molecules is probably one of the rate limiting steps of the activation cascade and as such will affect both the kinetics and amplitude of the photoresponse. Morover the speed of the recombination of the PDE_{γ} subunits with the $PDE_{\alpha\beta}$ subunit may affect the rate of the termination of the photoresponse. The lateral diffusion of photopigment in photoreceptor membranes shows a Q_{10} of $\sim$2.5 (Liebman *et al.*, 1982). Baylor *et al.* (1983) and Lamb (1984) suggest that the changes in kinetics seen in the photoreceptors may be mediated by this reduction in diffusion rate. Consequently this membrane may be expected to show some degree of homeoviscous adaptation (Sinensky, 1974; Section 1.4.3.1) to offset the effects of the change in temperature. However to date no work on homeoviscous adaptation in photoreceptor outer segments has been carried out, so it is not known to what degree it may occur, if at all.

The potential for adaptive changes in the phototransduction mechanism by changes in the relative and absolute densities of different protein components, modulation of their activities (for example by phosphorylation) and changes in the isoforms of these proteins is also a possibility (see Section 1.4.3.1). Different steps in the phototransduction cascade might be expected to be differently affected by short term thermal changes and, as described by Hochachka (1988), the adaptive mechanisms used will have to accomodate these changes so that the complex interactions of these different amplification steps and their control can be, as far as possible, optimised for the longer term conditions.

The sensitivity of CNS synapses to thermal extremes and the consequent assumption that they are able to show some ability to acclimate (Section 1.4.3.3) would lead to the supposition that a component of the temperature sensitivity of the horizontal cell responses and the ability to acclimate may stem from the photoreceptor–horizontal cell synapse. If the cone responses increase with temperature with no maximum over the temperatures investigated, as the rod responses in toad (Baylor *et al.*, 1983; Lamb, 1984) and rat (Robinson *et al.*, 1993) appear to, then the decrease in horizontal cell V_{max} at high temperatures may be due to changes in the synaptic transmission. Although, as discussed in Section 1.4.3.3, direct evidence of CNS synaptic acclimation is not easy to demonstrate directly it is thought to occur (Roots and Prosser, 1962; Largerspetz, 1974; Prosser and Nelson, 1981) and could explain the change in sensitivity to higher temperatures. However, to establish which mechanisms are responsible for the changes seen in the horizontal cells, for both short and long term changes in temperature, the phototransduction and synaptic components would need to be investigated separately.

At any one acclimation temperature the temperatures over which the dynamic range of the horizontal cells in the isolated retinal preparation is maximum is relatively small ($\sim$5°C) and in the cases of the fish acclimated to the upper and lower limits does not exactly coincide with the acclimation temperature. However accross the normal active range of the fish ($\approx$10°C–28°C) the dynamic range is maintained remarkably wall, as long as the temperature changes are slow enough for the fish to acclimate to the new temperatures, as shown by the ability to maintain V_{max} at over $40mV$ accross this temperature range (Fig. 2.11). Moreover Schellart *et al.* (1974) found that the thermal sensitivity of ERGs recorded from the isolated retina

was greater than when recorded from the retina in intact animals. Consequently while these results demonstrate the temperature sensitivity of the horizontal cell response to temperature and the ability of the responses to acclimate to long term temperature changes, it cannot be assumed that the thermal sensitivity in the *in vivo* responses is as acute as those presented here.

Chapter III

Voltage Clamp of Isolated Horizontal Cells Using the Whole Cell Patch Clamp Technique.

3.1 INTRODUCTION

3.1.1 The Patch Clamp Technique

One of the most important recent developments in electrophysiology was the introduction of the patch clamp technique. By placing a glass micropipette against denervated frog muscle fibres Neher and Sakmann (1976) were for the first time able to record individual channel currents. The electrical resistance of the gap between the glass and the membrane (seal resistance) was considerably higher than that of the pipette (about $50M\Omega$ and $2M\Omega$ respectively) so the current passing through a membrane channel enclosed by the tip of the pipette would predominately pass through the pipette and could therefore be recorded.

The greater the seal resistance, compared to the pipette resistance, the better the signal–to–noise ratio becomes and the greater the control over the potential across the membrane patch enclosed by the pipette. In 1981 Hamill *et al.* presented an improved patch clamp technique in which the seal resistance was measured in gigaohms. These 'giga–seals', as they are conventionally referred to, not only greatly improved the signal–to–noise ratio of single channel recording but also, because of their mechanical stability, allowed new techniques to be developed, see Fig. 3.1. It was for the development of these techniques that Neher and Sakmann won the Nobel Prize for Physiology or Medicine in 1991 (see Neher and Sakmann, 1992). The technique used to voltage clamp isolated horizontal cells was one of these — 'whole-cell recording'.

Briefly a glass pipette of suitable dimensions (i.e. a tip diameter of $\sim 0.5 - 2\mu m$) filled with a solution simulating the intracellular ionic environment is positioned close to a cell. When the pipette tip makes contact with the cell membrane a

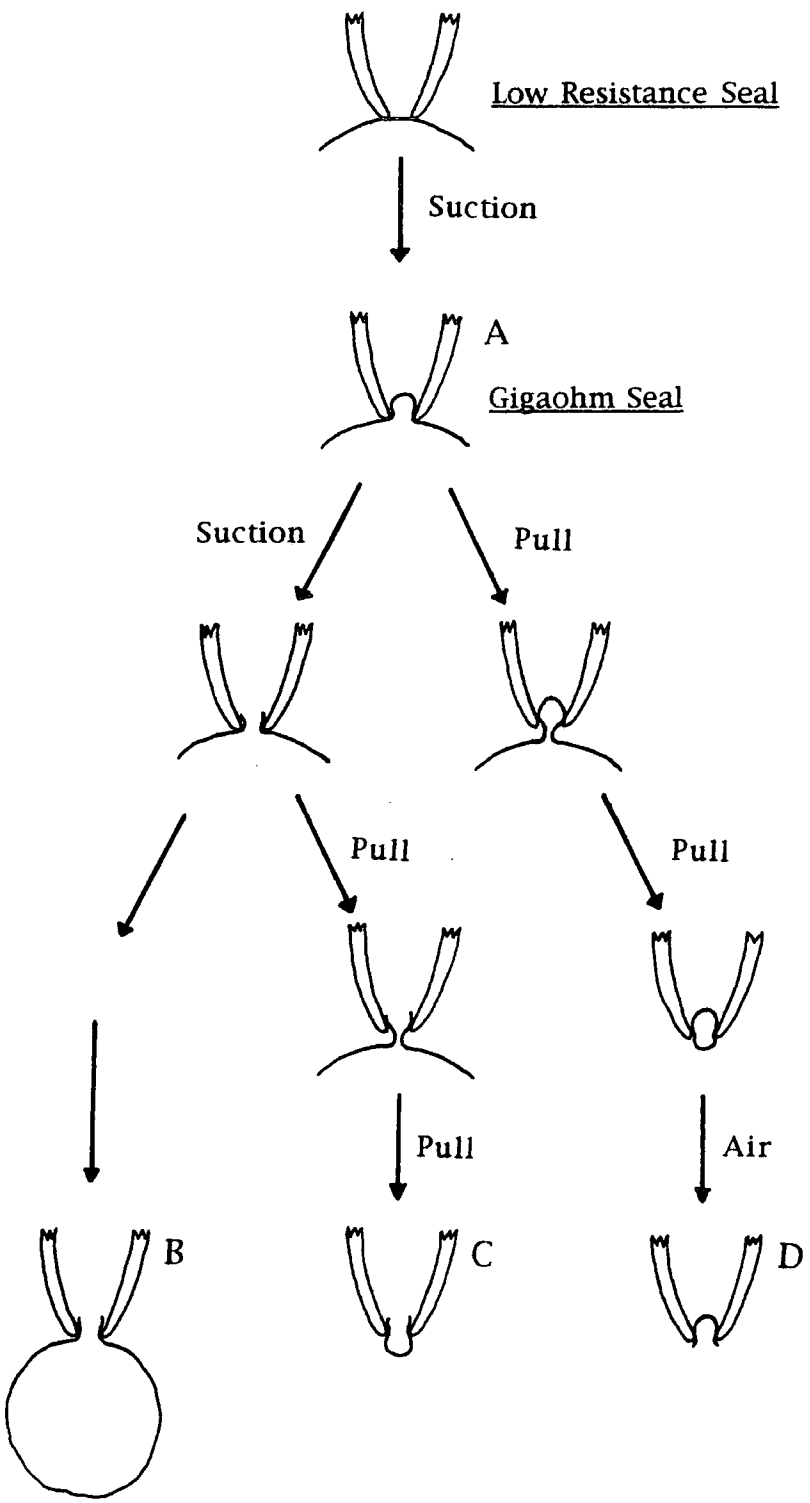
Low Resistance Seal
Suction
A
Gigaohm Seal
Suction
Pull
Pull
Pull
Pull
Air
B
C
D

giga–seal can be formed if the pipette tip and the cell surface are both perfectly clean. A portion of the membrane is drawn into the pipette and it is thought that direct molecular contact is made between the phospholipid head groups of the membrane lipids and the glass of the pipette, because the estimates of the gap between these two are around 1 Angstrom (Hamill *et al.*, 1981; Corey and Stevens, 1983). If a rapid pulse of negative pressure is applied to the pipette then the area of membrane enclosed by the pipette can be ruptured without breaking the giga–seal or damaging the cell. This results in a low electrical resistance access to the cell interior. When used on cells of small dimensions, e.g. $<30\mu m$, the currents generated by voltage clamping the cell are not of a magnitude great enough to cause a potential change of more than a few millivolts across this access resisitance (when up to 90% of the access resistance can be electronically compensated for as described in Section 3.2.4). Consequently the cell can be voltage clamped with this single pipette being used to both pass current and monitor potential.

The obvious advantage of this technique over using microelectrodes is that the access resistance is much lower. It is also clear that small cells are damaged much less by this technique than by conventional microelectrode recording (Fenwick *et al.*, 1982a; Marty and Neher, 1983). The large diameter (relative to a conventional microelectrode) of the pipette tip means that the cell contents and the pipette solution rapidly equilibrate. This washout of the cytoplasm, which is of a much smaller volume than the pipette solution, can be used, for example, to control the intracellular concentrations of various second messengers or to apply blockers of membrane channels intracellularly. However it also can result in the decline of membrane currents which are modulated by intracellular mechanisms such as ATP and free calcium concentrations or by protein phosphorylation as these modulating molecules are washed out of the cell (e.g. Fenwick *et al.*, 1982b; Marty and Neher, 1983; Bean, 1992).

3.1.2 Voltage Clamping Horizontal Cells

The majority of the work done involving voltage clamping horizontal cells has involved using the patch clamp technique on isolated cells (Shingai and Christensen, 1983, 1986; Lasater, 1986; Mallchow *et al.*, 1990; Sullivan and Lasater, 1990, 1992; Gollard *et al.*, 1992; Ueda *et al.*, 1992; Akopain and Witkovsky, 1994).

The syncitial nature of horizontal cells in the intact retina means that it is very difficult to effectively voltage clamp cells in the intact retina because the applied current will dissipate through the low electrical resistance gap junctions between the cells and not polarize the cell membrane as required.

However Werblin (1975) attempted to voltage clamp horizontal cells in the intact retina using a double–barrelled micoelectrode in the mudpuppy retina. Although there were large leakage currents he was able to show some inward rectification (see below). Byzov *et al.* (1977) attempted to overcome the problem by voltage clamping the whole syncitium by uniformly polarizing the horizontal cell layer by passing a current across the retina. As the current passes into the horizontal cell layer it results in a potential change across the horizontal cell membrane. In the illuminated retina (which removes any photoreceptor neurotransmitter mediated effects on the horizontal cells by hyperpolarizing the photoreceptors) a nonlinear current–voltage (I–V) relation was observed with a negative conductance region with some similarities to the results seen in isolated cells. Murakami and Takahashi (1987) also tried to control the membrane potential of the whole horizontal cell syncitium by pharmacologically treating an isolated retina (with elevated extracellular Ca^{2+} and potassium channel blockers) so that a calcium action potential across the whole syncitium could be induced. They were able to measure the reversal potential of the light response, but because they could not clamp the membrane potential to a set level as they were relying on the dynamic action potential, accurate current–voltage relationships were not recorded. Miyachi and Murakami (1989) attempted to prevent the current leak between the horizontal cells in the intact carp and turtle retinas by ionophoretically injecting cyclic AMP into the cells which blocked the gap junctions between the cells and consequently increased the input resistance of the cells, again allowing the measurement of the reversal potential of the light response. The combined techniques of using a double–barrelled microelectrode and increasing the electrical resistance between horizontal cells, in this case using exogenous dopamine, were used by Low *et al.* (1991) to successfully voltage clamp cells in the isolated intact carp retina. Again the reversal potential of light evoked currents was estimated and current–voltage relationships showing a region of negative resistance were recorded.

However the ability to identify individual cell types after enzymatic dissociation of the retina (Drujan and Svaetichin, 1972; Kaneko *et al.*, 1976) means that solitary horizontal cells can be studied free from the problems of synaptic input and electric coupling. These cells, from numerous fish and reptilian species, have been isolated and voltage clamped. The usual method is with the patch clamp electrode using the whole cell technique, although Tachibana (1983a,b), for example, used a single microelectrode switching alternately from current injection to membrane potential sampling at $1KHz$. The results from different classes of horizontal cells (where they could be identified) and from different species show few distinct differences (Kaneko and Tachibana, 1986), although the relative magnitudes of the currents can vary between species and cell types within a species (e.g. Lasater, 1986, and see below).

3.1.3 Isolated Horizontal Cell Currents

Fig. 3.2 shows the current responses of a carp horizontal cell to voltage commands from a hold potential of $-60mV$. The results can be split into two distinct types; transient responses and sustained responses. These are shown in Fig. 3.3 and are typical of isolated horizontal cell total current–voltage relationships (Tachibana, 1983b; Shingai and Christensen, 1986; Lasater, 1986; Golard *et al.*, 1992), although there are qualitative differences between different species and within species between different horizontal cell types.

Different current types carried by different ions contribute to different parts of the I–V relationship. Horizontal cells from different species tend to have the same current types, though their relative magnitudes vary. These currents are the same as or similar to currents observed in other cell types which are summarised below. The two currents investigated in this study (the anomalous/inward potassium rectifier and the sustained inward calcium current) are discussed in considerably more detail than the others.

3.1.4 Transient Outward Potassium Current

This current is similar to the A type current (I_A) distinguished from other potassium currents by Conner and Stevens (1971a,b). The I_A current is normally activated at potentials more positive than about $-60mV$ and increases with further

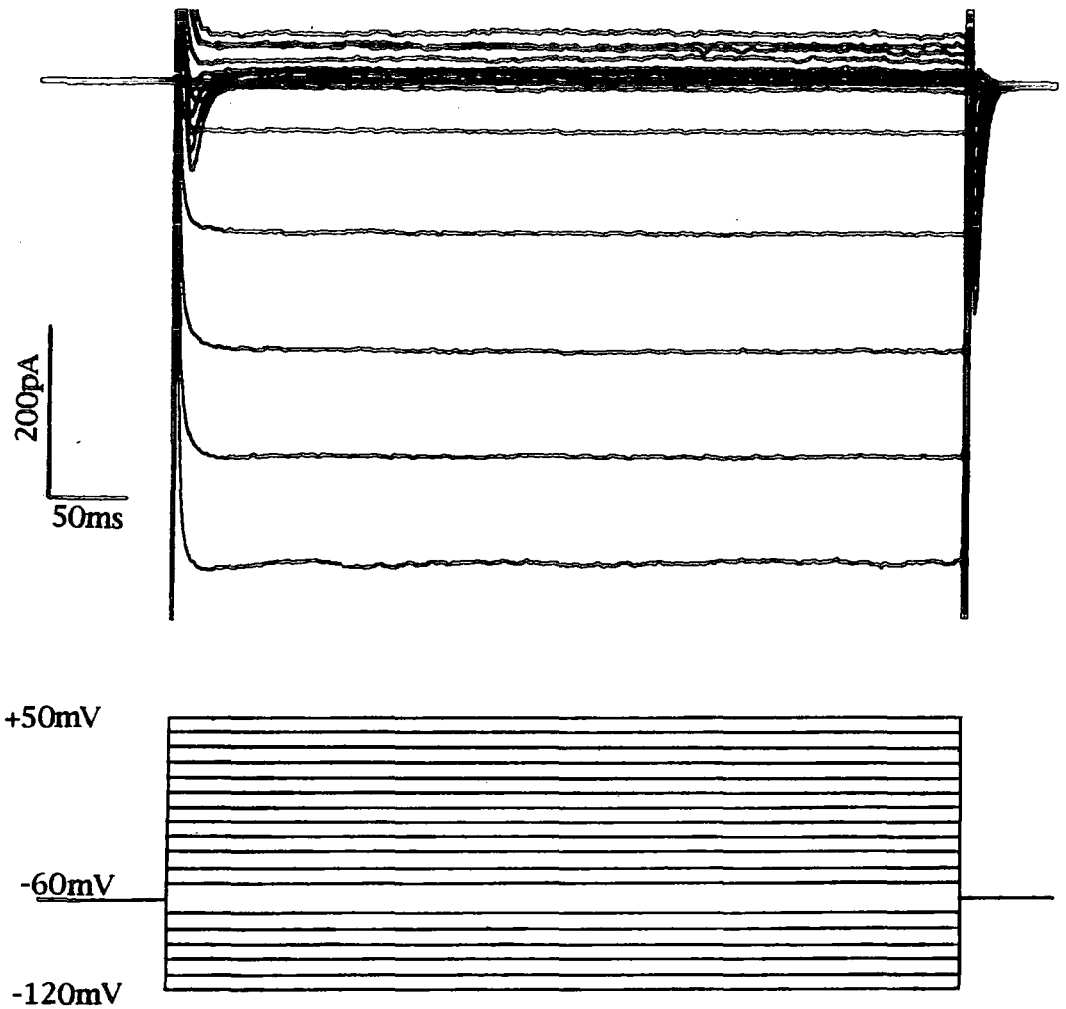
200pA
50ms
+50mV
-60mV
-120mV

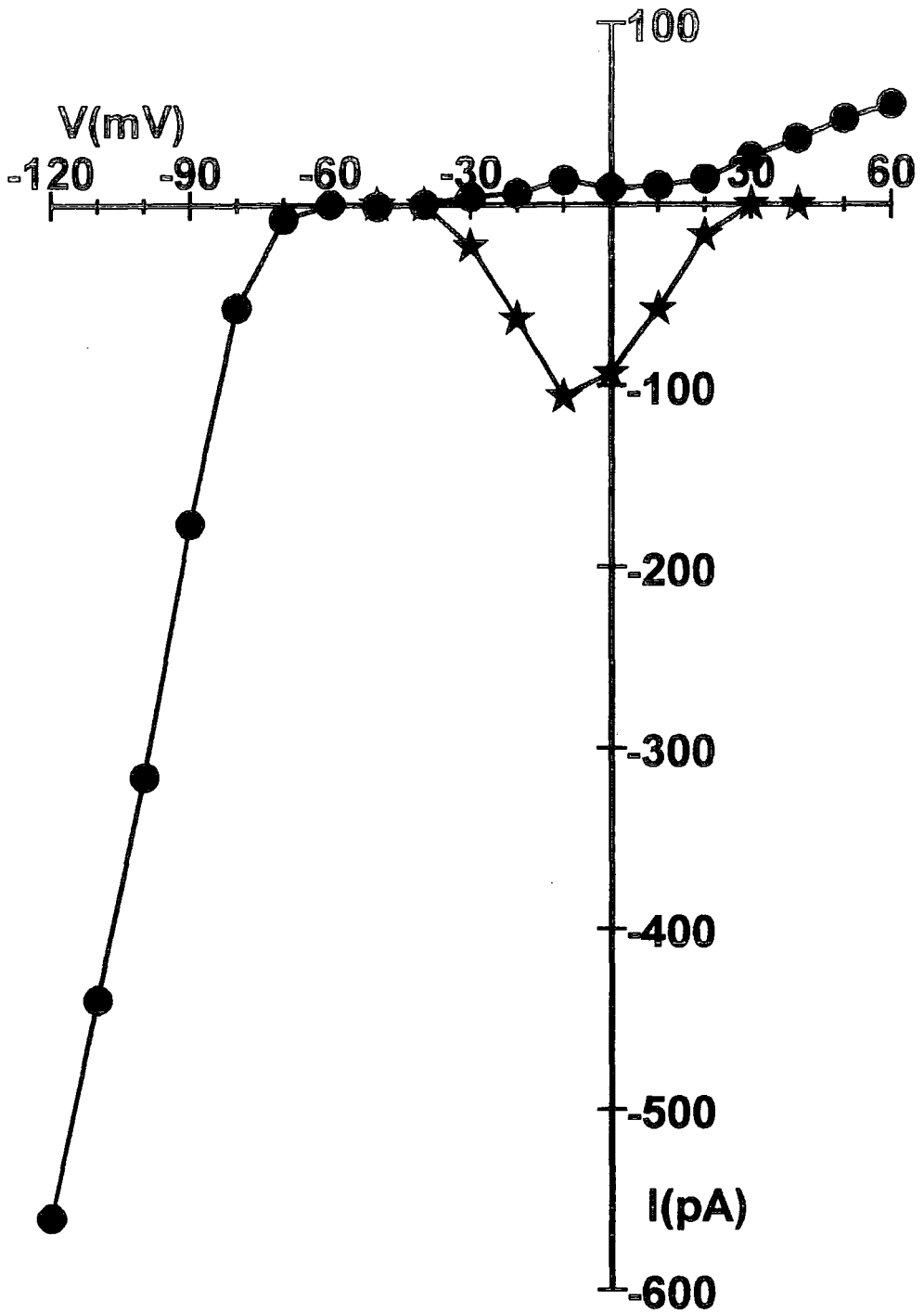
V(mV)
-120
-90
-60
-30
30
60
100
-100
-200
-300
-400
-500
I(pA)
-600

depolarizations. It shows an exponential decrease with time, with a time constant of around $50ms$ in vertebrate neurones, although in molluscan neurones where it was first demonstrated the time constant can be longer ($\sim 150ms$). The current can be inactivated by either a depolarized hold potential (Conner and Stevens, 1971b) or $100\mu M$ concentrations of 4–AP (Gustafsson *et al.*, 1982).

3.1.5 Delayed Potassium Rectifier

All horizontal cells have a sustained outward current which is similar to the delayed rectifier, which is the major potassium current in many neurones (Hodgkin and Huxley, 1952; Rudy, 1988). The delayed rectifier is normally activated by depolarization beyond $-80mV$ to $-40mV$ in vertebrate neurones and unlike the transient outward current does not show inactivation. It can normally be blocked by 10–$20mM$ extracellularly applied TEA (Connor and Stevens, 1971b; Stanfield, 1983).

3.1.6 Transient Sodium Current

This current is a rapidly activating and inactivating inward current similar to sodium currents seen in other neuronal tissue (Hodgkin and Huxley, 1952; Hille, 1992). It is activated by depolarizations beyond about $-40mV$ and reaches a maximum at potentials of about $+10mV$. It is blocked by TTX and inactivated by depolarization of the hold potential (Narahashi *et al.*, 1963).

3.1.7 The Anomalous/Inward Potassium Rectifier

Katz (1946) found that frog skeletal muscle had a higher membrane conductance for inward current injection than for outward current injection. This inward rectification was termed an anomalous rectification to distinguish it from the 'normal' delayed rectification, the anomaly being that the conductance increases with hyperpolarization. Inward rectifying currents carried by potassium have been shown in various cell types, from cardiac muscle (Sakmann and Trube, 1984) to tunicate embryos (Miyazaki *et al.*, 1974) and starfish eggs (Hagiwara *et al.*, 1976). It has also been shown to occur in horizontal cells for example from mudpuppy (Werblin, 1975), goldfish (Tachibana, 1983a,b), white perch (Lasater, 1986), catfish (Shingai and Christensen, 1986) and turtle (Golard *et al.*, 1992).

The inward current is activated by hyperpolarizing the cell to potentials more negative than those near the potassium equilibrium potential. At potentials more positive than this the current is outward but many times smaller. By changing the extracellular potassium concentration the voltage dependence of the current can be altered (Miyazaki *et al.*, 1974; Hagiwara *et al.*, 1976) shifting along the voltage axis by $RT\mathrm{Ln}[K^+]_o$. Rather than the voltage–gating being dependent on the potassium equilibrium potential as is often stated, Hagiwara and Yoshii (1979) and Leech and Stanfield (1981) performed experiments which demonstrate that the voltage–gating is not affected by changes in the intracellular potassium concentration. The channel gating is therefore dependent on the extracellular potassium concentration and the membrane potential. However the intracellular potassium concentrations usually used in patch pipettes mean that the gating of this channel is often close to the potassium equilibrium potential.

The rectification of this current appears to be in the main part due to the block of the channel at potentials more positive than the potassium equilibrium potential by intracellular magnesium ions (Vandenberg, 1987; Ishihara *et al.*, 1989). However there is also probably some intrinsic voltage–gating of the channels, with the magnesium block mechanism accounting for the instantaneous current seen on hyperpolarization and voltage–gating for the slightly delayed increase in current seen in some preparations, which develops exponentially with time constants from milliseconds to half a second (Ishihara *et al.*, 1989).

The presence of these channels in cardiac tissue gives some suggestion as to their function. These cells spent a large proportion of their time in a depolarized state as a result of repeated prolonged action potentials. The absence of significant outward currents at depolarized potentials allows prolonged repeated depolarizations with the minimum of metabolic outlay. In fact the conductance of nonpacemaker cardiac cells can be lower during the plateau phase of the action potential than at the resting potential (Hille, 1992). The large inward current present at potentials more negative than the potassium equilibrium potential prevents excessive hyperpolarization which could be caused by electrogenic pumps, especially in cells with low conductivities.

The current can be blocked by barium at μM concentrations (Standen and

Stanfield, 1978; Hagiwara *et al.*, 1978) and by rubidium at mM concentrations, (Mitra and Morad, 1991; Silver *et al.*, 1994) although these channels are slightly permeable to rubidium.

Recently a number of inward rectifier channels have been cloned and expressed in Xenopus oocytes and it is clear that they form a family of channels distinct from other voltage activated potassium channels, although there is similarity in the amino acid sequence of the region of the peptides forming the pore of the channel with other potassium channels (Ho *et al.*, 1993; Kubo *et al.*, 1993; Ishii *et al.*, 1994; Koyama *et al.*, 1994; Morishige *et al.*, 1994).

3.1.8 Calcium Currents

3.1.8.1 Introduction

The presence of an action potential in crustacean muscle fibres which was not dependent on sodium ions (Fatt and Katz, 1953) was correctly explained as being a 'calcium spike' (Fatt and Ginsborg, 1958), an action potential driven by the concentration gradient of calcium ions across the cell membrane and controlled by voltage–gated calcium channels. It has since been shown that voltage–gated calcium channels are present in all excitable cells examined from animal phyla as well as in many other cell types (Hille, 1992).

The role of voltage–gated calcium channels is basically twofold. The translation of electrical activity through membrane potential changes to the activation of cellular functions and the shaping of the electrical activity.

The normally very low intracellular free calcium concentration can increase markedly on calcium influx through these channels. As calcium is an intracellular second messenger and is maintained at a low intracellular concentation the membrane potential changes causing a calcium current to pass across the membrane will also be resulting in an increase in the intracellular calcium concentration (see Chapter 4). This can trigger other cellular mechanisims such as muscular contraction and neurotransmitter release in the short term, the activation of calcium dependent enzymes such as phosphorylases mediating medium term responses and responses like gene expression and neurite outgrowth in the longer term.

However the voltage–gated calcium channels can also contribute to, as well as respond to, membrane potential changes. As has already been described crustacean muscle action potentials are generated by these channels alone. In many vertebrate as well as invertebrate cells the shape of action potentials can be significantly affected by voltage gated calcium channels, especially in cardiac cells where the sinoatrial pacemaker cells form action potentials with no voltage–gated sodium channels present (see Hille, 1992 for other examples). Also the non–uniform distribution of voltage–gated calcium channels in the dendrites of many cells means that the integration of synaptic inputs is possibly affected by localized action potentials and membrane resistance changes within the dendritic tree (Llinás and Sugimori, 1980).

3.1.8.2 Voltage–gated Calcium Channel Diversity

Due to the wide distribution and diverse characteristics of the voltage gated calcium channels attempts to classify them tend to have the detrimental effect of forcing currents into pidgeonholes which are not totally appropriate and might obscure a continuum of properties. However the generally accepted classification of these current into four different types is useful, even though some currents may meet some of the charateristics of a particular 'pidgeonhole', but not all.

Three distinguishable voltage–gated calcium channel types were shown to coexist in sensory neurones in the chick dorsal root ganglion (Nowycky *et al.*, 1985a; Fox *et al.*, 1987) and were referred to as L–, T– and N–types. They were primarily distinguished on the basis of their voltage–dependent kinetics and derive their labels from these characteristics, as summarized in Table 3.1. The L–type for Long–lasting, the T–type for Transient and the N–type for Neither (as it has some features in common with the L– and N–type currents but is distinct from both.) Conveniently N–type currents have only been observed in neurons to date, a more fitting root for the label, especially as N–type currents are not the only type which are neither L– nor T–types (see below). It should also be noted that there are other names used to refer to these groupings. For example L–type currents are also referred to as being high voltage activated (HVA) and I_{slow} although the former definition often encompases the N–type and other channel types (see below). The T–type currents are conversely referred to as being low voltage activated

(LVA) and I_{fast} (e.g. Hess, 1990).

However these electrical properties are not the only way these current types are distinguished. For example one of the simplest methods of distinguishing T–type currents from L– and N–types is the relative sensitivity to block by Ni^{2+} and Cd^{2+}. T–type channels are more sensitive to Ni^{2+} while L– and N–type channels are more sensitive to Cd^{2+} (Fox *et al.*, 1987). Also in both L– and N–types using Ba^{2+} as the charge carrier rather than Ca^{2+} results in an increase in the current amplitude, while there is little change in the current amplitude of T–type currents (Bean, 1985; Tsien *et al.*, 1988). L–type channels can be distinguished by their sensitivity to various lipid soluble drugs. Verapamil will preferably block L–type channels over T– and N–types (Hille, 1992) and L–type channels are more sensitive to low concentrations of dihydropyridines, which can either enhance or inhibit them. For instance, $5\mu M$ Bay K 8644 greatly increased L–type single channel current averages in chick sensory neurones but had no effect on T– and N–type currents (Nowycky *et al.*, 1985a,b) while $10\mu M$ nifedipine blocked up to 60% of the L–type current with little or no effect on the T– and N–type currents (Fox *et al.*, 1987). Although L–type currents are more sensitive to the dihydropyridines there is a wide degree of variation between currents from different tissues (Bean, 1989).

The electrical properties of the T–type current, primarily its activation by relatively small depolarizations, means that it is relatively easy to distinguish from the L– and N–type currents, which are sometimes collectively referred to as the high voltage activated currents. Increasingly the substances being used to distinguish the ever increasing numbers of high voltage activated calcium channels are short polypeptides referred to as ω–toxins. (To date no ω–toxin has been isolated which blocks T–type currents.) The ω–toxins are derived from two sources; the predatory (especially the fish hunting) marine snails of the genus *Conus* giving rise to the ω–conotoxins (Olivera *et al.*, 1985) and spiders, primarily the American funnel–web spider *Agelenopsis aperta*, giving rise to the ω–agatoxins (Adams *et al.*, 1990). The first ω–conotoxin used, ω–conotoxin GVIA, is specific for N–type channels in mammalian preperations (Mogul and Fox, 1991; Kasai and Neher, 1992), but seems to have a broader action, blocking L–type currents in lower vertebrates too (Olivera *et al.*, 1994). It was the inability of this peptide to block a calcium current with similar electrical properties to the N–type current in purkinje cells that lead

Table 3.1 Summary of L–, T– and N–type Calcium Channel Characteristics. Not all channels, or currents, described demonstrate all of the characteristics for any one channel type, but can still be described as primarily showing the properties of the most appropriate channel type.

	Current Type		
	L–type	T–type	N–type
Activation Range	Positive to $-10mV$	Positive to $-70mV$	Positive to $-20mV$
Inactivation Range	-60 to $-10mV$	-100 to $-60mV$	-120 to $-30mV$
Inactivation Rate	V.Slow (τ>500)	Rapid ($\tau\approx5-50ms$)	Moderate ($\tau\approx50-80ms$)
Ion Block	$Cd^{2+} > Ni^{2+}$	$Ni^{2+} > Cd^{2+}$	$Cd^{2+} > Ni^{2+}$
Relative Conductance	$Ba^{2+} > Ca^{2+}$	$Ba^{2+} \approx Ca^{2+}$	$Ca^{2+} > Ba^{2+}$
Verapamil Block	Sensitive	Resistant	Resistant
Dihydropyridine Sensitivity	Sensitive	Resistant	Resistant

Llinás *et al.* (1989) to introduce a new current type — the P–type. They suggested that the P–type current could be selectively blocked by a polyamine–containing fraction from *Agelenopsis aperta* venom called FTX (funnel–web toxin), although its specificity to this type is doubtful (Olivera *et al.*, 1994). However a toxin more specific to this channel type, ω–agatoxin IVA, was identified by Mintz *et al.* (1992). Various other ω–toxins have been isolated and are used to selectively block different voltage–gated calcium channels (see Olivera *et al.*, 1994 for a recent review). A few of the more common ones are described in Table 3.2, but as only a very small fraction of the predatory species from which these peptides are found have been closely studied the potential for increasing numbers of these compounds is vast.

However these are not the only sources of polypeptide voltage–gated calcium channel blockers. A 60 amino acid peptide calciseptine, isolated from black mamba venom, appeares to be the only polypeptide antagonist of L–type channels discovered to date (De Weille *et al.*, 1991).

As has already been stressed the voltage–gated calcium channels are much more diverse than the classification into four types would suggest. For instance

Table 3.2. The relative sensitivity of L–, N– and P–Type calcium currents to various ω–toxins.

	Current Type		
	L–Type	N–Type	P–Type
ω–conotoxin GVIA	Resistant*	Sensitive	Resistant
ω–Conotoxin MVIIA	Resistant	Sensitive	Resistant
ω–conotoxin MVIIC	Resistant	Sensitive	Sensitive
ω–agatoxin IIIA**	Sensitive	Less Sensitive	Least Sensitive
ω–agatoxin IVA	Resistant	Resistant	Sensitive

* — Appears to be sensitive in lower vertebrates.

** — Binds strongly to all three channel types but blocking decreases from 100% of the L–type current in the sequence L>N>P.

the differences in blocking effects of ω–conotoxin GVIA between mammalian and non–mammalian channels is only one example of how current properties can vary between species and tissue types. For example within retinal horizontal cells Sullivan and Lasater (1992) found a sustained voltage–gated current which had many properties of an L–type current. However 10–50μM nifedipine had no consistent effect on it, although 1–10μM Bay K 8644 significantly increased the current amplitude. This is an example of the phenomenon mentioned earlier where a current meets most, but not quite all, of the criteria of one of the four current types described.

The basis of the great diversity of voltage–gated calcium channels is thought to be primarily derived from the multiple isoforms present. Since the initial cloning of skeletal L–type channel (Tanabe *et al.*, 1987) much has been learnt about the structure of these channels. It has been suggested that much of the diversity of the $\alpha 1$ subunit may be attributable to alternate splicing as well as multiple genes (Tsien *et al.*, 1991; Snutch and Reiner, 1992; McCleskey, 1994). There is the potential for hundreds of different isoforms of the L–type channels which show slightly different current–voltage relationships and pharmacological properties. Large numbers are

already described with slight variations and as the numbers of toxins avaliable to characterise these channels increases and the structures of more and more are discovered the restrictions of the four channel type definitions described will be increased. Additional channel–type definitions are suggested (Olivera *et al.*, 1994) and the shortcomings of the present method pointed out (e.g. Llinás *et al.*, 1989; Hille, 1992). However at present the definitions of L–, N–, P– and T–types are still widely used.

3.1.8.3 Divalent Ion Selectivity

Work on the selectivity of voltage–gated calcium channels for Ca^{2+} and other divalent ions has been largely restricted to L–type channels. These channels are very strongly selective for divalent ions only when they are present, transmitting large currents conducted by alkali metals in their absence (Almers and McCleskey, 1984; Hess and Tsien, 1984). The block of this alkali metal ion current by very low Ca^{2+} concentrations indicates high–affinity Ca^{2+} binding sites (with dissociation constants in the micromolar range), which is not compatible with an apparent dissociation constant in the millimolar range calculated from single channel current amplitudes (Hess *et al.*, 1986).

This apparent anomaly can be solved by a two–site model of the channel pore (Almers and McCleskey, 1984; Hess and Tsien, 1984) which suggests that the channel pore allows ions to pass through in single file only and has two high affinity binding sites each of which can bind monovalent or divalent ions. As the divalent ions are bound more tightly they can prevent the monovalent ions from passing through the channel even when the divalent ions are present at low concentrations. At higher divalent ion concentrations the presence of two divalent ions in the channel results in increased probability of the extrusion of one due to electrostatic repulsion. Consequently the presence of divalent ions will prevent monovalent ions passing through the channel and if they are present in high enough concentrations can rapidly pass through by alternating between single and double occupancy of the channel.

A similar model relies on only one divalent ion binding site which can bind to one ion with high affinity or two with lower affinity (Armstrong and Neyton, 1992; Yang *et al.*, 1993) while a 'long pore' model with multiple high affinity and

low affinity sites has also been proposed (Kuo and Hess, 1993). They are both, however, based on the principle of a pore able to conduct ions in single file only, with only divalent ions having a high probability of displacing other divalent ions from binding sites in the pore.

3.1.8.4 Calcium Currents in Horizontal Cells

Two calcium currents have been observed in horizontal cells; a transient one and a sustained one, although the transient one is not present in cells from all species recorded from to date (see Table 3.3 B for details and references). Both are activated by depolarization beyond about $-40mV$ and are at a maximum at about $-10mV$ and $+10mV$ respectively. The former reaches a maximum within a few milliseconds and then decreases rapidly with time and is referred to as having mainly T–type properties, while the latter usually shows very little inactivation and is referred to as having mainly L–type properties.

3.1.9 Interspecies Horizontal Cell Current Variations

The observations of a number of studies into the ionic conductances in horizontal cells from various species are given in Table 3.3. This shows how the currents in horizontal cells differ from the various current types described above and the variations in currents between species.

As can be seen from Table 3.3 A all horizontal cells recorded from have demonstrated an anomalous rectifier current, although the amplitude of this current varies between not only cells from the same species but also different cell types. The degree of conservation of this current across the range of species presumably demonstrates the importance of this current in the horizontal cells.

The outward potassium currents are much less consistent in magnitude and expression between the species with, for example, the lack of any transient outward current in the catfish. Interestingly, Lasater (1986) states as an unpublished observation that carp horizontal cells also do not demonstrate a transient outward current. However, where present the voltage dependencies of these inward potassium currents in the various horizontal cells represented in Table 3.3 A were

reasonably consistent, with the transient current being activated by depolarizations beyond about $-30mV$. This is more depolarized than is usual for the I_A current described by Conner and Stevens (1971a,b). The sustained current is also activted at more depolarized levels than is usual for this current type (see Rudy, 1988). In most cases these currents do not appear to be significantly activated at the potentials experienced by the cells *in vivo* and only contribute significantly to the I–V relationship at positive membrane potentials. However Perlman *et al.* (1993) have shown that in the isolated turtle retina these currents speed up the recovery of the horizontal cell membrane potential from the effects of bright light stimuli and in doing so improve the frequency response of the cells.

The inactivation of the transient current with 4–AP is consistent with the properties of the I_A current, while the unpredictable and incomplete inactivation of the sustained current by TEA is unusual although not unprecedented (Rudy, 1988).

Table 3.3A: Potassium Currents in horizontal cells.

Species	Anomalous/Inwards Rectifier	Transient Outwards Current (I_A)	Sustained Outwards Current	Reference
Goldfish	Hyperpolarisation from the resting potential evoked a large steady inwards current with an almost linear I–V curve beyond $-70mV$. Depolarisation evoked a very much smaller outwards current. The I–V curve was shifted along the voltage axis by changing $[K^+]_E$ as predicted by Nernst.	A transient K^+ current was activated by depolarisation beyond $-25mV$, and increased with increased depolarisation. It could be inactivated either by depolarisation of the of the hold potential to $-30mV$ or by $10mM$ 4–AP.	A sustained K^+ current was activated by depolarisation beyond $-20mV$, and increased with increased depolarisation. It increased to a maximum within a few hundred ms and was maintained during sustained depolarisation.	Tachibana, 1983a,b.
Catfish	This current was present, with the same characteristics as described above (Tachibana 1983a,b). It was not affected by hold potential, but was inactivated by $100\mu M$ Ba^{2+}.	Not present.	A very small sustained K^+ current was blocked by $15mM$ TEA or intracellular Cs^+. It appeared to activate only at potentials more positive than $+20mV$.	Shingai and Christensen, 1986
White Perch	As in Tachibana, 1983a,b. Shows some variation in amplitude between cell types, but not in kinetics. An instantaneous and delayed component of the activation were observed, the kinetics of which were dependent on the degree of hyperpolarisation.	A large transient K^+ current was activated by depolarisations beyond $-30mV$. It was inactivated by a depolarised (beyond $-30mV$) hold potential, $10mM$ 4–AP or intracellular Cs^+. The amplitude and time constant of its decay varied between cell types.	A small sustained K^+ current was activated by depolarisation beyond $-30mV$. The degree of inactivation by $20mM$ TEA varied between cells. It was inactivated by intracellular Cs^+, but only after 10–15 minutes exposure.	Lasater, 1986
Skate	As in Tachibana, 1983a,b. No inactivation over a six second hyperpolarising pulse.	A very large transient K^+ current was activated by depolarisation beyond about $-30mV$. It was inactivated by a hold potential more depolarised than $-40mV$ or $10mM$ 4–AP.	A relatively small sustained K^+ current was activated by depolarisation beyond $-20mV$. It was partially blocked by $20mM$ TEA (varied between cells).	Mallchow *et al.* 1990.
White Bass	Observed, but not described.	A large transient K^+ current was activated by depolarisation beyond $-30mV$. It was inactivated by a depolarised hold potential ($-30mV$) or $2.5mM$ 4–AP (though a 'slowly inactivating' component was not affected.) There was variation in the time constant of decay of the current between cell types.	A sustained K^+ current was present which was very small below $-10mV$. It was not affected by up to $50mM$ TEA.	Sullivan and Lasater, 1990

Table 3.3A continued: Potassium Currents in Horizontal Cells.

Species	Anomalous/Inwards Rectifier	Transient Outwards Current (I_A)	Sustained Outwards Current	Reference
Cat	As in Tachibana, 1983a,b. Blocked by $0.5\mu M$ Ba^{2+} or $10mM$ Rb^{+}. Similar in axonless and short axoned cells.	The most prominent current in these cells, activated by depolarizations beyond $-40mV$, decaying rapidly with time ($< 25ms$ decay time). Inactivated by a depolarized hold potential and blocked by $10mM$ 4-AP.	A sustained K^+ current was activated by depolarizations beyond -5 to $-10mV$. It was inactivated by $30mM$ TEA and partially by a depolarized hold potential.	Ueda *et al*, 1992.
Turtle	As in Tachibana, 1983a,b. Two components of the activation time course were observed as in Lasater, 1986.	A transient K^+ current was activated by depolarisation beyond $-30mV$. It was inactivated by a depolarised (beyond $-30mV$) hold potential or $5mM$ 4-AP. After activation the current was inactivated, taking minutes to recover.	No sustained component of the inwards K^+ current was observed.	Gollard *et al*, 1992.
Xenopus	This current was present in cells, but varied in amplitude between cell types. It was not discussed in detail.	A large transient K^+ current was activated by depolarisation beyond around $-45mV$. It was inactivated by a depolarised (beyond $-40mV$) hold potential or $5mM$ 4-AP. The depolarisation dependent inactivation could be modulated by both intracellular GTP and intracellular Ca^{2+}.	A sustained K^+ current was activated by depolarisation beyond $-20mV$. It was reduced but not eliminated by $20mM$ TEA.	Akopain and Witkovsky, 1994

Table 3.3B: Sodium and Calcium Currents in horizontal cells.

Species	Transient Sodium Current	Transient Calcium Current	Sustained Calcium Current	Reference
Goldfish	Not observed, because of insuficient recording speed.	Not Observed.	A sustained Ca^{2+} current was activated on depolarisation beyond $-45mV$, reaching a maximum at $0mV$, and reversing at an estimated $+50mV$. It was inactivated by Ca-mediated Ca inactivation and $4mM$ Co^{2+}.	Tachibana, 1983a,b.
Catfish	A typical TTX sensitive fast inwards Na^{+} current was activated by depolarisation to beyond $-50mV$. The maximum current was reached in less than $5ms$ on depolarisation to $+10mV$.	In the presence of TTX, and with $30mM$ extracellular Ca^{2+} depolarisation induced a transient inwards current activating at $-30mV$ and maximal at $+25mV$.	A small sustained current was observed in $30mM$ extracellular Ca^{2+} which was activated at $-30mV$ and was maximal at $+25mV$. It demonstrated little or no inactivation over depolarisation steps lasting for seconds.	Shingai and Christensen, 1983
White Perch	A current similar to that described by Shingai and Christensen (1983) was observed. It was inactivated by either TTX or no extracellular Na^{+}. It was maximal at $-10mV$ and activated at about $-50mV$.	Not Observed.	A small sustained current was activated by depolarisation beyond $-30mV$ in $20mM$ Ca^{2+}, which reached a maximum at $+20mV$ and reversed at about $+50mV$. There was no sign of inactivation over $800ms$ depolarising steps. It was inactivated by $5mM$ Co^{2+}.	Lasater, 1986
Skate	A fast inwards current was inactivated by $1\mu M$ TTX and activated by depolarisation beyond $-30mV$ and reached a peak at $0mV$. The amplitude varied widely between cells.	Not observed.	A sustained current which could be inactivated by $4mM$ Co^{2+} or 100 μM Cd^{2+} was activated by depolarisations beyond $-40mV$. The maximum was reached at 0 to $+10mV$ and reversed at about $+40mV$.	Malchow *et al,* 1990
White Bass	Not Studied, though TTX was used to block any Na^{+} currents present.	A large transient current inwards was observed in $10mM$ Ca^{2+} and was activated by depolarisation beyond -60 to $-50mV$ and reached a broad peak at -20 to $+10mV$ (to some degree depending on the cell type) and reversed at around $+50mV$.	A sustained inwards current was observed in $10mM$ Ca^{2+} and activated by depolarisation beyond $-30mV$. It was maximal at $+10mV$ and reversed at around $+40$ to $+50mV$. Some cells showed no inactivation over 15–60 second depolarisations, where as others did, in a voltage dependent manner ($\tau \sim 13.5s$).	Sullivan and Lasater, 1992

Table 3.3B continued: Sodium and Calcium Currents in Horizontal Cells.

Species	Transient Sodium Current	Transient Calcium Current	Sustained Calcium Current	Reference
Cat	A TTX sensitive Na^+ carried current which inactivated rapidly was recorded on depolarizations beyond $-45mV$, reaching a maximum at $-25mV$. It was observed in axonless cells only.	Not observed.	A sustained Ca^{2+} current (in $10mM$ Ca^{2+}) activated by depolarization beyond $-40mV$, reaching a maximum at $+15mV$. It was blocked by $10mM$ Co^{2+} and sensitive to the dihydropyridines nifedipine and Bay K 8644.	Ueda *et al*, 1992.
Turtle	A current with the same kinetics described in Lasater, 1986 was recorded. The amplitude varied widely between cells. The current was inactivated by $2\mu M$ TTX.	Not observed.	A very small sustained current was activated by depolarisation beyond $-40mV$ in $20mM$ Ca^{2+}. It reached a maximum at about $+10mV$ and reversed at about $+60mV$. It was greatly increased by $10\mu M$ Bay K 8644.	Golard *et al*, 1992
Xenopus	A fast inwards current was blocked by $1\mu M$ TTX, but was not described further.	A transient Ca^{2+} current was reported in luminosity, but not chromaticity cells, but was not described further.	A sustained Ca^{2+} current was reported in all the cell types, but was not described further.	Akopain and Witkovsky, 1994

3.2 METHODS

3.2.1 Whole Cell Patch Electrodes

The requirements of a patch clamp electrode are significantly different from those of a conventional intracellular microelectrode. Rather than having a glass pipette with a long shank which tapers very gradually to a tip of $\sim 0.1 \mu m$, the patch clamp pipette should taper steeply to a tip of about $0.5–2 \mu m$. This ensures a low pipette resistance, ideally $<5 M\Omega$, when filled with $150 mM$ KCl.

Patch pipettes are pulled from similar types of glass to microelectrodes, but a two step pulling process is used (Rae and Levis, 1992). The glass is heated in a heating coil and has a mild pulling tension applied to it. A mechanical stop is used to terminate the primary pull, usually after $6–10 mm$, so that the glass has at an external diameter of about $200 \mu m$ at the thinnest point. This thinnest point is then repositioned to the centre of the heating coil and the glass is heated for a second time, again with a mild pulling tension, at which time the tubing breaks forming two electrodes. Once the current through the heating coil and drop distance required for the first pull have been set, the exact dimensions of the pipette tip can usually be controlled quite accurately by slightly varying the current through the heating coil for the second pull.

The simplest method for estimating the dimensions of the tip of the pipette is to bubble it in methanol. The pressure required to expell air from the tip in methanol is dependent on the external diameter of the pipette tip (Mittman *et al.*, 1987). By connecting the pipette to a $10 ml$ syringe with narrow gauge tubing the amount of depression of the syringe plunger needed to form bubbles can be observed. This figure is known as the 'bubble number' (Corey and Stevens, 1983) and is commonly used to compare pipettes.

Initially the glass tubes used in this study to make electrodes were Drummond $100 \mu l$ microcaps. Electrodes were made in the apparatus shown in Fig. 3.4. This simply holds the glass in the heating coil and puts a low pulling tension on one end. The distance of the first pull was controlled by the position of the stop and the temperature of the coil by the current through it. The heating coil was $6mm$ long with an internal diameter of about $4mm$ and a total of six turns of $0.5mm$

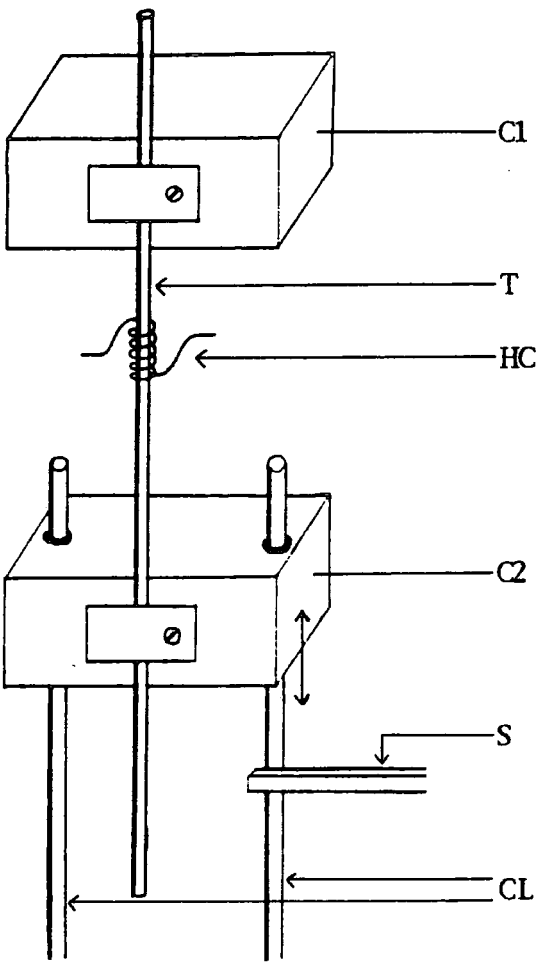
C1
T
HC
C2
S
CL

diameter nicrome wire. For the first pull $3.8V_{\mathrm{RMS}}$ was put across the coil and the drop was $8mm$. The glass was then repositioned up $3.5mm$ and 2.90–$3.05V_{\mathrm{RMS}}$ put across the coil for the second pull. The dimensions of the pipette tip varied with the heat of this second pull — increasing the heat of the coil decreased the diameter of the pipette tip and consequently increased the resistance, as shown in Fig. 3.5.

Although seal resistances in the gigaohm range were achieved when using these electrodes the success rate for breaking the enclosed membrane patch to go 'whole cell' without rupturing the cell or breaking the glass–membrane seal was very low. This problem was largely solved by using a different glass tubing – Clark Electromedical Instruments GC150–10. This is a thick walled (i.e. $1.2mm$ outer diameter, $0.94mm$ inner diameter) borosilicate tubing. The same electrode puller was used, initially with the same heating coil. The potential required for the first pull was higher, due to the thicker glass, and the drop used longer, $4.8V_{\mathrm{RMS}}$ and $10mm$ respectively. After positioning the thinnest part of the tube in the centre of the heating coil the second pull was carried out with 3.00–$3.05V_{\mathrm{RMS}}$ across the coil, to give pipettes with bubble numbers of about 5.2–5.6 and resistances of about 10–12 $M\Omega$. The whole cell recording success rate with these electrodes was considerably higher than with those made from the Drummond microcaps (see Section 3.2.4).

However the thicker walled glass tubing has the disadvantage that the taper to the pipette tip is less steep than for thin walled glass (Sakmann and Neher, 1983). Consequently the resistance is higher for the same pipette tip internal diameter. A second heating coil was made (two turns of $0.5mm$ diameter Nicrome wire, internal diameter about $3.5mm$ and about $2mm$ tall) to give a much more localized heat for the second pull. This should result in a steeper taper to the tip, and consequently a lower resistance for the same pipette tip characteristics (Armstrong and Gilly, 1992). However it was only moderately successful, as is shown in Fig. 3.6, which compares the relationship between the resistances and the bubble numbers for pipettes made with and without this smaller second coil. A potential of 2.09–$2.12V_{\mathrm{RMS}}$ across the coil gave pipette resistances of 8–10 $M\Omega$ and bubble numbers of 5.2–5.6.

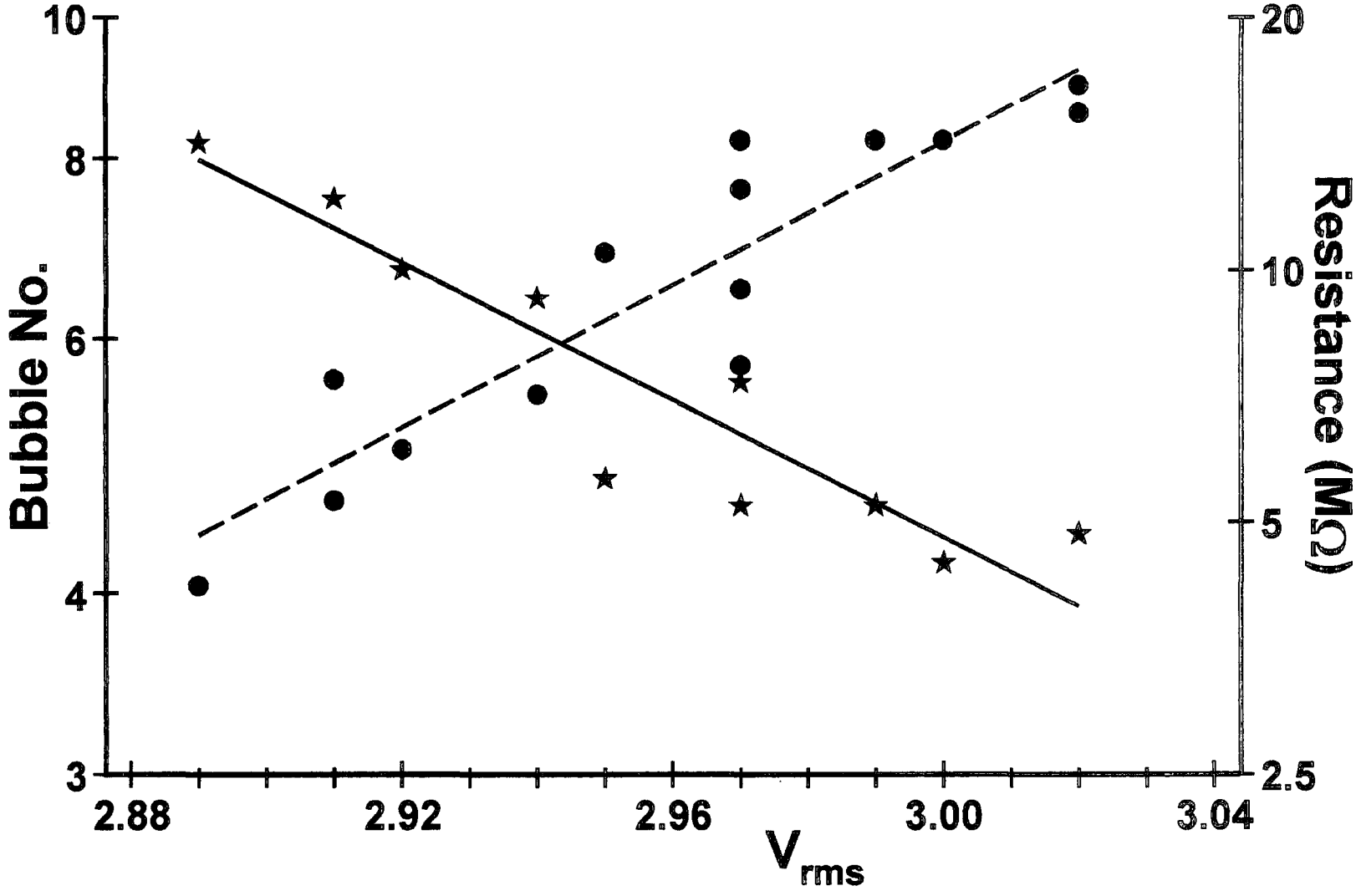
10
8
6
4
3
Bubble No.
20
10
5
2.5
Resistance (MΩ)
2.88
2.92
2.96
3.00
3.04
V_{rms}

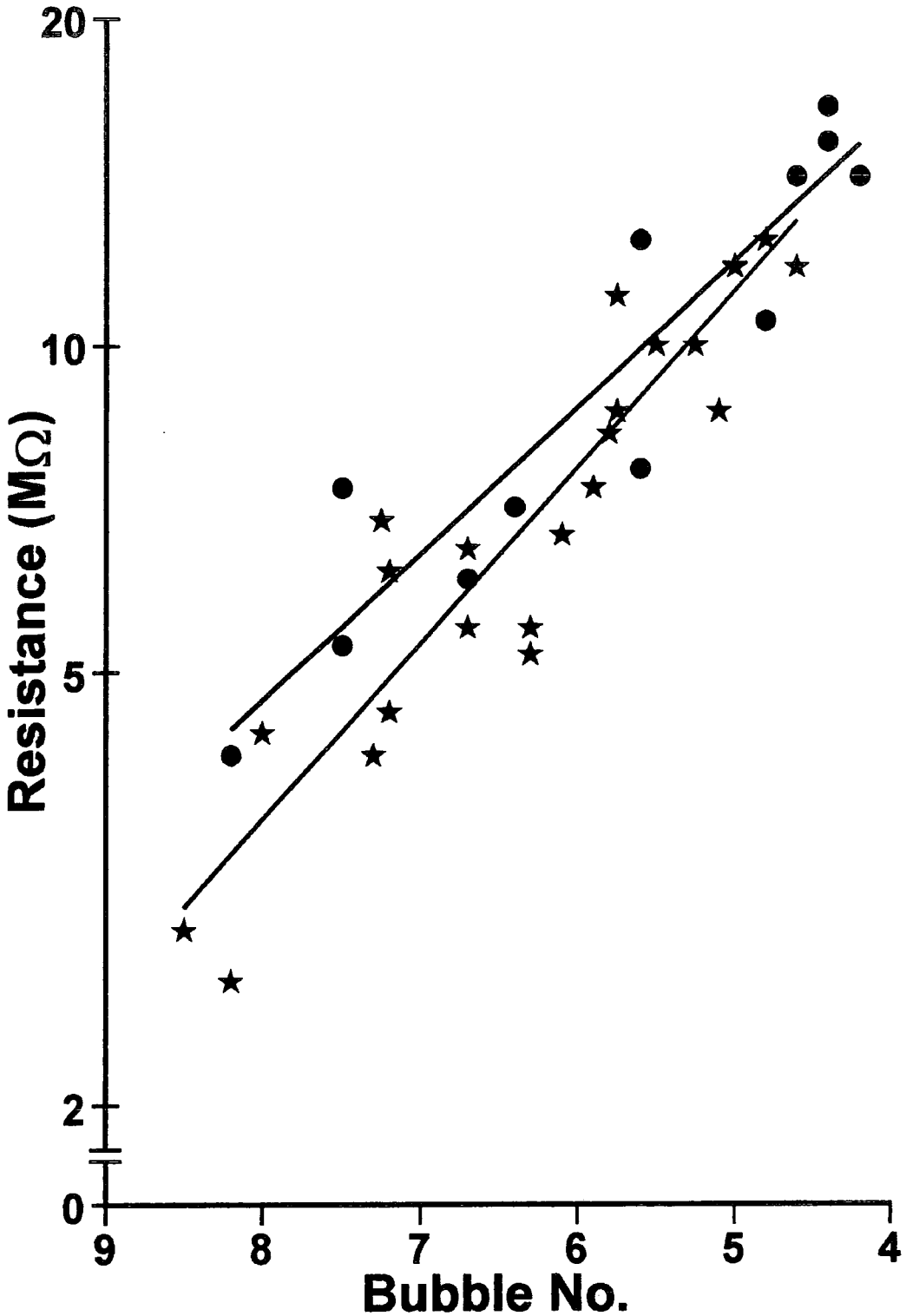
20
10
5
2
0
Resistance (MΩ)
9
8
7
6
5
4
Bubble No.

The pipette solution used was a standard low calcium whole cell patch clamp solution consisting of (in mM): KGluconate, 130; NaCl, 4; $MgCl_2$, 1; $CaCl_2$, 1; EGTA, 11; HEPES, 8.4, buffered to pH7.4 with KOH. This gives a calculated final Ca^{2+} concentration of $8.3nm$ (Sullivan and Lasater, 1992). Before the pipettes were filled the solution was filtered through a $0.22\mu m$ filter to ensure that there was no particulate material in it. Pipettes were then filled by sucking the solution into the pipette to fill the tip and back filling the rest of the pipette using a hypodermic syringe.

3.2.2 Cell Isolation.

The method used to isolate the horizontal cells was similar to those described in a number of publications (e.g. Lasater and Dowling, 1982). Fish were dark adapted and a retina isolated as described previously (Section 2.2.2). They were incubated in hyaluronidase (1000 $units/ml$, Sigma type V) for 15 minutes at 22°C to remove any vitreous humour (Heidelberger and Matthews, 1992). This gave more consistent results as the amount of vitreous humor adhering to the retina varied between preparations. The retina was then washed briefly in saline and incubated in $0.5mg/ml$ of protease (Sigma Type XIV) for 30 to 45 minutes at 22°C.

After washing in saline at least three times, the retina was then cut into about $2mm$ pieces and transferred to a 30% Liebovitz L-15 solution (Sigma). These pieces were then further broken up by triturating them with fire polished pipettes with diameters ranging from about $2mm$ to $0.75mm$. After each passage the remaining pieces of retina were transferred to new medium so that a series of suspensions was produced. The best yield of cells was generally from the final triturations when the retina fragments were very small. These later suspensions were placed on $10mm$ diameter round coverslips (Lamb Thickness No. 0) in Petri dishes. They were left for at least 90 minutes to allow the cells to adhere to the glass and the base of the Petri dish was then covered with medium. They were then kept in a moist incubator at 16°C. All solutions were filter sterilized and procedures after the enzyme incubations were carried out in a flow cabinet.

After isolation horizontal cells could be distinguised from other cell types due to their characteristic morphology in culture (e.g. Drujan and Svaetichin, 1972;

Tachibana, 1983a,b, Dowling *et al.*, 1983; Yagi and Kaneko, 1988). They had a large flat cell body and short thick dendrites immediately after isolation (Plate 3.1). Over a period of days the dendrites tended to elongate slightly and fine processes grew from them as shown in Plates 3.1 and 3.2. The cells were usually used one to five days after isolation.

3.2.3 Apparatus

The stage of an inverted microscope (a Zeiss Axiovert inverted microscope, with a phase contrast ×32 objective) held an open perfusion micro-incubator (Medical Systems Corp. PDMI-2) which was used to control the experimental temperature. This device, designed by Ian Forsyth, uses peltier devices to regulate the temperature, controlled by a graded feedback current (Medical Systems Corp. Bipolar Temperature Controller TC-202) to prevent deviation from the set temperature (see Forsyth, 1991 for details).

The microincubator is designed to take Corning 35*mm* petri dishes. These were modified by replacing a suitable area of the plastic base with a glass one (cf. Bray, 1970). This enabled the higher power objective lens to be used as it had a very short working distance. The area removed was diamond shaped and just large enough to take the coverslips used (see Fig. 3.7). This area of the dish was continually perfused with saline. It was pumped (by a Watson Marlow 501 peristaltic pump) into the microincubator where it first passed around the temperature control plate in a thin walled tube so that it reached the appropriate temperature before entering the petri dish. A bubble trap was included in the perfusing system to reduce any fluctuations in the perfusion rate.

As stated previously, the main requirements of the cells and the pipette tip for successful patch clamp recordings are that they are both clean and do not move relative to each other. The continuous perfusion of the cells ensured that loose debris on the coverslip was washed off rapidly and that the air–liquid interface was clean. The microscope and micromanipulator (Huxley–Goodfellow) used to position the electrode were independently mounted on a vibration absorbing stack of alternating concrete and polystyrene slabs which damped any ground vibrations. The electrode was held in an electrode holder connected to the head stage amplifier,

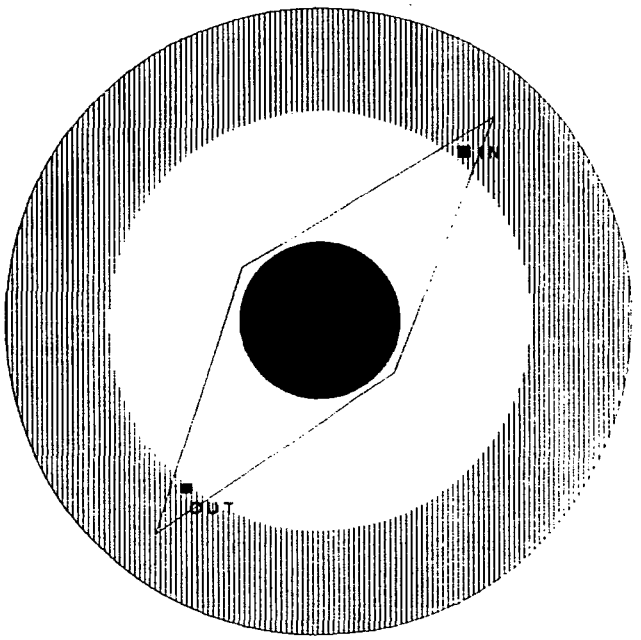

Figure 3.7. Diagram of the modified petri dish in the microincubator. The outer shaded area is part of the temperature control plate and supports the dish. The central circle is the coverslip positioned on the glass of the cut away area of the petri dish (diamond shape). The saline entered and left the dish at the points indicated and was restricted to the cut away area of the dish.

which was attached to the micromanipulator. The three main requirements of the electrode holder are:-

1 To provide an electrical connection between the pipette solution and the pin of a BNC connector, which plugs into the head stage amplifier.

2 To allow positive or negative pressure to be applied to the pipette interior.

3 To hold the pipette completely immobile, especially during pressure changes in the pipette.

The holder used (Fig. 3.8) held the pipette in an O–Ring which also provided an air tight seal. The side of the holder had an opening which was connected to a length of thin tubing so that pressure changes could be applied to the pipette interior. The BNC pin fitted into the head stage amplifier which was attached

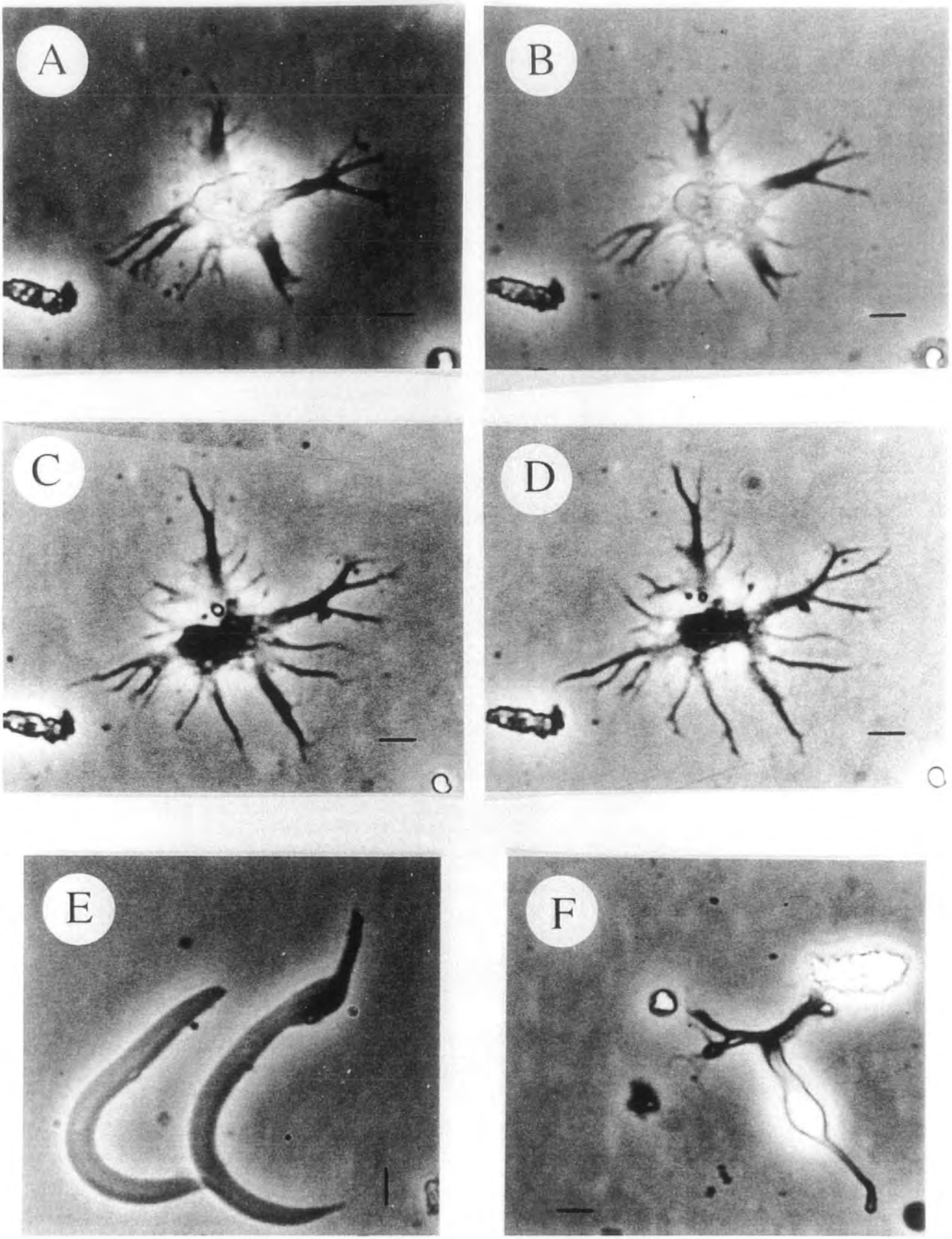
A
B
C
D
E
F

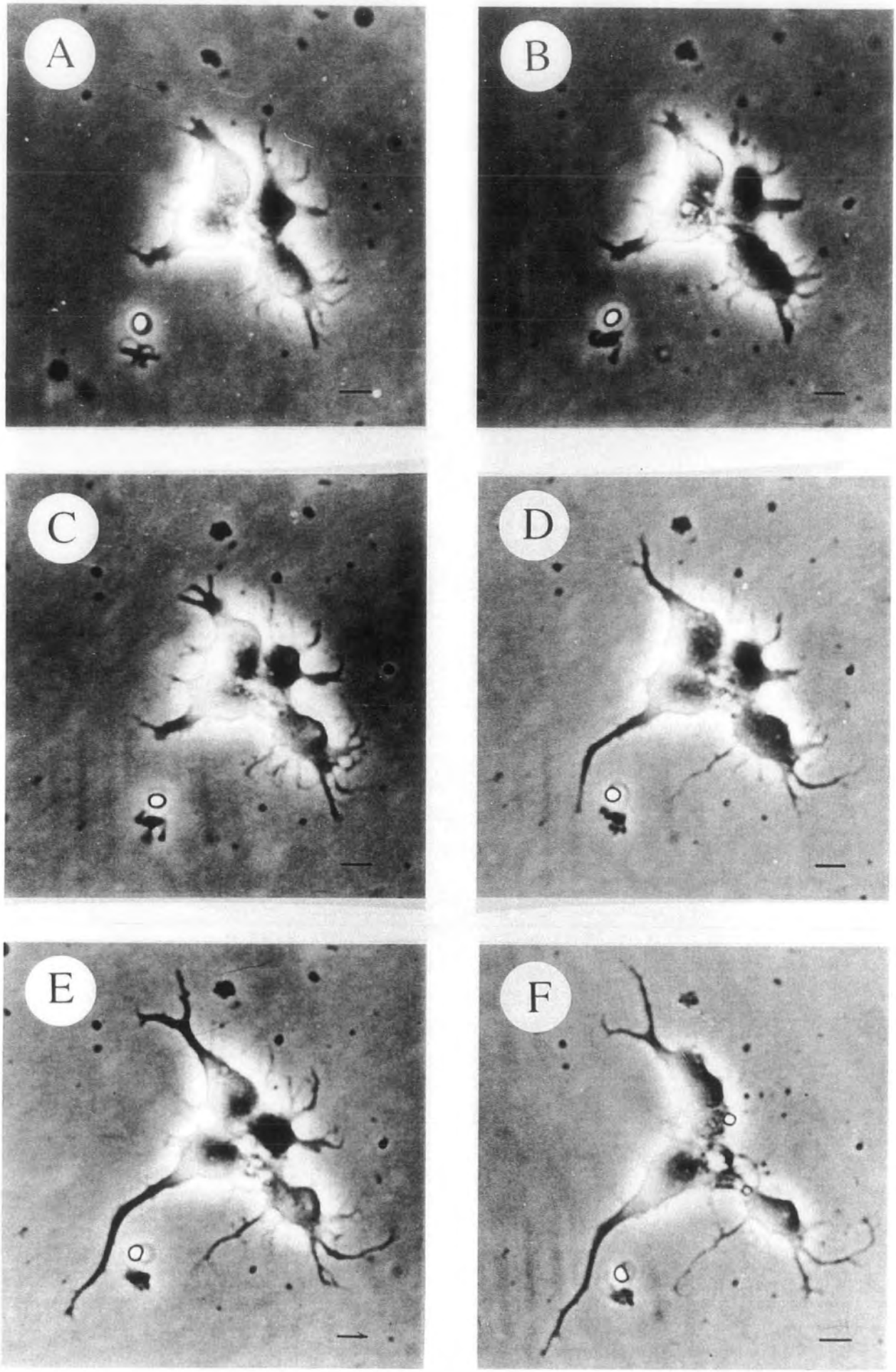
A
B
C
D
E
F

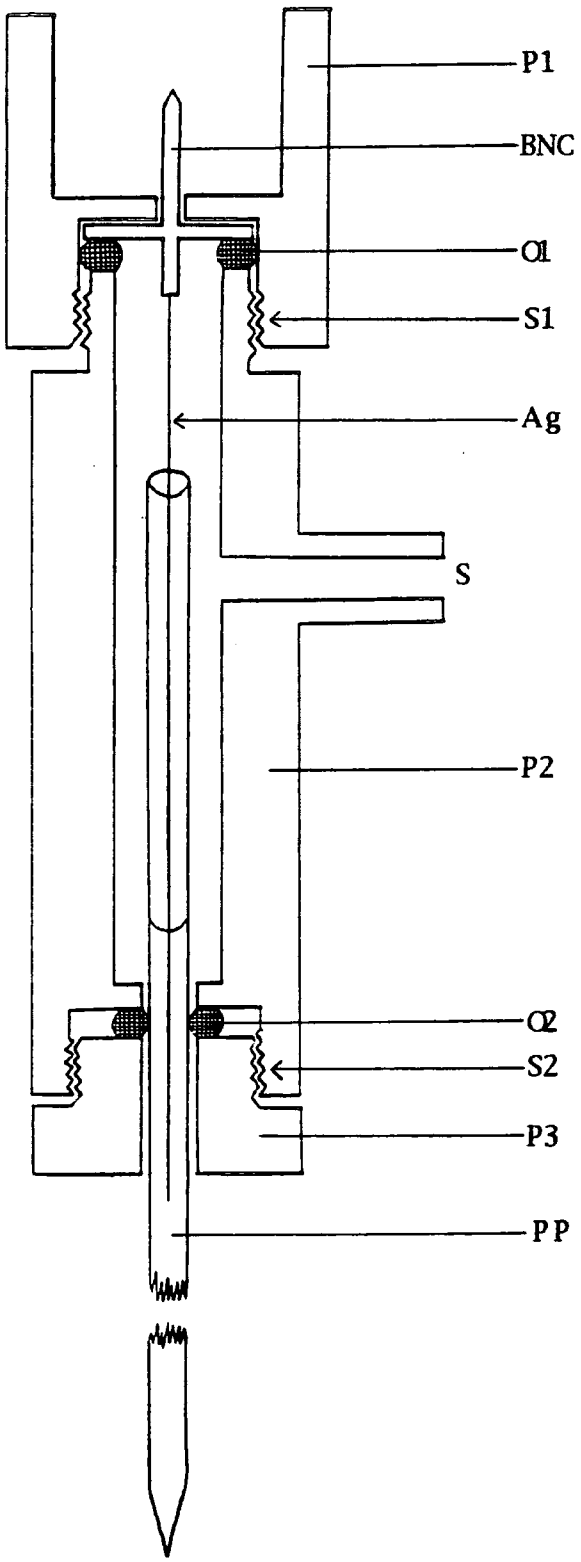
P1
BNC
O1
S1
Ag
S
P2
O2
S2
P3
PP

to a micromanipulator by a piece of pyrex. Although the use of pyrex presented considerable problems due to its fragility it was the only substance which was found to provide the electrical insulation required and did not bend slightly with changes in air temperature, as, for example, perspex and teflon were found to. The BNC pin and the pipette solution were connected by a silver wire coated with silver chloride. Care was taken to avoid scratching the wire on the end of the pipette as exposure of the silver resulted in rapidly varying junction potentials.

The patch clamp amplifier used was a Bio–Logic RK 300. The head stage current to voltage converter was set to $100M\Omega$ at all times to allow currents of up to $10nA$ to be recorded. Voltage commands were generated by a 'home made' patch clamp program controller (made by D. Hyde in 1988) and fed into the patch clamp amplifier. The patch clamp program controller was based on the design of Gitter and Theis (1987) and generated rapid voltage pulses of variable duration, amplitude and signal. The signal was filtered by a low–pass 5–pole Tchebicheff filter with a cut–off frequency of $300Hz$ before viewing on a storage oscilloscope and recording onto computer disk using the Strathclyde Electrophysiological Software package (J. Dempster, Strathclyde University) and a Data Translation analogue to digital converter (DT2812).

3.2.4 Technique

The technique used attempted to maintain the cleanliness of both the pipette tip and the target cell, as was described as being the most important single factor in the sucess rate for achieving giga–seals in the original paper by Hamill *et al.* (1981).

Patch clamp electrodes were made as required, so that there was less chance of their picking up debris on the tip, and filled with solution just before use. After the electrode was positioned firmly in the holder with the tip of the wire in the pipette solution and the holder was securely placed in the head stage amplifier a slight positive pressure was applied to the pipette. This meant that a slow flow of pipette solution was forced out of the tip of the pipette, helping to keep it clean. The pipette was then positioned just above a suitable cell.

Before contact was made with the cell the resistance of the pipette was measured and the junction potentials offset. A $2mV$ pulse was passed across the pipette and the resulting current measured to calculate the resistance. A junction nulling dial on the patch clamp amplifier could apply up to $\pm 200mV$ to the headstage to provide an equal and opposite potential to the various junction potentials in the circuit. These arise from liquid–solid junction potentials between the reference Ag–AgCl electrode and the extracellular solution and the electrode Ag–AgCl wire and solution and the liquid–liquid junction potential at the electrode tip. The liquid–solid junction potentials will be constant over recording time periods provided that the chloride covering on the silver has not been damaged and can therefore be effectively nulled. The liquid–liquid potential however will change if the solution composition changes on either side of the pipette tip as occurs when a whole cell recording is made. Moreover as the experiment proceeds the cell contents progressively equilibrate with the pipette solution resulting in a continually changing junction potential. Fenwick *et al.* (1982a) measured the magnitude of this potential for a high KCl pipette solution in a high NaCl solution and found it to be $3–5mV$. No attempt was made to calculate the magnitude of this potential and the junction potential compensation was adjusted for no current flow with the pipette tip in the saline. This was done in the voltage clamp mode by altering the applied potential until no current was observed indicating no potential difference across the pipette tip. This was checked before attaining a giga–seal to ensure no drift in the juntion potentials. If significant drift was occuring, indicating damage to the Ag–AgCl electrodes, the wires were cleaned and rechlorided in a Cl^- containing solution.

With a stable junction potential the electrode was lowered towards the cell surface a few microns at a time. The magnitude of current measured on a test potential pulse of $2mV$ was used to monitor the position of the electrode tip relative to the cell. When the tip was almost touching the cell the current through the pipette was reduced because of the increased resistance. When this occurred the positive pressure was removed from the pipette interior. This often resulted in the immediate formation of a giga–seal indicated by a great reduction in current measured for the $2mV$ potential pulse. Sometimes, however, suction on the pipette interior was also required. This was applied either by mouth or using a $1ml$ syringe.

Once in the 'cell attached' configuration the application of a $20mV$ test pulse was used to measure the resistance of the seal. Initially with the Drummond microcap pipettes, the resistances recorded were $0.5–5G\Omega$. Subsequently using pipettes made from the thicker walled tubing the resistances recorded were usually $10–40G\Omega$. These differences were probably due to the increased area of contact between the membrane and glass using the thicker walled pipettes. As would be expected with the application of rapid potential changes across a high resistance, capacitance transient currents were recorded due to the various capacitances in the head stage input. In the 'cell attached' configuration these are produced by the pipette, the pipette holder and the head stage amplifier. The amplitude of these capacitances and their time constants was minimised by keeping the head stage amplifier and pipette holder clean and dry and by preventing saline from the bath creeping up the outside of the pipette by having a very shallow saline depth and applying petroleum jelly to the shoulder of the pipette. The patch clamp amplifier could also be used to apply equal and opposite currents directly to the head stage amplifier using a capacitance transient compensation circuit. The Bio–Logic RK 300 has three such circuits with different time constants. The fast and medium time constant circuits (up to $200\mu s$) could compensate for most of the capacitance current seen in the 'cell attached' configuration, (see Fig. 3.9 A and B).

Before attempting to rupture the pipette enclosed–cell membrane, the hold potential was set to $-60mV$. Then short sharp pulses of suction were applied to the pipette interior using a $1ml$ syringe. Between each suction pulse a rapid $20mV$ change in the hold potential was used to test whether the membrane was ruptured and the 'whole cell' configuration had been obtained. This was signified by a large increase in the capacitance current on the potential changes (Fig. 3.9 C) caused by the capacitance of the cell membrane. The slow time constant (up to $2.0ms$) capacitance transient compensation circuit of the patch clamp amplifier was used to cancel this current out (Fig. 3.9 D). The amplitude of capacitance currents was not only dependent on the capacitance of the circuit, but also the rate of change of the potential. The cell membrane currents being measured were sustained currents so a facility on the patch clamp amplifier to add a $1ms$ rounding to the command potential changes was used to reduce the capacitance currents, without affecting the membrane currents.

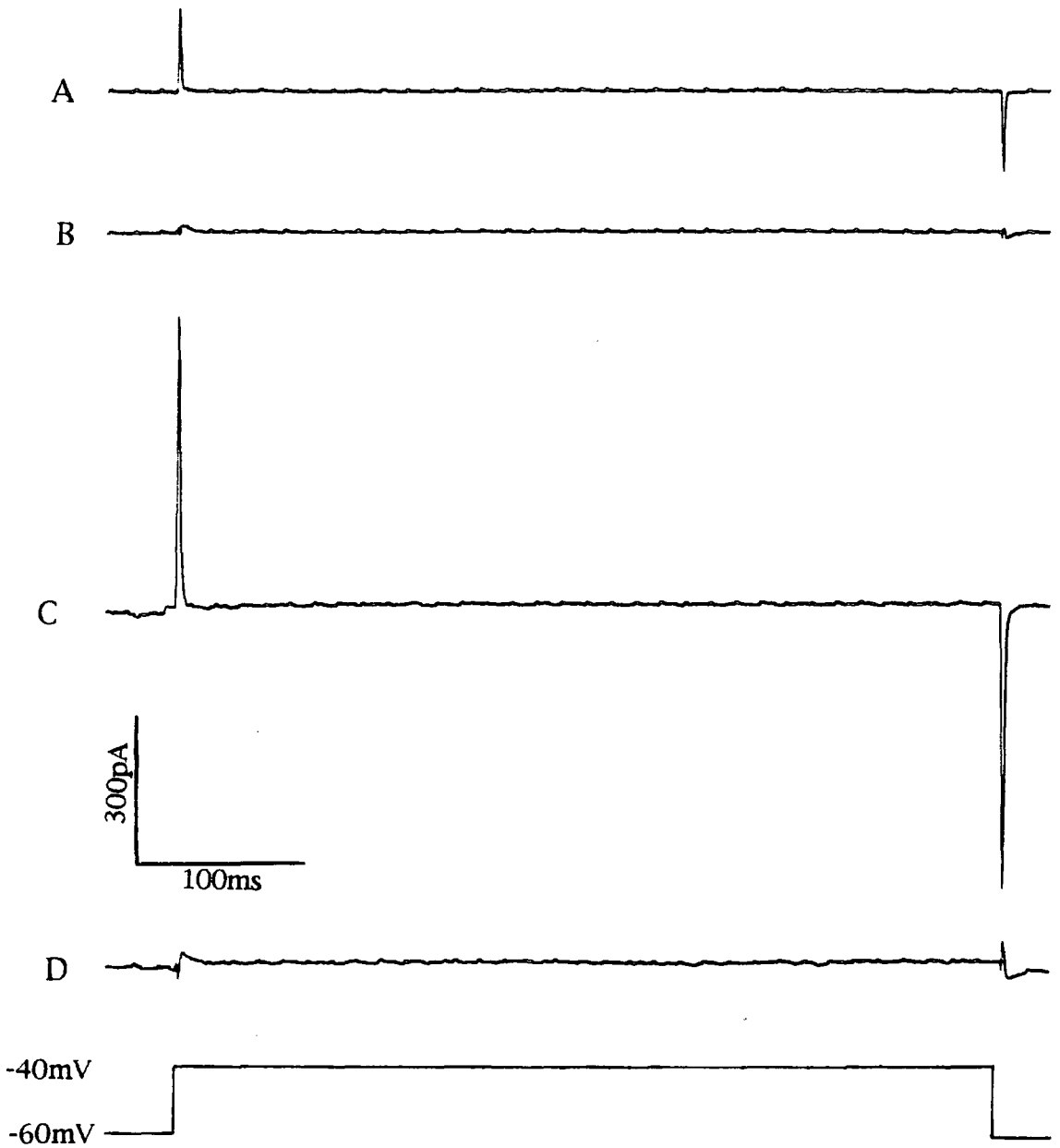
A
B
C
300pA
100ms
D
-40mV
-60mV

The sucess rate for achieving giga–seals with both pipette types was reasonably high (about 50% of the time), though this seemed to vary inexplicably on a day to day basis. However, as stated previously, the success rate for achieving 'whole cell' configuration was markedly different for pipettes made from the two different types of tubing. With pipetts made from the thinner–walled tubing the cells did not seem to remain attached to the pipette when the suction pulse ruptured the enclosed cell membrane. Even using a wide range of pipette tip diameters and controlled progressive increases in suction, the tendency was for the membrane not to rupture, or the cell to be destroyed. It was only possible on a few occasions to sucessfully make whole cell recordings using these pipettes. The giga–seals formed with the thicker walled pipettes were much more stable, possibly due to the increased membrane–glass contact. The success rate for achieving whole cell recordings with a seal of over $20G\Omega$ was about 50%.

Recently Bohle and Benndorf (1994) have reported that using very thick walled ($2mm$ outer diameter, $0.5mm$ inner diameter) glass tubing the patch pipettes can be used repeatedly simply by breaking off the tip of the pipette to expose a new clean glass surface. They claim that giga–seals are formed more frequently without the need for negative pressure in the pipette, but as the pipette resistances used vary from a maximum of $80M\Omega$ this technique is not suited to whole cell recording.

Once in the 'whole cell' configuration with the capacitance transients adequately compensated the series resistance compensation was applied. The pipettes used usually had resistances of 8–$10M\Omega$ and as the currents measured were up to $1.5nA$, a potential drop of up to $15mV$ could occur across the pipette. Consequently the membrane potential would not be held at the potential indicated by the user. In fact the access resistance is invariably considerably higher than the pipette resistance because of some degree of blockage of the pipette or incomplete rupturing of the cell membrane. However this access resistance can be calculated. The cell capacitance C_m is a fixed value dependent on the cell, but the time constant τ is dependent on the series resistance in the circuit, which is effectively the access resistance R_{access}:-

$$\tau = C_m R_{\text{access}}$$

Both C_m and τ can be read off the slow capacitance transient compensation circuit which compensates for the cell capacitance. The access resistance could consequently be calculated. It was found to be 2.19±0.10 (n=20) times the pipette resistance, which is similar to the increase reported by Marty and Neher (1983). This increased access resistance would mean that large discrepancies between the set and actual voltage clamp conditions would occur. Moreover during rapid changes in current amplitude, e.g. when transient currents are activating and inactivating, the membrane potential can escape control of the pipette potential and fluctuate widely over the duration of the transient currents (Armstrong and Gilly, 1992). The problem with sustained currents is less acute, but distortions in the current amplitude and current–membrane potential relationships can arise (e.g. see Armstrong and Gilly, 1992, Figure 6).

The function of series resistance compensation is to electronically reduce the effect of the voltage drop across the access resistance. An additional voltage command is applied to the pipette which is dependent on the amplitude of the current passing through the pipette and a variable scaling factor which is set by the user. This should cancel out the voltage drop across the access resistance. However the positive feedback nature of this circuit means that there is a tendency for oscillations to be set up. The scaling factor is consequently set to the maximum value possible without causing the clamp to 'ring', which usually represents 80–90% of the access resistance. The proportion of the access resistance which can be compensated for in this way is dependent on how efficiently the capacitance currents have been compensated and the speed of the feedback circuitry (Sigworth, 1983).

The value of the resistance which is being compensated for was read off the dial on the patch clamp amplifier. The series resistance compensated was 84.4±1.7% (n=20) of the calculated access resistance. When recording very large currents (e.g. $1000pA$) the resulting voltage drop across the pipette was about $5mV$, although for most currents (e.g. the calcium currents which were usually less than $300pA$) the error was less than $2mV$.

3.3 RESULTS

All results are, unless otherwise indicated, at an experimental temperature of 17°C and from cells from fish acclimated to 16°C.

3.3.1 Whole Cell Total and Leakage Currents

A typical example of the currents recorded from isolated carp horizontal cells have already been shown in Fig. 3.2. It shows the currents recorded for $500ms$ changes in membrane potential from a hold potential of $-60mV$ to a range of potentials, varying from $-120mV$ to $+60mV$. As is conventional, inward currents are represented as negative (down the page) and outward currents as positive (up the page). Large sustained inward currents were generated in response to clamp potentials more negative than $-70mV$, with very small sustained outward currents in comparison, at potentials more positive than $-60mV$. However at potentials between $-30mV$ and $+20mV$ transient inward currents were observed. The maximum current observed was $113pA$ at a potential of $-10mV$, reaching its peak after $12ms$. Although transient currents of this magnitude were often seen they were not studied further.

The sustained currents were measured after about $450ms$ and the current–voltage (I–V) relationship for the cell is shown in Fig. 3.10. This curve is clearly dominated by the large inward current observed at potentials more hyperpolarized than $-70mV$. The I–V relationship was approximately linear between $-80mV$ and $-120mV$ and reached more than $0.5nA$ at $-120mV$. Between $-70mV$ and $+20mV$, which includes the normal *in vivo* potentials of these cells, the sustained currents were also approximately linear. The apparent membrane resistance of the cell between $-120mV$ and $-80mV$, calculated by the slope of the appropriate points on the curve, was $0.079G\Omega$, while at potentials of $-70mV$ to $+20mV$ it was $4.1G\Omega$, over a 50–fold difference.

When the cells were incubated with a solution containing $20mM$ TEA, $10mM$ 4–AP and $5mM$ Co^{2+} sustained currents induced by depolarizing voltage commands from $-60mV$ up to $0mV$ were blocked, although small transient currents often remained. The I–V relation of the sustained leakage current was consequently

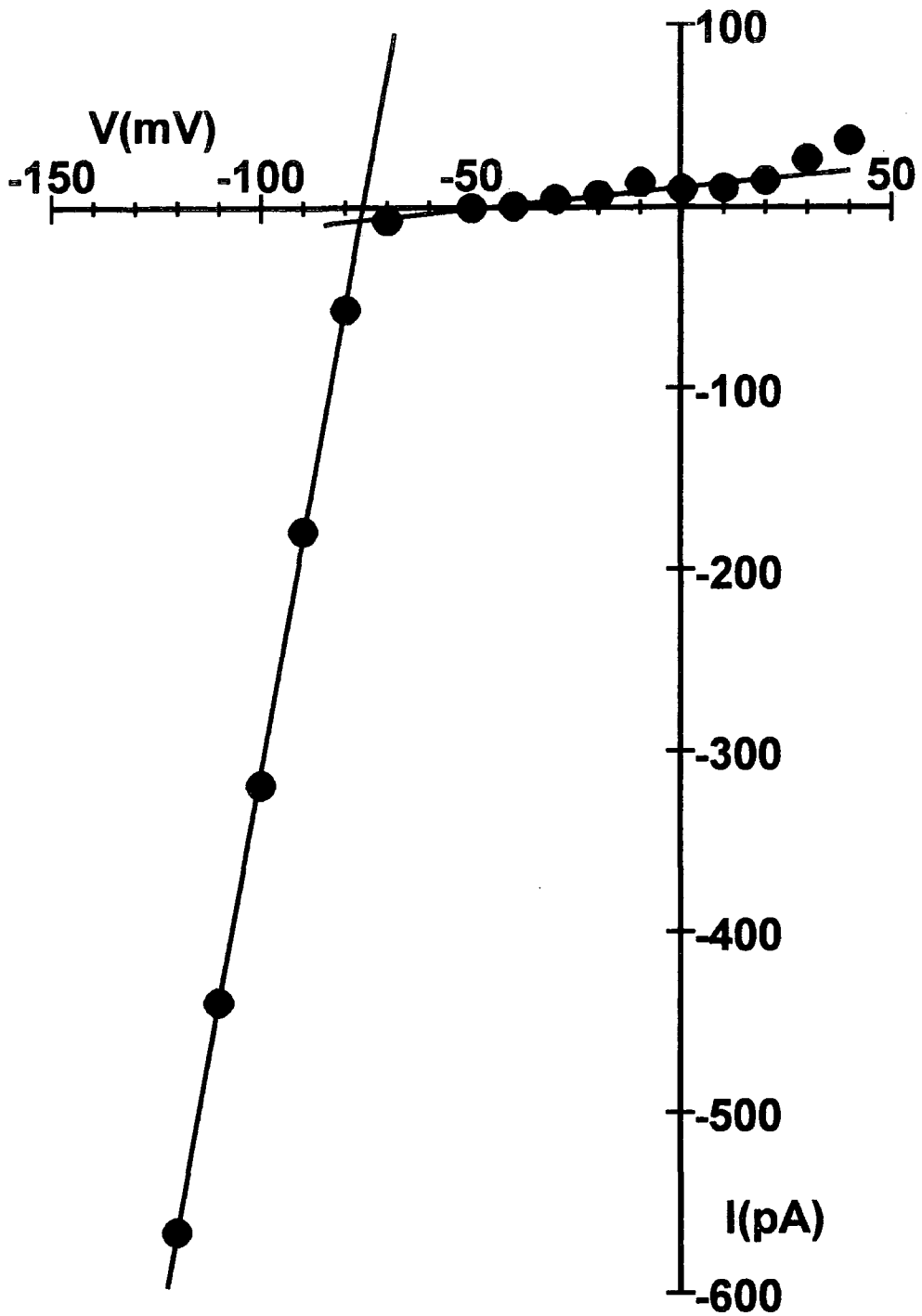
V(mV)
-150
-100
-50
50
100
-100
-200
-300
-400
-500
I(pA)
-600

linear (see Fig. 3.19 B and C) over this range and the input resistance of the cells could be calculated. This was found to be $1.64 \pm 0.17 G\Omega$, mean $\pm$ S.E.M. $n = 33$.

3.3.2 The Potassium Anomalous Rectifier Current

3.3.2.1 Current–Voltage Relationship

The large inward current demonstrated in Fig. 3.2 is typical of the behaviour of the potassium inward rectifier current, or the anomalous rectifier, which has been well documented in horizontal cells (see Table 3.3 A for references). Hyperpolarization resulted in large inward currents with the I–V curve approximately linear for potentials more negative than $-80mV$ while depolarization produced much smaller outward currents. No attempt was made to study the small outward currents, as this would have required blocking the various other currents present at these potentials. However the inward current totally dominated the I–V relationship at potentials more negative than $-80mV$ so it was not necessary to block other currents in order to study it at these potentials.

The voltage dependence and magnitude of this current was not affected by the hold potential used, as shown in Fig. 3.11. Two hold potentials ($-50mV$ and $-70mV$) were used and although the I–V relationship was affected at potentials more positive than around $-30mV$ there was no difference in the voltage dependence and magnitude of the large inward current evoked by hyperpolarization beyond $-80mV$. As long as the hold potential was more positive than the potassium equilibrium the magnitude and I–V relation of the hyperpolarization induced inward current was not affected ($n = 5$).

However, the magnitude of the current observed in different cells varied widely. The mean current from 11 cells at potentials more negative than the hold potential of $-60mV$ is shown in Fig. 3.12. The large error bars are indicative of the wide range of current amplitudes measured in different cells. For example the current measured on a $50mV$ hyperpolarizing pulse from the hold potential varied from $219pA$ to $1220pA$.

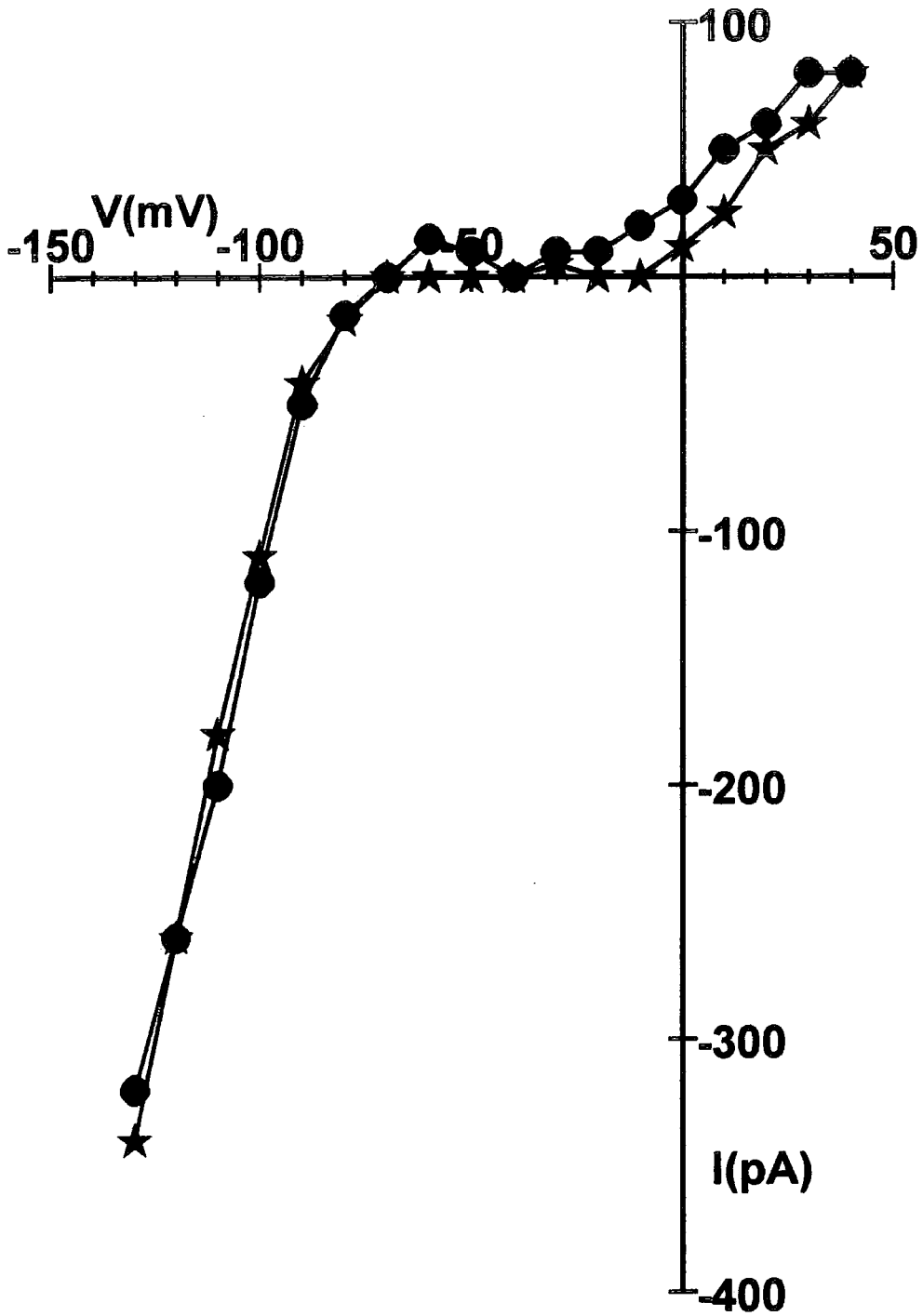
100
V(mV)
-150
-100
-50
50
-100
-200
-300
I(pA)
-400

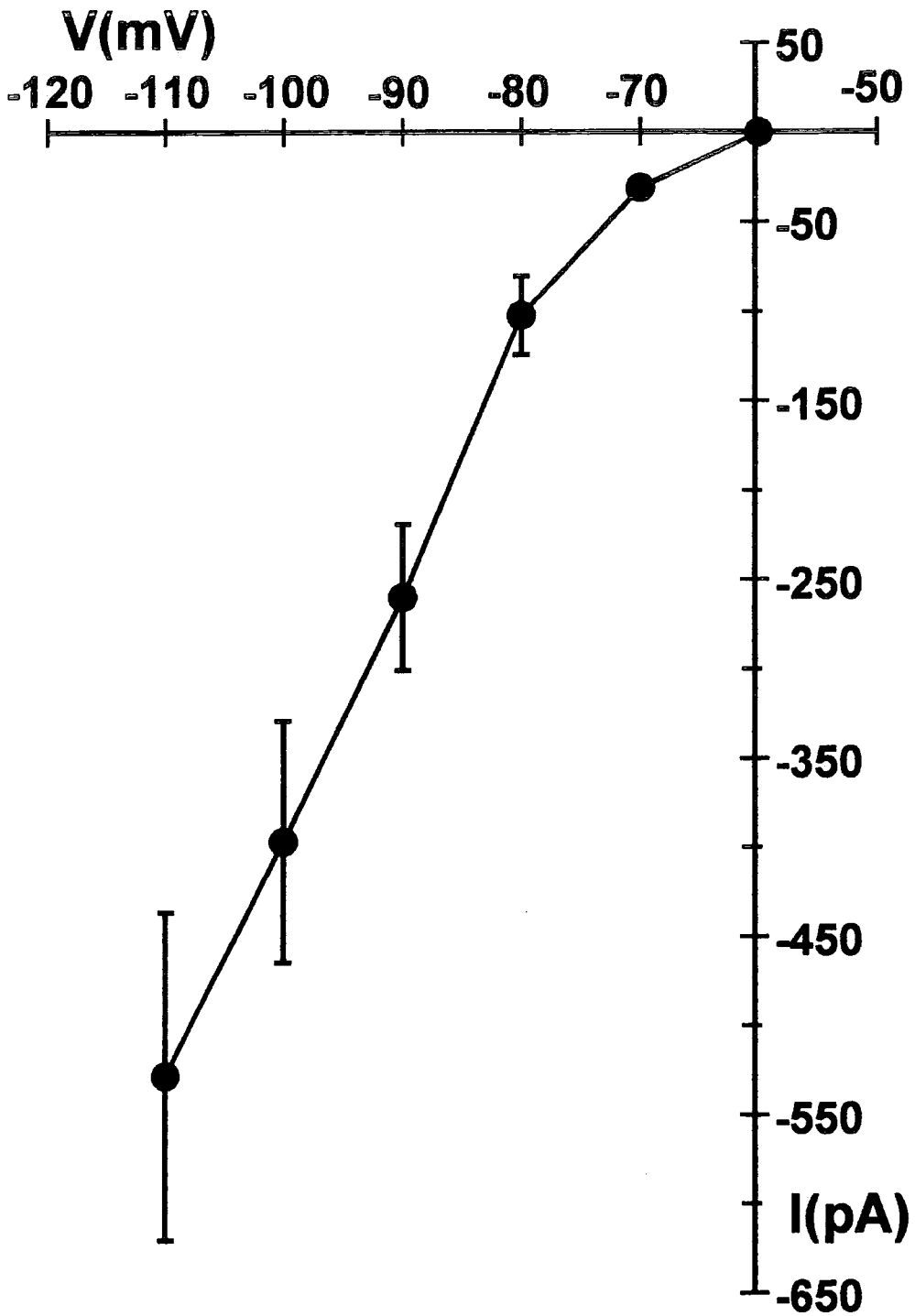
V(mV)
-120
-110
-100
-90
-80
-70
50
-50
-50
-150
-250
-350
-450
-550
I(pA)
-650

3.3.2.2 Effect of Rubidium and Barium

The effect of barium and rubidium on this current was tested. The addition of $1mM$ barium to the saline reduced the inward current by more than 90% (Fig. 3.13). The difference between the I–V relationship in the presence and absence of the Ba^{2+} shows the characteristic strong rectification of the anomalous rectifier (Fig. 3.13 B). The addition of the same concentration of rubidium ($1mM$) also reduced the current amplitude, in this case by about 60% (Fig. 3.14). If however all the potassium in the saline ($4mM$) was replaced by rubidium the current amplitude was reduced by more than 90% (Fig. 3.15).

3.3.2.3 Effect of Varying Extracellular Potassium Concentration

The voltage dependence of the current was found to shift as a result of changes in the extracellular potassium concentration (Fig. 3.16). The same cell was exposed to increasing extracellular potassium concentrations rising from $4mM$ to $100mM$ (with corresponding reductions in sodium concentration). The onset of the large inward current occured at more depolarized potentials as the extracellular potassium concentration was increased. The shift in voltage dependence brought about by a 1 log change in the extracellular potassium concentration (from $10mM$ to $100mM$) was about $58mV$. This is as would be expected (Hagiwara *et al.*, 1976; Hille, 1992) because the voltage characteristics of this current type are effectively controlled by the potassium equilibrium potential (Section 3.17). The gradient of the I–V curve increased, in the region of the maximum current, with increasing potassium concentration because of the increase in number of ions able to carry charge through the channels. The membrane resistance of the cell was calculated as being (in $M\Omega$) 54.2, 32.3, 22.6 and 12.4 for extracellular potassium concentrations of (in mM) 4, 10, 30 and 100 respectively.

If the points at which the linear regions of the I–V curves cross the zero current axis (indicated by arrows in Fig. 3.16) are plotted against log extracellular potassium concentration they should form a straight line with a gradient of 57.5 (assuming a base 10 log scale and a temperature of 17°C) as predicted by Nernst (Hille, 1992). The results from four cells exposed to the same extracellular potassium concentrations are shown in Fig. 3.17. They all show the same linear relationship, at least at the higher potassium concentrations, with gradients reasonably close

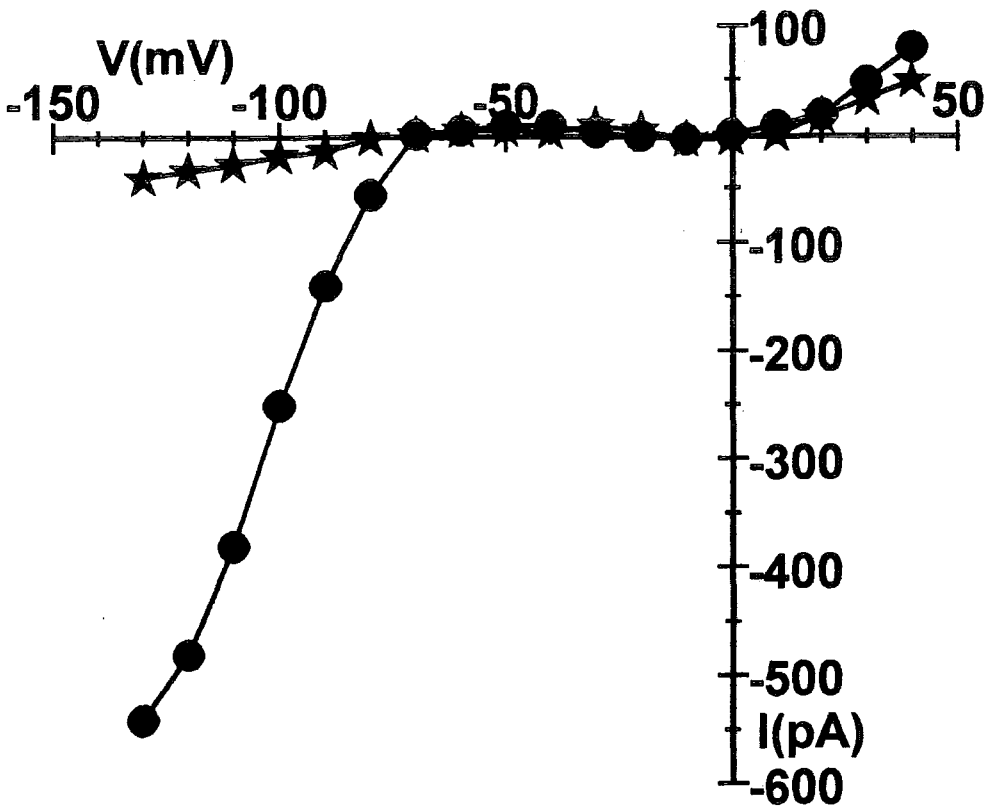
V(mV)
-150
-100
-50
50
100
-100
-200
-300
-400
-500
I(pA)
-600

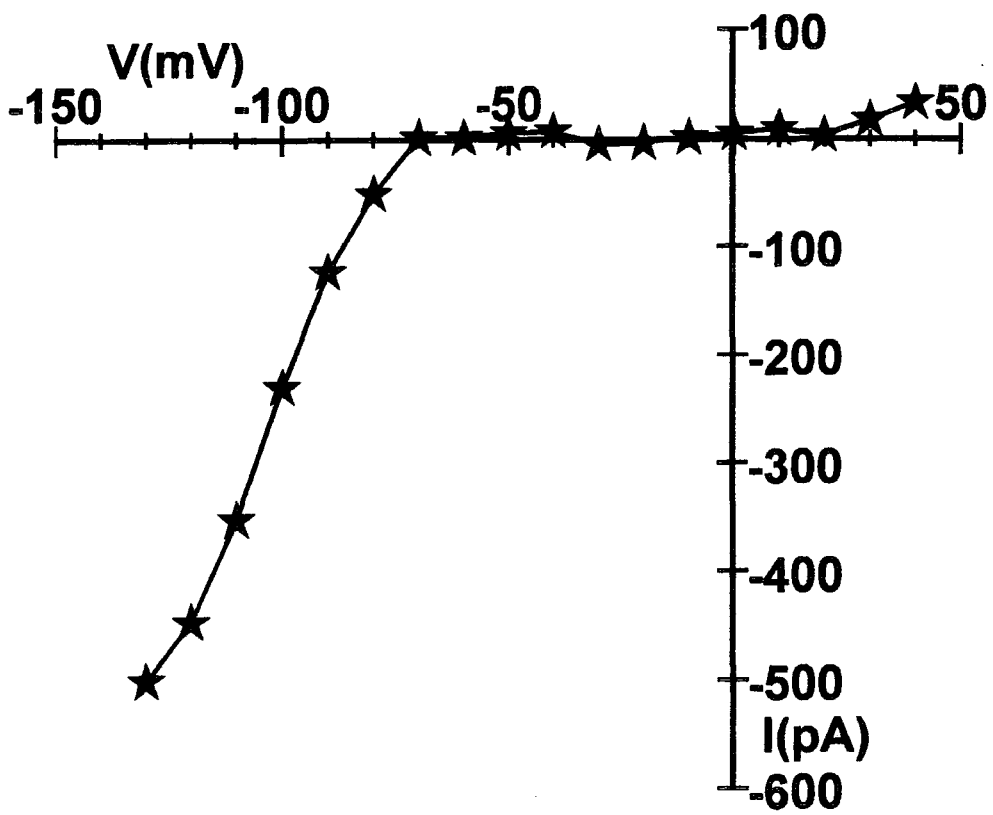
V(mV)
-150
-100
-50
50
100
-100
-200
-300
-400
-500
I(pA)
-600

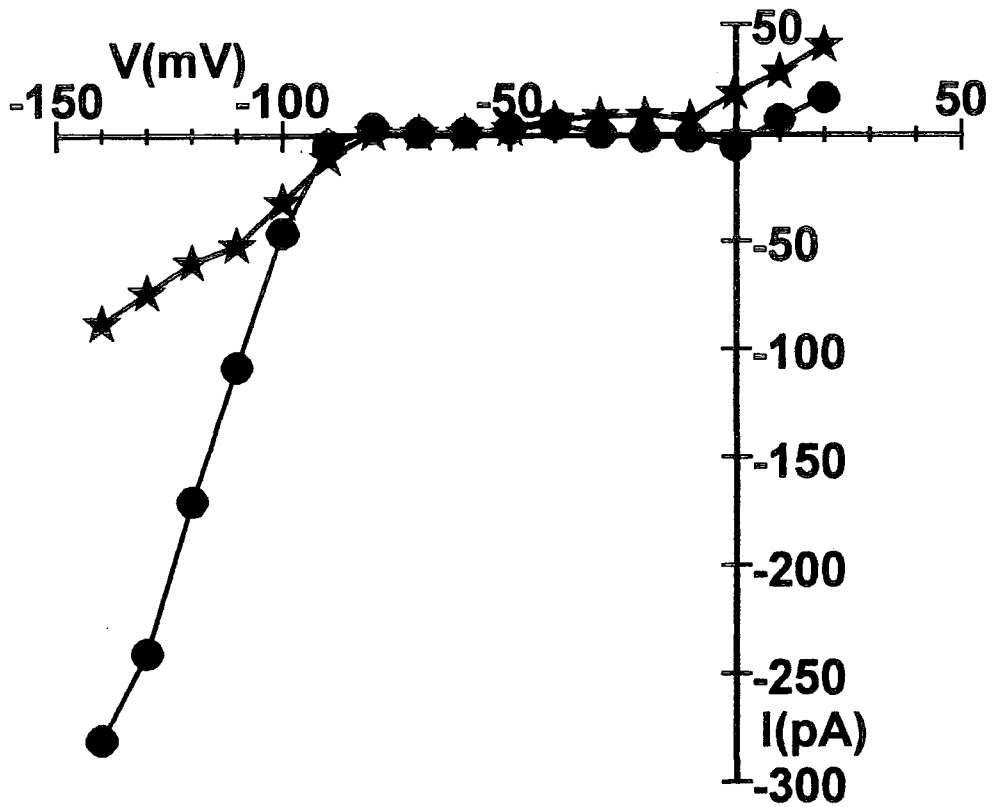
V(mV)
-150
-100
-50
50
50
-50
-100
-150
-200
-250
I(pA)
-300

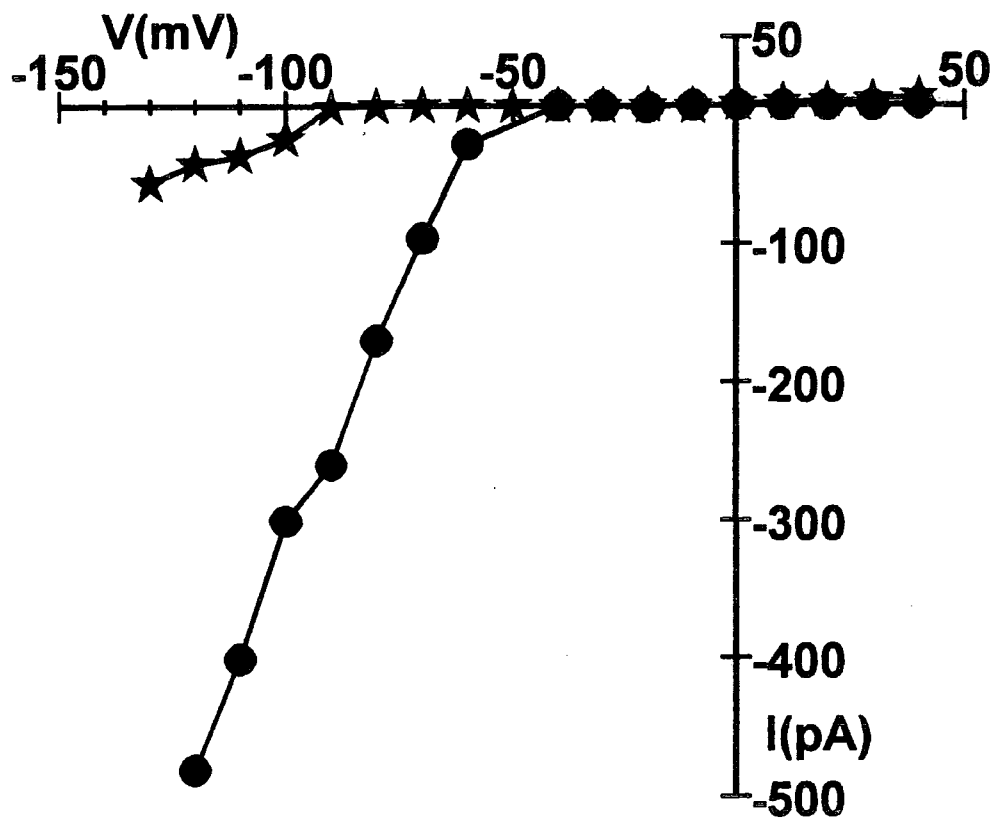
V(mV)
-150
-100
-50
50
50
-100
-200
-300
-400
I(pA)
-500

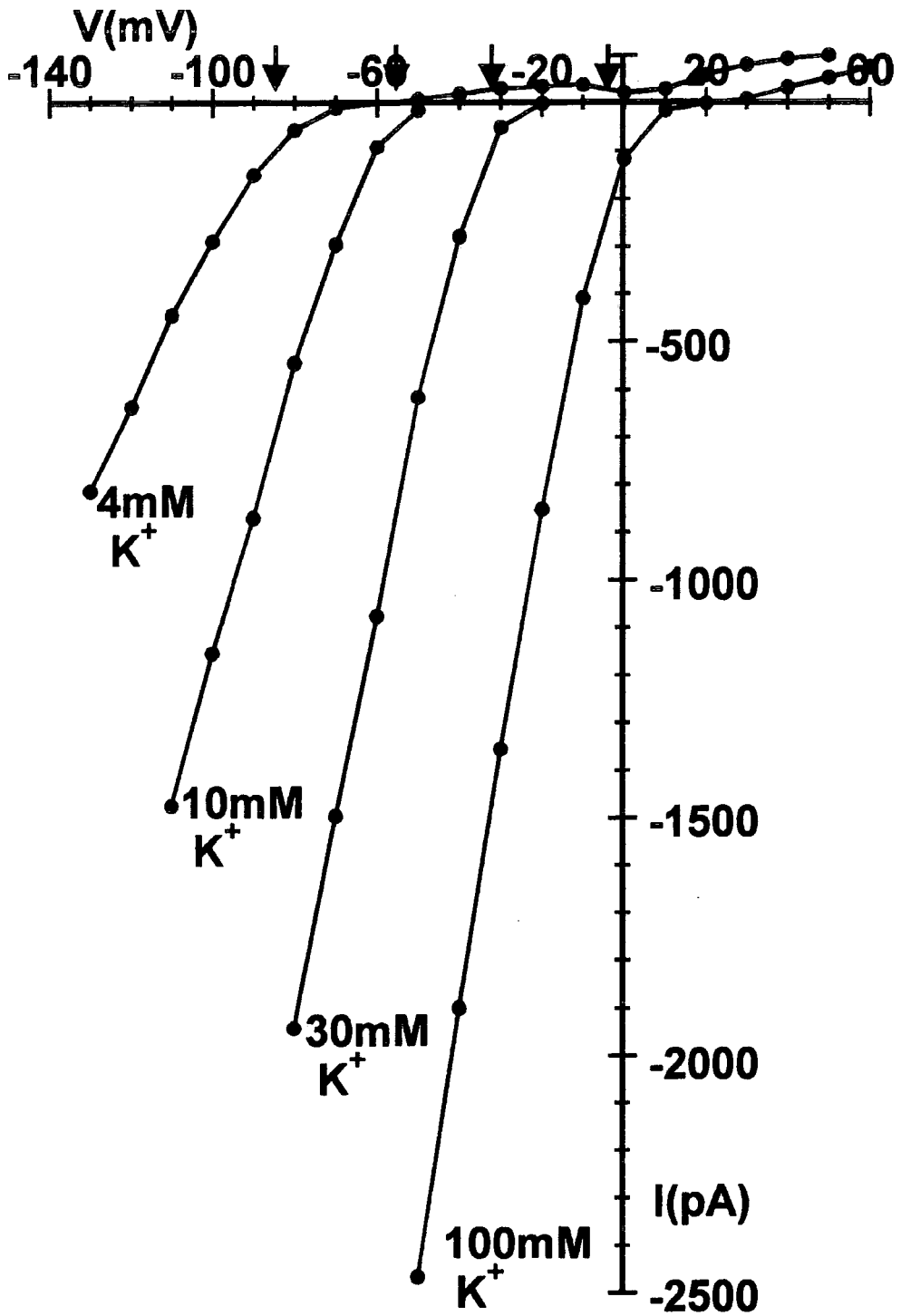
V(mV)
-140
-100
-60
-20
20
60
-500
-1000
-1500
-2000
-2500
I(pA)
4mM
K+
10mM
K+
30mM
K+
100mM
K+

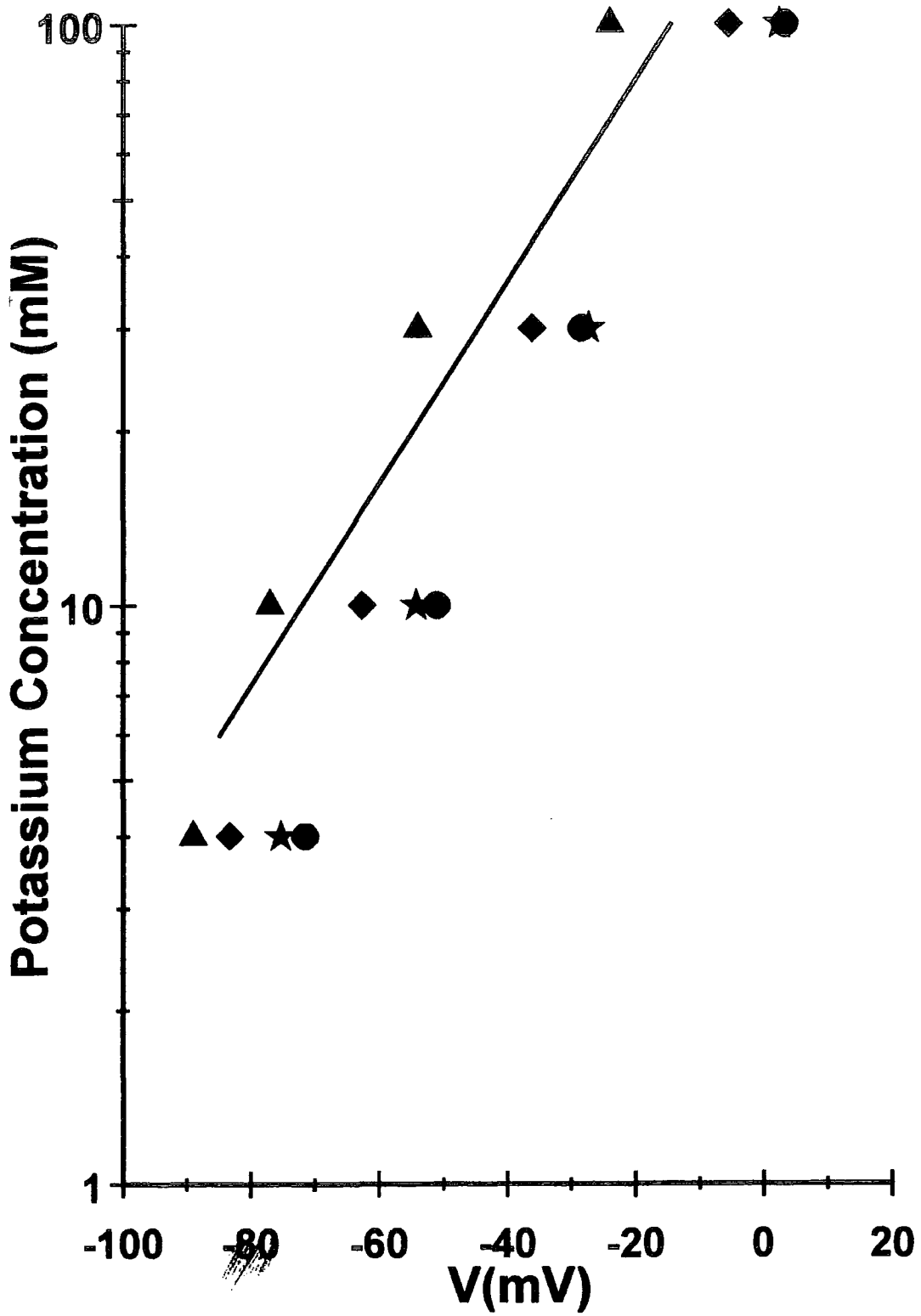
100
10
1
Potassium Concentration (mM)
-100
-80
-60
-40
-20
0
20
V(mV)

to 57.5 as predicted. However there is variation between the individual cells with some displacement of the lines along the potential axis.

3.3.2.4 Effect of Acclimation Temperature

As already mentioned all the results up to now have been at experimental temperatures of 17°C and the cells have been from retinas from fish acclimated to 16°C. Fish were acclimated to 8°C, 16°C and 26°C, as described in Section 2.2.1, and the results were compared to find out if there was any change in the current characteristics brought about by the acclimation process. All experiments were carried out at 17°C.

As can be seen in Fig. 3.18 the wide variation in current amplitudes resulting in very large error bars means that there is no significant difference between any of the current amplitudes at the same potential for the different acclimation temperatures. In order to compare the voltage dependence of the current from cells from different acclimation temperatures the point at which the linear region of the I–V curve crossed the zero current line was calculated for the different cells in saline containing $4mM$ potassium (Table 3.4).

Table 3.4. The effect of acclimation temperature on the voltage dependence of the anomalous rectifier at an experimental temperature of 17°C.

Acclimation Temperature	Mean ± S.E.M.	n
8°C	78.1 ± 2.1	8
16°C	72.2 ± 2.1	11
26°C	76.5 ± 4.0	11

There was no significant difference between any of these results ($p > 0.05$ Students t–Test) suggesting that there was no significant change in the voltage dependence of the anomalous rectifier current with temperature acclimation.

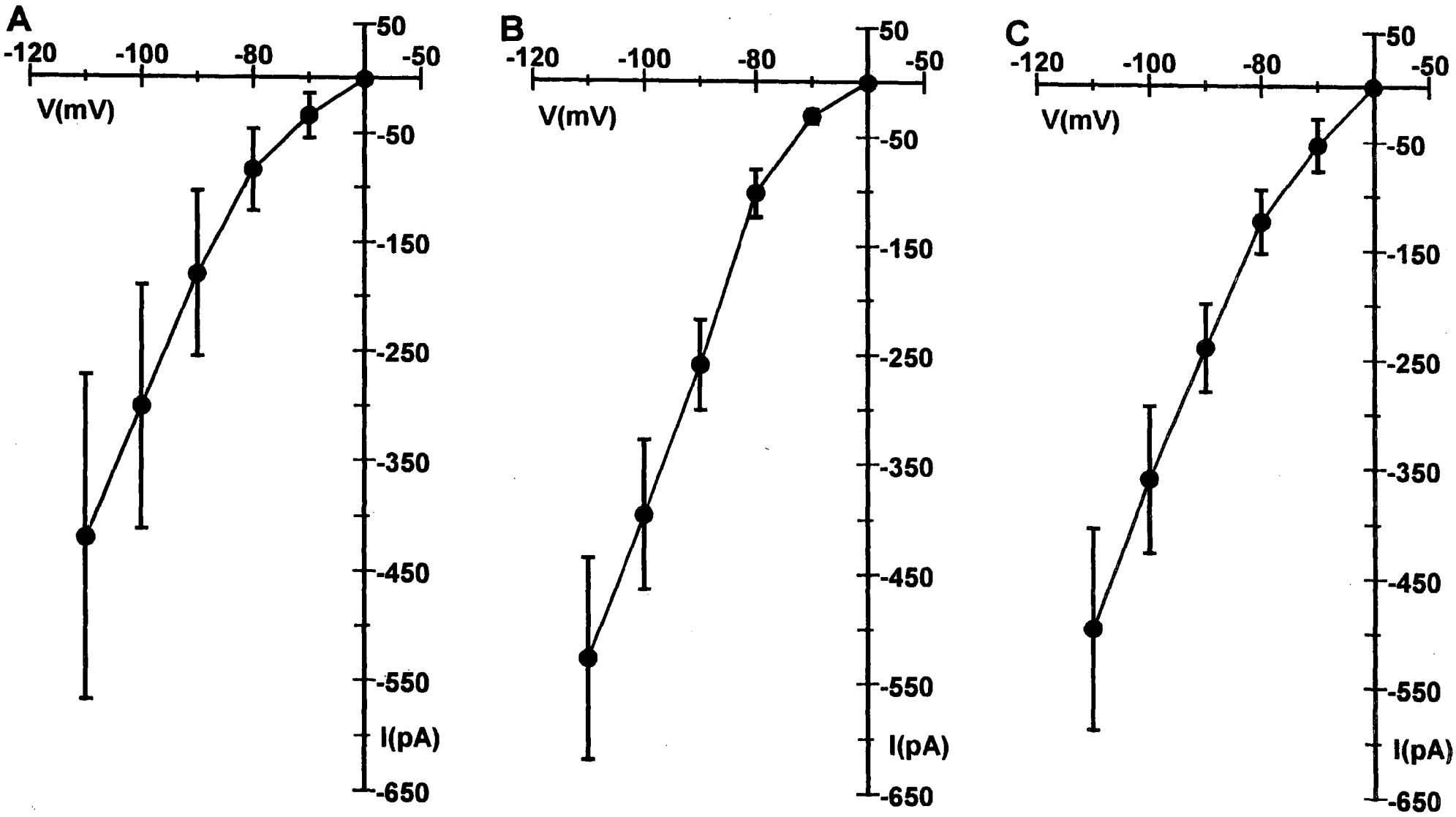
A
-120
-100
-80
-50
V(mV)
50
-50
-150
-250
-350
-450
-550
I(pA)
-650
B
-120
-100
-80
-50
V(mV)
50
-50
-150
-250
-350
-450
-550
I(pA)
-650
C
-120
-100
-80
-50
V(mV)
50
-50
-150
-250
-350
-450
-550
I(pA)
-650

3.3.3 The Sustained Calcium Current

3.3.3.1 Current–Voltage Relationship

A sustained calcium current has been demonstrated in horizontal cells from many different species (Table 3.3 B). In order to demonsrate a Ca^{2+} current inward potassium currents were blocked with extracellular TEA and 4–AP, and Ba^{2+} was used as the charge carrier. The saline used consisted of (in mM): NaCl, 79; TEA, 20; 4–AP, 10; $BaCl_2$, 10; KCl, 4; $MgCl_2$, 1; HEPES, 10; Glucose, 10; buffered to pH 7.5 with NaOH/HCl. The use of Ba^{2+} has a number of advantages (Bean, 1992). For example it blocks the inward retifier (Fig. 3.13) and magnifies the current passing through L–type calcium channels (Fox *et al.*, 1987). The inward transient current was still observed in many of the recordings, but as it is fully inactivated well within $100ms$ and the sustained currents were only measured after voltage changes of at least $450ms$ this did not interfere with the results.

The results of a typical recording are shown in Fig. 3.19 A. The cell was voltage clamped to potentials from $-50mV$ to $+60mV$ for $500ms$, in $10mV$ steps, from a hold potential of $-60mV$. An inward current was activated at potentials more positive than $-10mV$ and reached a maximum at a clamp potential of $+10mV$ before reducing and showing an apparent reversal potential of $+50mV$. There was no sign of inactivation over the $500ms$ depolarization of this current although a small transient inward current was seen at less depolarized potentials.

This sustained inward current could be blocked with $5mM$ Co^{2+} to leave only a leakage current (see Section 3.3.1) which was linear at potentials between $-60mV$ to $0mV$ (Fig. 3.19 B). This current was subtracted from the sustained current in Fig. 3.19 A to give the total Co^{2+} sensitive current as shown in Fig. 3.19 C. The mean current from 9 cells is shown in Fig. 3.20. There was less variation in the current amplitude for this current than for the potassium inward rectifier (cf. Fig. 3.12). The current activated at around $-30mV$, reached a maximum at $+10mV$ and appeared to reverse at about $+60mV$.

3.3.3.2 Effect of Dopamine and Dibutyryl cAMP

Pfeiffer–Linn and Lasater (1993) showed that the sustained calcium current

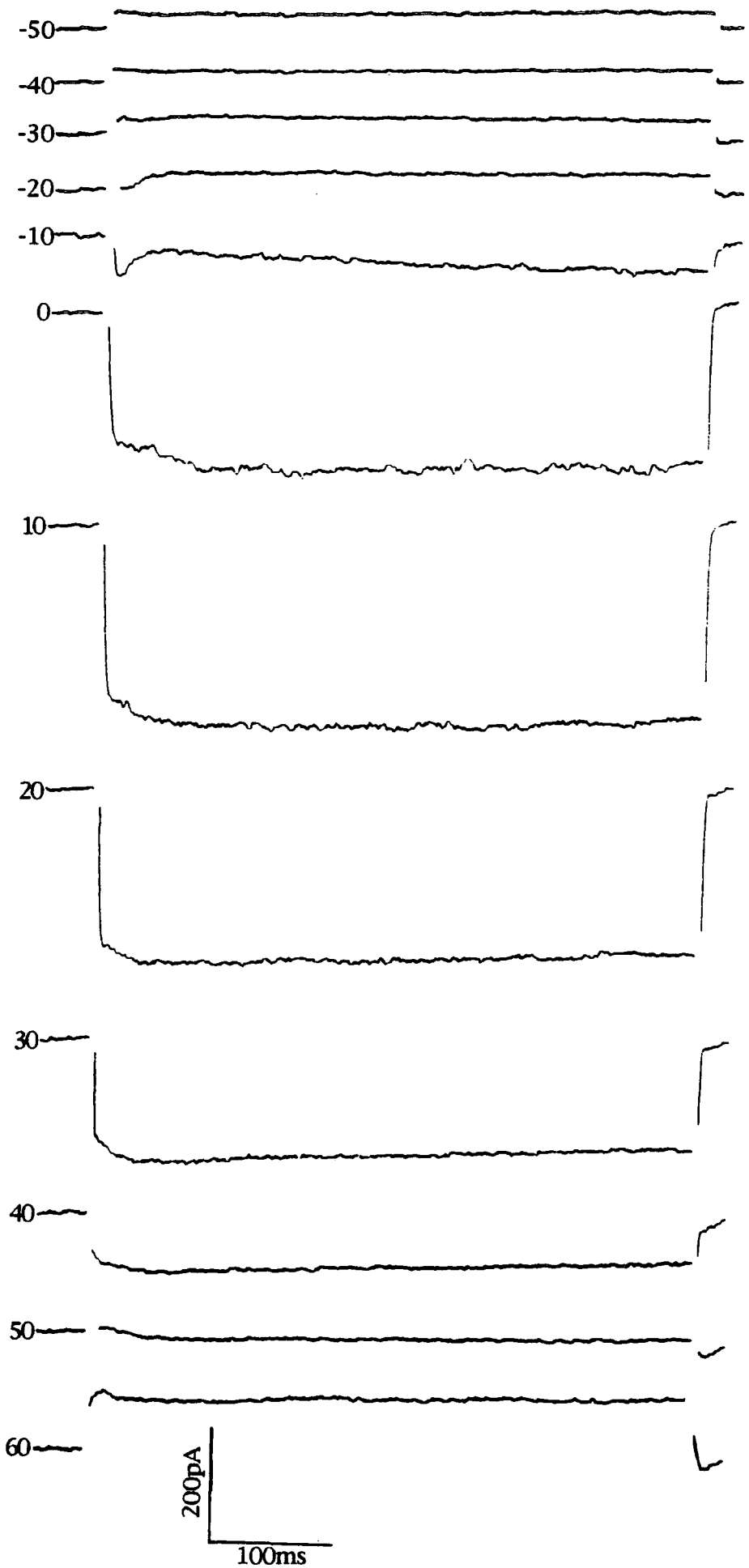
-50
-40
-30
-20
-10
0
10
20
30
40
50
60
200pA
100ms

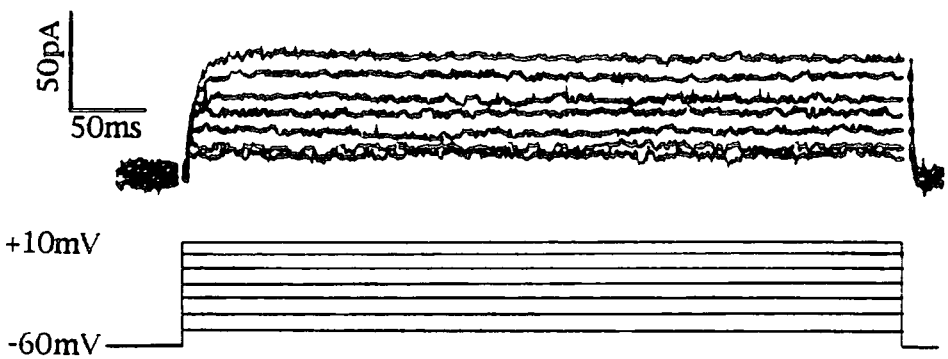
50pA
50ms
+10mV
-60mV

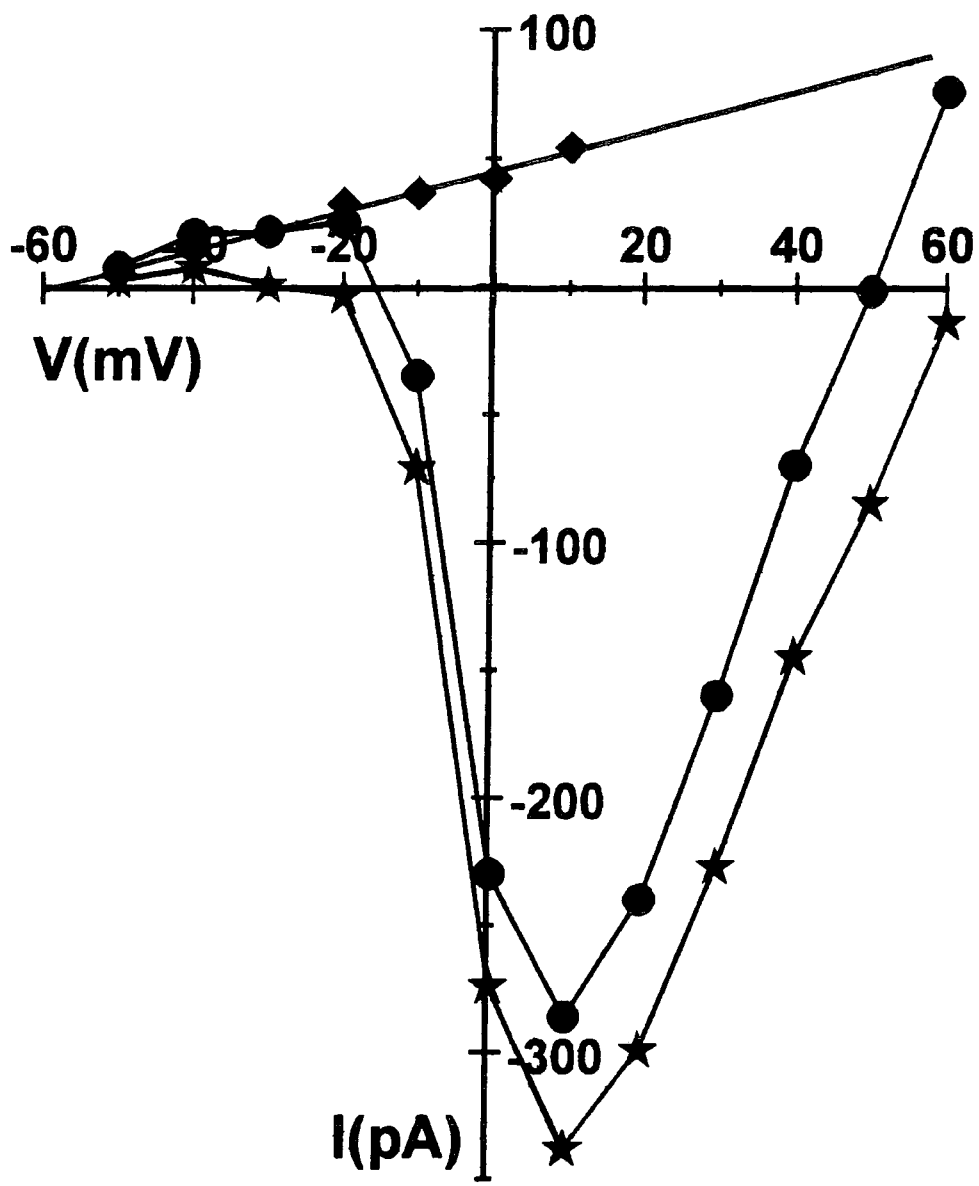
100
-60
-20
20
40
60
V(mV)
-100
-200
-300
I(pA)

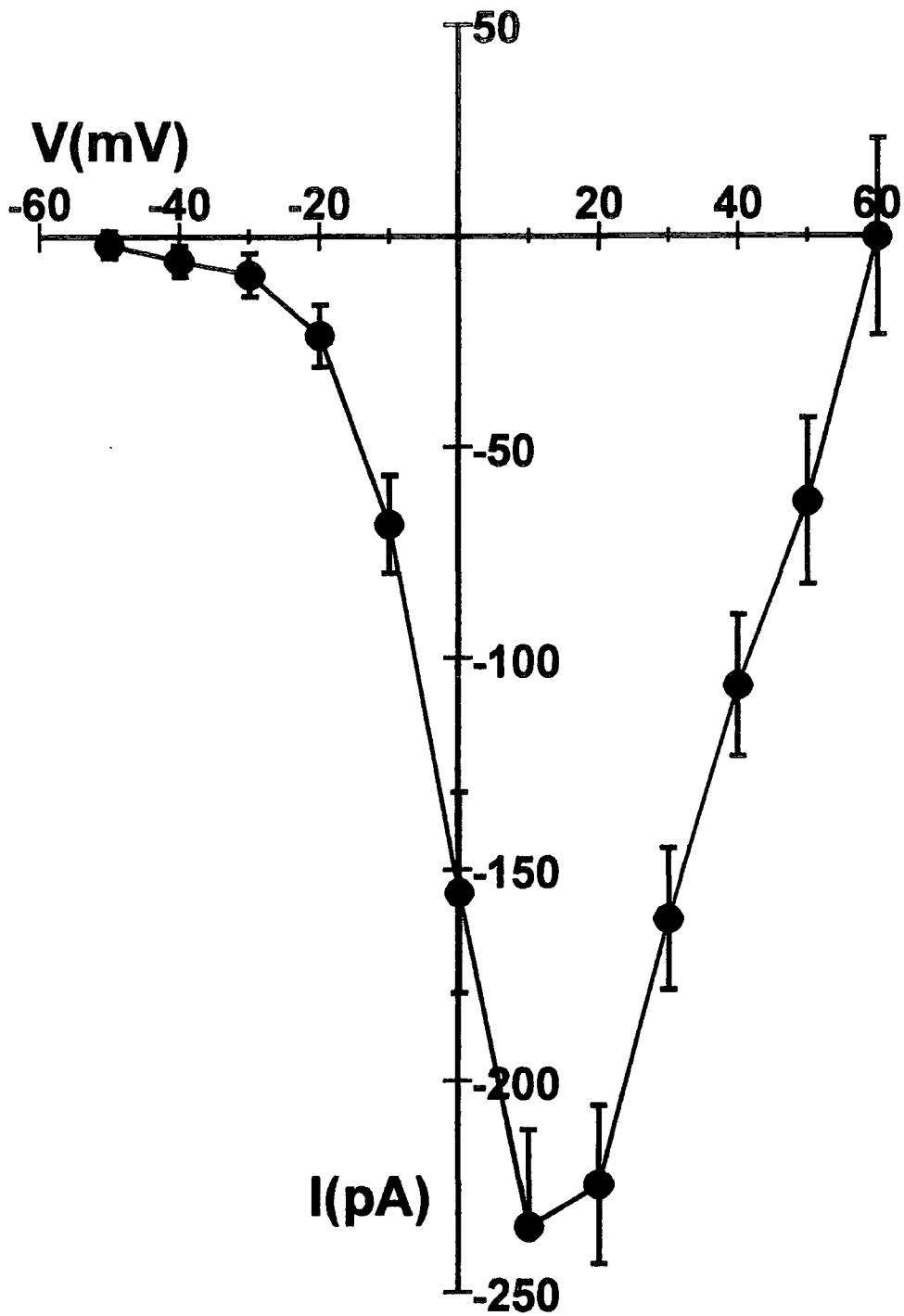
V(mV)
-60
-40
-20
20
40
60
50
-50
-100
-150
-200
-250
I(pA)

in white bass horizontal cells was increased by dopamine acting via cAMP. They found that dopamine concentrations of $20\mu M$ and above achieved the maximum effect, which was similar to the effect of the application of a membrane permeable derivative of cAMP at a concentration of $50\mu M$. Van Buskirk and Dowling (1981) found that carp horizontal cells demonstrate an at least 400 fold increase in intracellular cAMP concentration on application of $200\mu M$ dopamine. The response shown by white bass horizontal cells reached a maximum after about three minutes. In order to study the effect of comparable concentrations of dopamine and dibutyryl cAMP over a similar time period the current induced by depolarizing cells from a hold potential of $-60mV$ to $0mV$ for $500ms$ was recorded every thirty seconds for five minutes. The cells were exposed to $200\mu M$ dopamine or $50\mu M$ dibutyryl cAMP after 1 minute. Controls, where no drug was added, were also carried out.

In the control results the amplitude of the calcium current surprisingly showed a slight increase over the first $\sim 1\frac{1}{2}$ minutes after rupturing the cell membrane to make whole cell recordings, before subsequently declining (Fig. 3.21). After five minutes the current was 88.3 $\pm$ 6.4% (mean $\pm$ S.E.M. n=3) of the initial amplitude recorded.

The addition of $200\mu M$ dopamine and $50\mu M$ dibutyryl cAMP had no effect on the amplitude of the current over this time period (Fig. 3.22). The current amplitude was slightly increased after $\sim 1\frac{1}{2}$ minutes when the dopamine/dibutyryl cAMP was added but the time–amplitude relationship of the currents under the three conditions were indistinguishable.

3.3.3.3 Effect of Acclimation Temperature

Sustained calcium currents were recorded from cells from fish acclimated to 8°C, 16°C and 26°C at an experimental temperature of 17°C to see if the acclimation temperature had any effect on the current–voltage relationship or current amplitude. A total of 8, 9 and 14 cells from these acclimation temperatures respectively were recorded and the current–voltage relationships are compared in Fig. 3.23. A comparison of various aspects of the current recorded from cells from fish acclimated to the different temperatures is given in Table 3.5.

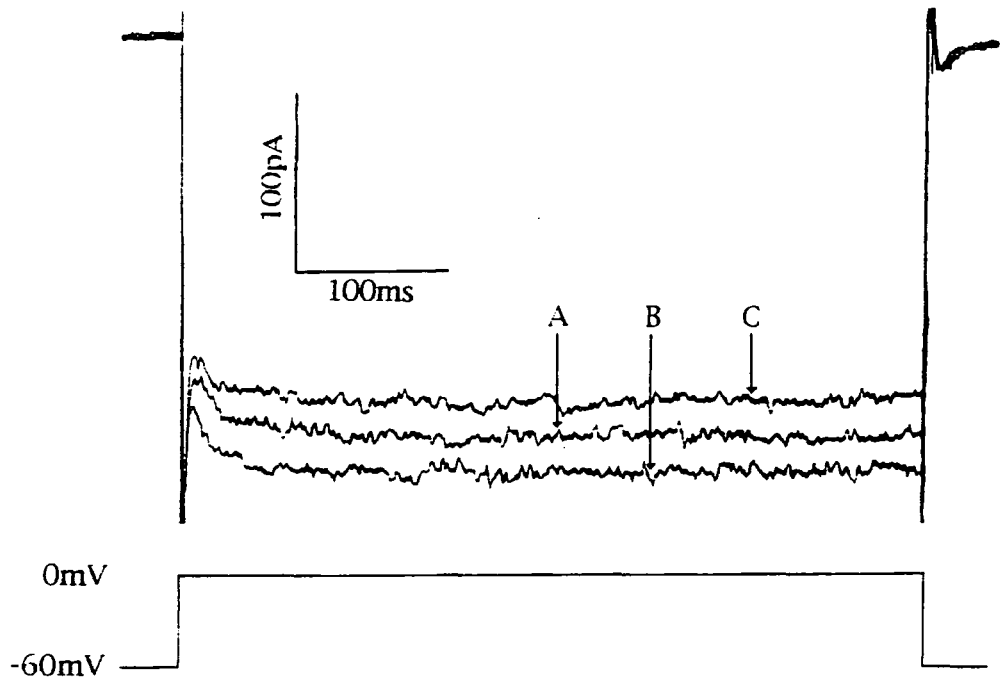

Figure 3.21. The amplitude of the inward current recorded on a $500ms$ test potential of $0mV$ from a hold potential of $-60mV$ A, 30 seconds B, 90 seconds and C, 300 seconds after the start of whole cell recordings.

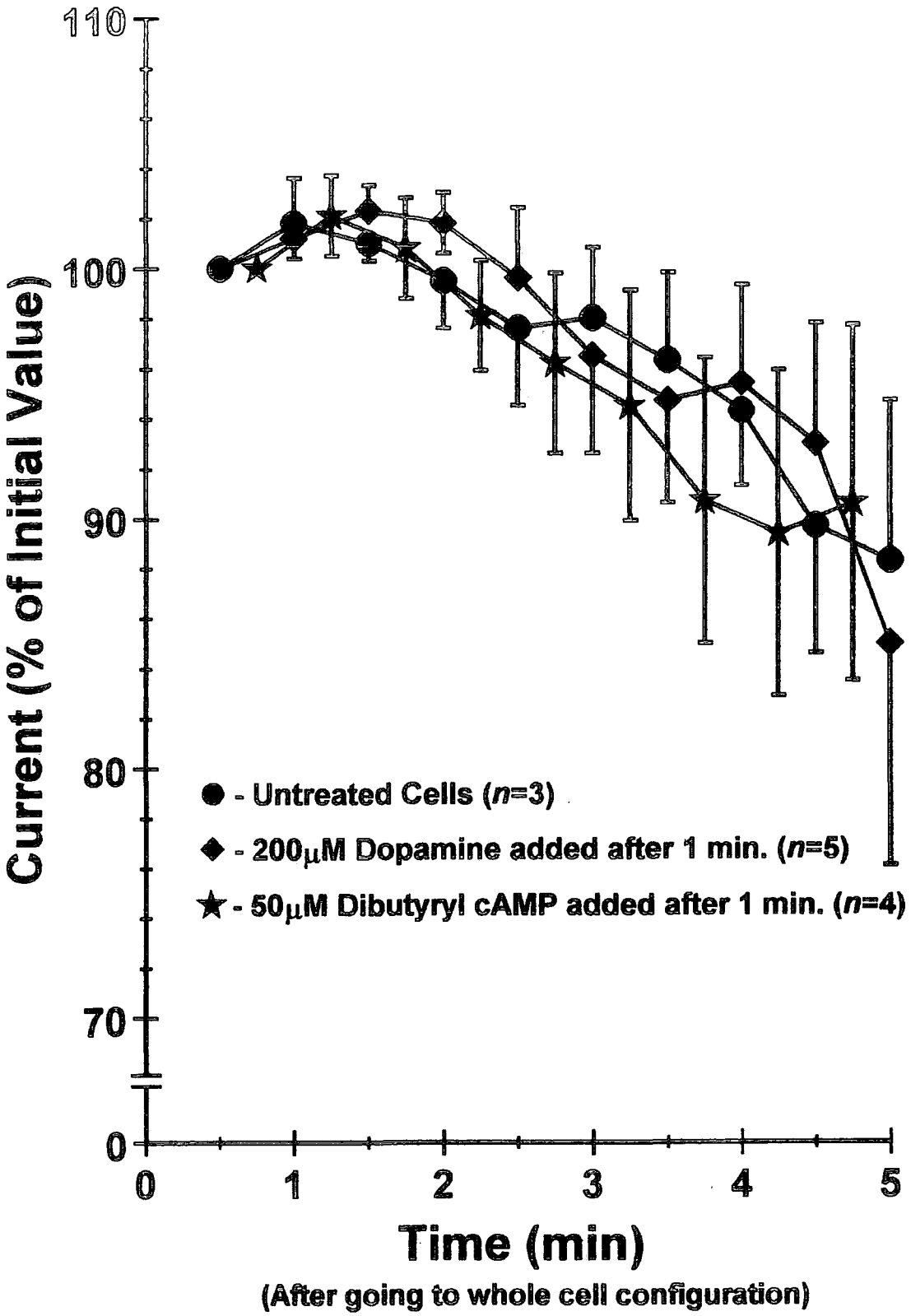
110
100
90
80
70
0
0
1
2
3
4
5
Current (% of Initial Value)
Time (min)
(After going to whole cell configuration)
● - Untreated Cells (n=3)
◆ - 200μM Dopamine added after 1 min. (n=5)
★ - 50μM Dibutyryl cAMP added after 1 min. (n=4)

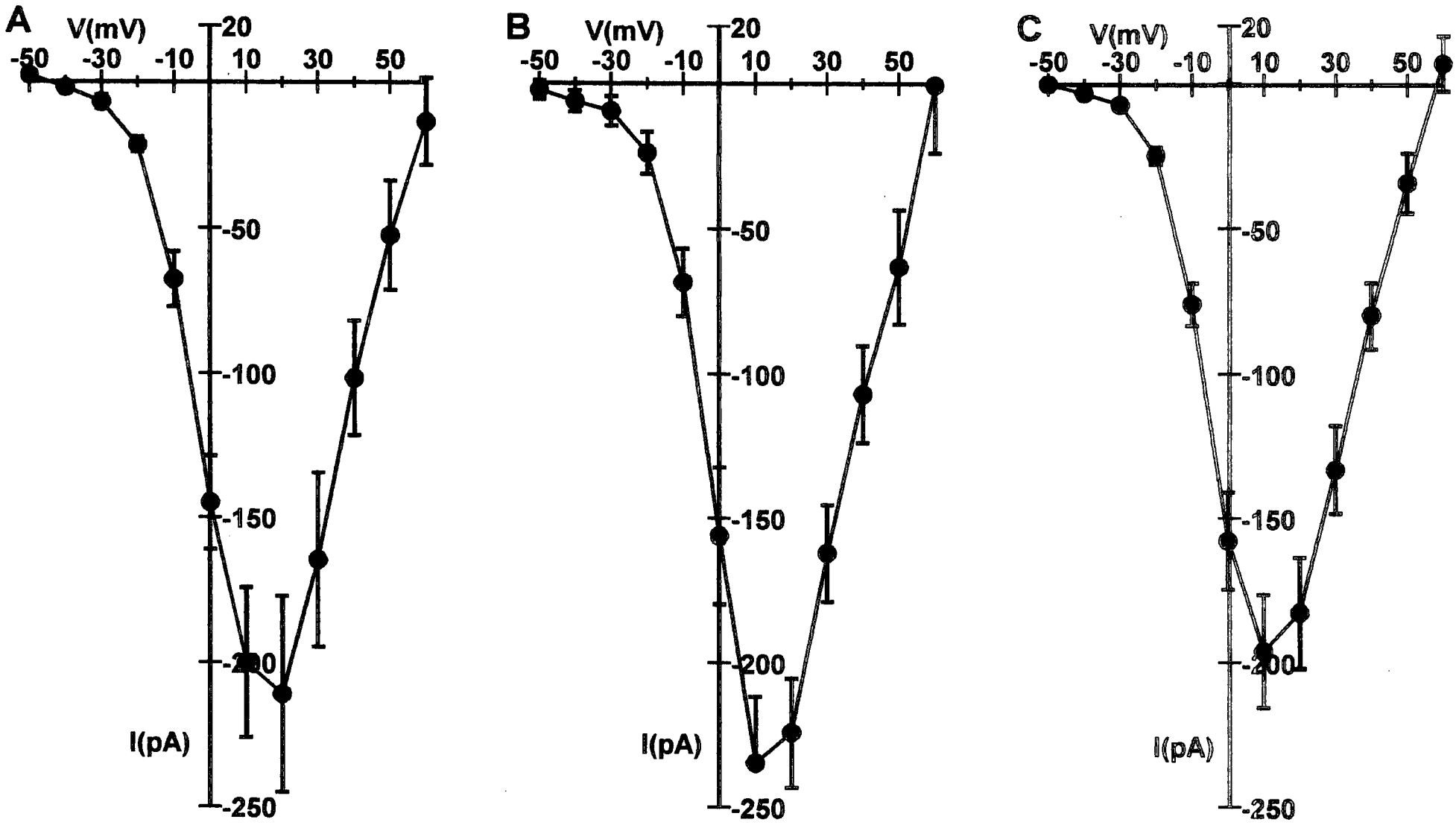
A
V(mV)
-50
-30
-10
10
30
50
20
-50
-100
-150
-200
-250
I(pA)
B
V(mV)
-50
-30
-10
10
30
50
20
-50
-100
-150
-200
-250
I(pA)
C
V(mV)
-50
-30
-10
10
30
50
20
-50
-100
-150
-200
-250
I(pA)

Table 3.5. The effect of acclimation temperature on the mean (± S.E.M.) of the maximum current amplitude, the membrane potential at which it was recorded, the estimated membrane potential at which 10% of the maximum current occured, and the estimated reversal potential of the current. All results were at an experimental temperature of 17°C.

	Acclimation Temperature		
	8°C	16°C	26°C
Maximum Current Amplitude	$212 \pm 34pA$	$235 \pm 23pA$	$196 \pm 20pA$
Membrane Potential for 10% of Maximum Current	$-21mV$	$-20mV$	$-23mV$
Membrane Potential for Maximum Current	$+20mV$	$+10mV$	$+20mV$
Estimated Reversal Potential	$+65mV$	$+61mV$	$+58mV$

As can be seen the characteristics in Table 3.5 do not show much variation between the acclimation temperatures. In fact the current amplitudes measured at any single test potential from cells from fish acclimated to different temperatures were not significantly different ($p > 0.05$ Student's t–Test).

3.4 DISCUSSION

3.4.1 Whole Cell Total and Leakage Currents

The total current–voltage relationship recorded from isolated carp horizontal cells on depolarizing and hyperpolarizing voltage–clamp test potentials from a hold potential of $-60mV$ are similar to those recorded from white perch (Lasater, 1986), turtle (Golard *et al.*, 1992), *Xenopus* (Akopain and Witkovsky, 1994) and zebrafish (McMahon, 1994). The presence of a large anomalous rectifier current on hyperpolarization beyond about $-70mV$ to $-80mV$ (in an extracellular potassium concentration of 3 to $4mM$) and the activation of a small sustained current on depolarization beyond about $-20mV$ is common. The rapidly inactivating transient inward current on depolarization is also found in horizontal cells from all these species except the zebrafish where it was not reported (McMahon, 1994). The main difference in the results from the carp horizontal cells is in the outward current activated on large depolarizing test potentials. Depolarization beyond around $-20mV$ does result in progressively larger (on increasing depolarization) outward currents, but unlike the results from the above species there is no time dependent inactivation of the current (Fig. 3.2). However this is in agreement with the unpublished observation by Lasater (1986) that there is no transient outward potassium current in carp horizontal cells.

In the intact retina the membrane potentials recorded from horizontal cells range from a resting potential of about $-15mV$ to $-30mV$ in the dark to around $-70mV$ to $-80mV$ when the retina is brightly illuminated (see Chapter 2). Over the greater part of this range the lack of sustained currents means that the membrane resistance of the cells is high. This contributes to the lateral spread of the signal in the horizontal cell syncitium and also means that the energy requirement to maintain the membrane potential in the dark is low.

It has been suggested (Perlman *et al.*, 1993) from studies on the effects of TEA and 4–AP on horizontal cell responses in the intact retina, that the outward potassium currents seen in the isolated turtle horizontal cells may be involved in the shaping of the cells' responses to the offset of bright light stimuli in the intact retina. The rapidly inactivating inward current (Figs. 3.2 and 3.3 and seen in almost all other isolated horizontal cells) is usually attributable to a TTX

sensitive sodium current (though see Sullivan and Lasater (1992) where a transient calcium current contributes). Although a TTX sensitive transient current might also be expected to contribute to the rapid depolarization seen on the offset of a light stimulus there is no observable change in the horizontal cell response from an intact retina when it is superfused with TTX (Djamgoz and Stell, 1984; Perlman *et al.*, 1993).

The ability to block all sustained currents, at least between the membrane potentials of $-70mV$ and $0mV$, results in the linear current–voltage relationship of the leakage currents (Fig. 3.19). The measured membrane resistance between these potentials ($1.64 \pm 0.17G\Omega$ n=33) was similar to that recorded by Tachibana (1983a, b) from goldfish horizontal cells ($2.2 \pm 0.6G\Omega$ n=21).

3.4.2 The Anomalous/Inward Rectifier

The inward current seen at potentials more hyperpolarized than about $-70mV$ in $4mM$ extracellular potassium is typical of all isolated horizontal cells studied to date (see Table 3.3 A for references). The shift in voltage dependence on changes in extracellular potassium concentration and the block by barium and rubidium are all indicative of the anomalous rectifier current (see section 3.1.7).

The wide variation in the amplitude of this current in the horizontal cells (Fig. 3.12) cannot be attributed to differences in the surface area of the cells, as if this were the case the calcium currents and leak currents of the cells would have shown similar large variations in amplitude. However if the inward rectifier is acting primarily as a 'latch' on the membrane potential preventing it from hyperpolarizing much beyond the potassium equilibrium potential but allowing it to 'swing free' when the cell is depolarized from the potassium equilibrium potential (Hille, 1992), then the absolute amplitude of the current would be less important than the fact that it is large compared to the other currents in the cell.

The variations in the current–voltage dependence of the current (Fig. 3.17 and Table 3.4) are less easily explained. If the voltage gating is entirely dependent on the potassium equilibrium potential then by controlling both the intracellular and extracellular potassium concentrations there should have been no variation in the potential at which the inward current was activated. The small tip diameter of the

patch pipette might suggest that the equilibration of the potassium concentrations may not occur rapidly and the variation in activation potentials may therefore be due to variations in the intracellular potassium concentration affecting the potassium equilibrium potential. However this seems unlikely because the time taken for small ions such as Na^+ and K^+ to reach equilibrium in a whole cell recording has been calculated as being at most a few tens of seconds (Marty and Neher, 1983). Also Hagiwara and Yoshii (1979) and Leech and Stanfield (1981) showed that the inward potassium rectifier in the starfish egg and frog skeletal muscle respectively was independent of the intracellular potassium concentration.

A more likely source of the variation comes from the effect of perfusing the cells while the experiments were being carried out. Randriamampita and Trautmann (1987) in macrophages and Perlman *et al.* (1988) in white perch horizontal cells showed that both the voltage gating and the amplitude of the inward potassium rectifier was affected by the movement of saline relative to the cell. The changes caused by perfusion (an up to $15mV$ negative shift in voltage gating and a significant reduction in the current amplitude) lead Perlman *et al.* to conclude that they were the result of changes in the boundry layer around the cell, and consequently the effective potassium concentration in the microenvironment around the cell. It is possible that, although the total perfusion rate was constant, the speed of the saline in different regions of the dish was different and this contributed to the variability in the voltage gating of the inward potassium current. The variations in the amplitude of the current between cells seen in these results are greater than those seen in white perch as a result of changing the perfusion rate and may not therefore be fully attributed to fluctuations in perfusion rate, although it may have contributed.

The action of a 'latch' on the free swinging membrane potential seems to be the most likely role for the inward rectifier current, i.e. ensuring that the membrane potential does not become too hyperpolarized in the light–stimulated state by effectively clamping the membrane potential close to the potassium equilibrium potential (Lasater, 1986, 1992). However if the inward rectifier does function in this way the position of the 'latch' will vary as the extracellular potassium concentration varies. The small extracellular space in the retina means that changes

in the fluxes of ions into and out of cells can have a significant effect on the extracellular concentrations of these ions. Different regions of the retina show different variations in the extracellular potassium concentration on illumination (Oakley and Green, 1976). The horizontal cell layer is affected both by a slow decrease in concentration originating in the photoreceptor layer and faster increases in concentration derived from the bipolar cells. The changes in potassium concentration actually experienced in the retina are reduced by the spatial buffering of the extracellular potassium concentration by the Muller cells (Newman *et al.*, 1984) but may vary over the range of $1.5mM$ to $5mM$ (Oakley and Steinberg, 1982). It is not possible to tell if the horizontal cells experience variations in extracellular potassium concentration over as large a range as this or to what extent it might affect the voltage gating of the inward rectifier, as at lower potassium concentrations the shift in voltage dependence of the current is less than is predicted by Nernst, due to competition by other ions (see Fig. 3.17).

The lack of any significant difference between the voltage gating and amplitude of the current from cells from fish acclimated to different temperatures (Fig. 3.18 and Table 3.4) suggests that there has not been any change in the charateristics of this channel type in response to the various acclimation temperatures.

3.4.3 The Sustained Calcium Current

The sustained inward current carried by Ba^{2+} in the presence of TEA and 4–AP and blocked by $5mM$ Co^{2+} (Fig. 3.19 C) is probably conducted through calcium channels (Byerly *et al.*, 1985; Bean, 1992). The amplitude and current–voltage relationship was more consistent for this current than for the anomalous rectifier (cf. Figs 3.20 and 3.12). It should be noted that by using $10mM$ Ba^{2+} the current–voltage relationship observed is not the same as that which the Ca^{2+} current in the intact retina would exhibit.

The increased extracellular concentration of the charge carrying divalent ion relative to the *in vivo* state and the different ionic species both alter the driving force of the ions through the channels. The higher concentration will depolarize the equilibrium potential and therefore shift the current–voltage relationship to the right on the potential axis (e.g. Byerly *et al.*, 1985, Figures 2 and 3). The altered external surface potential of the barium ions compared to the calcium ions

will also affect the influence of the membrane potential on the driving force on the ions shifting the current–voltage relationship on the potential axis (Fox *et al.*, 1987).

The effect of these factors on the positioning of the current–voltage relationship on the potential axis is probably reasonably small and presumably usually affect recordings of currents through calcium channels, as elevated extracellular divalent ion concentrations are the usual method of amlifying these currents (Bean, 1992). It is still clear that the current activates at and reaches a maximum at potentials typical for high voltage activated or L–type currents, as is the case in horizontal cells from other species (Table 3.3 B). Chapter 4 includes details of pharmacological experiments carried out on depolarization–induced increases in intracellular calcium (Sections 4.4.6 and 4.4.7) which provide further evidence that this is a L–type current, namely sensitivity to blocking agents and various metal ions.

The apparent reversal of the current at around $+60mV$ (Fig. 3.20) is not at the equilibrium potential for Ba^{2+}, although it is in good agreement with the reversal potentials previously recorded from isolated horizontal cells (Table 3.3 B). Table 3.3 B also shows that for horizontal cells from various species TEA, even at $20mM$, does not completely block the sustained outward potassium rectifier, especially at potentials more positive than $+20mV$. Consequently the inward Ba^{2+} current at potentials more positive than this is probably being increasingly underestimated. The TEA and 4–AP resistant outward potassium currents in white perch could be blocked by using intracellular Cs^{+} (Lasater, 1986). However the block of the sustained current took up to fifteen minutes after the whole cell recordings started due to the slow diffusion of the Cs^{+}, so this method of blocking the outward currents was not suitable because of the time–dependent rundown of the inward current (Fig. 3.22). Moreover, Lasater (1986) found that calcium currents were never observed when CsCl was used in the patch pipette in white perch horizontal cells and assumed that it was having some sort of blocking effect on the channels, although intracellular Cs^{+} has been sucessfully used to block potassium currents in teleost retinal neurones when recording goldfish bipolar cell calcium currents (Heidelberger and Matthews, 1992). In fact, as horizontal cells in the intact retina are not depolarized to these potentials and the leakage current was linear up to

$+10mV$, the possible inaccuracies in the current at the more depolarized potentials can be accepted.

The true reversal potential of these currents i.e. if all other outward currents were completely blocked, would actually be more negative than the Ba^{2+} equilibrium potential (or if Ca^{2+} was the main extracellular divalent ion present the Ca^{2+} equilibrium potential). This is because of monovalent ions moving outward through the channels (Reuter and Schloz, 1977; Lee and Tsien, 1984). The intracellular potassium concentration is about 10^6 times the concentration of the divalent charge carrying ions (the pipette potassium concentration was $130mM$ and free calcium concentraton $8.3nM$). Consequently, even if potassium ions are 10^{-4} times as permeable as the divalent ions, at depolarized potentials the driving force on the potassium ions will mean that they will contribute to the net current passing through the channels, in an outward direction (Hille, 1992). If the main intracellular cation was Cs^+ instead of K^+ the reduced permeability of this ion through the calcium channels would mean that the reversal potential would be closer to the Ba^{2+} equilibrium potential, but again this is not practical for the reasons mentioned above.

The Ba^{2+} currents recorded showed little or no inactivation over the $500ms$ potential changes used (Fig. 3.19 A). This is in common with the sustained currents recorded from horizontal cells from many other species (Table 3.3 B). The inactivation observed by Tachibana (1983a, b) in goldfish was described as being calcium–mediated calcium inactivation while in contrast Sullivan and Lasater (1992) described voltage dependent inactivation of the sustained current in some white bass horizontal cells ($\tau \sim 13.5 \pm 2.3$ seconds) whereas in some it did not inactivate over depolarizing test potentials of 15–60 seconds.

It should be noted that another effect of using Ba^{2+} as the charge carrier is that the intracellular Ca^{2+} concentration should not increase when the cells are depolarized. This means that the calcium–induced calcium inactivation exhibited by many L–type calcium channels will not occur as Ba^{2+} does not seem to substitute for Ca^{2+} in this role (Bean, 1985; Byerly and Hagiwara, 1988). This is compounded by the use of EGTA in the patch pipette which will maintain the very low intracellular calcium concentration levels. In fact these two methods of reduc-

ing or eliminating calcium–mediated calcium inactivation were used by Tachibana (1983b) to demonstrate the calcium dependence of the goldfish horizontal cell calcium current inactivation. Also the duration of the test potentials ($500ms$) means that inactivation with a time constant greater than $\sim$10 seconds might not be easily detected.

Although the caveat that the calcium channels passing the current are not experiencing the same physiological conditions which they would in the *in vivo* state (Bean, 1992; Hille, 1992) must be remembered, the advantages of using Ba^{2+} as the charge carrier, primarily the increased current amplitude through L–type calcium channels, seem to outweigh these problems (Bean, 1992). The current–voltage relationships of this current and the sustained calcium currents observed in other isolated horizontal cells show activation of the current at $-30mV$ to $-40mV$ reaching a peak at $0mV$ to $+20mV$ (Table 3.3 B and Fig. 3.20). As horizontal cells are not normally depolarized beyond about $-10mV$ in the intact retina the amplitude of this current must be small in the *in vivo* state and consequently the influence of the calcium current on the total current–voltage relationship of the horizontal cell is probably quite small. However the fact that, in isolated cells, in 'normal' extracellular calcium concentrations of $\sim 2mM$, depolarization of the membrane by either current injection or the application glutamate produces a calcium action potential (Johnston and Lam, 1981; Tachibana, 1981; Lasater and Dowling, 1982; Dowling *et al.*, 1983; Ariel *et al.*, 1984, and see Section 4.5.2) shows that this current can control the membrane potential of the cell under these conditions.

The sustained inward nature of the current means that it will be antagonistic to the sustained outward potassium current. It therefore contributes to the flat I–V relationship of the isolated cells over the potential range of $-60mV$ to $+10mV$ when measuring the total membrane currents. It could therefore be reducing the amount of neurotransmitter release required to maintain the depolarized membrane potential in the dark. However whether it contributes significantly to the membrane potential responses of the horizontal cells in the intact retina is difficult to tell. The functional role of voltage gated channels in cells which respond *in vivo* with graded potentials only, especially voltage gated channels which only appear to be significantly activated at potentials more positive that those experienced by

the cells *in vivo* is difficult to assess. In the case of calcium channels the changes in intracellular calcium concentration caused by the influx of extracellular calcium might be expected to have some second messenger role, for example controlling the release of neurotransmitter. This is discussed in more detail in Chapter 4 where data on the depolarization–induced intracellular calcium concentration changes in these cells is reported.

Dopamine and dibutyryl cAMP did not appear to have an effect on the amplitude of this current, in contrast to the results of Pfeiffer–Linn and Lasater (1992) on bass horizontal cells where it was shown that the L–type current was potentiated by dopamine. The action of dopamine on the bass horizontal cells was via increases in intracellular cAMP (Pfeiffer–Linn and Lasater, 1992). The application of dopamine to carp horizontal cells is known to increase the intracellular cAMP concentration (Van Buskirk and Dowling, 1981; Watling and Dowling, 1981). The actions of cAMP in horizontal cells are multiple (Section 1.3.5), but this study demonstrates that they are not the same in different teleost species.

The temporary increase in current amplitude over the first few minutes whole cell recording (Figs. 3.21 and 3.22) was less than 10% but was consistently observed using the recording protocol described. The reason for the slight increase in current amplitude was not clear. One possibility was that the intracellular calcium concentration was lowered by the pipette EGTA and calcium dependent inactivation is removed, although it is not known whether calcium dependent inactivation occurs in carp horizontal cells as has been reported in goldfish horizontal cells (Tachibana, 1983a, b). A reduction of the current amplitude with time is common when recording calcium currents using the whole cell patch clamp technique (Fenwick *et al.*, 1982b; Bean, 1992) and is usually attributed to the progressive washing out of the cell of regulatory factors in the cytoplasm, such as protein kinases.

As with the potassium inward rectifier current there was no significant difference between the current amplitude and voltage gating of the current from cells from fish acclimated to the different temperatures (Fig. 3.23; Table 3.5). Previous studies on the effects of temperature on L–type calcium currents indicate that they are temperature sensitive. A common finding was an increase in current amplitude with an increase in temperature with a Q_{10} of 1.6 to 2.5 (Narahashi *et al.*,

1987; Wang *et al.*, 1991; Herve *et al.*, 1992; Van Lunteren *et al.*, 1993), although this varied over the temperature ranges studied. In some cases the current amplitude demonstrated a temperature dependent maximum. Mouse neuroblastoma cells exhibited a calcium current with a maximum amplitude at 30°C (Narahashi *et al.*, 1987), whereas the cuurent in rat smooth–muscle cells was at a maximum at 35°C (Wang *et al.* , 1991). Guinea–pig and ground squirrel myocytes and bull-frog sympathetic neurones did not show comparable maximums (Herve *et al.*, 1992 and Van Lunteren *et al.*, 1993 respectively). The effect of acclimation to different temperatures on calcium currents was not reported in any of these papers. No data on the current amplitude at experimental temperatures other than 17°C was systematically recorded in this study. However the results from cells from fish acclimated to different temperatures suggests that there was no acclimatory change in this current to compensate for any temperature dependent changes which might occur.

Chapter IV

Intracellular Calcium Measurements in Isolated Horizontal Cells

4.1 INTRODUCTION

4.1.1 Historical Perspective

The roles of cytoplasmic free calcium ions as an intracellular messenger are now widely investigated and are of such importance that the subject warrants its own journal — Cell Calcium. However the importance of its intracellular functions was for a long time not fully recognised, even though some early work provided evidence of now well known roles. It is important to point out that any potential second messenger function is carried out by free calcium ions in solution and not the total intracellular calcium. Chandra *et al.* (1994) showed that the total calcium concentration is hundreds of times the free calcium concentration in tumor mast cells because of the large proportion of calcium which is bound to intracellular chaelators or sequestered in intracellular stores. Throughout this chapter any references to intracellular calcium refer to the free ionic calcium, unless clearly indicated otherwise.

Ringer demonstrated, over 100 years ago, the absolute requirement for extracellular calcium to maintain many diverse cellular functions, from the beating of the frog's heart to the development of various fertilized eggs (e.g. Ringer, 1890). Pollack (1928) seems to have been the first to attempt to study the intracellular calcium concentration. He microinjected the dye alizarin sulphonate into an amoeba and concluded that the appearance of red crystals close to a pseudopodia formation was due to an increase in intracellular calcium, because the calcium salt of the dye has a very low solubility. Heibrunn (1943) suggested that the source of intracellular calcium changes could be from intracellular stores, as well as the extracellular solution, because of the asymmetry of calcium distribution within cells.

However it was not until the work on muscle contraction showed a definite role and mechanism for calcium as an intracellular messenger in the years up to the early 1960s that the 'Calcium Hypothesis' became widely accepted (see Campbell, 1983 for review). Now the importance of intracellular free calcium ions as second messengers in a great diversity of cell types is accepted, especially neurones (see Section 4.1.5). Changes in the free cytoplasmic calcium are generally accepted as originating primarily from intracellular stores, or from the extracellular environment through channels in the cell membrane. The most important channels are probably the voltage gated channels, although receptor gated channels (e.g. the glutamate NMDA channel) and potentially intracellular second messenger gated channels may have a significant effect (Milani *et al.*, 1990).

4.1.2 Intracellular Stores

The importance of intracellular calcium stores in intracellular calcium signalling is well known (e.g. Tsien and Tsien, 1990; Pozzan *et al.*, 1994) and their occurance in many different types of neurone widely reported (Henzi and MacDermott, 1992).

There appear to be two basic types of intracellular calcium release; inositol 1,4,5–trisphosphate (IP_3) induced calcium release and calcium induced calcium release mediated by two families of receptor.

1 Calcium Induced Calcium Release (CICR)

Endo (1977) showed that sarcoplasmic reticulum released calcium in response to mM concentrations of caffeine in a reversible manner. This was mediated by what is now known as the Ryanodine receptor, due to its sensitivity to ryanodine at very low concentrations and its subsequent isolation (Inue *et al.*, 1987; Meissner, 1994). This molecule is directly affected by caffeine which causes an increase in the frequency and duration of channel open events (Rosseau and Meisser, 1989). It is normally stimulated by an increase in intracellular calcium concentration and the subsequent efflux in calcium from the store results in a rapid positive feedback induced transient response.

2 IP_3 Induced Calcium Release (IICR)

In cells not sensitive to caffeine other agents have been able to cause an increase in intracellular calcium concentration by calcium release from intracellular stores. Abramson and Salama (1987) showed that sulphydryl oxidation of a sarcoplasmic reticulum protein caused an increase in the sarcoplasmic reticulum membrane permeability. Miyazaki *et al.* (1992) have shown that thimerosal induced release in hamster eggs, which do not respond to caffeine, is from an IP_3 receptor.

However, is not clear how independent these two types of intracellular calcium release are. Models of calcium oscillations involving intracellular stores usually involve interactions between both types of release mechanism (e.g. Berridge, 1990). In fact it is possible that there is only one intracellular calcium store, with two receptor types, as was demonstated by Iino (1987) in guinea-pig smooth muscle. Moreover there is a great degree of homology between the two different receptor types and commonality of control mechanisms (Pozzan *et al.*, 1994). For instance IP_3 can open ryanodine receptors and increases in cytosolic calcium appear to act as a co-agonist to IP_3 during IICR (Finch *et al.*, 1991).

4.1.3 Voltage Gated Calcium Channels

The presence of an inward calcium current in the cell membrane would be expected to result in an increase in the intracellular calcium concentration. Large numbers of cells have been shown to have significant calcium currents with different voltage and time dependencies (Section 3.1.8). The effect of such currents on the intracellular calcium concentration will depend on the current amplitude and duration and the intracellular calcium buffering mechanisms such as calcium chelators and membrane bound calcium pumps which can either pump the calcium into the extracellular space or intracellular stores. Consequently the influence of calcium currents measured electrophysiologically (as in the previous chapter) on the intracellular calcium concentration cannot be assumed without directly measuring the intracellular calcium concentration.

4.1.4 Intracellular Calcium Dyes

Early monitoring of intracellular calcium concentration with calcium sensitive

dyes usually involved the use of the luminescent photoprotein aequorin. This naturally occuring protein (it is extracted from the bioluminescent jellyfish *Aequorea aequorea*) emits light in an aequeous solution in a calcium dependent manner (Shimomura and Johnson, 1976). Its potential as a calcium concentration indicator was suggested as early as 1963 (Shimomura *et al.*, 1963) although it was first used for intracellular calcium monoitoring by Ridgeway and Ashley (1967), who injected it into the muscle fibres of an Acorn barnacle,

Metallochromic indicators, such as Arsenazo–III, show changes in absorbance at relatively long wavelengths (600–700nm) as a result of binding with calcium (Campbell, 1983; Mayer *et al.*, 1987; Thomas, 1991). However it can be difficult to relate changes in absorbance of the dye injected into a cell, to changes in calcium concentration, because of the poor selectivity of the dye for calcium over protons and magnesium and its variable stoichiometry.

It has become more usual to use fluorescent indicators derived from calcium chelators as intracellular calcium indicators, although aequorin and the metallochromic dyes are still used. (For instance a novel method has been developed to use aequorin as an intracellular calcium concentration indicator, in cells which are not suitable for more recently developed dyes, by transforming the cell type with apoaequorin cDNA so that the dye can be expressed intracellularly. This has been sucessfully achieved in slime moulds (Saran *et al.*, 1994) and there appears to be no reason as to why it should not work in other cell types (Cobbold and Lee, 1991).) However fluorescent indicators are generally easy to use, have a better signal to noise ratio than photoproteins and better temporal resolution than techniques such as ion sensitive electrodes and NMR studies (Thomas and Delaville, 1991).

The first frequently used fluorescent indicator was Quin 2, developed by Tsien (1980), when it was referred to as ligand 3b. It fluoresces maximally at about 492nm when excited with ultra–violet light at about 339nm. The fluorescence intensity is about five times greater when it is calcium saturated (i.e. at about 1μM Ca^{2+}) than when in calcium free solution. If cells are incubated with the acetoxymethyl ester of the dye this lipid soluble molecule will diffuse across the cell membrane into the cytosol, where the cells' acetylesterases hydrolyse it to the lipid

impermeable free acid form, trapping it in the cell (Tsien, 1981), thus preventing the potentially damaging need to inject it directly into the cell.

However Quin 2 does have a number of drawbacks. The fluorescence intensity measured is not simply dependent on the calcium concentration, but also on the Quin 2 concentration and the autofluorescence of the cells. Consequently a complex calibration is required for each cell sample used, involving lysing the cells in solutions of known calcium concentration and then measuring the fluorescence intensity (Tsien *et al.*, 1982). Another problem with Quin 2 is the buffering effect of the dye. As it is required in quite high concentrations (tenths of millimolar), to counteract the autofluorescence of the cells, transient changes in the calcium concentration will be underestimated (Tsien *et al.*, 1982), because of the calcium binding properties of the dye. Moreover as the dye saturates at 1–2μM changes in calcium concentration cannot be accurately resolved at or above this range.

It was suggested (Tsien *et al.*, 1982) that if a dye could be developed which fluoresced strongly and indicated calcium concentration not as a change in the fluorescence intensity, but as a shift in the emission spectra, then the ratio of the fluorescence intensity at two appropriate wavelengths would indicate the calcium concentration independently of the dye concentration. Grynkiewicz *et al.* (1985) introduced new dyes based on the calcium chaelator BAPTA which did have these charateristics. Two of the most commonly used are Indo-1 and Fura-2 (Fig.4.1). The former behaves as described above, with a shift in emission maxima dependent on calcium concentration (Fig. 4.2 A). Consequently when using Indo-1 the dye is illuminated at one excitation wavelength and the intensity of the emitted light is measured at two appropriate wavelengths, the ratio of which indicates the calcium concentration. However Fura-2 shows a greater shift in excitation maxima than emission maxima (Fig. 4.2 B) so the ratio of fluorescence intensity at two appropriate excitation wavelengths is used. The intracellular concentrations required (tens of micromolar) are less than for Quin 2 because both these dyes fluoresce more strongly than Quin 2 and cellular autofluorescence is less at the excitation wavelengths used. The membrane permeant acetoxymethyl esters of both dyes can be used to introduce them to the cell cytoplasm in the same way as for Quin 2.

The dye predominantly used in this study was Fura-2. Isolated cells loaded

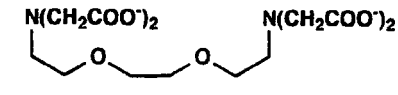

EGTA

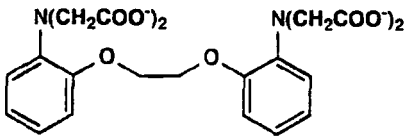

BAPTA

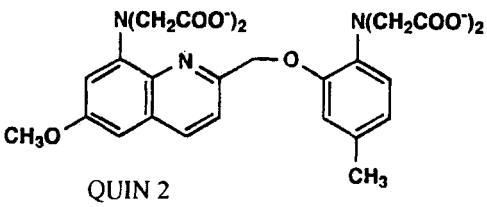

QUIN 2

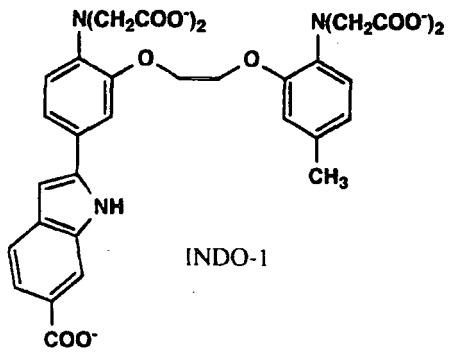

INDO-1

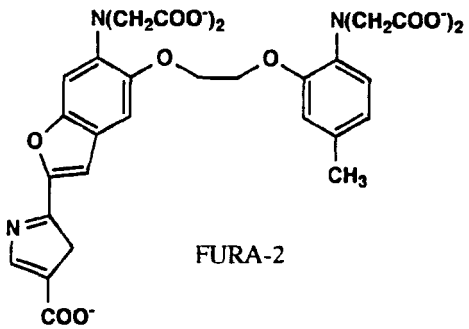

FURA-2

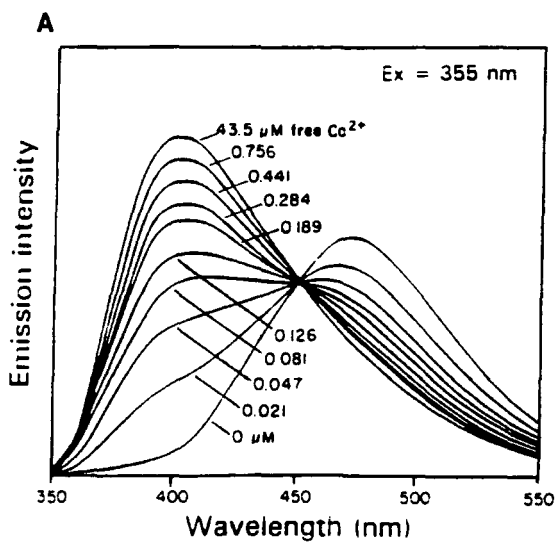

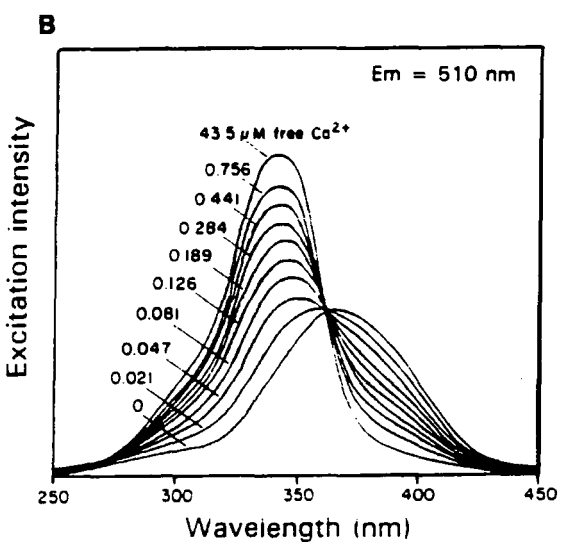

with the dye were alternately exposed to two ultra–violet excitation wavelengths over a one second time period and the corresponding fluorescence intensities measured. The ratio of these two values was calculated each second and was used to monitor the intracellular calcium concentration over a period of time. A calibration equation was calculated specifically for the apparatus and cell type used (Section 4.3) so the ratio values recorded could be converted into calcium concentrations.

To date the only other use of Fura-2 in single isolated retinal horizontal cells was by Schwartz (1987) on catfish cells. Although he demonstrated an intracellular calcium concentration increase on depolarization of a cell in a calcium rich saline the main aim was simply to demonstrate that the intracellular calcium concentration did not change on depolarization in calcium free saline.

4.1.5 Intracellular Ca^{2+} as a Second Messenger

The function of intracellular calcium as a second messenger is so widespread, involving both excitable and non–excitable cells and many different primary messengers, that there are not comprehensive reviews on the subject. However the basic mechanism involves the binding of a primary agonist to the cell which results in an increase in intracellular calcium concentration by an influx of extracellular calcium or the release of calcium from intracellular stores, or both. The subsequent cellular responses are mediated by calcium–modulated proteins in the cytoplasm which are distinct from the calcium–binding proteins which buffer the intracellular calcium concentration (Barritt, 1992). The diversity of responses mediated by intracellular calcium is demonstrated in Table 4.1, which is an obviously far from complete list!

The importance of calcium on neurones has already been alluded to and its role in modulating phototransduction mechanisms mentioned (Section 1.2). It is well established that an influx of extracellular calcium mediates vesicular neurotransmitter release (Katz, 1969; Llinás and Nicholson, 1975). This is probably the fastest second messenger mediated mechanism as the vesicles are already associated with the plasma–membrane (when they are referred to as being 'docked') in close proximity to voltage gated calcium channels (Kelly, 1993) so that when, on depolarization, the channels open, localised, rapid and large rises in intracellular calcium concentration are rapidly detected by a calcium modulated protein which

Table 4.1. Examples of some cellular responses mediated by changes in the concentration of free calcium ions in the cytoplasm (Barritt, 1992).

Cellular Response	Cell Type	Primary Messenger
Contraction	Skeletal Muscle	Various Neurotransmitters
Glycogenolysis	Liver Parenchymal	Adrenalin
Shape Change	Platelets	Thrombin
Growth (Proliferation)	Fibroblasts	Platelet–derived Growth Factor
Fertilization	Sea–urchin Eggs	Spermatozoa
Light Adaptation	Photoreceptors	Illumination (Section 1.2)

results in fusion of the vesicle to the plasma–membrane within $1ms$ (Almers, 1994; Von Gersdorff and Matthews, 1994; Jahn and Sudhof, 1994).

Intracellular calcium concentration changes can also modulate activity in excitable cells by a number of mechanisms. One of the simplest is by binding to and increasing the probability of opening of a potassium channel. There are a number of different calcium–modulated potassium channel types (Rudy, 1988; Hille, 1992). The probability of opening is usually affected by both the membrane potential (increased probability on depolarization) and the intracellular calcium concentration (increased probability on increased concentration), for example as demonstrated by Barrett *et al.* (1982). To date only horizontal cells from *Xenopus* retina have demonstrated a calcium dependent potassium current (Akopain and Witkovsky, 1994). Other membrane channels, both voltage– and ligand–gated are thought to show some intracellular calcium dependence (see Kostyuk, 1992).

Potentiation of synaptic transmission on various time scales is also mediated by intracellular calcium. Facilitation, where sucessive rapid depolarizations in the presynaptic cell result in increasing transmitter release, is generally accepted as being the result of residual calcium in the presynaptic cell resulting in progressively higher calcium concentrations (Katz, 1969; Zucker, 1989). Longer term modulation of synaptic transmission include changes in the structure of dendritic

spines which are also mediated by increases in intracellular calcium concentration, though the mechanisms are not yet understood (Madison *et al.*, 1991; Harris and Kater, 1994). The longest term changes in synaptic plasticity involve changes in DNA expression and it is suggested that this may also be mediated by intracellular calcium (Madison *et al.*, 1991; Kostyuk, 1992). It has been shown that increased proenkephalin mRNA expression in chromaffin cells in response to nicotine is mediated by increased intracellular calcium concentrations entering the cell through voltage–gated calcium channels (Kley, 1987).

Growth cones in neurones also demonstrate calcium dependent fusion of plasmalemma vesicles with the plasma membrane (Lockerbie *et al.*, 1991), but are unable to release vesicular neurotransmitter during growth and appear to use common mechanisms involved in the vesicle fusion differentially depending on whether growth or neurotransmitter release is required (Catsicas *et al.*, 1994).

4.2 METHODS

4.2.1 Introduction

Since the introduction of Fura-2 (Grynkiewicz, 1985) there have been a number of developments which make it increasingly attractive to use. The dye is commercially available and the hardware to use it with is continually improving. Photomultipliers, for example, are increasingly sensitive and less cumbersome to use. Custom built equipment is also now available to use with dual excitation dyes and computer software to run the equipment. For isolated cells adhered to a suitable substrate dye loading is straightforward and the cells can then be studied individually and exposed to different stimuli while at the same time monitoring the intracellular calcium concentration.

4.2.2 Cell Isolation

Cells were isolated as has been described in Section 3.2.2 and used one to five days after isolation.

4.2.3 Fura-2 Loading

The acetoxymethyl ester of Fura-2 (Fura-2 AM) was purchased from Molecular Probes. The $1mg$ sample was dissolved in $1ml$ of dry DMSO and this was split into $20\mu l$ aliquots, to which $10\mu l$ of 20% Pluronic F-127 in DMSO was added. These were stored at −20°C in the dark until required. The addition of Pluronic F-127, a nonionic dispersing agent which helps to solubilise large molecules in physiological solutions, is known to improve loading rates of Fura-2 AM (Poenie *et al.*, 1986).

When required for use, $2ml$ of saline (containing (in mM): NaCl, 119; KCl, 4; $MgSO_4$, 1; $CaCl_2$, 1; Glucose, 10; HEPES, 10 buffered to pH 7.5 using NaOH) was added to a Fura-2 aliquot and vortex mixed for five minutes. This gave a final dye concentration of approximately $10\mu M$ (MW of Fura-2 AM is 1002). This solution was placed in a $35mm$ petri dish and coverslips with cells adhered to them were removed from the culture medium and placed into the Fura-2 AM solution. Cells were usually incubated for 40–80 minutes at 16°C. During the 5–6 hour period that a Fura-2 AM solution was used the duration of the cells' incubation was increased.

This seemed to be necessary to keep the fluorescence intensity recorded from the different cells at about the same intensity (i.e. the intracellular dye concentration at a similar level). A gradual dilution of the Fura-2 AM concentration in the saline, caused by the progressive removal of the dye in cells and the addition of small volumes of saline with each coverslip could have been the reason for this. The coverslip, with Fura-2 loaded cells (Plate 4.1), was then placed in the experimental chamber, where any dye not trapped in the cells was washed off by the continuous perfusion.

4.2.4 Equipment

A Nikon inverted microscope (Diaphot Model TMD) was used with a Nikon CF fluor (×40) lens. The additional specialist equipment was purchased from Newcastle Photometric Systems, as was the software package used to run the equipment.

Fig. 4.3 shows the optical pathways used and the numbers in square brackets below refer to the labels in this diagram.

4.2.4.1 Excitation Pathway

The ultra–violet light source was a Xenon 75 watt short arc lamp (Ostram XBO) [2.1]. A Xenon lamp was preferable to a mercury lamp as it produces a more uniform illumination spectrum, especially over the wavelengths required (Thomas and Delaville, 1991; Ploem, 1993). During the experiments the excitation beam was alternated between two wavelengths by a servo driven filter wheel rotating between two positions each containing filters that selected the excitation wavelengths. The interference filters used were from Ealing Electro-Optics and had peak transmission at $380nm$ and $350nm$, with half bandwiths of $11.6nm$ and $10.3nm$ respectively [2.4]. The intensity of the excitation beam could be controlled using inconel on glass neutral density filters [2.3]. For nearly all experiments and the calibration a neutral density filter transmitting 9% of incident light was used. A dichroic mirror [2.5] was used to reflect the ultra–violet excitation beam into the objective lens [1.4]. The mirror (Nikon DM400) reflects wavelengths shorter than $\sim 400nm$ and transmits wavelengths longer than $\sim 400nm$, when orientated at 45°

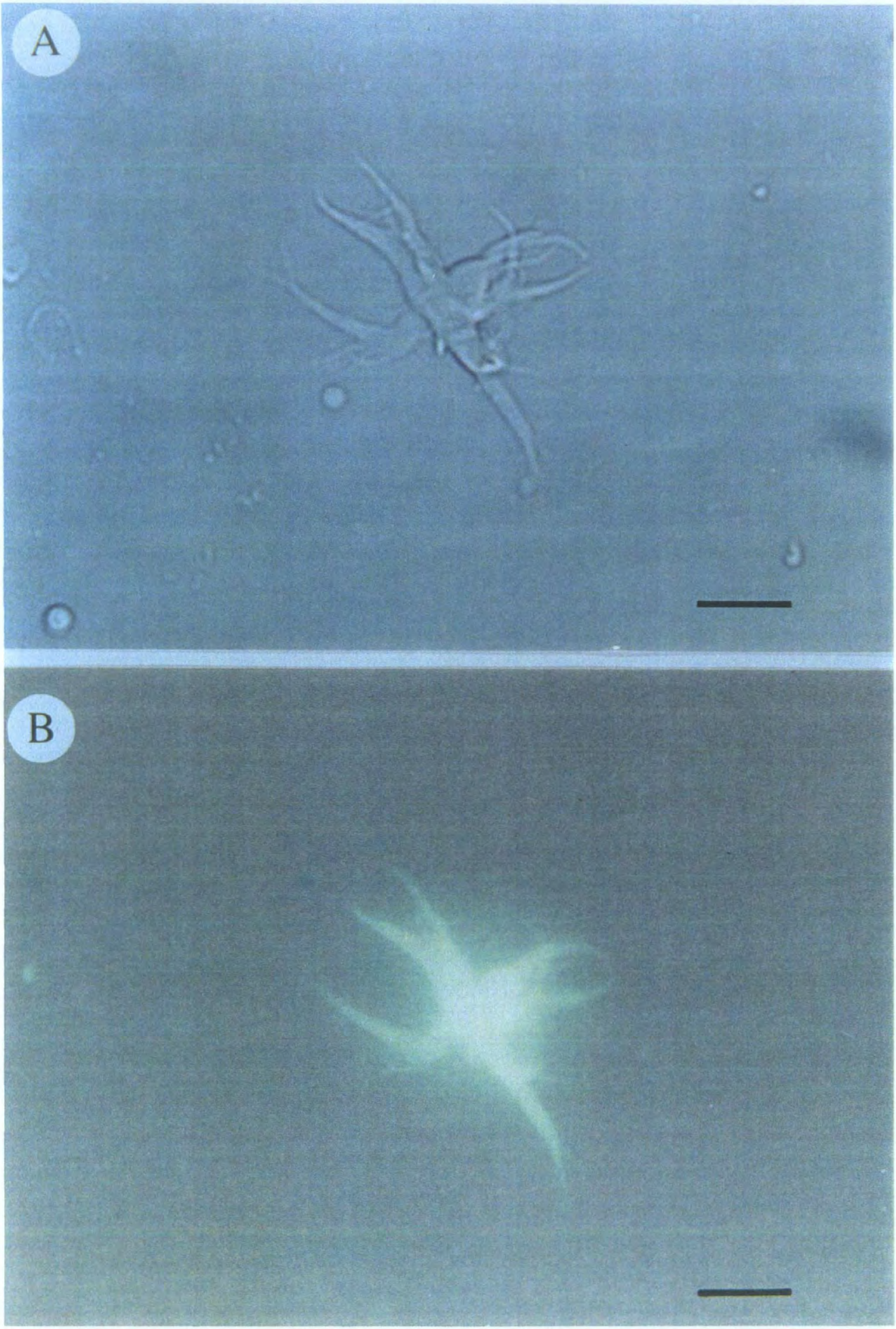
A
B

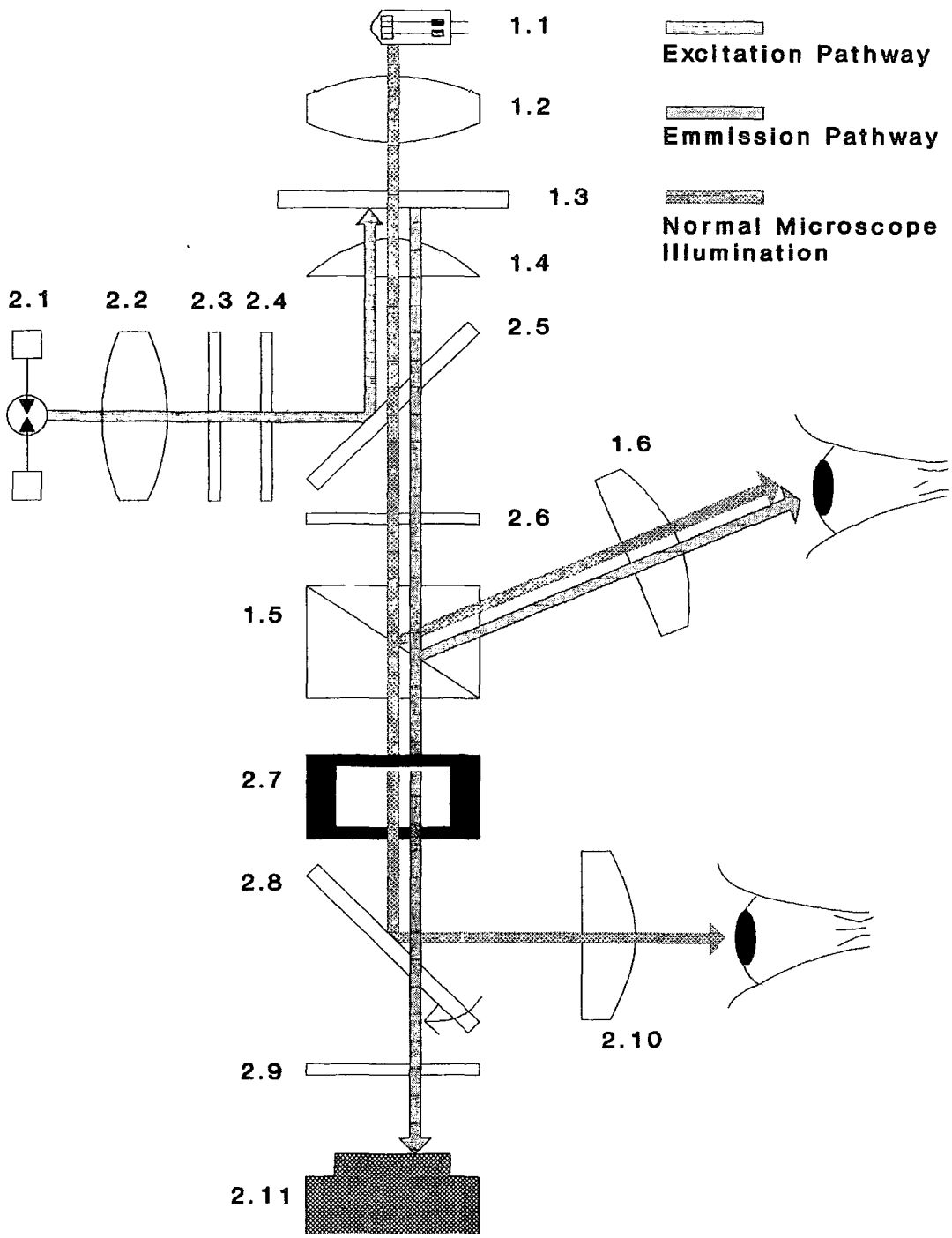
1.1
1.2
1.3
1.4
2.1
2.2
2.3
2.4
2.5
1.6
2.6
1.5
2.7
2.8
2.10
2.9
2.11
Excitation Pathway
Emmission Pathway
Normal Microscope Illumination

to the incident light. The objective lens then focused the excitation beam onto the specimen [1.3].

4.2.4.2 Emission pathway

The emitted light has a much longer wavelength than the excitation beam, so after passing through the objective lens it is transmitted through the dichroic mirror. A high pass filter (Nikon BA520) [2.6] was used to prevent wavelengths shorter than $\sim 520nm$ from passing through to the emission pathway. This ensured that any scattering of the excitation beam at the dichroic mirror did not get included in the emission path. The emission beam was then split by the microscope beam-splitting prism [1.5] with 20% going to the microscope eyepiece [1.6], and 80% going to the side camera port of the microscope.

Attached to the side camera port was a rectangular field diaphram [2.7], which was used to control the area of the emission pathway reaching the photomultiplier [2.11]. Between these two there was a photomicrographic attachment (Nikon Microflex PFX) [2.8, 2.9 and 2.10]. This consisted of a shutter [2.9] to control the exposure duration. When the shutter was closed a mirror [2.8] reflected the light to an eyepiece [2.10], so that the specimen could be viewed (usually with the normal microscope illumination). When the shutter was open this mirror lifted out of the emission pathway allowing all of the light to pass to the photomultiplier.

A photomultiplier, (Thorn EMI Type 9924B with a Thorn EMI Photomultipier Power Supply Type PM28B) operated in photon counting mode was used as the photometric sensor because of its sensitivity, fast response time and low noise characteristics (Stimson, 1974). This system operated at $5MHz$ and therefore had a theoretical maximum count rate of 5×10^6 counts per second. However, due to the random nature of photon emission, as the rate of photons entering the photomultiplier rises above about 1×10^6 per second an increasing proportion will not be detected. The fluorescence intensity of the dye was such that the number of counts detected in a $200ms$ count period was usually less than 80,000, or well inside the optimum detection frequency. The tendency of photomultipliers to have long timescale (minutes) changes in sensitivity was not important as the fluorescence ratio was calculated much more frequently. The photomultiplier used had an optimum operational power of -890 volts, as determined by the manufacturers.

Although using a larger power supply will give a larger signal, the signal–to–noise ratio will be less favourable, so a careful check was kept on the power source to ensure optimum signal to noise characteristics.

4.2.5 Computer Control

The software package used to run the experiments (Newcastle Photometric Systems Single Point Photon Counting System – Count 4.2) was run on an Amstrad PC3286. The software/hardware interface was a Newcastle Photometric Systems IBM computer board. It contained:

1 A pulse timer gating circuit to control the photon count period.

2 Two 32 bit photon counters.

3 Two servo filter wheel controllers.

4 A 4MHz crystal oscillator (to time events).

The equipment could be run in two distinct modes, either a filter changing mode for multiple excitation, or a single excitation mode where the emission beam was measured at one or more wavelengths. When using Fura-2 the multiple excitation wavelength mode was selected. The event timing sequence in this mode was:-

1 Check the count period has ended.

2 Read the counts from the interface board.

3 Move the filter to the next wavelength position.

4 Check the filter wheel move is complete.

5 Start a count sequence.

The sequence was then repeated for the next wavelength.

Each measurement cycle started with the data for the $350nm$ wavelength being counted and the sequence was then repeated for the $380nm$ wavelength. Then

the ratio of these two channels was calculated (350/380). The duration of each measurement cycle is given by:-

$$2 \times (\text{Photon count time period} + \text{Filter changing time})$$

The photon count time was set by the user (for Fura-2 $200ms$ was used) while the filter change time was about $300ms$. The total measurement cycle was therefore about one second. The time resolution of the system was limited by this value and any changes in intracellular calcium concentration over short time periods would not have been accurately recorded.

4.2.6 Protocol

The open perfusion micro-incubator (Medical Systems Corp. PDMI-2) was used to control the experimental temperature as described in Section 3.2.3 and was positioned on the stage of the inverted microscope. The modifications made to the petri dishes described in Section 3.2.3 and Fig. 3.7 (replacing an area of the base with coverslip glass) were also required for Fura-2 measurements as the ultra–violet excitation illumination would not pass through the plastic base of a petri dish satisfactorily.

It was essential to accurately control and change the composition of the saline surrounding the cell during experiments. The modifications to the petri dish resulted in a small experimental chamber which was continually perfused with saline using the same apparatus as for the patch clamp experiments, although the bubble trap was ommitted as it was not neccessary. Only the glass covered base of the dish was perfused, to a depth of approximately $1–2mm$, giving a volume of about $0.3ml$. This volume, in the experimental chamber, was kept to a minimum to increase the speed of changes in solution.

In order to test how efficiently changes in the perfusant concentration were transmitted in the experimental chamber a solution of potassium permanganate was used so that the transmission of light through the solution could be used to follow the concentration change (Fig. 4.4). With the normal microscope illumination at a very dim level the photomultiplier recorded ~180000 counts in the absence of potassium permanganate and ~18000 counts when it was present. When the

perfusing solution was changed between the two solutions the number of counts recorded by the photomultiplier changed rapidly. With the perfusion rate at $2ml$ per minute (the maximum recomended for use with the microincubator) switching between these two perfusants for 10 seconds resulted in a complete change in $KMnO_4$ concentration in the experimental chamber. In all experiments this perfusion rate was used and any changes in saline concentration were of a minimum of ten seconds.

A coverslip on which cells loaded with Fura-2 were present was put in the experimental chamber of the modified petri dish, in the microincubator. During the time used to select a suitable cell the perfusion system was on, to ensure that any extracellular Fura-2 AM and debris loosely attached to the coverslip were washed out. When a cell was located (clean from debris, as isolated from other other cells and attached debris as possible and preferably near the centre of the coverslip) it was positioned so that it could be seen through the photomicrographic attachment eyepiece. Using this eyepiece the field diaphram was adjusted to frame the cell ensuring that it was the only potentially fluorescent object in the field of view. In this way only Fura-2 from the cell was detected by the photomultiplier.

When there was no cell, or other fluorescent body, in the field of view and the shutter was opened to the photomultiplier a 'dark count' was recorded. This came from three main sources:-

1 The photomultipliers used had a dark count of about 200 counts per second.

2 Fluorescent objects, close to, but not in the field of view contribute slightly to the count values, due to light scattering.

3 Extraneous light from the room will be able to enter the emission pathway. This was reduced, but was never totally eradicated, by working in a light tight room with only a very dim red light.

In order to take account of these spurious signals a background count was subtracted from each channel before the ratio was calculated. This task was automatically carried out by the software package. First the cell was moved out of the field of view, without altering the field diaphram dimensions, and replaced with an adjacent blank area of coverslip in the field of view. With the shutter open the

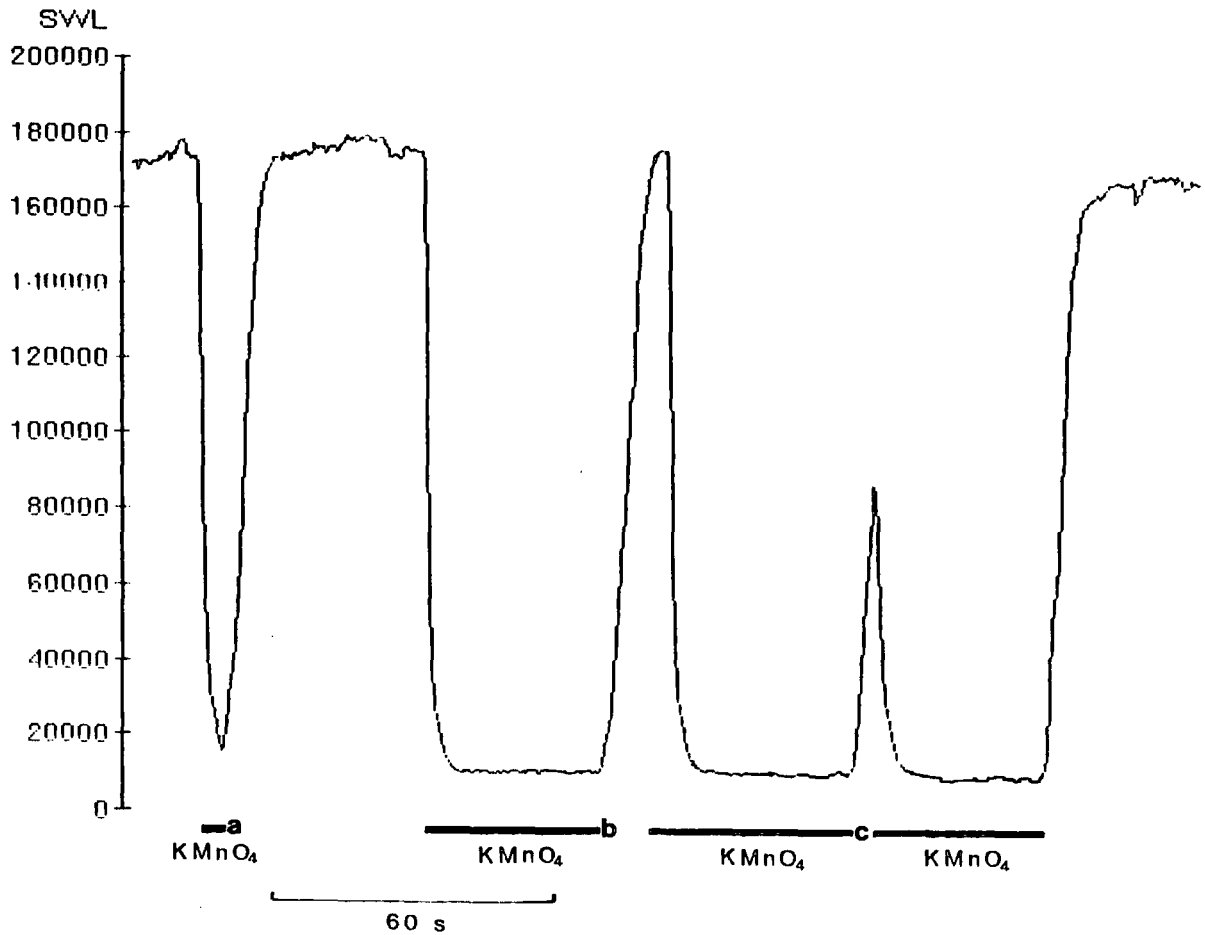
SWL
200000
180000
160000
140000
120000
100000
80000
60000
40000
20000
0
a
KMnO4
b
KMnO4
KMnO4
c
KMnO4
60 s

software package then ran the event timing sequence for ten cycles and the mean dark count value for each channel was calculated. The cell was then repositioned back into the field of view, again without making any change to the field diaphram dimensions. During any subsequent measurements these two dark count values were automatically subtracted from the appropriate channel before the data was displayed.

Except during the recording of background counts, the excitation pathway was blocked (to prevent excessive exposure of the cell to the ultra–violet light) and the shutter kept closed (to protect the photomultiplier from the normal microscope illumination). Both these obstructions were then removed and a fluorescnce ratio dependent only on the Fura-2 in the cell recorded. Every time a new cell was studied these procedures were repeated to generate new background values.

During experiments the data was displayed on the computer screen and saved on the hard disk. The cell's response to the stimuli could be observed in real time and the experiment conducted appropriately. In some experiments, over long time periods it was advantageous not to expose the cell to the excitation beam continuously (see Sections 4.5.1.6 on bleaching of the dye and Fig. 4.10 on ultra–violet damage to the cell). This was done by blocking the excitation pathway. When this occurred the photomultipier counts became less than the background counts for each channel. To avoid divide by zero errors when this occurred the software package rounded the count values up to one, to give a ratio value of one (e.g. Fig. 4.20).

4.3 CALIBRATION

4.3.1 Derivation of the Calibration Equation.

The fluorescence intensity was measured at two excitation wavelengths ($\lambda 1$ and $\lambda 2$) and the ratio ($\lambda 1/\lambda 2$) calculated from these measurements. If $\lambda 1$ is $350nm$ and $\lambda 2$ is $380nm$ then an increase in calcium concentration will be represented by an increase in ratio. The following account was based on that described by Grynkiewicz *et al.* (1985) and Bolsover *et al.* (1993). If the total fluorescence intensity upon excitation at $\lambda 1$ is $I_{\lambda 1}$ then

$$I_{\lambda 1} = S_{f\lambda 1}C_f + S_{b\lambda 1}C_b$$

where

$S_{f\lambda 1}$ = intensity of fluorescence of calcium free dye when excited at $\lambda 1$

$S_{b\lambda 1}$ = intensity of fluorescence of calcium bound dye when excited at $\lambda 1$

C_f = concentration of calcium free dye

C_b = concentration of calcium bound dye.

Similarly, at a second excitation wavelength $\lambda 2$:

$$I_{\lambda 2} = S_{f\lambda 2}C_f + S_{b\lambda 2}C_b$$

Due to the 1:1 stoichiometry of Fura-2 with Ca^{2+} (Grynkiewicz *et al.*, 1985), C_b can be expressed in terms of C_f and the effective dissociation constant of the dye (K_d):

$$C_b = C_f[Ca^{2+}]/K_d$$

$$\text{So} \quad I_{\lambda 1} = S_{f\lambda 1}C_f + S_{b\lambda 1}C_f[Ca^{2+}]/K_d$$

$$I_{\lambda 2} = S_{f\lambda 2}C_f + S_{b\lambda 2}C_f[Ca^{2+}]/K_d$$

$$\text{Thus} \quad R = \frac{I_{\lambda 1}}{I_{\lambda 2}} = \frac{S_{f\lambda 1} + S_{b\lambda 1}[Ca^{2+}]/K_d}{S_{f\lambda 2} + S_{b\lambda 2}[Ca^{2+}]/K_d}$$

Solving for $[Ca^{2+}]$ gives:

$$[Ca^{2+}] = K_d\left(\frac{RS_{f\lambda 2} - S_{f\lambda 1}}{S_{b\lambda 1} - RS_{b\lambda 2}}\right)$$

$$\text{or} \quad [Ca^{2+}] = K_d\left(\frac{R - S_{f\lambda 1}/S_{f\lambda 2}}{S_{b\lambda 1}/S_{b\lambda 2} - R}\right)\left(\frac{S_{f\lambda 2}}{S_{b\lambda 2}}\right)$$

The minimum ratio which can be achieved (in a zero calcium concentration) is $S_{f\lambda 1}/S_{f\lambda 2}$ and can be written as R_{min}, while the maximum ratio which can be achieved (in a saturating calcium concentration) is $S_{b\lambda 1}/S_{b\lambda 2}$ and can be written as R_{max}. Substituting these gives:

$$[Ca^{2+}] = K_d\left(\frac{S_{f\lambda 2}}{S_{b\lambda 2}}\right)\left(\frac{R - R_{min}}{R_{max} - R}\right)$$

$$\text{or} \quad [Ca^{2+}] = K_{\frac{1}{2}}\left(\frac{R - R_{min}}{R_{max} - R}\right)$$

where

$$K_{\frac{1}{2}} = K_d\left(\frac{S_{f\lambda 2}}{S_{b\lambda 2}}\right)$$

and $K_{\frac{1}{2}}$ = the calcium concentration when $R = \dfrac{R_{min} + R_{max}}{2}$

As can be seen above $K_{\frac{1}{2}}$ is dependent not only on K_d but also on the relative fluorescence of the free and bound dye when exposed to one of the excitation wavelengths. This value depends on variables such as the wavelength of the excitation beam, the bandwidth of the excitation beam, the spectral filtering of the emmision beam and so on, i.e. the specific characteristics of the apparatus being used. Likewise R_{min} and R_{max} are not the same for different apparatuses, so the values given in the literature for these three variables (e.g. Grynkiewicz *et al.*, 1985) should not be used. Hence the requirement for calibrating these values for a specific experimental apparatus.

4.3.2 Introduction to Methodology.

For the calibration the free acid form of Fura-2 was incubated with known free calcium ion concentrations and the ratio of the fluorescence intensities measured in as close to the experimental conditions as possible. This involved simply placing the Fura-2 in calcium–buffered solutions in the experimental equipment used, in the position normally occupied by the cells, and measuring the fluorescence ratio

for each solution used. This *in vitro* technique was therefore carried out using the same excitation and emission pathways and the same photomultiplier as in the experiments. However, it had the drawback that the dye was not in the same environment in an *in vitro* calibration as it was intracellularly, although it is possible to compensate for these differences (Poenie, 1990 and Section 4.3.3.3).

Ideally Fura-2 calibration should also involve an intracellular calibration of the dye with known values of intracellular calcium concentration in the cell type used, a so called *in situ* technique. This can be done either with a patch clamp electrode (Neher, 1988; Heidelberger and Mathews, 1992) or by using a calcium ionophore (Williams and Fay, 1990) to control the intracellular calcium concentration. These techniques have the problem that while the pipette and extracellular solution calcium concentrations can be accurately buffered, the intracellular concentration can be significantly different. Using the patch clamp technique the diffusion of the large calcium buffer molecules from the pipette into the cell may be limited. Also the speed of equilibration of the extracellular and intracellular calcium concentrations in the presence of a calcium ionophore can be very variable. The action of the cell's own calcium buffering system will be working to act against any changes in the intracellular concentration. This will include endogeneous calcium buffers (e.g. calmodulin) and the uptake and release of calcium to or from intracellular stores. For instance an EGTA concentration of $10mM$ in a patch pipette was found to be inadequate for large cells (Byerly and Moody, 1984). Moreover, diffusion from the cell into the pipette of any cellular constituents will mean that the Fura-2 will not be in the same environment during the calibration as in the experiment — the whole point of the *in situ* calibration.

The use of an ionophore to control the intracellular calcium concentration has been used with varying degrees of success. Williams *et al.* (1985) were able to generate a complete calibration curve for Fura-2 in smooth muscle cells using ionomycin, while Connor *et al.* (1987) found that variations in ratio recorded between rat cerebellar granule cells supposedly buffered to the same calcium concentration were too great to be able to calculate a calibration curve. However they found that the values for R_{min} and R_{max} were more consistent and used these to corroborate an *in vitro* calibration.

The calibration procedure used in this study was similar to that of Connor *et al.* (1987). An *in vitro* calibration, including a correction to take into account the difference between the calibration solution and the cellular environment, and an *in situ* calculation of R_{min} and R_{max} using an ionophore as well.

4.3.3 *In Vitro* Calibration

4.3.3.1 Calcium Buffered Solutions.

The calibration of the fluorescence of Fura-2 to calcium concentration changes was carried out at three temperatures; 10°C, 17°C and 25°C. Small volumes of calcium–EGTA buffered solutions containing the free acid form of Fura-2 were placed in the experimental chamber and the fluorescence ratio was measured. The free calcium concentrations used were in the range over which the dye is responsive, i.e. 10^{-9} to 10^{-6} Molar.

In order to have known accurate free concentrations of calcium in this range the dissociation constant of EGTA (Kd^{EGTA}) under the conditions used and the ratio of CaEGTA complex concentration to the free EGTA concentration must be known:-

$$[Ca^{2+}]_{\text{Free}} = \frac{Kd^{EGTA}[CaEGTA]}{[EGTA]}$$

A calcium buffer kit was purchased from Molecular Probes (Calcium Calibration Buffer Kit 2) with eleven samples, in $100mM$ KCl and $10mM$ MOPS, having different molar ratios of CaEGTA to EGTA in each.

As both the pH and temperature of the solution affect the Kd^{EGTA} the pH at the three temperatures used was taken using a Unicam Combination pH Electrode sensitive to three decimal places. There was little difference between the different samples at the same temperature:-

10°C $7.522 \pm .002$ $n = 4$

17°C $7.426 \pm .003$ $n = 4$

25°C $7.315 \pm .007$ $n = 4$

The effect of pH on the Kd^{EGTA} in $100mM$ KCl for two temperatures (37°C and 20°C) is given by Tsien and Possan (1989, Table 1). By using the assumption that the calcium association constant ($K'_{Ca^{2+}}$) varies linearly over the temperature range concerned, when plotted as an Arhenius plot (Harrison and Bers, 1987), the Kd^{EGTA} was calculated for the temperature and pH values required.

Using these values, the free calcium concentration was calculated for each of the samples provided at the three temperatures. The series of CaEGTA/EGTA calibration solutions are intended to be used for calibrations such as this and give suitable free calcium concentrations. They include one of zero free calcium to determine R_{min} and one at a calcium concentration high enough to saturate the dye to determine R_{max} ($>10\mu M$). The remaining nine solutions give free calcium concentrations in the nanomolar range (5 to 1000 nM).

4.3.3.2 Method.

The free acid (pentapotassium salt) form of Fura-2 was dissolved in DMSO ($1mg/ml$) and $2\mu l$ of this stock added to $200\mu l$ of each calcium buffer solution, to give a final concentration of about $12\mu M$. As the total EGTA concentration was $10mM$ the effect of this concentration of Fura-2 as an additional buffer of the free calcium concentration was negligible.

Glass bottomed cuvettes were made by sticking coverslips with epoxy resin onto the tops of a plastic cuvettes and cutting off the bottoms. These were used to hold $150\mu l$ of the dye mixture in the microincubator, in the experimental chamber. Importantly, the excitation and emission beams pass through the same glass combinations in this calibration setup as in an experiment. The fluorescence ratio was then measured for each calcium buffer solution at the three temperatures.

4.3.3.3 Viscosity Correction Factor.

Poenie (1990) has shown that the excitation spectrum of Fura-2 is affected by its solution environment, particularly the viscosity of the solution. Consequently the *in vitro* calibration, done in a low viscosity solution, was not directly applicable to the *in situ* environment of the cell cytoplasm. The calibration results were therefore be modified to take this into account before use.

The effect of the solution environment seems to be on the fluorophore part of the Fura-2 molecule only and not on the calcium binding region, as it has little or no effect on the Kd of the molecule. The fluorescence intensity of the dye increases in a more viscous environment, but preferentially at the longer wavelengths. Consequently the *in situ* ratio values will be lower for all calcium concentrations than the *in vitro* ratio value (Poenie, 1990). As this effect is independent of the calcium concentration a single multiplication factor can be applied to all the *in vitro* calibration results to adjust them appropriately. This is called the viscosity correction factor (V), although it also corrects for other errors such as the effect of proteins on the dye and preferential absorption of one or other of the excitation wavelengths by the cytoplasm. Although it varies for different cell types and experimental apparatus, the viscosity correction factor is usually between 0.7 and 0.85 (Poenie, 1990). It can be calculated by comparing the changes in fluorescence intensity at the two excitation wavelengths from *in situ* and *in vitro* calcium concentration changes (Poenie, 1990; Bolsover *et al.*, 1993).

A calcium concentration change causes changes in the fluorescence intensity at each excitation wavelength, but by different amounts and in opposite directions. If the change at the shorter and longer excitation wavelengths are denoted by $\Delta_{\lambda 1}$ and $\Delta_{\lambda 2}$ respectively then $\Delta_{\lambda 1}/\Delta_{\lambda 2}$ should be constant for all calcium concentration changes when the dye is in a constant environment. This value can be obtained for both the *in situ* and *in vitro* environments and the viscosity correction factor calculated as shown below:-

$$\text{If} \quad Z_{insitu} = \Delta_{\lambda 1}/\Delta_{\lambda 2} \quad \text{for intracellular dye}$$

$$\text{and} \quad Z_{invitro} = \Delta_{\lambda 1}/\Delta_{\lambda 2} \quad \text{for extracellular dye}$$

$$\text{then} \quad V = \frac{Z_{insitu}}{Z_{invitro}}$$

To calculate Z_{insitu} and $Z_{invitro}$ the fluorescence intensity from each excitation wavelength was monitored during a rapid calcium concentration increase, when the dye was both intracellular and in the calibration solution, as shown in Fig. 4.5. The drop in fluorescence intensity at the excitation wavelength of $380nm$ and the rise in fluorescence intensity at the excitation wavelength of $350nm$ was measured, to give $\Delta_{\lambda 1}$ and $\Delta_{\lambda 2}$. The corresponding 'Z' values were calculated and hence the

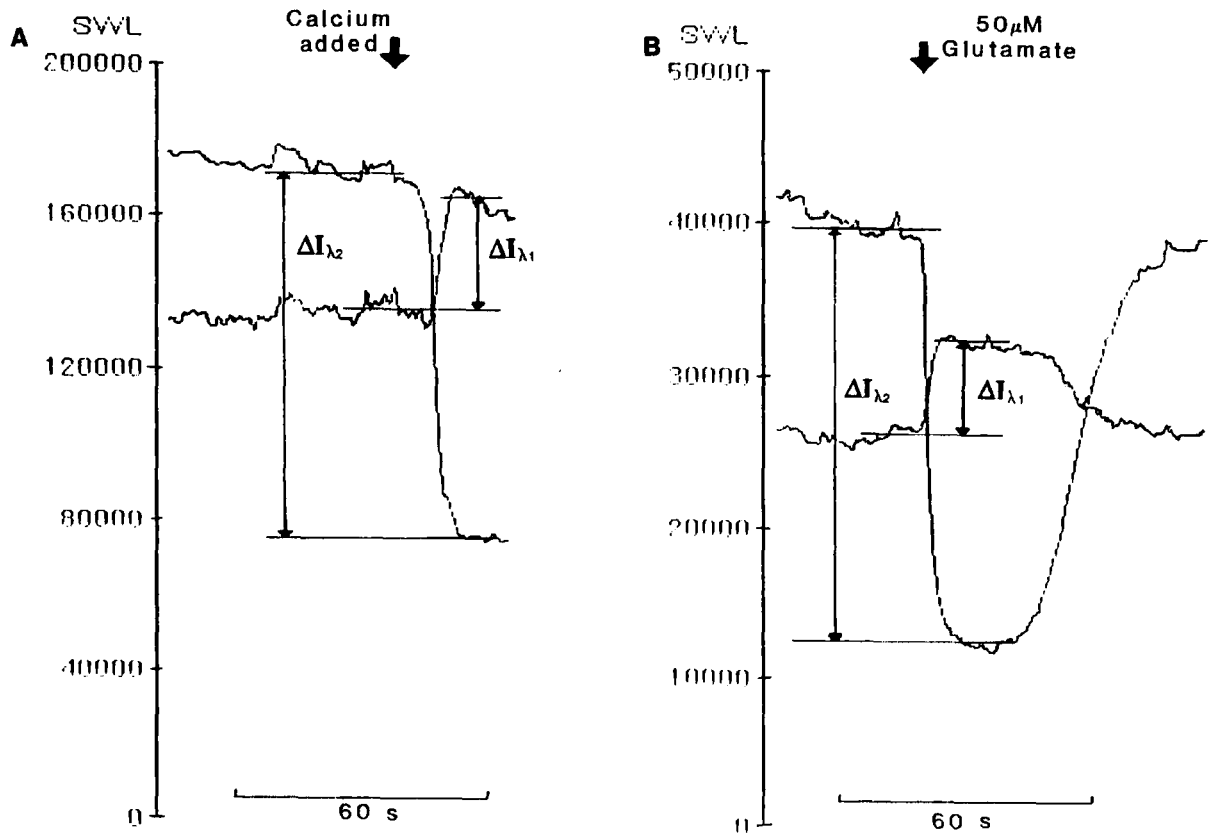
A
SWL
Calcium added
200000
160000
120000
80000
40000
0
$\Delta I_{\lambda 2}$
$\Delta I_{\lambda 1}$
60 s
B
SWL
50μM Glutamate
50000
40000
30000
20000
10000
0
$\Delta I_{\lambda 2}$
$\Delta I_{\lambda 1}$
60 s

value of V, as shown below:-

$$Z_{insitu} \quad 0.2434 \pm 0.0100 \quad n = 6$$

$$Z_{invitro} \quad 0.3268 \pm 0.0286 \quad n = 6$$

$$V = 0.745$$

4.3.3.4 Results and Calculation of Calibration Equation.

The ratio of fluorescence was measured a number of times for each calcium buffered solution at the three temperatures. These values were then multiplied by the viscosity correction factor, V. These data were then used to calculate the three unknowns in the calibration equation; R_{min}, R_{max} and $K_{\frac{1}{2}}$.

A computer program, based on the method of Wilkinson (1961) to fit a curve to the Michaelis Menten equation, was used. This required some manipulation of the original equation in order to have it in the form of a Michaelis–Mentin equation. The full equation is:-

$$[Ca^{2+}] = K_{\frac{1}{2}}\left(\frac{R - R_{min}}{R_{max} - R}\right)$$

If this curve is displaced, so that R_{min} = zero, i.e. subtracting R_{min} from all the ratio values, then this does not affect the shape of the curve or its position on the X axis. The equation becomes:-

$$[Ca^{2+}] = K_{\frac{1}{2}}\left(\frac{R'}{R'_{max} - R'}\right)$$

where

$$R' = R - R_{min}$$

$$R'_{max} = R_{max} - R_{min}$$

This equation can now be used to calculate R'_{max} and $K_{\frac{1}{2}}$ for any value of R_{min} chosen, using the computer program. If various values of R_{min} are used the sum of squares of the residuals about the curve (SSQ) can be seen to form a minimum (Fig. 4.6). This value of R_{min}, minimising the SSQ, was used and the

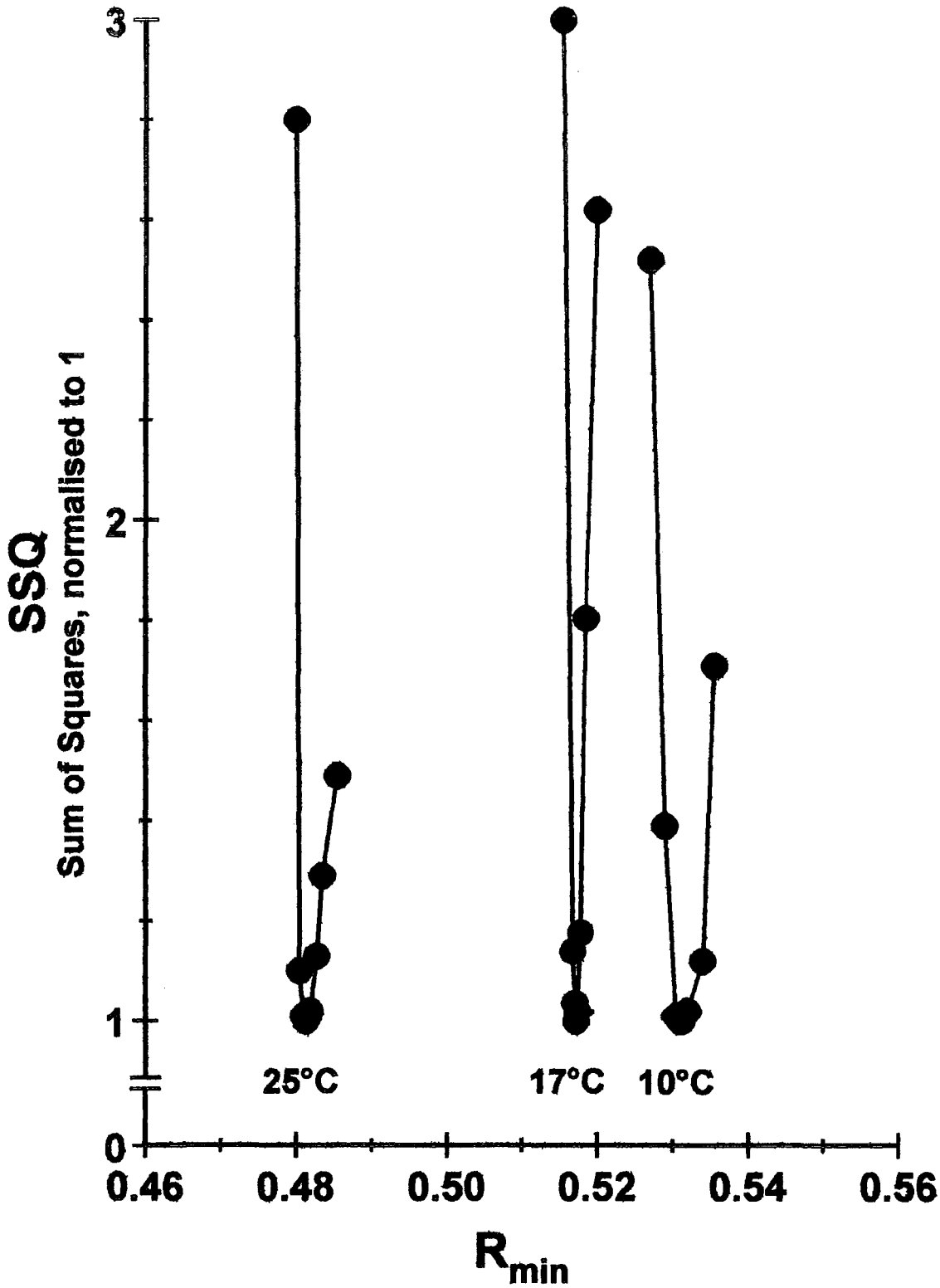
SSQ
Sum of Squares, normalised to 1
3
2
1
0
25°C
17°C
10°C
0.46
0.48
0.50
0.52
0.54
0.56
R_{min}

corresponding values of R'_{max} and $K_{\frac{1}{2}}$. R_{max} was then simply $R'_{max} + R_{min}$. For the three temperatures used the results are as shown in Table 4.1.

Table 4.1. The results of the *in vitro* calibration at three temperatures.

Temp.	$K_{\frac{1}{2}}$	R_{min}	R_{max}
10°C	$744nM$	0.531	9.34
17°C	$800nM$	0.517	9.32
25°C	$570nM$	0.481	9.25

The experimental results are shown in Fig. 4.7 along with the calculated calibration curves. Fig. 4.7 D shows the three calculated curves over the range of ratio values observed in the subsequent experiments, i.e. between the ratio values of 0.5 and 4. This shows that there was very little variation between the calibration curves at the three temperatures used over the ratio values observed *in situ*.

4.3.4 *In Situ* Calibration

4.3.4.1 Method.

As discussed the objective of the *in situ* calibration was to corroborate the values of R_{min} and R_{max} obtained from the *in vitro* calibration combined with the viscosity correction factor. The most frequently used calcium ionophores for intracellular calibration of fluorescent dyes are ionomycin (Williams and Fay, 1990) and the calcium ionophore 4-bromo-A23187 (Deber *et al.*, 1985), as these are nonfluorescent in the ultra–violet spectrum used, unlike the calcium ionophore A23187. Ionomycin was used in this study as it is more selective for calcium over magnesium than 4-bromo-A23187.

The method used was based on Protocol 5 from Thomas and Delaville (1991). The cells were loaded with Fura-2 and placed in the experimental chamber at 17°C in the normal way. The fluorescence intensity for each excitation wavelength was measured before the excitation pathway was closed. The cell was then perfused

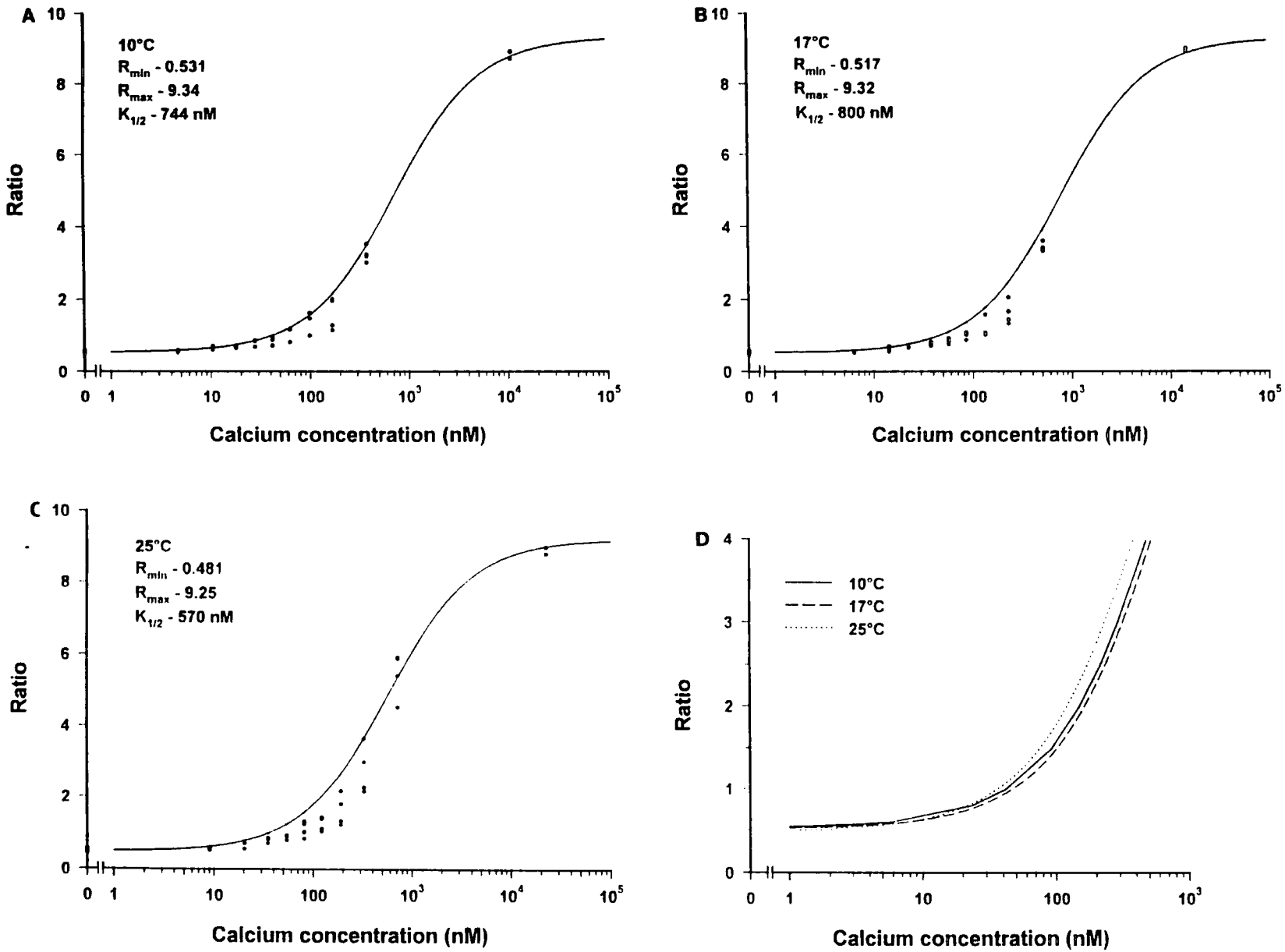
A
10°C
R_{min} - 0.531
R_{max} - 9.34
$K_{1/2}$ - 744 nM
Ratio
Calcium concentration (nM)
B
17°C
R_{min} - 0.517
R_{max} - 9.32
$K_{1/2}$ - 800 nM
Ratio
Calcium concentration (nM)
C
25°C
R_{min} - 0.481
R_{max} - 9.25
$K_{1/2}$ - 570 nM
Ratio
Calcium concentration (nM)
D
10°C
17°C
25°C
Ratio
Calcium concentration (nM)

with calcium free saline (containing $5mM$ EGTA) for a few minutes. With the perfusion stopped ionomycin (from a stock of $5mM$ dissolved in DMSO) was pipetted into the chamber to give a final ionomycin concentration of about $75\mu M$. This was left for 3–5 minutes to allow permeabilization of the cell membrane to calcium and thus the intracellular calcium concentration to equilibrate with the extracellular concentration.

The excitation pathway was then opened and the flourescence intensities remeasured during a number of changes in the perfusant (see Fig 4.8). Initially, in the EGTA containing saline, the intracellular free calcium concentration should have been close to zero and allowed calculation of R_{min}. However in some cases the fluorescence intensities had dropped significantly when compared to before the ionomycin was added. This was probably due to dye leakage from the cell (Roe *et al.*, 1990). If this occured (i.e. a drop of more than about 5%) then the experiment was discarded. However in most cases the perfusion was restarted and a high calcium concentration was added (usually $20mM$). Once the fluorescence intensities had stabilised at their new levels the intracellular Fura-2 should have been saturated with free calcium and R_{max} could be calculated. The perfusant was then replaced with a manganese containing solution ($5mM$ Mn^{2+}, $1mM$ Ca^{2+}), to quench the Fura-2, manganese being able to enter the cells in the presence of ionomycin. The values of R_{min} and R_{max} were calculated as shown in Fig. 4.8.

4.3.4.2 Results.

The *in situ* values for R_{min} and R_{max} were calculated for eight cells at 17°C and are compared to the *in vitro* values below:-

	in situ	*in vitro*
R_{min}	0.555±0.018	0.517
R_{max}	9.25±0.24	9.32

The *in situ* value for R_{max} was close to that calculated from the *in vitro* calibration, while the *in situ* R_{min} value was slightly larger than the corresponding *in vitro* value. The elevated *in situ* R_{min} value was possibly due to the intracellular

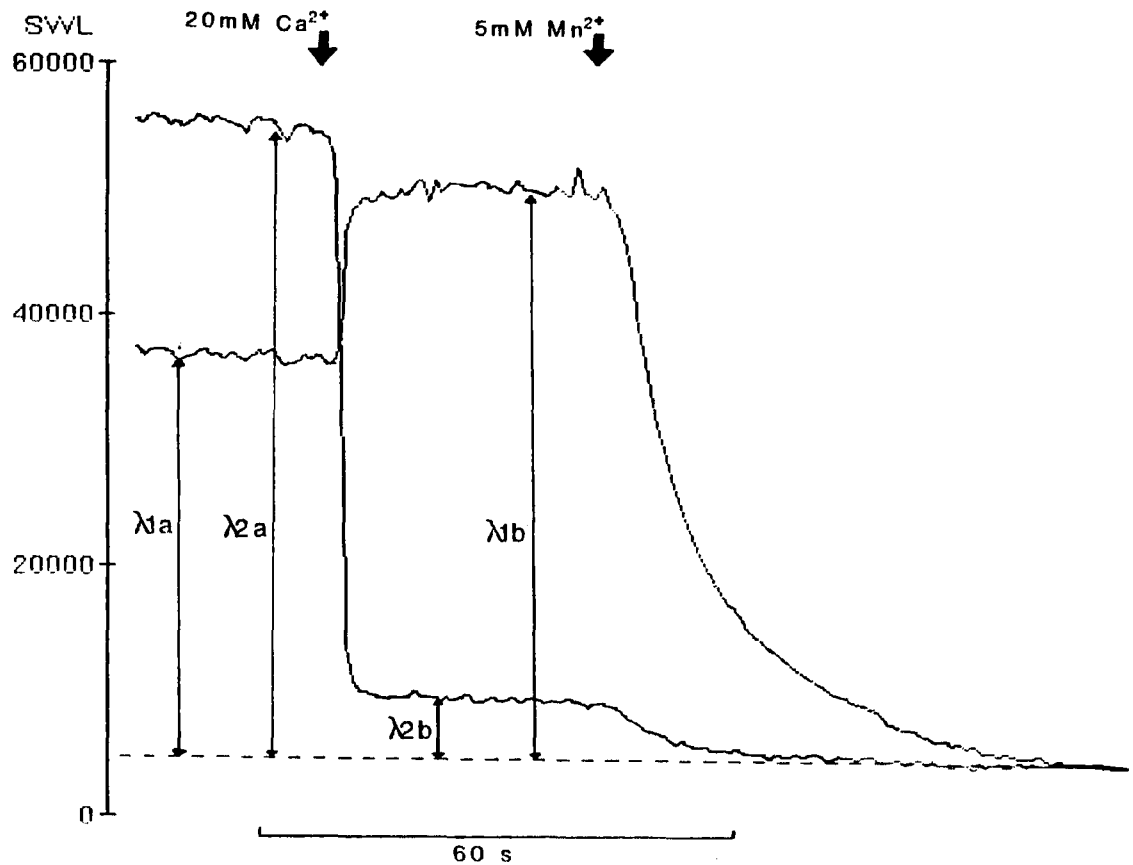
SWL
20mM Ca2+
5mM Mn2+
60000
40000
20000
0
λ1a
λ2a
λ1b
λ2b
60 s

calcium concentration not being completely buffered to zero because of the gradual release of calcium from intracellular calcium chaelators and intracellular stores. Taking this into account the *in situ* results corroborate the *in vitro* results reasonably well and in particular the value used for the viscosity correction factor.

4.3.5 Conclusion.

As can be seen from Fig. 4.7 D the relationship between the ratio measured, and the actual calcium concentration was not a linear one. Consequently when viewing results it must be remembered that a doubling in ratio is not analagous to a doubling in calcium concentration.

4.4 RESULTS

4.4.1 Introduction

The majority of the results presented in this section demonstrate stimulus–induced changes of intracellular calcium concentration in individual cells. In all cases, unless otherwise stated, the cells were from fish acclimated to 16°C and the temperature at which intracellular calcium concentration measurementes were made was 17°C.

Fig. 4.9 is a typical example demonstrating how the ratiometric measuring technique reports an increase in calcium concentration, in this case caused by the cell being exposed to $25\mu M$ L–glutamate. The lower half of the figure, labelled SWL (for Single Wavelength measurements), shows the fluorescence intensities recorded when the dye was excited at the two excitation wavelengths. In response to L–glutamate stimulation the Fura-2 fluorescence intensity when excited at $350nm$ increases, while the Fura-2 fluorescence intensity when excited at $380nm$ decreases. Consequently there is a marked change in the ratio of the fluorescence at the two excitation wavelengths recorded. This is shown on the upper half of the figure, labelled Ratio. Using the calculated calibration equation (Section 4.3) calcium concentrations were calculated for ratio values and a second axis displayed showing corresponding intracellular calcium concentrations.

As can be seen the response to the $25\mu M$ L–glutamate stimulus was a rapid rise in intracellular calcium concentration from the original level to over $300nM$ in a few seconds. The increase was sustained for about 25 seconds before returning rapidly to the resting level. The apparent fluctuations in calcium concentration at the peak of the response are probably due to increased noise in the signal. At this time the fluorescence intensity on excitation at $380nm$ is considerably lower than the either of the fluorescence measurements before the calcium concentration change. Consequently a small change in this fluorescence intensity value has a much greater influence on the calculated ratio than if the two intensities are similar in magnitude.

In many experiments the amplitude of the ratio changes observed decreased with time as a result of photobleaching of the Fura-2 (Becker and Fay, 1987). This

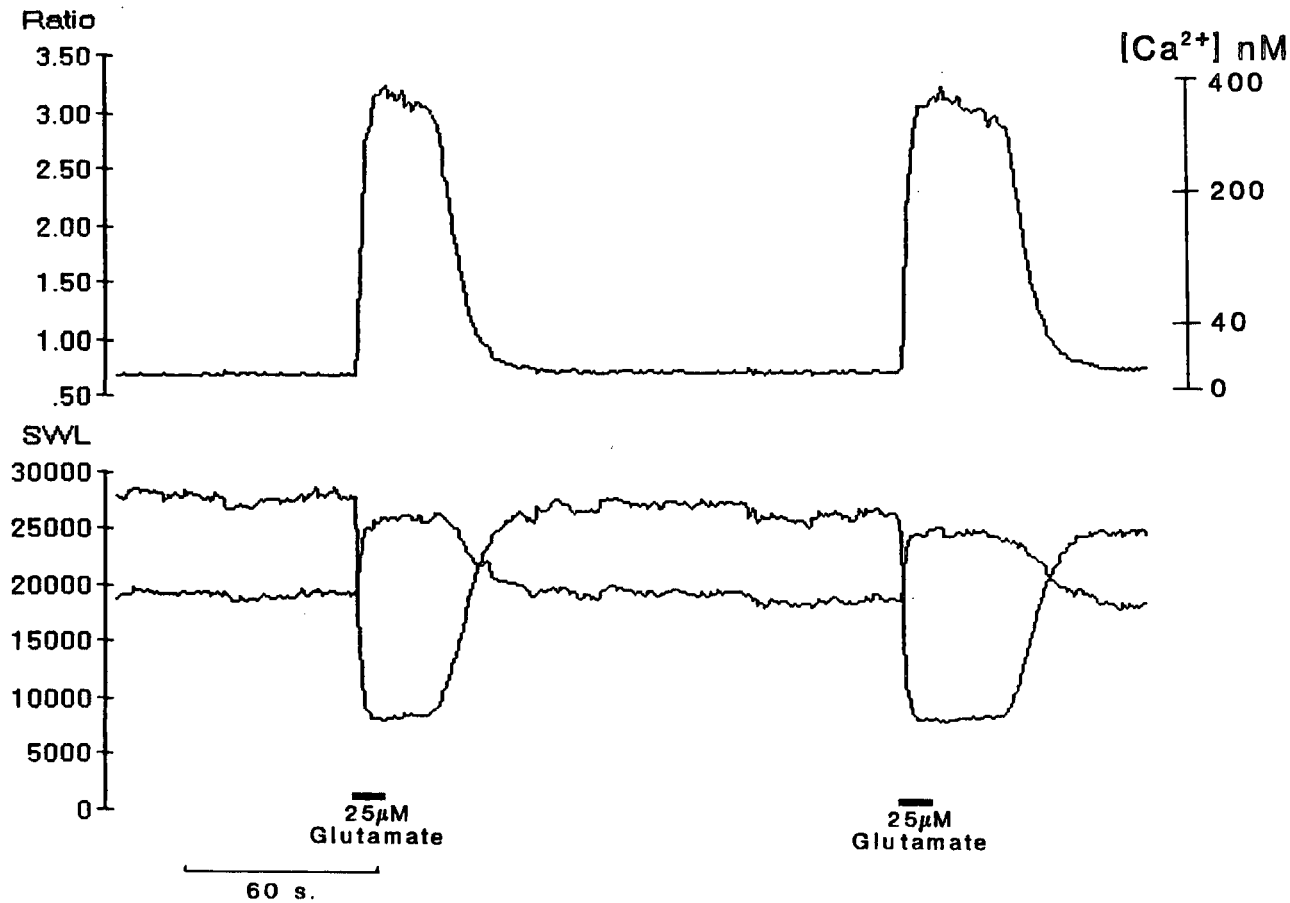
Ratio
3.50
3.00
2.50
2.00
1.50
1.00
.50
[Ca2+] nM
400
200
40
0
SWL
30000
25000
20000
15000
10000
5000
0
25μM
Glutamate
25μM
Glutamate
60 s.

problem is discussed fully in Section 4.5.1.6. However the problems it presents in making accurate measurements of intracellular calcium concentrations need to be recognized. Fig. 4.10 demonstrates an extreme example of photobleaching. Initially it appears that the increase in intracellular calcium concentration in response to sucessive 10 second exposures to $50\mu M$ L–glutamate was decreasing. However, if the fluorescence intensities of the two excitation wavelengths are examined it is clear that the fluorescence intensity, at elevated calcium concentrations, when excited at $380nm$, actually increased. This indicates the presence of a photobleaching product which has an excitation spectrum peak closer to $380nm$ than $350nm$ (Becker and Fay, 1987 report an excitation maximum at $375nm$ for the photobleaching product). Consequently the decrease in amplitude of the ratio change does not necessarily indicate a decrease in the maximum intracellular calcium concentration induced by the $50\mu M$ L–glutamate (cf. Fig. 4.9 where the response amplitude is consistent when there is no appreciable reduction in total fluorescence).

In this figure and in most subsequent ones a calcium concentration scale is not included. Although in most experiments the amount of photobleaching of the dye was much less than in Fig. 4.10 the caveat remains that the ratios recorded may not always correspond exactly to the calcium concentration calculated by the calibration equation (see also Section 4.5.1.6). However the fluorescence ratio changes observed are clearly indicative of intracellular calcium concentration changes of the order of magnitude indicated in Fig. 4.9. Although further figures do not normally show the fluorescence intensity values due to the separate excitation wavelengths a careful monitor of fluorescence intensities in subsequent experiments means that in most cases photobleaching during the experiments was not a frequent occurance, although in some cases it did occur and is commented on.

4.4.2 The 'Resting' Level of Intracellular Calcium

Throughout the rest of this chapter a cell in normal saline with no depolarizing stimuli is referred to as being in a 'resting' state. The fluorescence ratio recorded from 'resting' cells was usually 0.65 to 0.75. This corresponds to intracellular calcium concentrations of $12nM$ to $22nM$. For most experiments this ratio remained

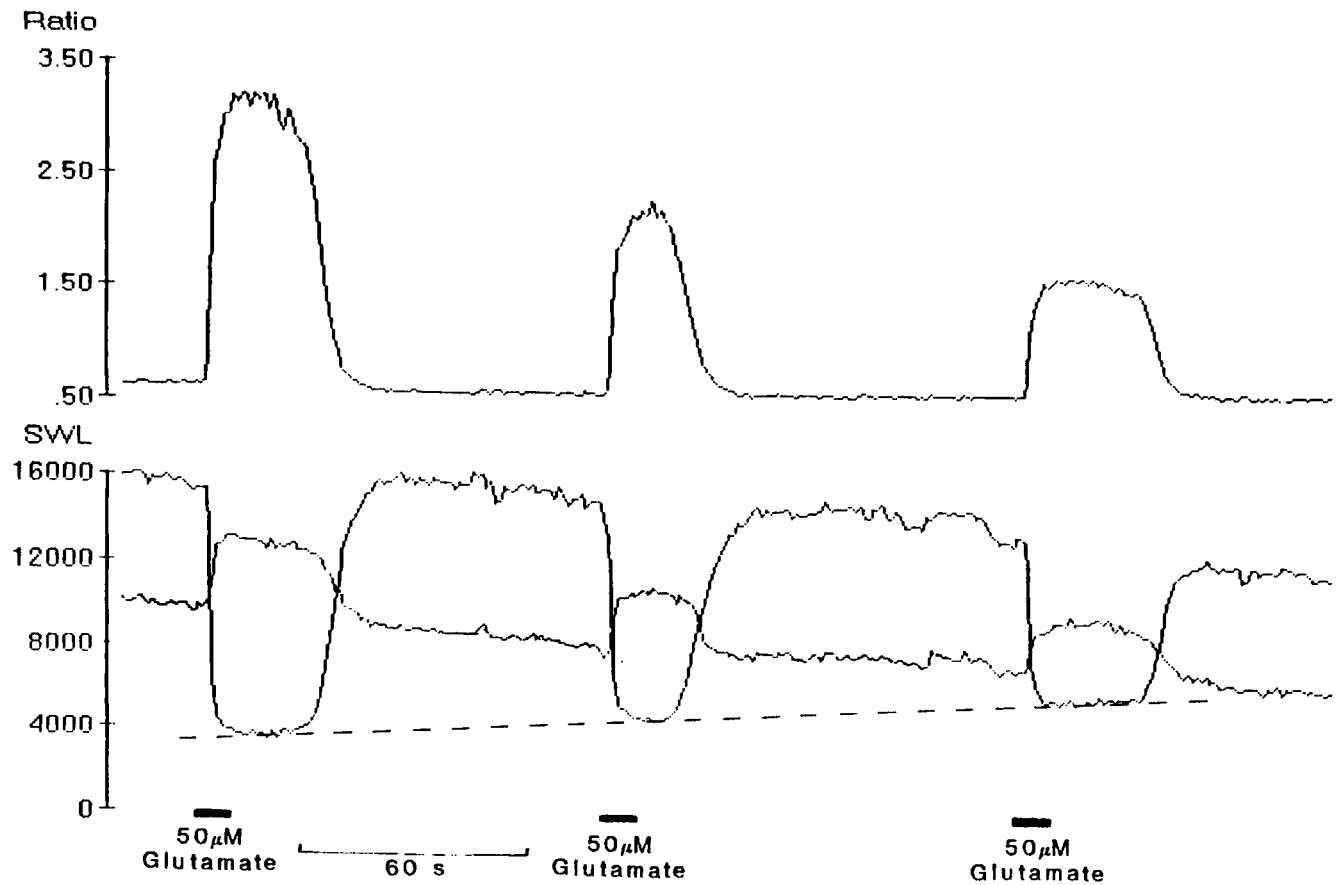
Ratio
3.50
2.50
1.50
.50
SWL
16000
12000
8000
4000
0
50μM
Glutamate
60 s
50μM
Glutamate
50μM
Glutamate

constant for considerable time periods (i.e. minutes) provided that the cells remained in the normal saline. However throughout the course of the experiments cells showed, on occasion, increases in intracellular calcium concentration, represented by increases in the ratio recorded, not associated with any applied stimulus. These varied considerably from cell to cell. They usually consisted of a series of rises in ratio recorded, each of a few seconds duration, which became more frequent until a persistently elevated ratio level was recorded (see Fig. 4.11 A). The amplitude of these 'spontaneous' changes varied widely from cell to cell, with peak ratio values of 1–3 being most common. Once the ratio reached the permanently elevated state it did not change in response to any external stimuli.

It was noticed that these 'spontaneous' changes in intracellular calcium tended to occur most frequently in cells which appeared less healthy, e.g. with dendrites rounded up or with surface irregularities. The appearence of cells tended to vary between different retinal preparations and was probably due to mechanical or protease damage during the cell preparation. However usually a cell preparation yielded reasonable numbers of viable cells, or, on occasion, none at all.

Cell photodamage has been recognised as a potential problem when using fluorescent dyes requiring illumination in the ultra–violet region of the spectrum (e.g. Moore *et al.*, 1990; Grapengiesser, 1993) and it was thought that the 'spontaneous' changes in intracellular calcium concentration could be due to ultra–violet. damage. Using cells all from the same retina (from a preparation where the cells were not as healthy as usual and therefore more susceptible to 'spontaneous' increases in ratio) single cells were illuminated with the excitation beam attenuated by a range of neutral density filters. The results (see Fig. 4.11) show that, for this cell preparation, the intensity of the ultra–violet illumination affected the mean time taken for the first 'spontaneous' intracellular calcium concentration rises to occur. If the excitation beam intensity was reduced then the ratio recorded remained constant for longer (e.g. with a neutral intensity filter attenuating the excitation beam to 24% of the full beam calcium concentration increases occured after 298±43 seconds (mean ± S.E.M. $n = 6$), while attenuation to 6% increased this time to 623±47 seconds (mean ± S.E.M. $n = 6$)), suggesting that the cells were indeed being damaged by the ultra–violet.

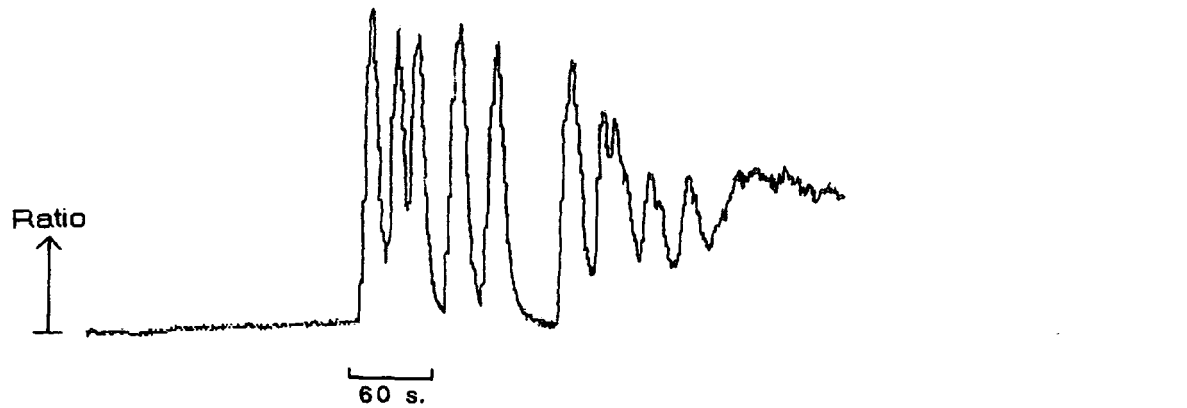
Ratio
60 s.

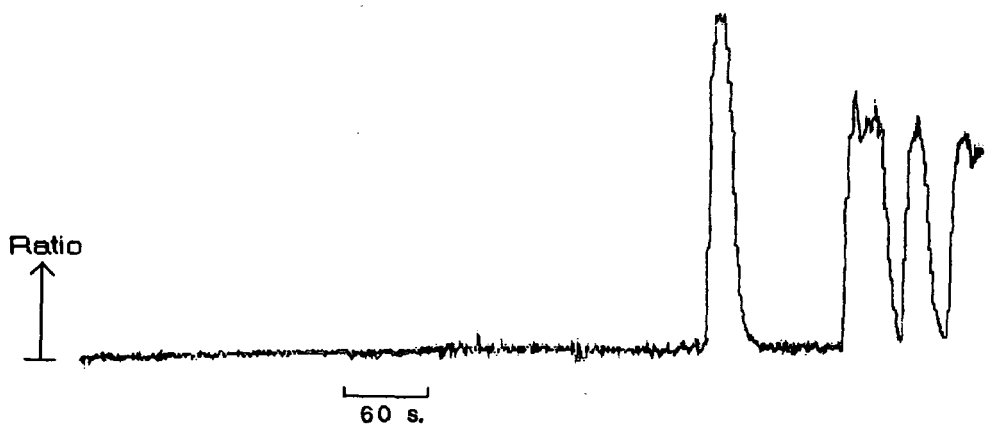
Ratio
60 s.

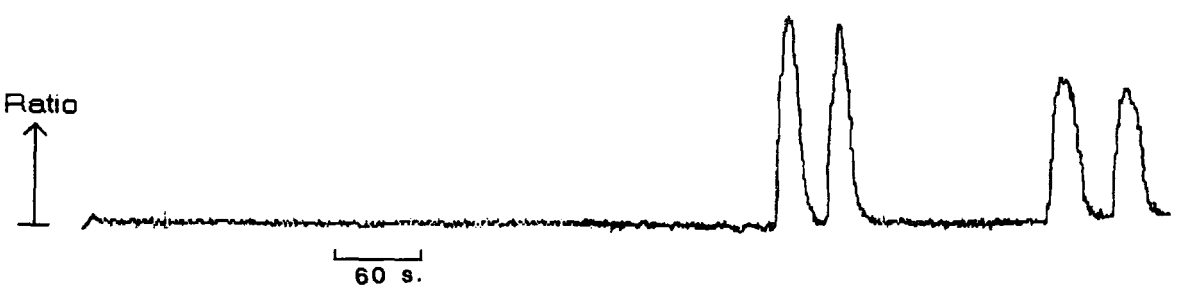
Ratio
60 s.

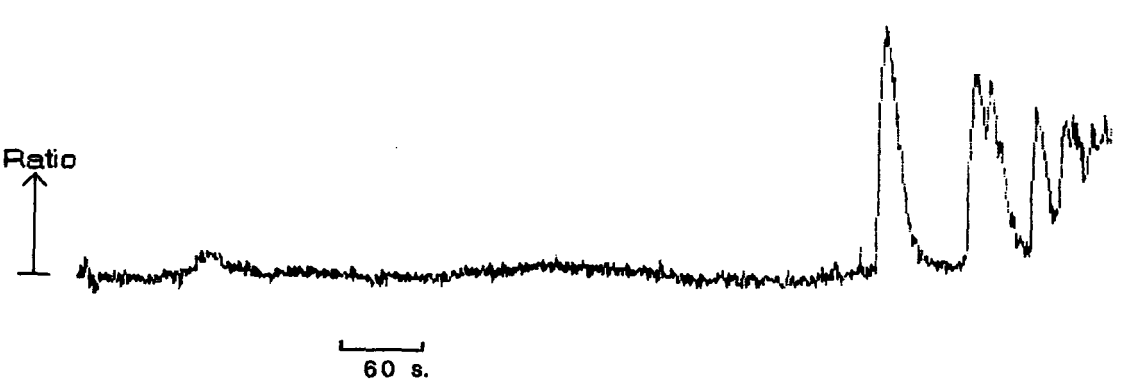
Ratio
60 s.

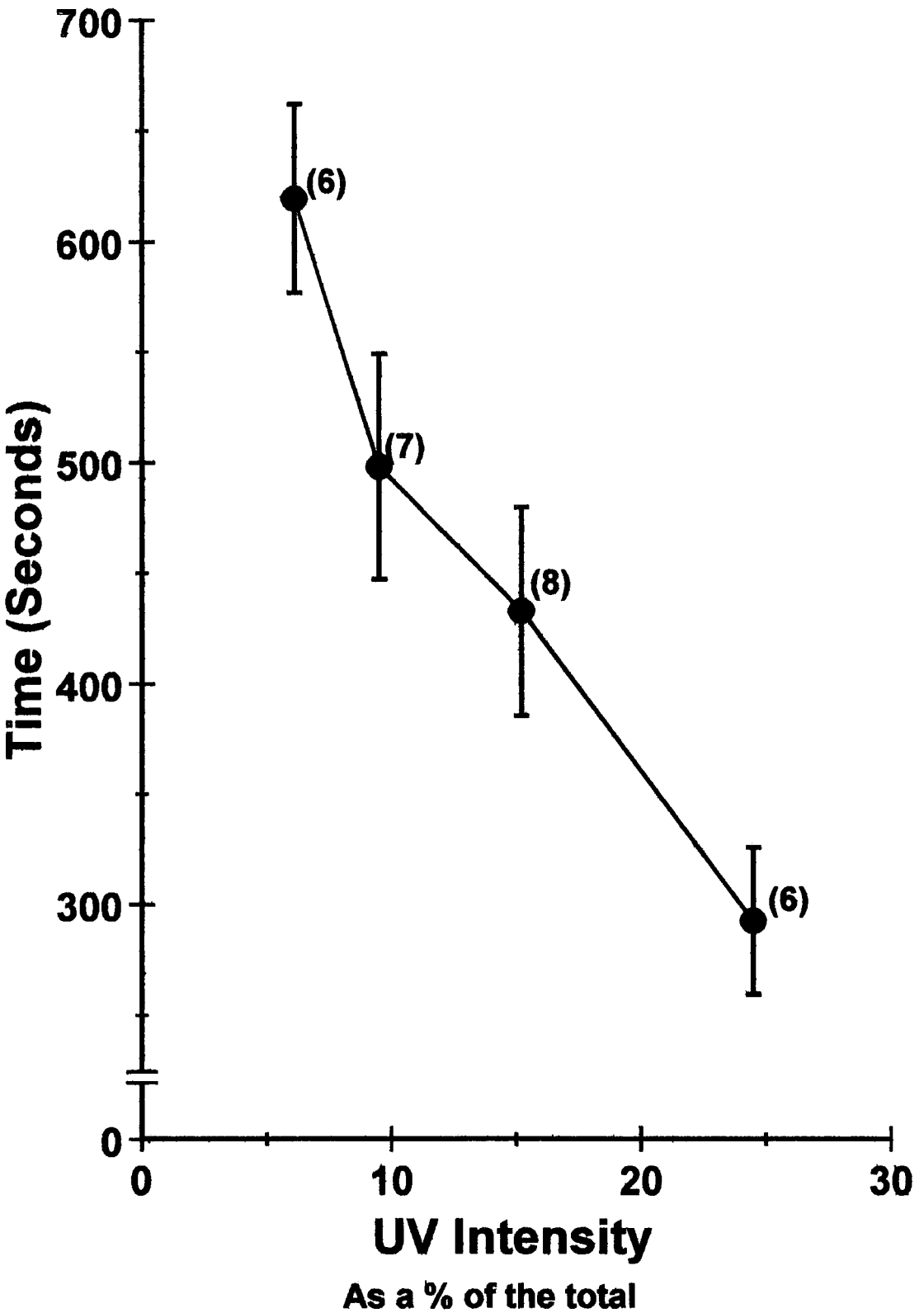
700
600
500
400
300
0
Time (Seconds)
(6)
(7)
(8)
(6)
0
10
20
30
UV Intensity
As a % of the total

For the subsequent experiments the neutral density filter used in the excitation pathway transmitted 9% of the full excitation beam. It was generally possible to run experiments over time periods well in excess of 500 seconds by blocking the excitation pathway during the experiment when the cells were not being stimulated and, more importantly, using only cells which appeared healthy. In this way the frequency of 'spontaneous' responses was kept very low. On those occasions where they did occur the experiment was discarded.

4.4.3 Characterization of Calcium Increases

Membrane depolarization caused an increase in intracellular calcium concentration. The membrane was depolarized by either the application of L–glutamate or by increasing the extracellular potassium concentration which results in a depolarization as shown by Tachibana (1981).

The response to L–glutamate appeared to be all or nothing for concentrations above a certain threshold value, e.g. in Fig. 4.12 glutamate concentrations of $25\mu M$ and $30\mu M$ elicited no increase in intracellular calcium concentration, while glutamate concentrations of $40\mu M$, $50\mu M$ and $250\mu M$ resulted in increases to about the same maximum. The duration of the rise in intracellular calcium concentration increased slightly on increased glutamate concentration, but this may well been due to the increased time taken to wash the glutamate out of the dish. The amplitude of the response to glutamate was most frequently from the 'resting' ratio to a peak of almost 3.5 representing a rise in intracellullar calcium concentration to about $400nM$. However there was variation in the amplitude of response, with a lower maximum recorded, possibly as a result of photobleaching of the Fura-2. The minimum concentration required to elicit a response varied between cells ($10\mu M$ to $40\mu M$) but was usually constant for any one cell. ($23.1 \pm 1.3\mu M$ mean $\pm$ S.E.M. n=29).

In contrast, the response to ten second increases in a range of extracellular potassium concentrations was graded (Fig. 4.13). It was assumed that the cells act as potassium electrodes, i.e. the increase in extracellular potassium results in the membrane potential being depolarized in a Nernstian way as shown by Tachibana (1981). The concentrations of extracellular potassium required to cause increases in the intracellular calcium concentration were more consistent between cells than

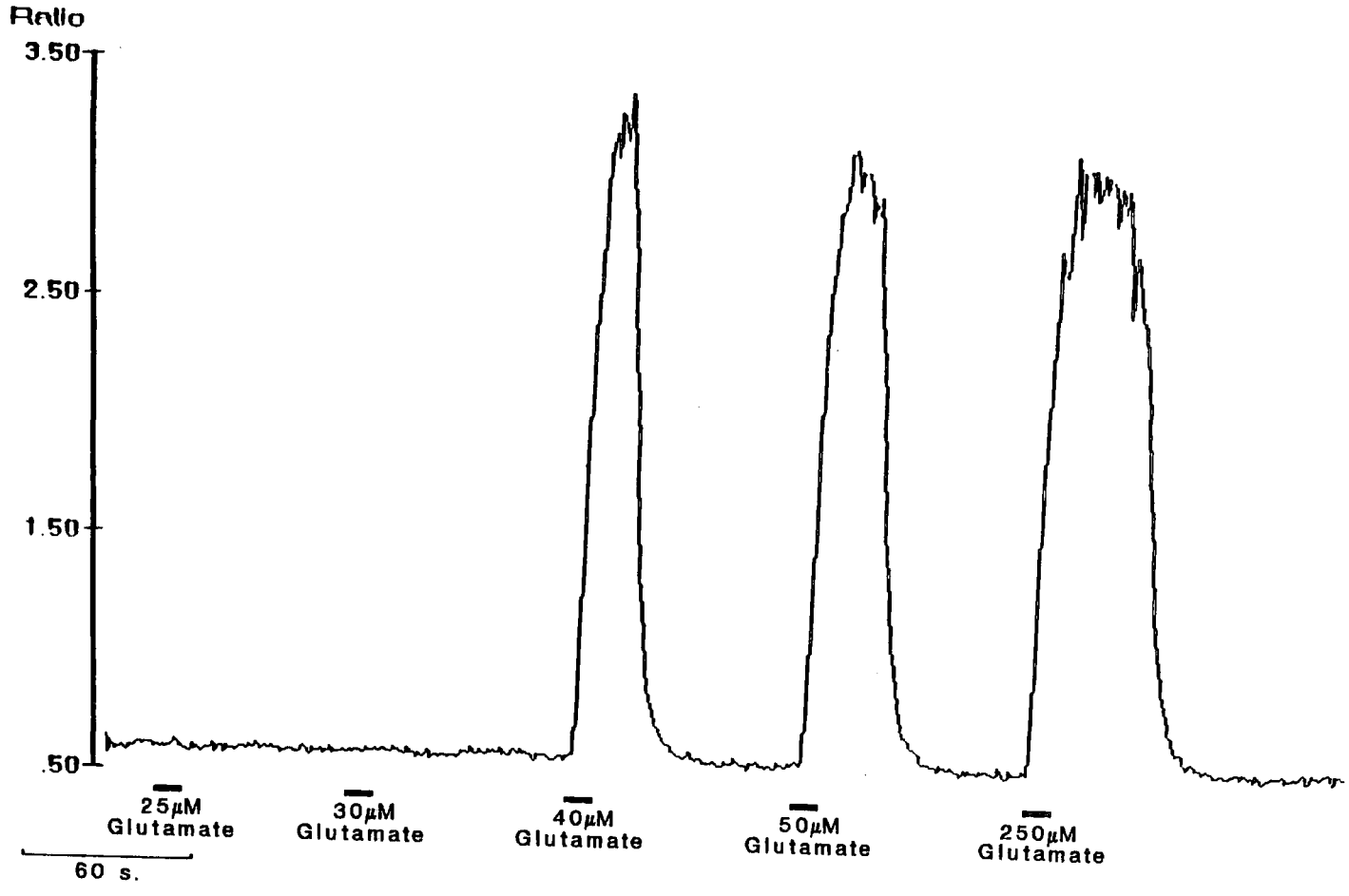
Ratio
3.50
2.50
1.50
.50
25μM Glutamate
30μM Glutamate
40μM Glutamate
50μM Glutamate
250μM Glutamate
60 s.

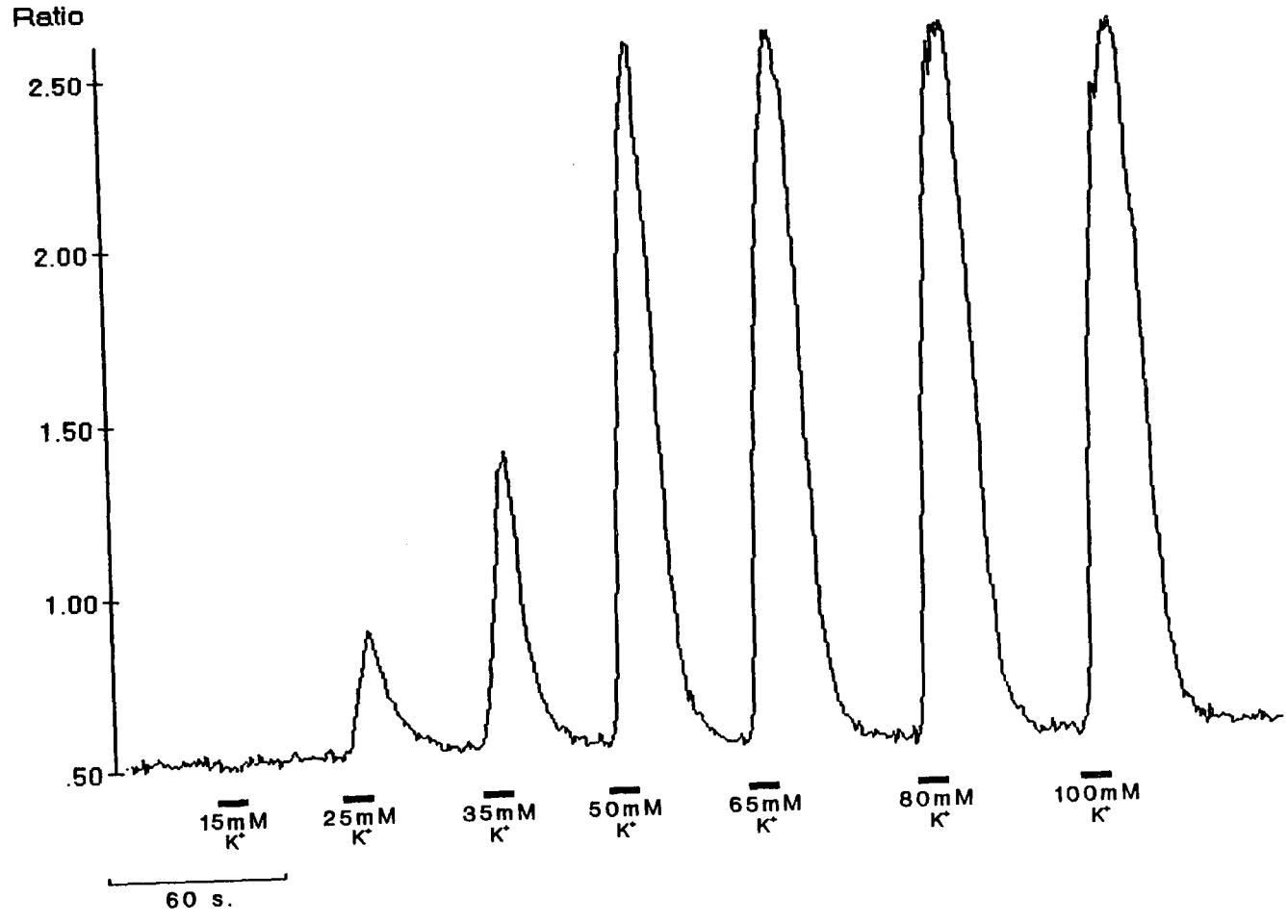
Ratio
2.50
2.00
1.50
1.00
.50
15mM K+
25mM K+
35mM K+
50mM K+
65mM K+
80mM K+
100mM K+
60 s.

was the case for the L–glutamate response. An extracellular potassium concentration of $25mM$ generally caused only a slight increase in intracellular calcium concentration, while an extracellular potassium concentration of $80mM$ caused a maximum increase in intracellular calcium concentration, to about $250nM$.

As both L–glutamate and potassium are known to depolarize isolated horizontal cells (Lasater, 1986 and Tachibana, 1981 respectively), it was decided to test whether the intracellular calcium concentration changes observed were due to an influx of calcium from the extracellular solution through voltage gated calcium channels, such as were demonstrated using the patch clamp technique (Chapter 3).

To test this possibility cells were depolarized in calcium free saline ($1mM$ Ca^{2+} replaced by $1mM$ EGTA) by both L–glutamate ($>50\mu M$) and an increased extracellular potassium concentration (to $65mM$). In both cases there was no increase in intracellular calcium, while on returning calcium to the saline the response was restored (n=6 and n=3 respectively), as shown in Fig. 4.14. If calcium was removed from the saline during a prolonged depolarizing stimulus, as shown in Fig. 4.15, then the intracellular calcium concentration returned to the 'resting' level, n=6. Moreover the magnitude of the intracellular calcium concentration increase in response to a $25\mu M$ L–glutamate stimulus was dependent on the extracellular calcium concentration — the higher the extracellular calcium concentration (between $0.25mM$ and $4mM$) the greater the increase in intracellular calcium concentration (Fig. 4.16), n=3. These results indicate that the source of the intracellular calcium concentration changes was an influx of extracellular calcium.

The effect on intracellular calcium concentration of aspartate and various glutamate analogues was tested. Even at concentrations of over $500\mu M$ aspartate did not have any effect on the intracellular calcium concentration (Fig. 4.17 A). The potent agonists of glutamate, kainate (Johnston *et al.*, 1974) and quisqualate (Bisco *et al.*, 1975), both produced all or nothing responses similar to those generated by L–glutamate (Fig. 4.17 B and C). The concentrations used ($50\mu M$) were similar to those required for L–glutamate. However NMDA did not cause an increase in intracellular calcium, even at concentrations of $250\mu M$ and in magnesium free saline (Fig. 4.17 D).

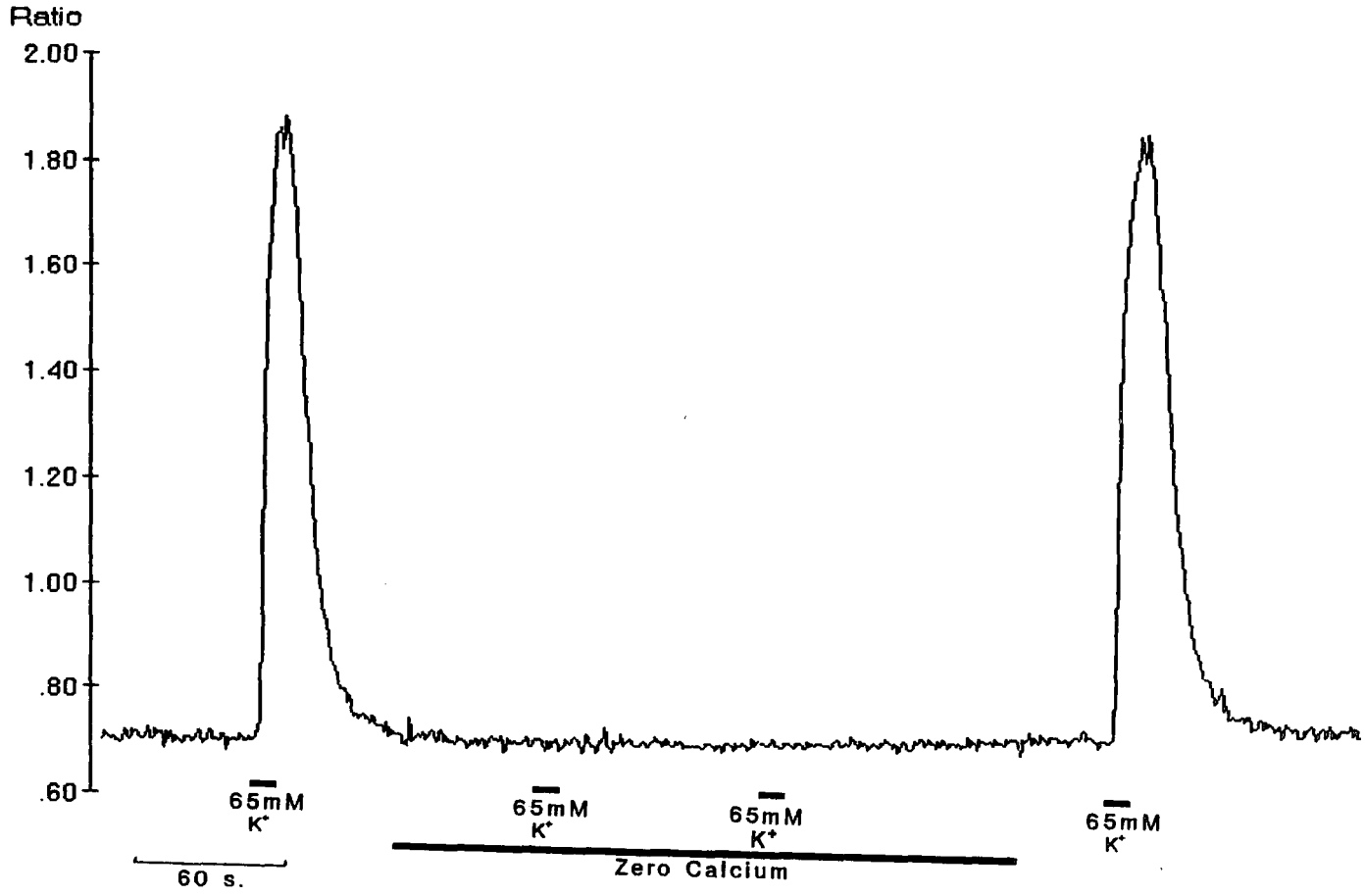
Ratio
2.00
1.80
1.60
1.40
1.20
1.00
.80
.60
65mM K+
65mM K+
65mM K+
65mM K+
60 s.
Zero Calcium

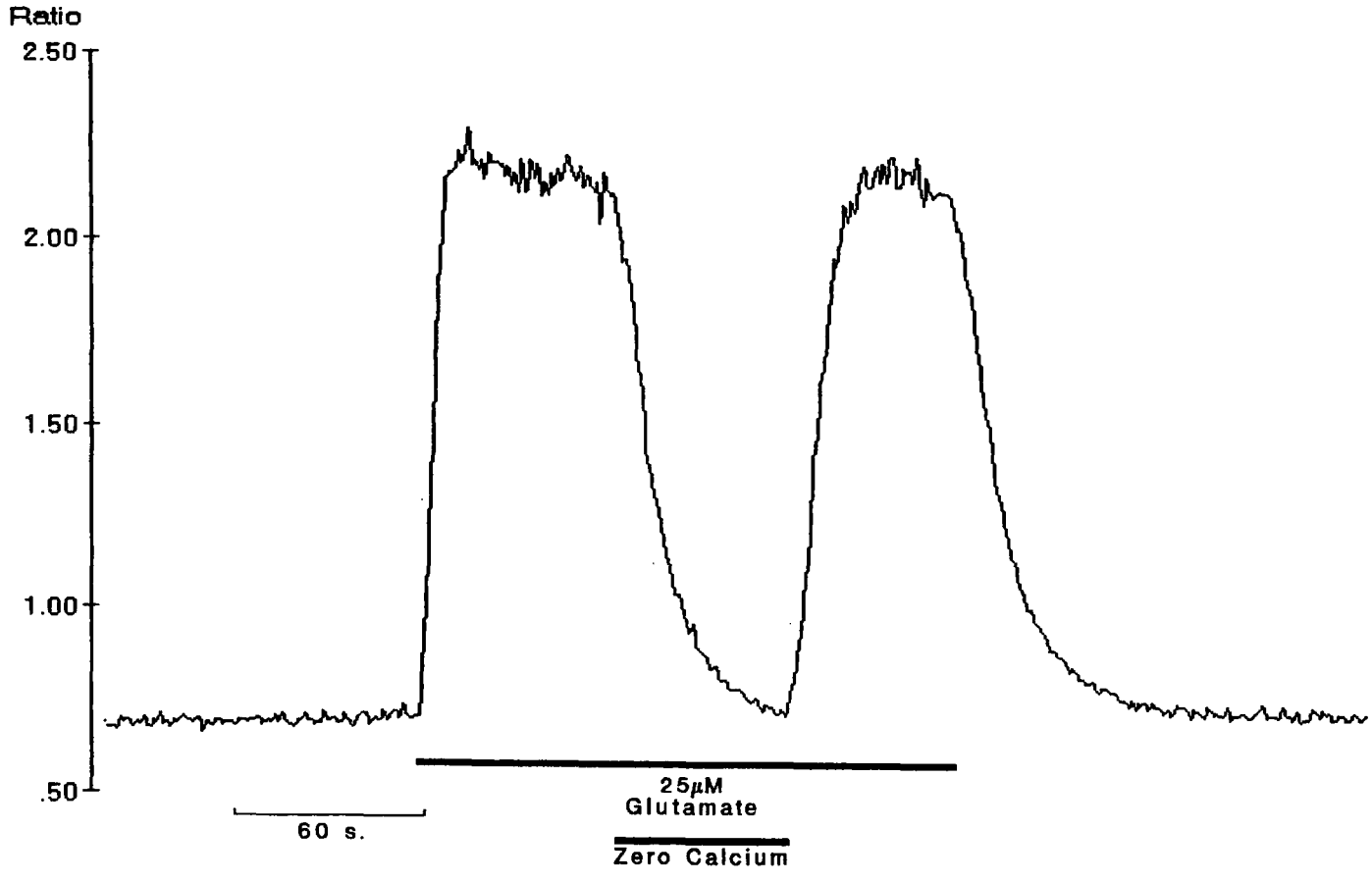
Ratio
2.50
2.00
1.50
1.00
.50
60 s.
25μM
Glutamate
Zero Calcium

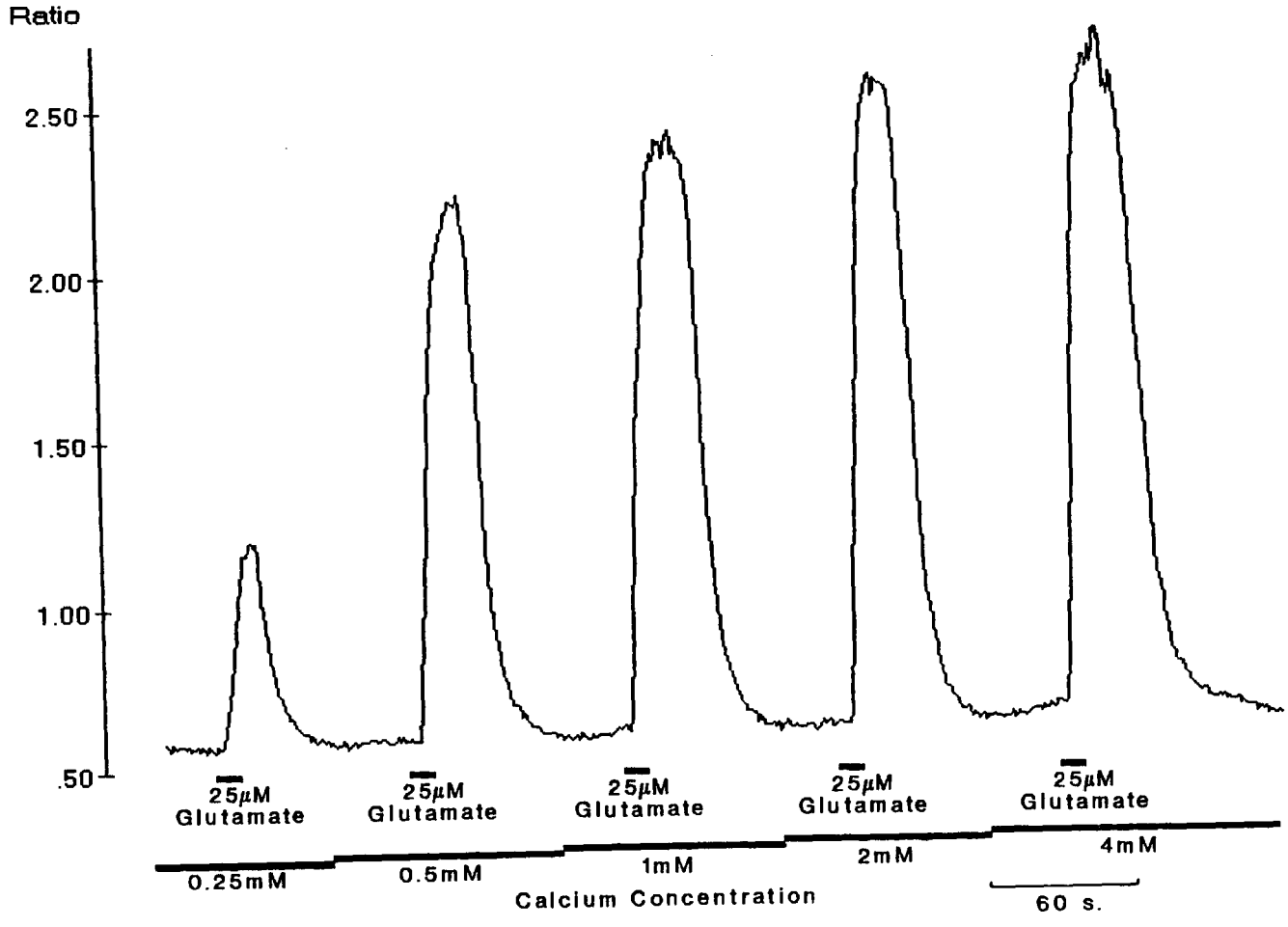
Ratio
2.50
2.00
1.50
1.00
.50
25μM Glutamate
25μM Glutamate
25μM Glutamate
25μM Glutamate
25μM Glutamate
0.25mM
0.5mM
1mM
2mM
4mM
Calcium Concentration
60 s.

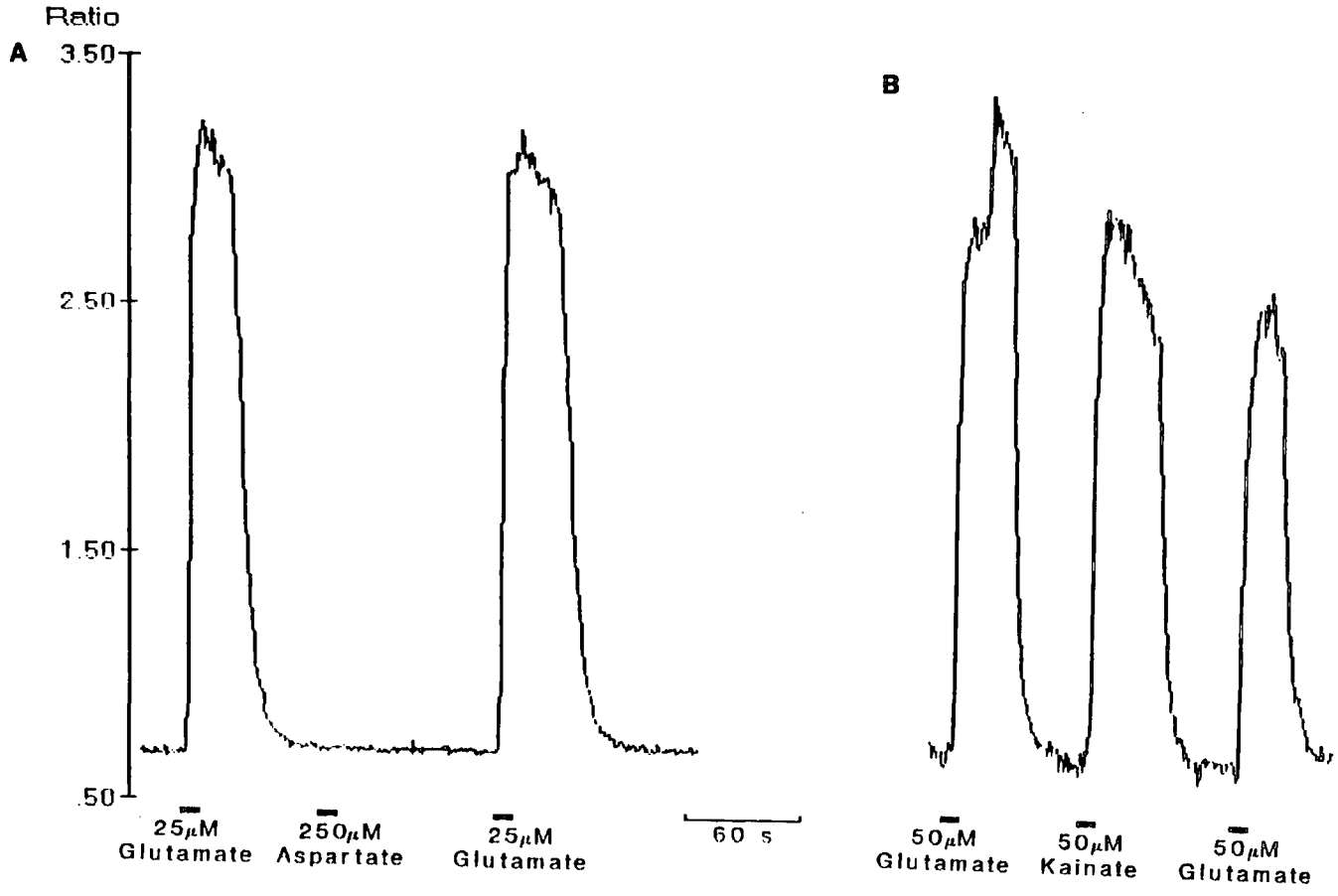
Ratio
A
3.50
2.50
1.50
.50
25μM
Glutamate
250μM
Aspartate
25μM
Glutamate
60 s
B
50μM
Glutamate
50μM
Kainate
50μM
Glutamate

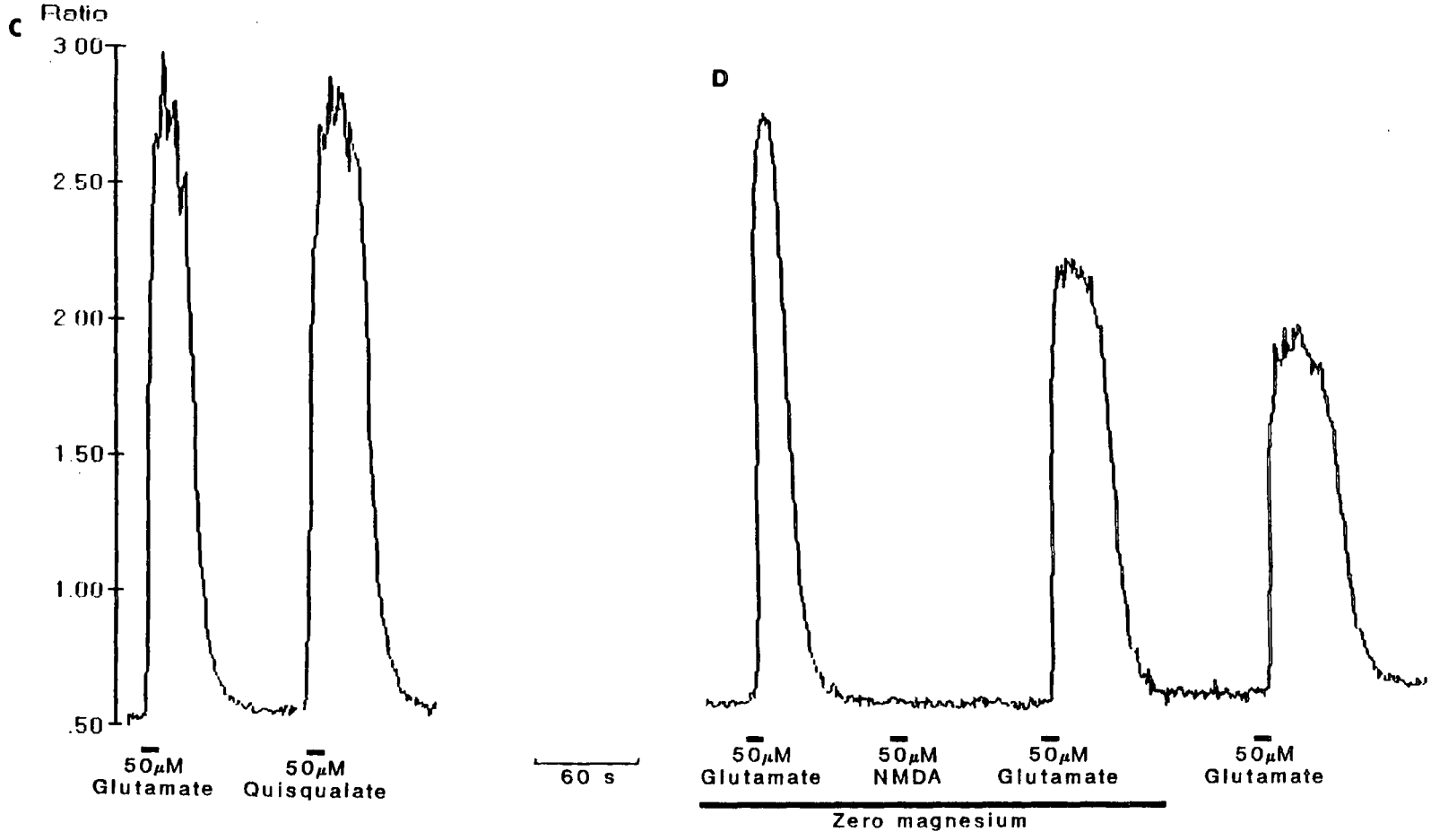
C
Ratio
3.00
2.50
2.00
1.50
1.00
.50
50μM
Glutamate
50μM
Quisqualate
60 s
D
50μM
Glutamate
50μM
NMDA
50μM
Glutamate
50μM
Glutamate
Zero magnesium

Horizontal cell axon terminals (Plate 3.1) were found to take up Fura-2, as well as the horizontal cell soma, so the effect of L–glutamate and elevated extracellular potassium on their intracellular calcium concentration was also examined. The 'resting' intracellular calcium concentration was about the same as in the horizontal cell soma. There was no apparent response to L–glutamate at $50\mu M$ or $500\mu M$ ($n = 50$). In a few cases when the extracellular potassium concentration was raised to $65mM$ the intracellular calcium concentration rose slightly as indicated by a ratio change. However, this was only slightly above the noise level of the ratio measurements (a ratio change of about 0.05) and it is not realistic to calculate the calcium concentration change it represents (Fig. 4.18).

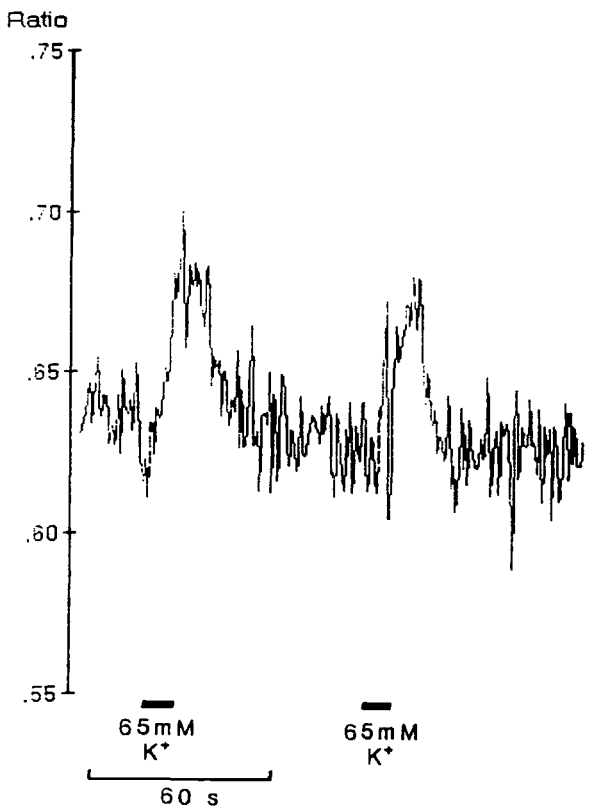

Figure 4.18. The effect of $65mM$ extracellular potassium concentration depolarizing stimuli on the intracellular calcium concentration of an axon terminal.

4.4.4 Potential Contribution of Intracellular Stores

Although it has been shown that the depolarization induced increase in intracellular calcium concentration is dependent on the presence of extracellular calcium, it is possible that a significant proportion of this increase was due to release of calcium from intracellular stores, as a result of calcium induced calcium release, triggered by the influx of extracellular calcium concentration. The potential contribution of CICR was investigated using caffeine to stimulate the Ryanodine receptor and result in the release of calcium from the intracellular stores (Endo, 1977; Rosseau and Meissner, 1989).

Cells were exposed to $20mM$ caffeine for about 40 seconds (Fig. 4.19). They responded with a rapid increase in intracellular calcium concentration to a maximum of about $75nM$, which then declined back to the 'resting' concentration within the 40 seconds. If the caffeine stimulus was repeated the response to the second stimulus was very small, or not detectable. However the response to caffeine recovered if the cell was depolarized in a calcium containing saline before a subsequent caffeine stimulus, as in Fig. 4.19. The caffeine–induced response was not dependent on the presence of extracellular calcium, as exposure to caffeine in calcium free saline resulted in a similar increase in intracellular calcium concentration (Fig. 4.19).

4.4.5 The Effect of Long Term Depolarizations

Horizontal cells in the intact retina are continually depolarized in the dark, due to the continuous release of photoreceptor (Trifonov, 1968, and Section 1.3.2). In order to attempt to simulate this condition in isolated cells they were depolarized by prolonged exposure to L–glutamate, kainate or elevated extracellular potassium. Fig. 4.20 shows the effect of exposures of $\sim$5 minutes of these three drugs on the same cell, with a gap of $\sim$5 minutes between stimuli. In all three cases the intracellular calcium concentration rose to a peak (Ratio $\approx$ 2.9) and then declined to a plateau level, which was still considerably elevated in comparison to the 'resting' level (Ratio $\approx$ 1.6). The time course of the decline from the peak intracellular calcium concentration to the plateau concentration, measured as a half time, was similar for the L–glutamate, kainate and the elevated extracellular

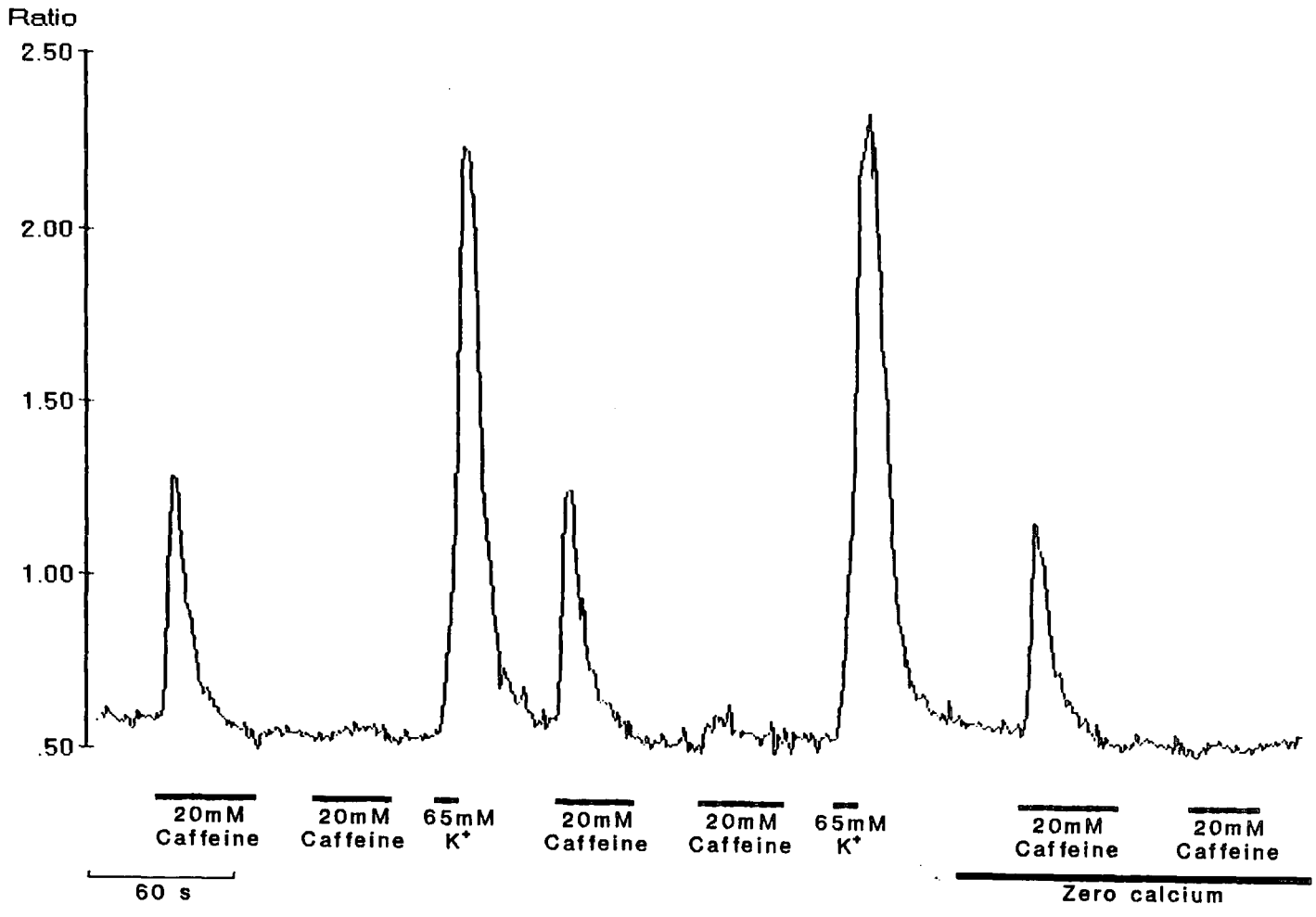
Ratio
2.50
2.00
1.50
1.00
.50
20mM Caffeine
20mM Caffeine
65mM K+
20mM Caffeine
20mM Caffeine
65mM K+
20mM Caffeine
20mM Caffeine
60 s
Zero calcium

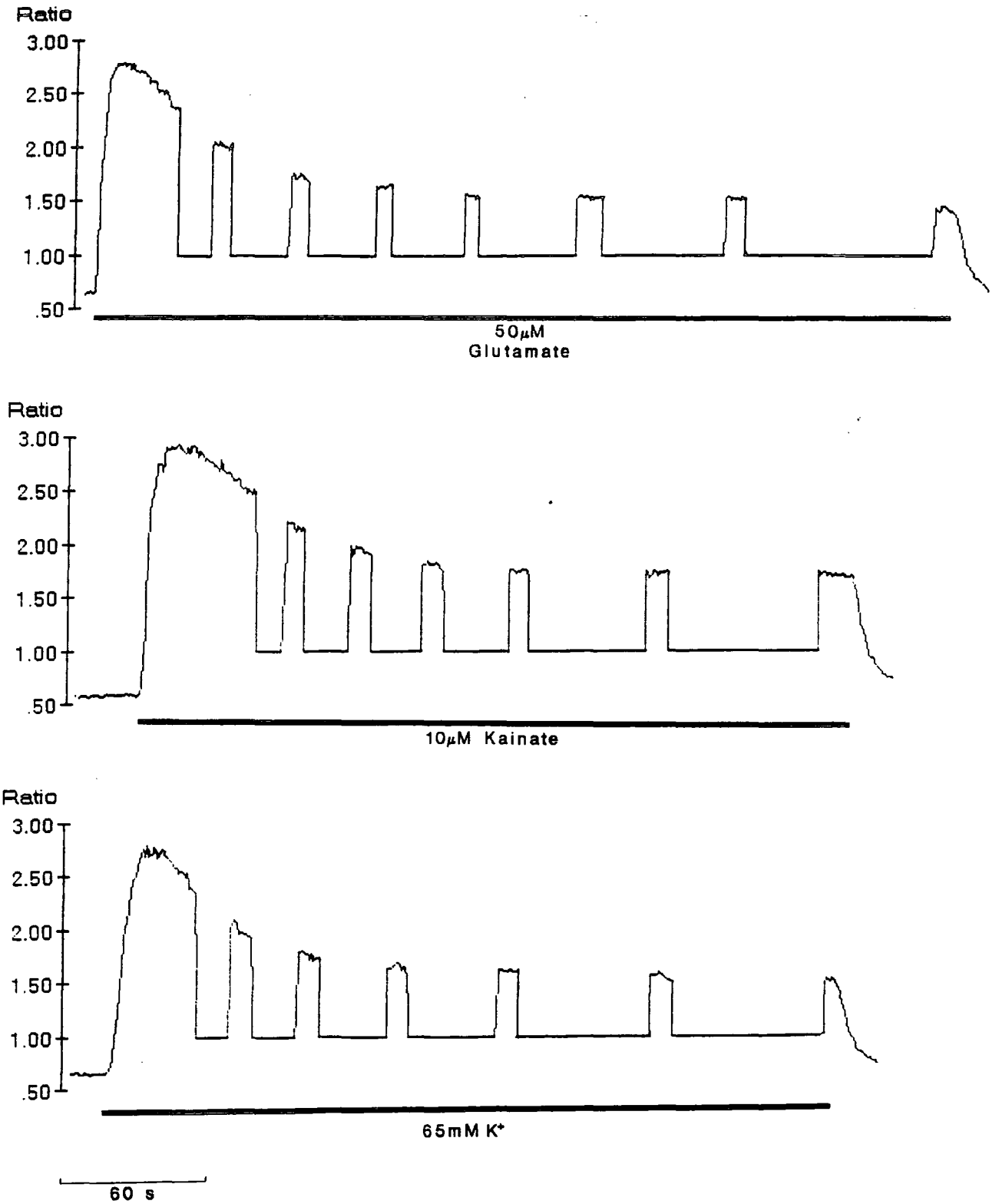
Ratio
3.00
2.50
2.00
1.50
1.00
.50
50μM
Glutamate
Ratio
3.00
2.50
2.00
1.50
1.00
.50
10μM Kainate
Ratio
3.00
2.50
2.00
1.50
1.00
.50
65mM K+
60 s

potassium stimuli (36.4, 41.5 and 35.6 seconds respectively). Once the depolarizing stimuli was removed the intracellular calcium concentration rapidly fell to the 'resting' level. Fig. 4.21 shows, for a different cell, that the plateau level of elevated intracellular calcium was stable for periods of at least 15 minutes, as long as the depolarizing stimulus was kept constant.

However, if, once the calcium concentration reached a stable level on a prolonged depolarization, the degree of depolarization was varied, then the intracellular calcium concentration also varied. For example in Fig. 4.22 the extracellular potassium concentration was changed from $50mM$ to $30mM$ and $100mM$ and the intracellular calcium concentration rose and fell on these changes. Thus controlling the membrane potential, by varying the extracellular potassium concentration, meant that the intracellular calcium concentration could be 'clamped' to any value over about a one log range.

4.4.6 Sensitivity to Verapamil and Nifedipine

Voltage clamp studies have demonstrated the presence of voltage gated calcium channels in isolated horizontal cells from a variety of species (Table 3.3 B and Section 3.3.3). These usually demonstrate predominantly L–type channel characteristics. In order to establish whether the increases in intracellular calcium concentration observed are due to L–type channels the sensitivity of the increases to various inhibitors of L–type channels was established.

A ten second increase in extracellular potassium, to $65mM$, was followed by three minutes exposure to the voltage gated calcium channel blockers Verapamil or Nifedipine. Both these drugs preferentially block L–type calcium channels (Fox *et al.*, 1987; Hille, 1992). The $65mM$ extracellular potassium stimulus was then repeated, still in the presence of the channel blocker. The first depolarizing stimulus acted as a control, so that the effect of the drug on depolarization–induced changes in intracellular calcium concentration could be calculated. During the exposure to the drug the excitation pathway was blocked to prevent photobleaching of the dye and cellular photodamage and was opened prior to the second depolarizing stimulus being applied.

Although there was some variation beween the response amplitudes of different

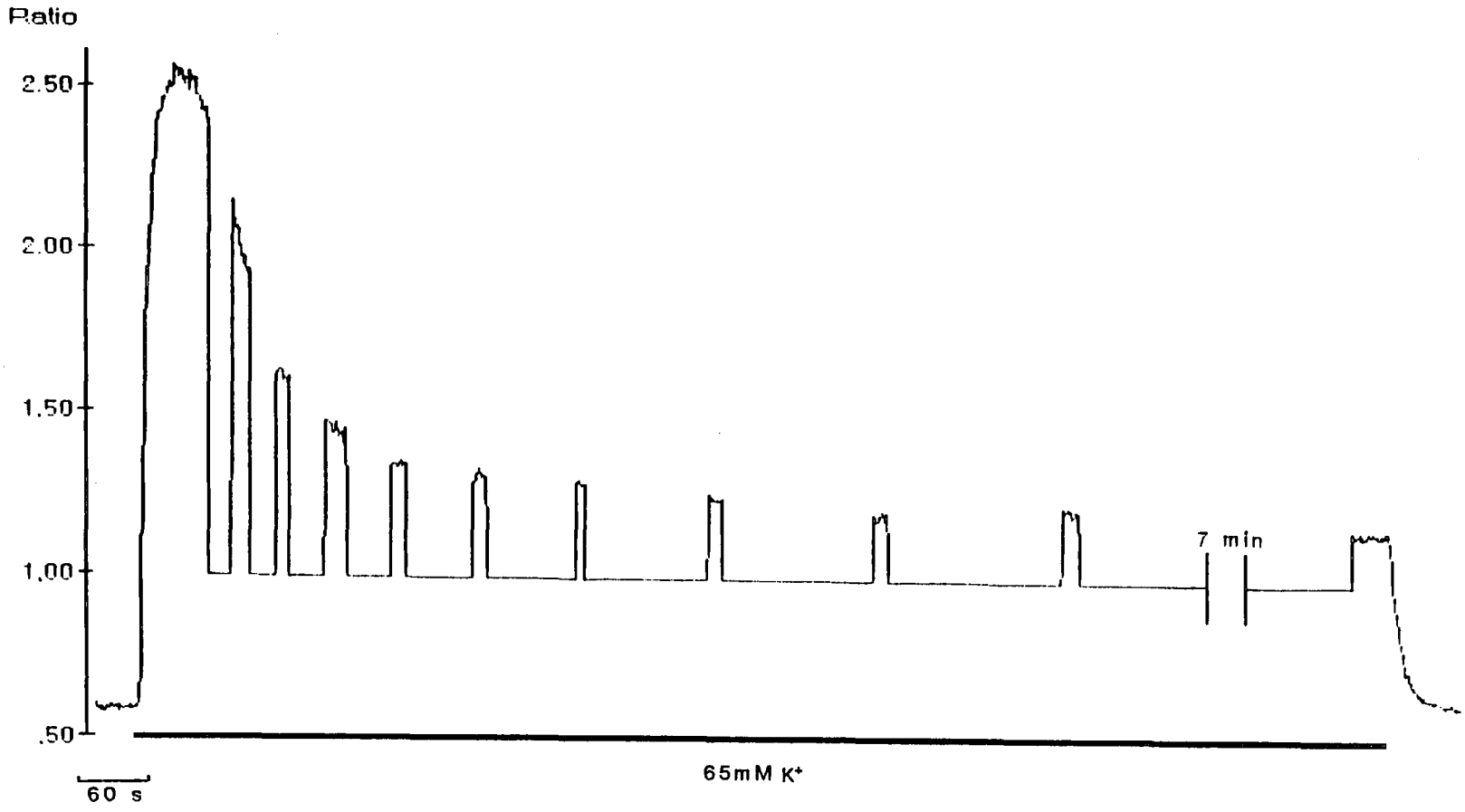
Ratio
2.50
2.00
1.50
1.00
.50
7 min
60 s
65mM K+

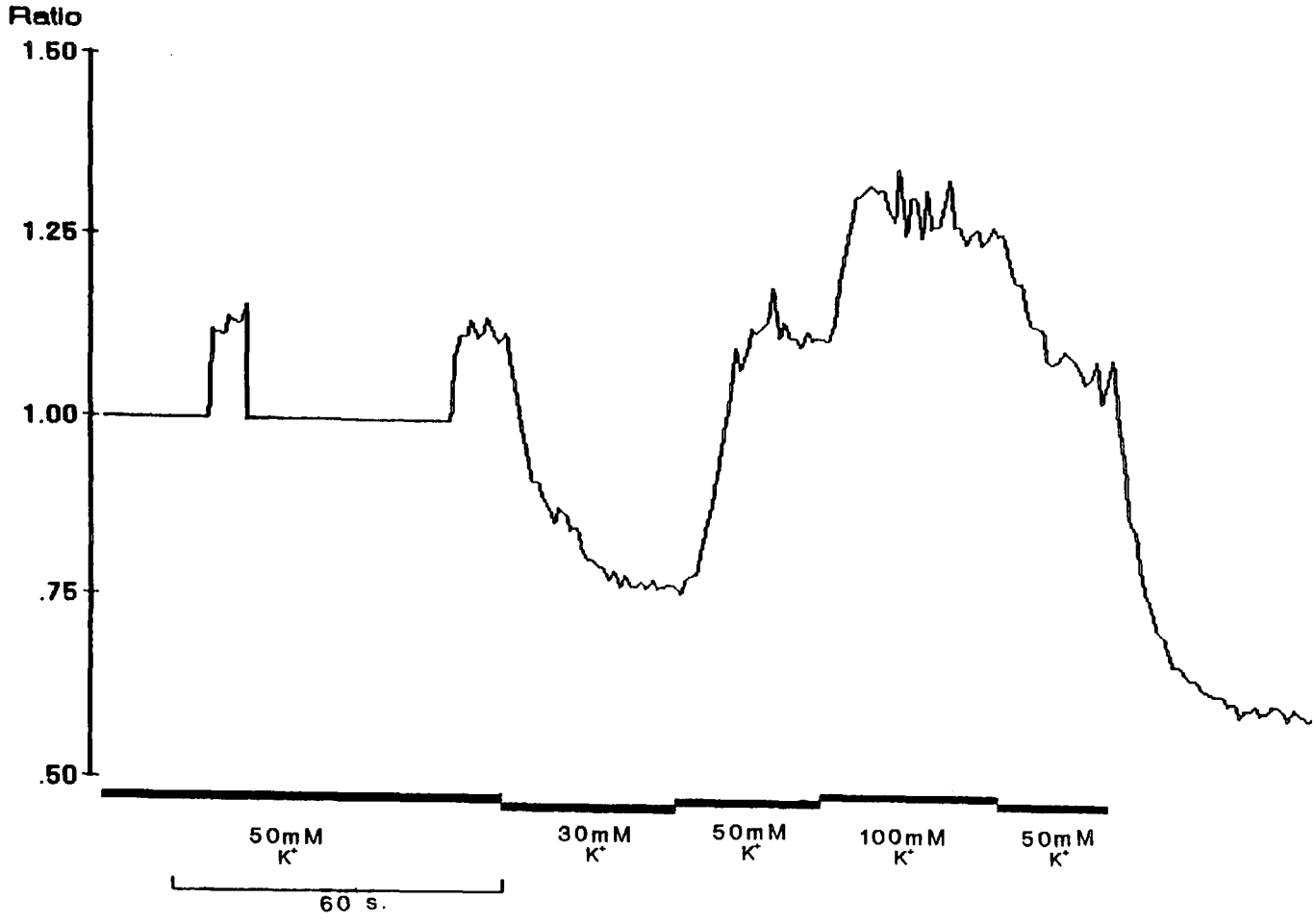
Ratio
1.50
1.25
1.00
.75
.50
50mM K+
30mM K+
50mM K+
100mM K+
50mM K+
60 s.

cells to the $65mM$ extracellular potassium stimulus, there was very little variation between the response amplitudes of the same cell, before and after excitation pathway block, when there was no drug present. (The second response was 101.1±2.8% of the first response n=6.) However as can be seen in Fig. 4.23 there was a reduction in the response amplitude induced by the $65mM$ extracellular potassium when a cell was exposed to verapamil. In this example the cell was exposed to increasing verapamil concentrations ($50\mu M$, $100\mu M$ and $200\mu M$) for three minutes, with the drug being washed out for the same length of time between exposures. The depolarization–induced increase in intracellular calcium concentration was reduced by the verapamil in a concentration dependent manner. The effect of verapamil was totally reversible on washing the drug out. The concentration dependence of the effect of verapamil was investigated and concentrations as low as $10\mu M$ were found to have a detectable effect while concentrations above $500\mu M$ totally abolished the depolarization–induced increase in intracellular calcium concentration.

For each verapamil concentration the increase in intracellular calcium concentration in the presence of verapamil was calculated as a percentage of the increase in the absence of verapamil and plotted against the log verapamil concentration (Fig. 4.24). The data was fitted (using the computer program described in Section 2.3.1 based on the methods of Wilkinson (1961) and Atkins (1973)) to the equation:

$$Y = \frac{100}{1 + \frac{[Verapamil]^h}{K_{1/2}^h}}$$

where Y is the response amplitude in the presence of verapamil, expressed as the percentage of the response before the drug was applied, $K_{\frac{1}{2}}$ is the half maximum blocking concentration and h is the Hill coefficient. For verapamil these values were $42\mu M$ and 1.56 respectively.

A similar experimental protocol was carried out with various concentrations of nifedipine and although these results were considerably less consistent a concentration dependent partial block of the response was observed (Figs. 4.24 and 4.25). There was a greater degree of variation in the effect of the nifedipine than there was for the verapamil, as is demonstrated by the much larger standard errors

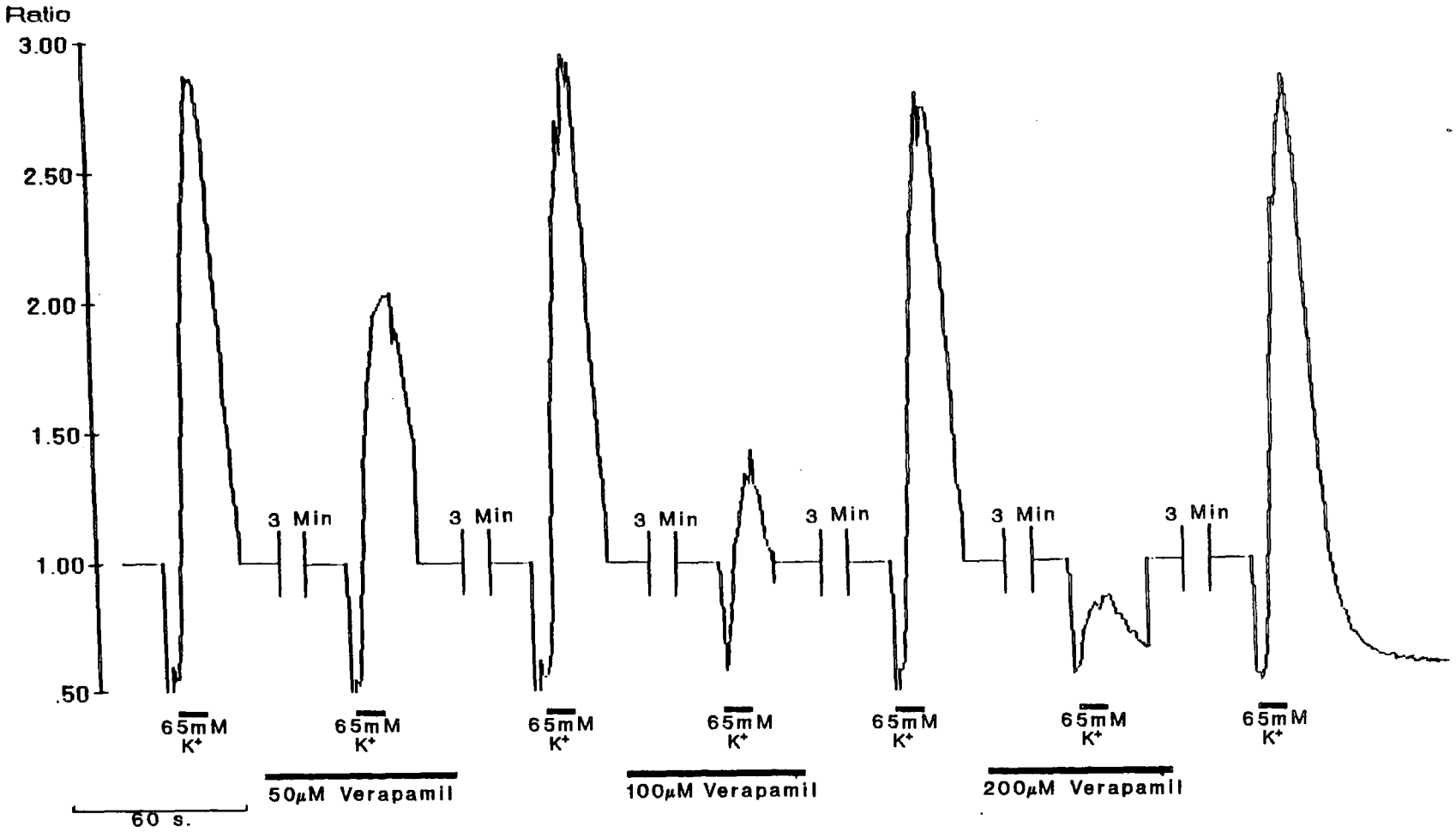
Ratio
3.00
2.50
2.00
1.50
1.00
.50
3 Min
3 Min
3 Min
3 Min
3 Min
3 Min
65mM K+
65mM K+
65mM K+
65mM K+
65mM K+
65mM K+
65mM K+
50μM Verapamil
100μM Verapamil
200μM Verapamil
60 s.

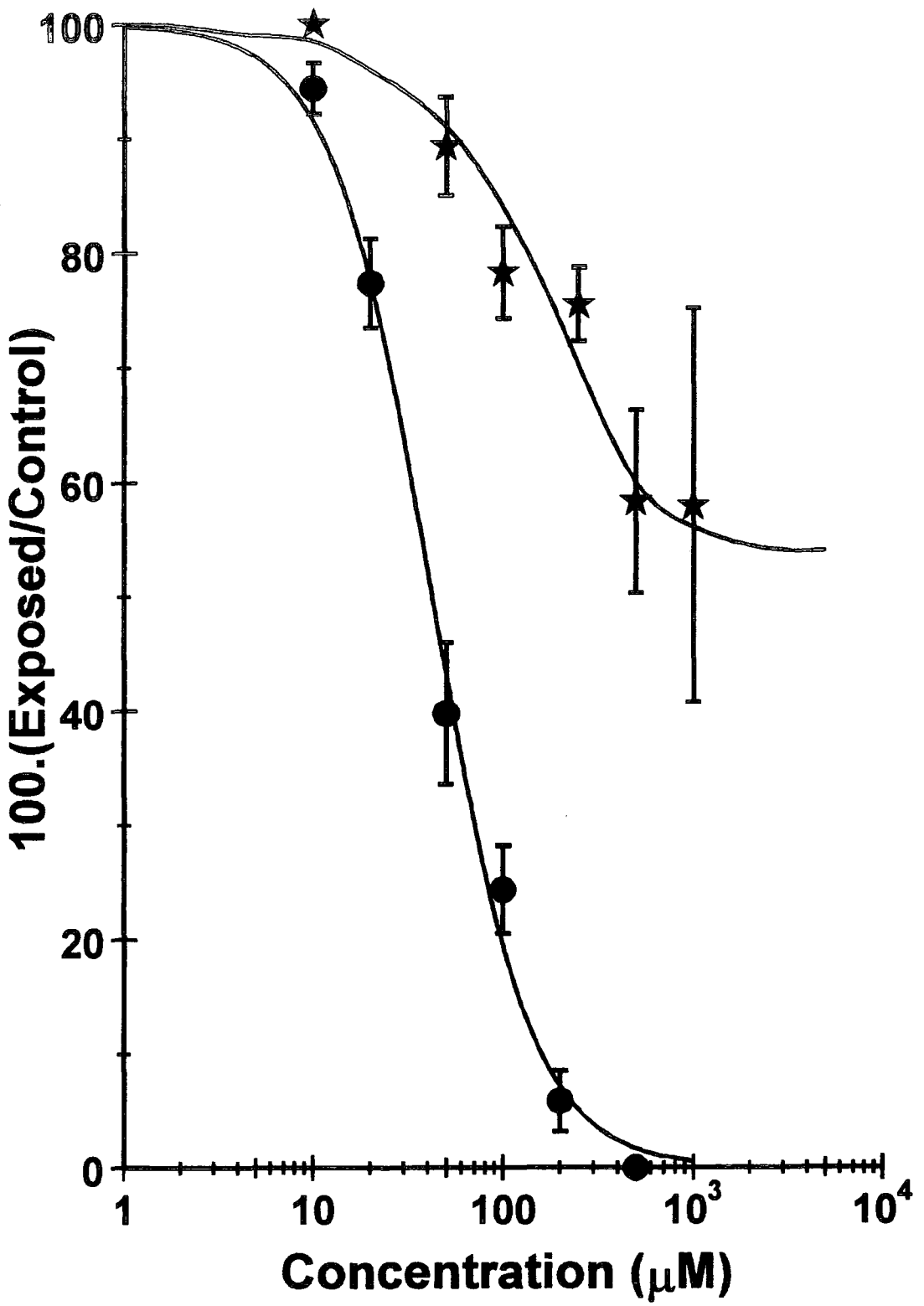
100
80
60
40
20
0
100.(Exposed/Control)
1
10
100
10^3
10^4
Concentration (μM)

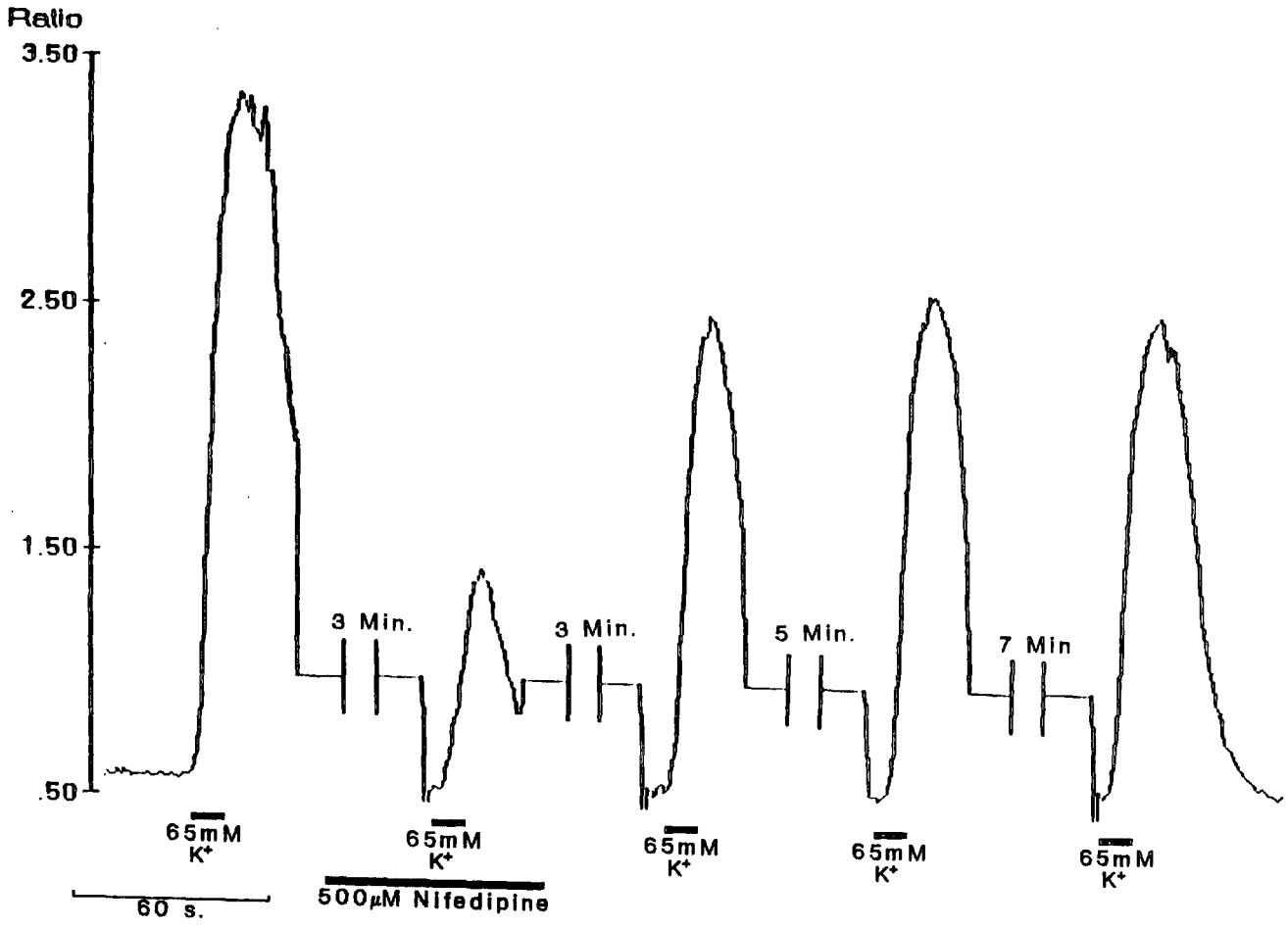
Ratio
3.50
2.50
1.50
.50
3 Min.
3 Min.
5 Min.
7 Min
65mM K+
65mM K+
65mM K+
65mM K+
65mM K+
60 s.
500μM Nifedipine

for this drug (Fig. 4.24). Also the effect was not always totally reversible, as is shown in Fig. 4.25 where exposure of a cell to $500\mu M$ nifedipine for three minutes resulted in a reduction of the depolarization–induced intracellular calcium concentration increase to ~33% of the control, but prolonged washout of the drug (for over 15 minutes) did not result in a complete recovery of the response.

4.4.7 Sensitivity to Various Metal Ions

The sensitivity to block by various divalent and trivalent metal ions can also be used to distinguish different calcium voltage–gated channels. The inhibitory effects of various concentrations of La^{3+}, Cd^{2+}, Cu^{2+}, Co^{2+} and Ni^{2+} on the response to a $65mM$ extracellular potassium stimulus were studied. The cells were exposed to the ion being tested for three minutes, using the same protocol as for the drugs in the previous section. After the $65mM$ extracellular potassium stimulus was repeated, in the presence of the inhibiting ion, the ion was then washed out for a further three minutes. In all cases a wash out time of three minutes resulted in a complete recovery of the depolarization–induced increase in intracellular calcium concentration. Examples of different concentrations of these ions are given in Figs. 4.26–4.28 (Fig. 4.26, $2\mu M$ and $50\mu M$ Cd^{2+}; Fig. 4.27, $250\mu M$ Ni^{2+} and $1\mu M$ La^{3+}; Fig. 4.28, $10\mu M$ Cu^{2+} and $500\mu M$ Co^{2+}).

Inhibition curves were constructed to the same equation as for Verapamil for each ion (Fig. 4.29) and the Hill coefficients and $K_{\frac{1}{2}}$ values calculated are given in Table 4.2.

4.4.8 Sensitivity to Dopamine and Dibutyryl cAMP

Dopamine and dibutyryl cAMP did not appear to have an effect on the amplitude of the sustained calcium current recorded using the patch clamp technique (Section 3.3.3.2). Pfeiffer–Linn and Lasater (1993), using the whole cell patch clamp technique, demonstrated that the L–type voltage–gated calcium current in white bass horizontal cells was potentiated by the application of either dopamine or a membrane permeant form of cAMP. There is the possibility that the lack of response to dopamine and dibutyryl cAMP observed in the voltage clamp recordings in Section 3.3.3.2 was due to diffusion of some intracellular factor from the cell into the patch pipette, although Pfeiffer–Linn and Lasater found that using the

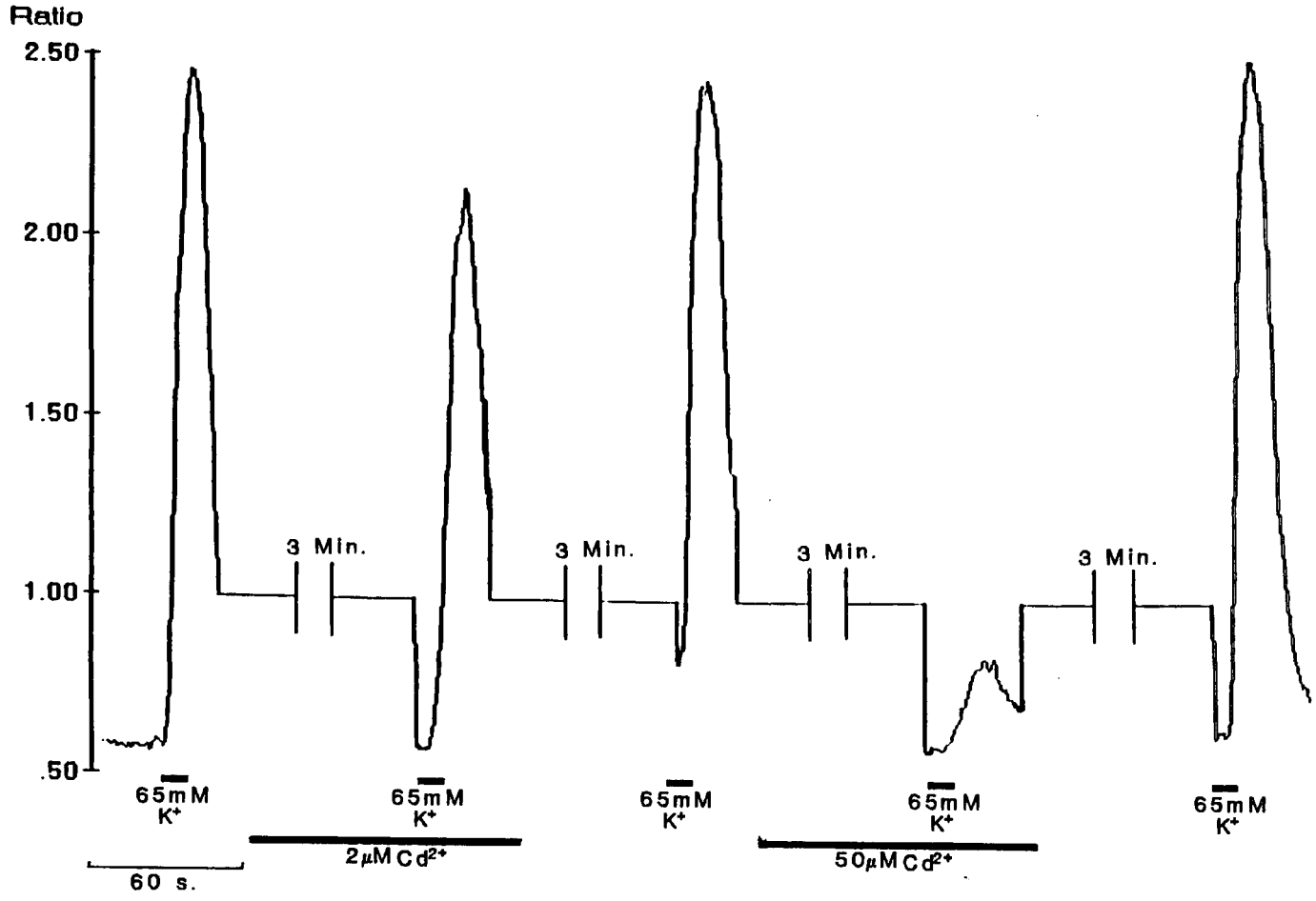
Ratio
2.50
2.00
1.50
1.00
.50
3 Min.
3 Min.
3 Min.
3 Min.
65mM K+
65mM K+
65mM K+
65mM K+
65mM K+
2μM Cd2+
50μM Cd2+
60 s.

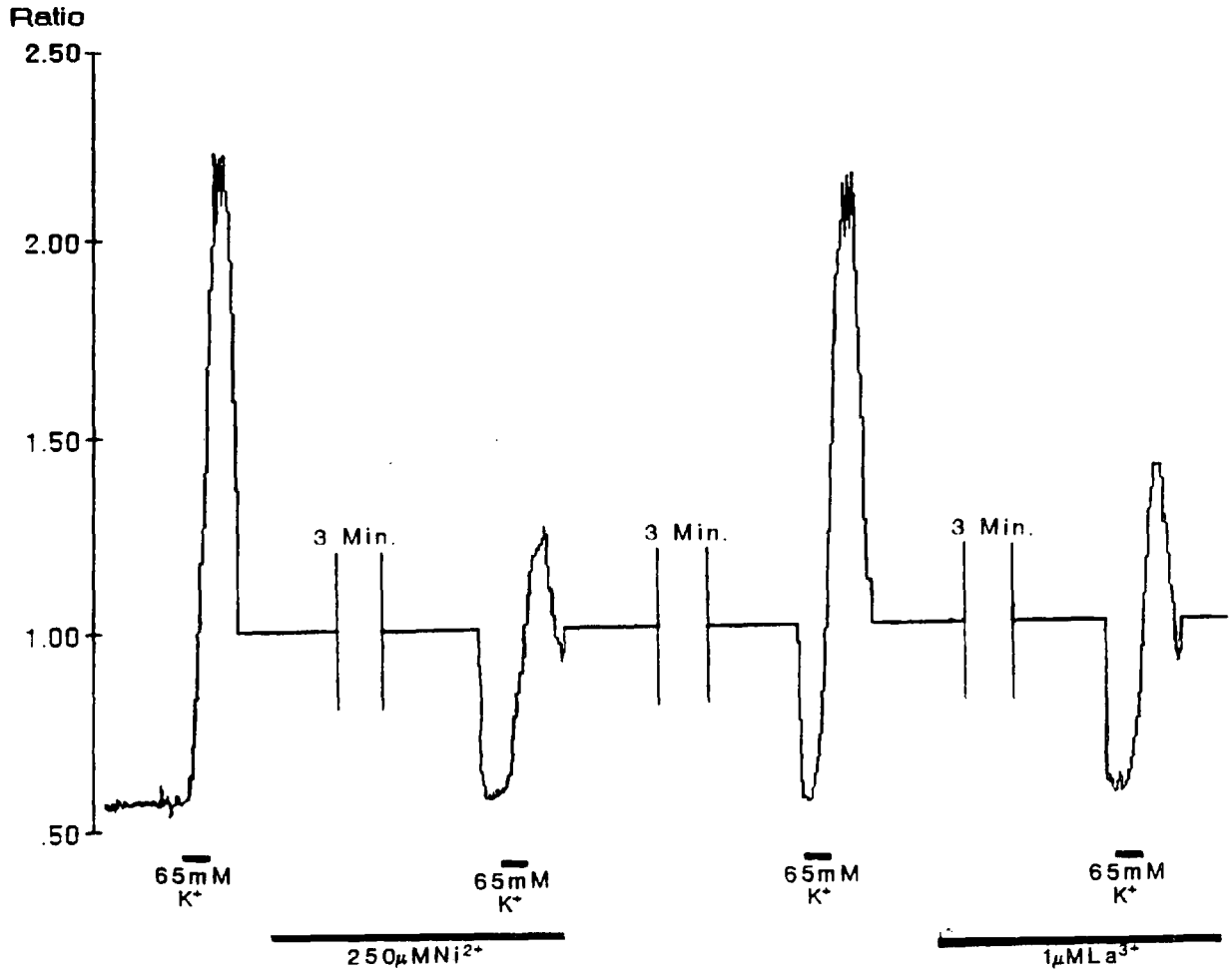
Ratio
2.50
2.00
1.50
1.00
.50
3 Min.
3 Min.
3 Min.
65mM K+
65mM K+
65mM K+
65mM K+
250μMNi2+
1μMLa3+

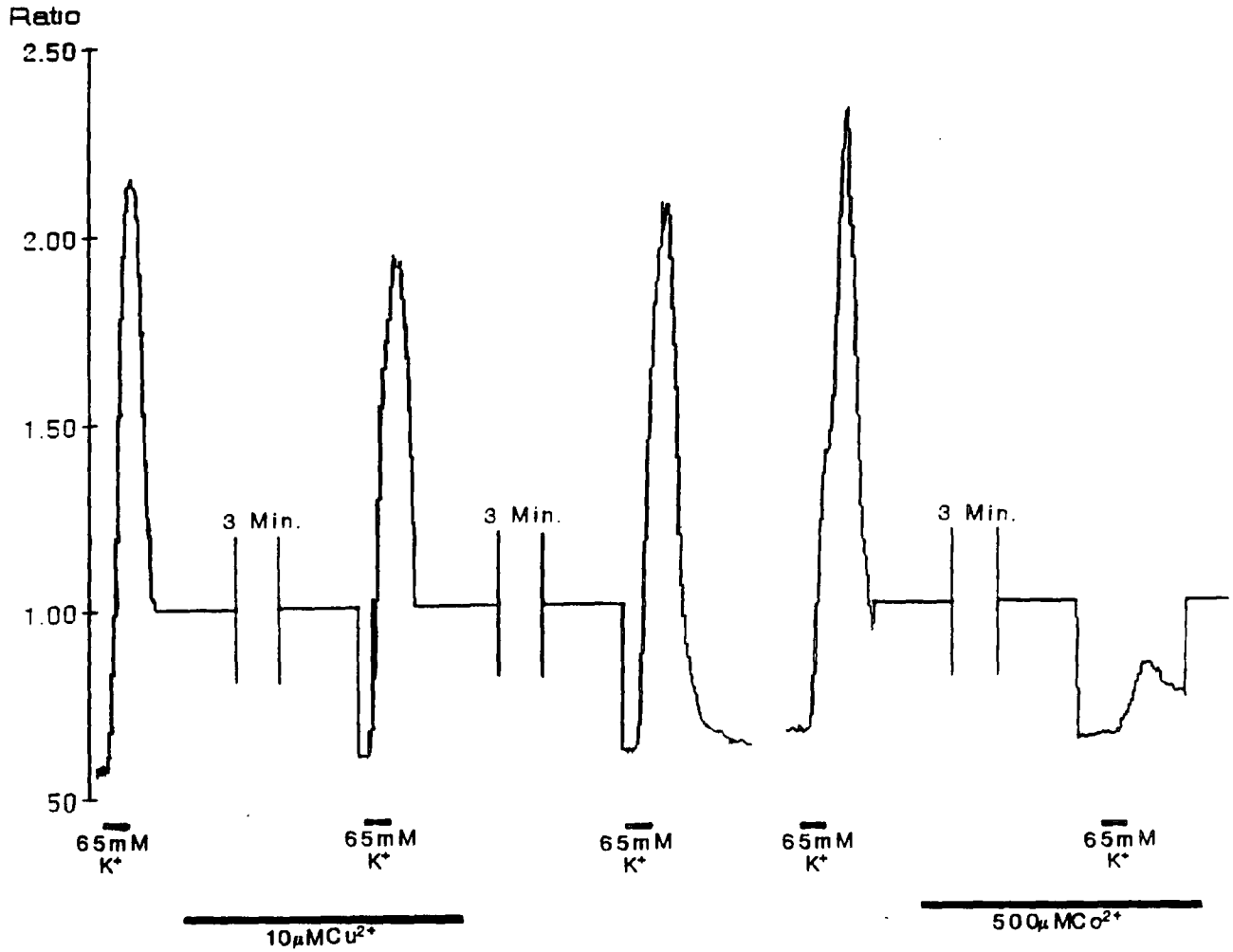
Ratio
2.50
2.00
1.50
1.00
50
3 Min.
3 Min.
3 Min.
65mM K+
65mM K+
65mM K+
65mM K+
65mM K+
10μMCu2+
500μMCo2+

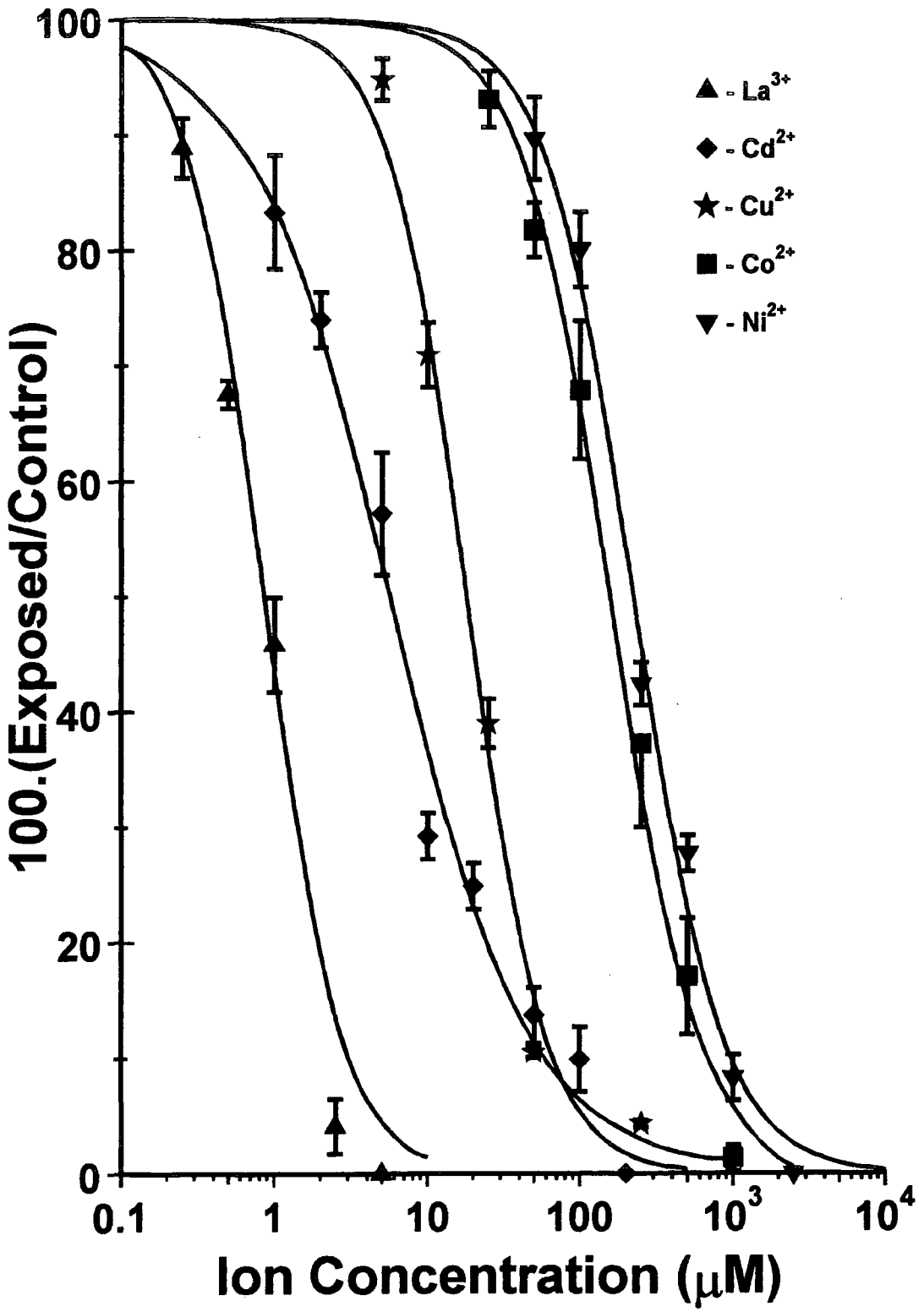
100
80
60
40
20
0
100.(Exposed/Control)
0.1
1
10
100
10^3
10^4
Ion Concentration (μM)
▲ - La3+
◆ - Cd2+
★ - Cu2+
■ - Co2+
▼ - Ni2+

Table 4.2. $K_{\frac{1}{2}}$ and Hill Constant h values for the inhibition of the depolarization induced increase in intracellular calcium concentration by various divalent and polyvalent ions.

Ion	$K_{\frac{1}{2}}$ (μM)	h
La^{3+}	0.86	1.73
Cd^{2+}	5.1	0.95
Cu^{2+}	18	1.68
Co^{2+}	150	1.50
Ni^{2+}	230	1.50

nystatin patch clamp technique (Horn and Marty, 1988), which prevents macromolecule movements between the patch pipette and the cell contents, did not affect their results. However, Heidelberger and Matthews (1994) showed that in goldfish bipolar cells dopamine resulted in significantly larger increases in intracellular calcium concentration (measured using Fura-2) when the cells were exposed to the same depolarizing stimulus and yet were unable to reveal any increases in amplitude of the calcium current using whole cell patch clamp techniques. They suggested that this was due to diffusion of some intracellular factor out of the cell. It was therefore necessary to establish whether dopamine, or a membrane permeable form of cAMP, had any effect on the depolarization induced changes in intracellular calcium concentration. The effect of both dopamine and dibutyryl cAMP, at the same and higher concentrations than were used in the voltage clamp experiments, was studied on the depolarization induced increases in intracellular calcium concentration.

After a control depolarizing stimulus ($65mM$ extracellular potassium) cells were exposed to saline with $200\mu M$ or $500\mu M$ Dopamine or $50\mu M$ dibutyryl cAMP. The dopamine solutions were always used within 30 minutes of being prepared to prevent excessive dopamine oxidation. The duration of exposure to these drugs varied from three to eight minutes to ensure that any possible second messenger mediated effects had time to take place. The time taken for the maximum dopamine induced response was about three minutes in the bass horizontal cells

(Sullivan and Lasater, 1992) and similar in goldfish bipolar cells (Heidelberger and Matthews, 1994). The same depolarizing stimulus was then repeated and the response amplitude before and after the dopamine/dibutyryl cAMP incubation was compared, as in the previous two sections (e.g. Fig. 4.30). The depolarizing stimuli used were $65mM$ extracellular potassium or $50\mu M$ L–glutamate. The results are summarized in Fig. 4.31 where the size of the second response is expressed as a percentage of the previous for the different treatments. The presence of dopamine or dibutyryl cAMP had no observable effect on the responses to the depolarizing stimuli — there was no significant change in the response amplitude for any of the experimental groups (control, $200\mu M$ Dopamine, $500\mu M$ Dopamine and $50\mu M$ dibutyryl cAMP) with either of the depolarizing stimuli ($p > 0.05$ Students t–Test).

4.4.9 Effect of Temperature on Calcium Rate of Change

The rates of increase and decrease in intracellular calcium in response to an L–glutamate stimulus appeared to be affected by temperature as shown in Fig. 4.32, where the rate of change of ratio with time at an experimental temperature of 25°C was over twice that of a cell at an experimental temperatue of 10°C. The variations in rates of change of intracellular calcium could be calculated to compare the response from cells from fish acclimated to different temperatures. However the tendency of the response amplitude to vary as a result of photobleaching (e.g. Fig. 4.10) means that the gradient of the response is dependent on this factor as well as the experimental temperature.

If the time taken for the ratio change to rise from 0.2 to 0.8 of its maximum and to fall from 0.8 to 0.2 is calculated (termed the rise time and fall time respectively) these values are more consistent for a series of responses which demonstrate significant photobleaching. For example the three ratio changes in Fig. 4.10 would have very different rates of change of ratio because of the decrease in response amplitude, but the rise and fall times calculated for each response do not differ by more than 5% .

Fish were acclimated to high, medium and low temperatures (8°C, 16°C and 26°C respectively) as described in Section 2.2.1. The rise times and fall times were calculated for cells acclimated to these temperatures at experimental temperatures

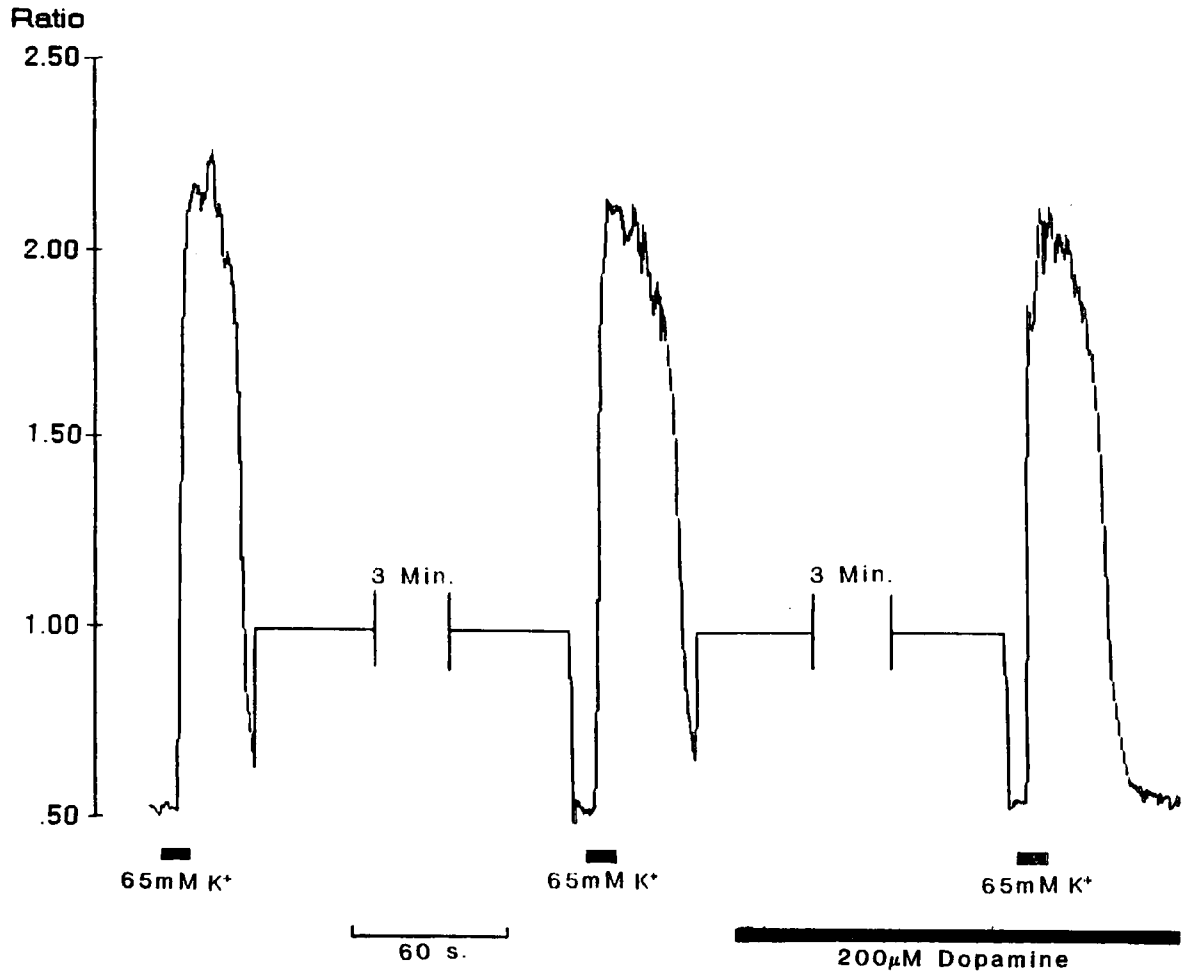
Ratio
2.50
2.00
1.50
1.00
.50
3 Min.
3 Min.
65mM K+
65mM K+
65mM K+
60 s.
200μM Dopamine

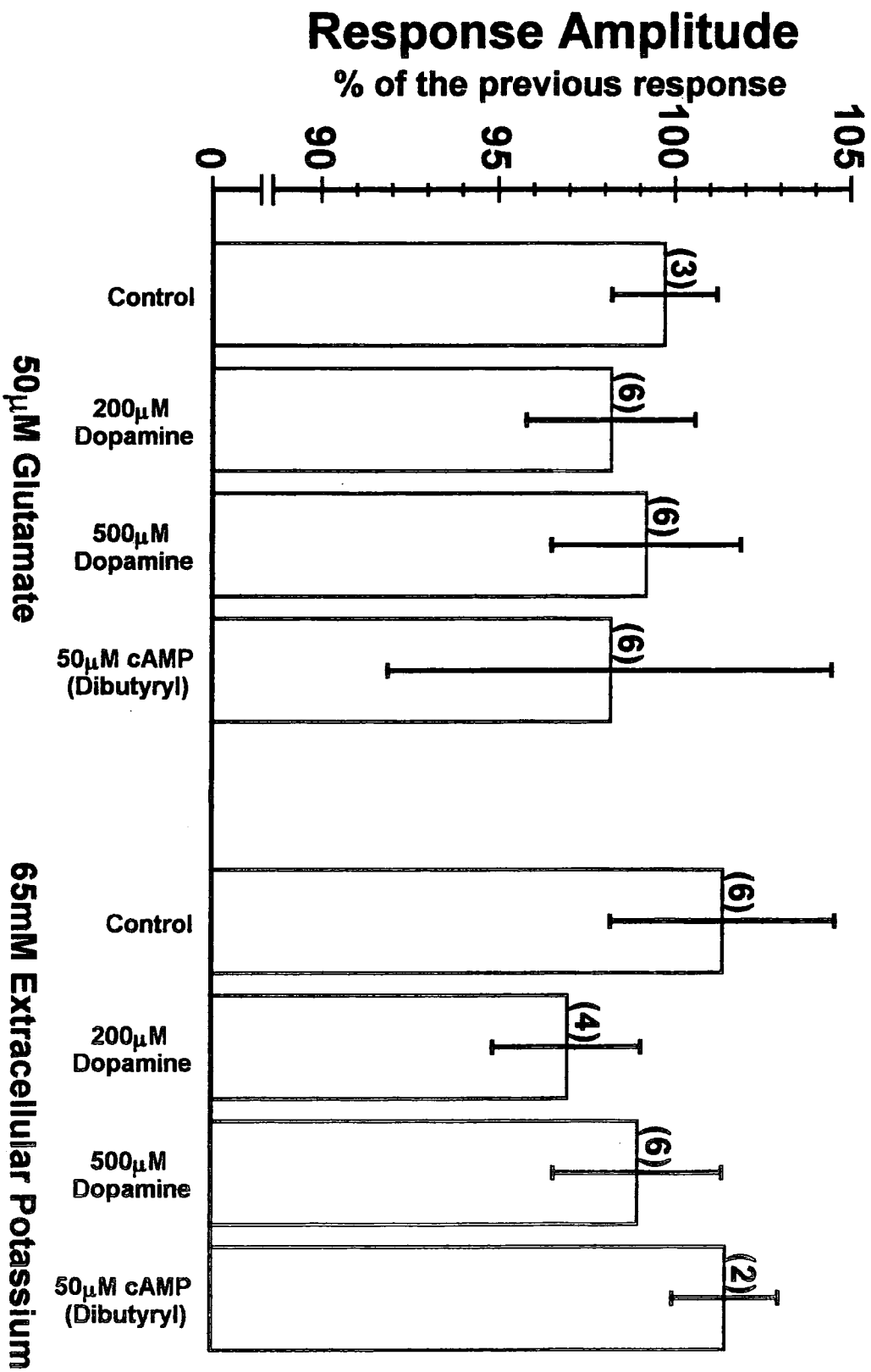
Response Amplitude
% of the previous response
0
90
95
100
105
50μM Glutamate
Control
200μM Dopamine
500μM Dopamine
50μM cAMP (Dibutyryl)
65mM Extracellular Potassium
Control
200μM Dopamine
500μM Dopamine
50μM cAMP (Dibutyryl)
(3)
(6)
(6)
(6)
(6)
(4)
(6)
(2)

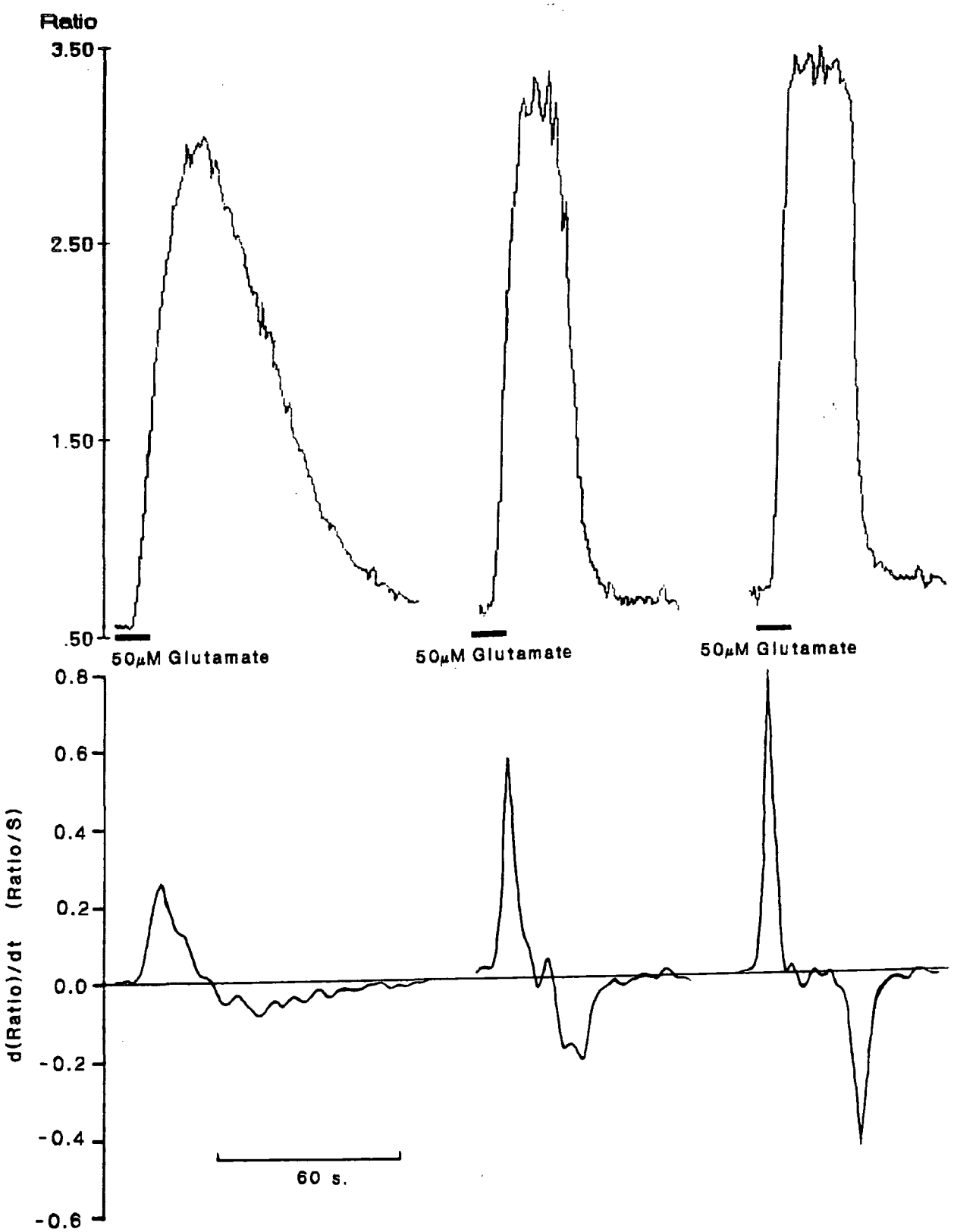
Ratio
3.50
2.50
1.50
.50
50μM Glutamate
50μM Glutamate
50μM Glutamate
0.8
0.6
0.4
0.2
0.0
-0.2
-0.4
-0.6
d(Ratio)/dt (Ratio/S)
60 s.

of 10°C, 17°C and 25°C. The results are given in Figs. 4.33 and 4.34 which show the mean fall and rise times respectively at the three experimental temperatures from cells from fish from the three acclimation temperatures.

The differences in fall times between cells from fish acclimated to different temperatures, in experiments at the same temperature, were not significant in any example ($p > 0.05$ Students t–Test). Conversely the differences in fall times between cells in experiments at 10°C and at 25°C, from the same acclimation temperature, were always significant ($p < 0.02$ Students t–Test). The results for the rise times followed a similar pattern. There was no significant difference between acclimation groups, but there was a significant difference between the results at experimental temperatures of 10°C and 25°C ($p < 0.001$ Students t–Test). There was one exception — the results at 17°C from fish acclimated to 8°C. These data are significantly different from the results from the different acclimation groups at the same experimental temperature ($p < 0.01$ Students t–Test).

The two sets of graphs taken together seem to indicate that there was no effect of acclimation on the rates of change of the intracellular calcium concentration between the 16°C and the 26°C acclimated groups, but that the cells from fish acclimated to 8°C were affected. Although the results were not significanlty different at the experimental temperature of 10°C, for both the rise and fall results, the cells from 8°C acclimated fish do show the lowest rise and fall times and seem to show different temperature sensitivities compared to the cells from the fish acclimated to the higher temperatures.

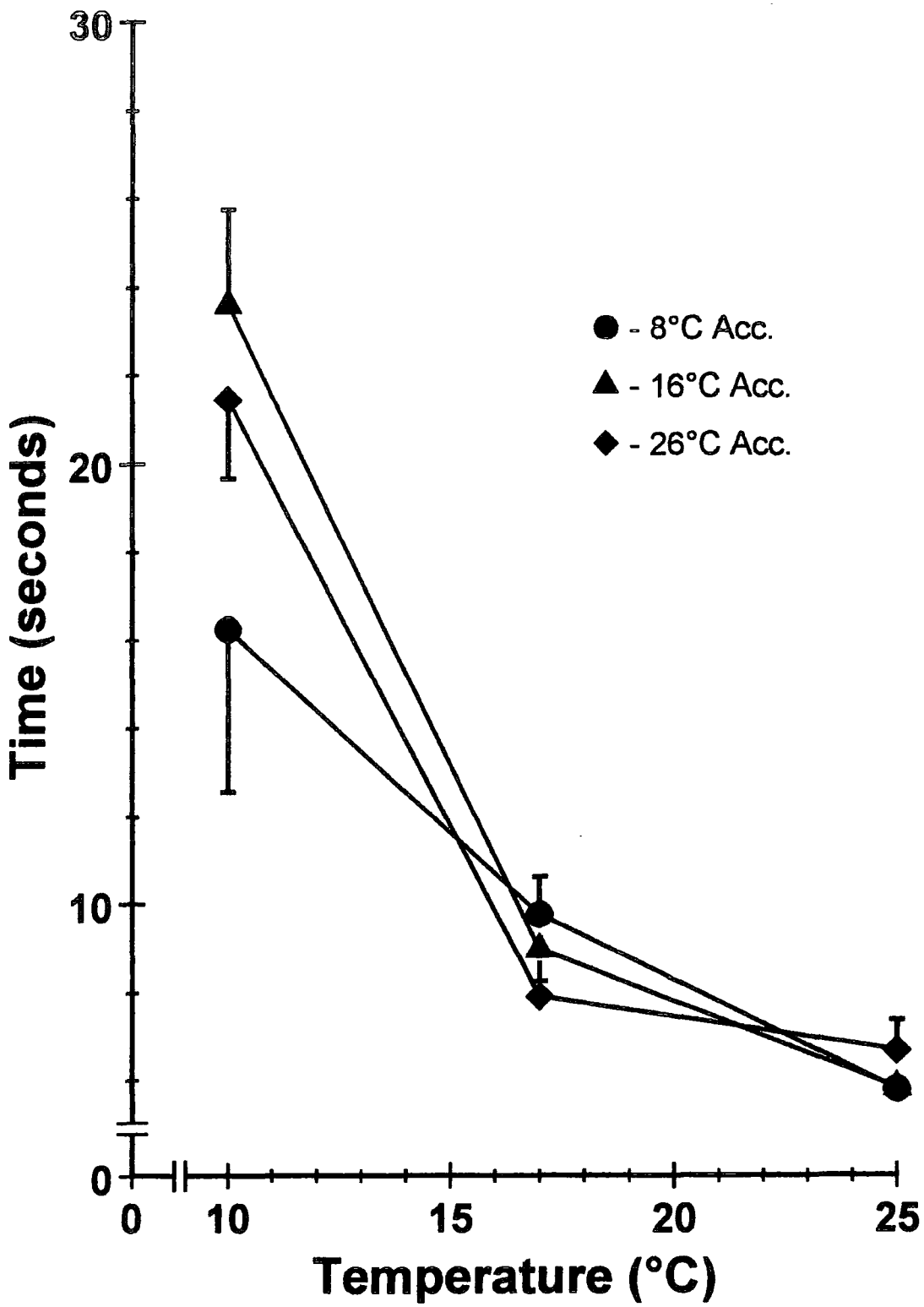
30
20
10
0
Time (seconds)
● - 8°C Acc.
▲ - 16°C Acc.
◆ - 26°C Acc.
0
10
15
20
25
Temperature (°C)

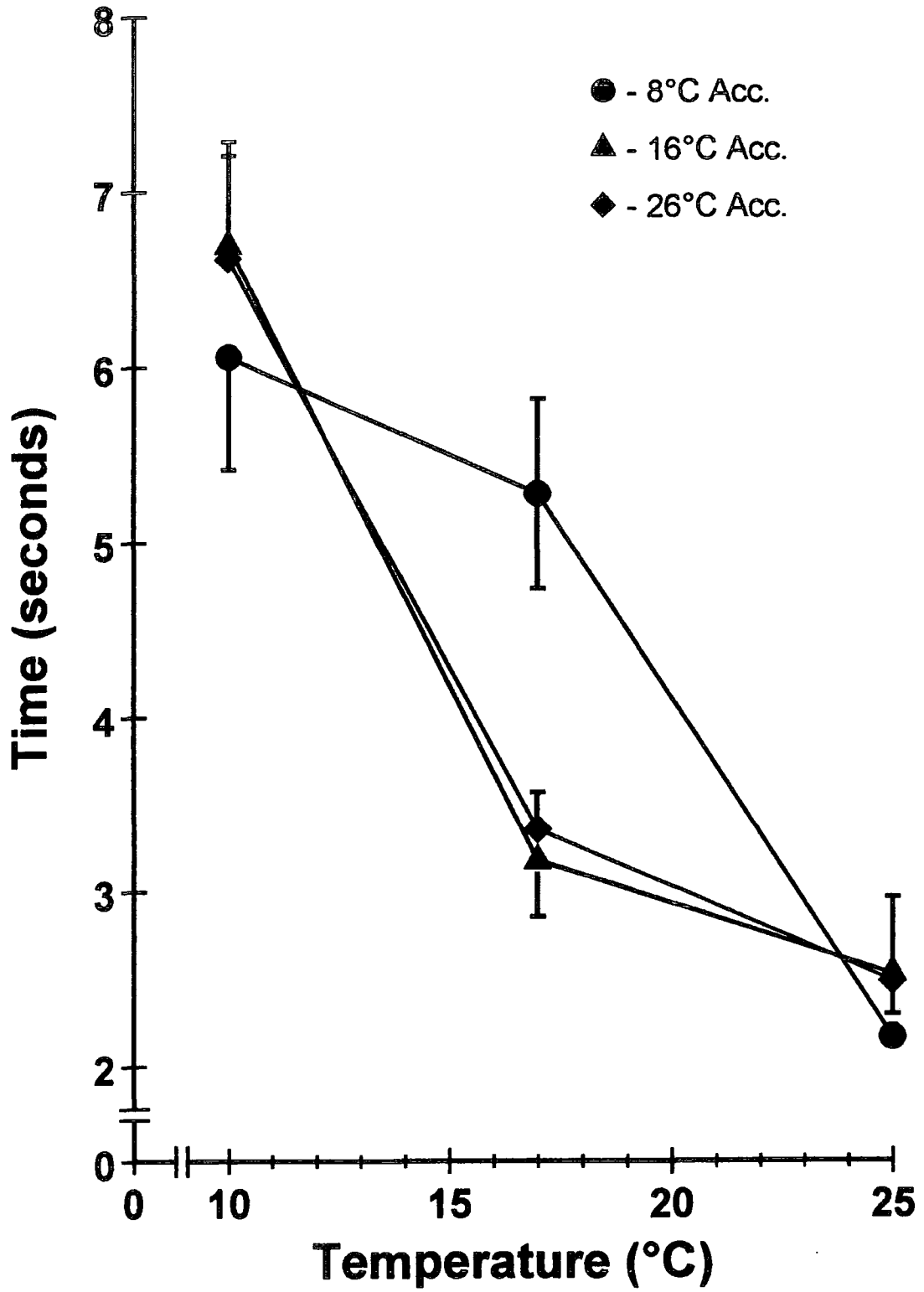
8
7
6
5
4
3
2
0
0
10
15
20
25
Time (seconds)
Temperature (°C)
- 8°C Acc.
- 16°C Acc.
- 26°C Acc.

4.5 DISCUSSION

4.5.1 Assessment of the Technique.

The increase in understanding of the role of intracellular calcium brought about by the introduction of the fluorescent dyes developed by Tsien and his co-workers is indicative of their importance. The diversity of their application, from measuring the intracellular calcium concentration in plant cells (Callam and Hepler, 1991) to simultaneous spatial and temporal resolution of Ca^{2+} changes in various cell types (Mason *et al.*, 1993) demonstrates their flexibility and relative ease of use. Reviews on the use of Fura-2 and Indo-1 are increasingly common (e.g. Tsien, 1988; Moore *et al.*, 1990; Roe *et al.*, 1990; Thomas and Delaville, 1991; Uto *et al.*, 1991; Bolsover *et al.*, 1993; Haugland, 1993; Hoyland, 1993; Hayashi and Miyata, 1994) and they underline the importance of the ratio measurement technique and the ability to load most cell types with these dyes in a non disruptive manner. However, these reviews also emphasise that there are a number of potential problems with these dyes. For accurate ratio measurements the photomultiplier should receive inputs from only two sources; fluorescence from cytoplasmic calcium bound dye and fluorescence from cytoplasmic calcium free dye. However there are a number of other potential sources of signal which will affect the ratio measurements and consequently the results, to varying degrees. These potential sources of error, their importance and methods of reducing their influence are disscussed below.

4.5.1.1 Background Light

Background light from the room can enter the emission pathway and although working in a blacked out room obviously reduces this there are some light sources, such as a dim red light necessary for the experimenter and the light produced by the computer screen. However as long as these are kept to the minimum required the amount of light reaching the photomultiplier should be very low and will be included in the subtraction of a background count (Section 4.2.6).

4.5.1.2 Equipment Fluorescence

The experimental equipment contributing to the optical pathway will generate some fluorescence. This should be low from the microscope attachments such as the

objective lens as they are designed for fluorescence use, but could be significant from, for example, the cell chamber. However this source of fluorescence will be constant and is therefore removed from the signal by the background count subtraction (Section 4.2.6).

4.5.1.3 Cellular Autofluorescence

When using Quin 2 at micromolar concentrations the cellular autofluorescence can be a significant proportion of the emitted light (Tsien and Pozzan, 1989). When using a single wavelength measurement system this can be accomodated if the cells remain present during the calibration (e.g. Protocols 2 and 3 in Thomas and Delaville, 1991), but when using a ratio technique it is potentially much more of a problem. The approximately 30–fold brighter fluorescence of Fura-2 compared to Quin 2 means that the relative intensity of autofluorescence compared to the dye fluorescence is much lower than for Quin 2. As is the case for all intracellular dyes the more dye loaded in the cell the less the potential contribution of the autofluorescence. In order to assess its contribution, the autofluorescence from a cell was measured under the same conditions as in the experiments, but without loading the dye. The counts recorded were 269±8 and 322±11 (mean ± S.E.M.) when excited at $350nm$ and $380nm$ respectively. In comparison with fluorescence readings of tens of thousands of counts for each excitation wavelength during the experiments it is clear that the cellular autofluorescence made very little contribution to the recorded fluorescence intensities.

4.5.1.4 Sub–cellular Compartmentalization

The trapping of the dye in various intracellular organelles can be a significant problem when using intracellular calcium indicators, as it is not exposed to the cytoplasmic free calcium. The calcium concentration of intracellular organelles differs significantly from the cytoplasmic concentration (e.g. Meldolesi *et al.*, 1988), so contributions to the intracellular calcium concentration measurements from these areas will affect the 'resting' concentration measured and reduce the changes in cytoplasmic concentration measured (Almers and Nehre, 1985; Malgaroli *et al.*, 1987; Steinberg *et al.*, 1987; Roe *et al.*, 1990; Moore *et al.*, 1990; Blatter and Wier, 1990). The acetoxymethyl ester form of Fura-2 is lipid soluble, so that it can

cross the plasma membrane, but this means that it is able to cross intracellular membranes as well.

The proportion of the dye which enters the cell's organelles is dependent on two main factors; the relative concentrations of esterases in the organelles compared to the cytoplasm and the proportion of the cell's volume occupied by the organelles. It is known for instance that rat liver mitochondria are able to hydrolyse Fura-2 AM to the free acid form (Gunter *et al.*, 1988). Cardiac cells, for example, which often have up to 40% of their volume taken up by mitochondria, are particularly prone to subcellular compartmentalization (Blatter and Wier, 1990). Another mechanism by which Fura-2 can enter organelles is by active uptake of micelles of the dye by the endoplasmic reticulum, usually close to the nucleus, to form a perinuclear ring of trapped Fura-2 (Bolsover *et al.*, 1993).

The use of alternative loading methods can prevent the problem of sub-cellular compartmentalization. For single cells pressure injection of the free acid form of the dye through a micropipette, or diffusion from a patch pipette in the whole cell mode can be used. There are various other methods more suited to cell populations involving a temporary disruption of the plasma membrane (Moore *et al.*, 1990). These include scrape loading for cultured cells, hypo-osmotic shock treatment, a short duration high voltage pulse, or exposure to millimolar concentrations of ATP which, in some cell types, opens large non-selective pores.

However, Fura-2 AM loading is much easier and more reliable than the above methods and is much less likely to damage the cells. The relatively low density of organelles, such mitochondria, in carp horizontal cells, as shown by electron microscopy (Yamada and Ishikawa, 1965), should mean that this problem is less acute in these cells than in some others. Additionally the dye loading environment can have a significant effect. The use of Pluronic F127 in the loading medium is found to greatly reduce the active uptake of the dye by the endoplasmic reticulum (Bolsover *et al.*, 1993). In many cell types reducing the temperature of loading helps limit the compartmentalization of the dye, which can often be visualized quite easily, for instance from photographs, by spatial variations in the fluorescence intensity (e.g. Roe *et al.*, 1990 Figure 1). The temperature used in this study to load horizontal cells was 16°C. There were no visually obvious 'hot spots' of

fluorescence observed in these cells (such as those in Roe *et al.*, 1990), which would indicate compartmentalization.

Moreover the close agreement between the viscosity corrected *in vitro* and the *in situ* calibrations (Section 4.3.4.2) suggests that there was little or no Fura-2 which was not free in the cytoplasm. Ionomycin is unable to enter the cell and therefore should not affect the calcium concentration in intracellular organelles, so a significant proportion of Fura-2 in these structures would have influenced the *in situ* calibration results.

4.5.1.5 Incomplete Fura-2 AM Hydrolysis

Incomplete hydrolysis of Fura-2 can produce a lipid impermeable product which will still fluoresce, but not in a calcium dependent way (Scanlon *et al.*, 1987). The Fura-2 AM molecule has five acetoxymethyl groups to be removed, each of which requires hydrolysis. Consequently during dye loading the cell will contain varying concentrations of partially hydrolyzed intermediates. If measurements are taken before this process is complete these molecules will contribute to the signal. This effect will grow progressively less with time as the intermediates are fully hydrolyzed.

In cell suspensions this problem is compounded by the fact that the cells cannot be easily removed from the extracellular source of Fura-2 AM, even with repeated washing. All of this extracellular dye must be taken up and fully hydrolyzed before fluorescence measurements are made (Thomas and Delaville, 1991). When single cells, or cells adhered to a substrate, are used the Fura-2 AM can be washed off and time allowed for the intracellular intermediates to be fully hydrolyzed. The time taken to find a cell and measure the background counts, i.e. the time between removing the cell from the Fura-2 AM and the first ratio measurements being taken, was usually over five minutes. This appears to have been adequate for complete hydrolysis of the dye, as usually no gradual changes in the resting ratio recorded were observed which would indicate the progressive hydrolysis of dye intermediates.

4.5.1.6 Photobleaching

As already mentioned (Section 4.4.1) one effect of illuminating Fura-2 with ultra–violet light is photobleaching. If this bleaching simply produced the equivalent of a gradual reduction in the concentration of the dye then there would be no change of the ratio recorded for any calcium concentration, only an increase in the noise of the signal as the fluorescence intensity decreased.

However, one of the intermediates of the breakdown process has been shown to be fluorescent, but not sensitive to calcium concentration in the range concerned, and will cause inaccuracies in the ratio recorded (Becker and Fay, 1987). Becker and Fay found that at a high calcium concentration their $380nm$ signal actually increased with time while their $340nm$ signal decreased. Naturally this decreased the ratio recorded for a constant calcium concentration. This effect was rapid, reducing the ratio by about 33% in 20 seconds. An example of the importance of photobleaching is shown in Fig. 4.10, where the ratio change in response to repeated $50\mu M$ glutamate stimuli decreases rapidly with time and the fluorescence intensity at high calcium concentrations when excited at $380nm$ (i.e. when this fluorescence is low) actually increases.

The only effective way to reduce photobleaching was to reduce the intensity of the excitation beam, although this would also reduce the signal–to–noise ratio. In order to optimise the signal–to–noise ratio the intracellular concentration of Fura-2 could be increased (by controlling the cells incubation in the Fura-2 AM) so that the fluorescence intensity was increased for any excitation intensity. Also the apparatus must be set up to ensure that as little of the emission signal as is possible is lost and the signal–to–noise ratio of the photomultiplier is at its maximum so that lower excitation intensities could be used, e.g. by running the photomultiplier at its ideal power rating. The neutral density filter used (9%) gave reasonable signal–to–noise results and usually reasonably little bleaching over the time scales used.

It is not possible to tell whether the variations in changes in ratio seen in response to the same depolarizing stimulus applied to different cells is due to genuine differences in the increase in intracellular calcium, or an effect of the

photobleaching. For example the response to super–threshold concentrations of L–glutamate usually resulted in an increase in ratio to almost 3.5 (see Figs. 4.9, 4.10, 4.12, 4.17 A and B, 4.20, 4,32) while on occcasion it did not exceed a ratio of 3.0 (see Figs. 4.15, 4.16, 4.17 C and D). Even in those cells where little photobleaching seems to occur during the experiment, as observed by changes in the fluorescence intensities, the possibility that photobleaching product from unavoidable normal microscope illumination is already contaminating the signal remains, although the exposure of dye loaded cells to any light before recording was kept to a minimum.

As a result of these uncertainties changes in the intracellular calcium concentration from different cells could not be directly compared. In the experiments studying the effects of various chemicals on the magnitude of the increase in intracellular calcium each cell acts as its own control. It was not possible to compare the responses of cells from fish acclimated to different temperatures or at different experimental temperatures, except when comparing the time taken for the ratio to change between 0.2 and 0.8 of its maximum (Section 4.4.9) which was not significantly affected by the photobleaching (Fig. 4.10).

4.5.2 Changes of intracellular calcium concentration

4.5.2.1 Introduction

Chapter 3 demonstrates the presence of an inward current carried through voltage–gated calcium channels. Similar currents, with various amplitudes, have been shown in many different retinal horizontal cells (Table 3.3 B). One of the main reasons for the magnitude of the calcium current amplitudes recorded in the carp horizontal cells is the extremely favourable conditions used to detect the current. The use of elevated extracellular divalent ion concentrations and calcium chelating compounds in the patch clamp solution are both commonplace in recording calcium currents (Bean, 1992) and act to amplify the current to probably many times its normal amplitude by increasing the driving force through the channels and preventing increases in intracellular calcium concentration.

The effect of this current, in physiologically more realistic extracellular calcium concentrations, on the intracellular calcium concentration will be dependent on the interaction of the current amplitude and the horizontal cell intracellular calcium

buffering mechanisms. It is therefore not possible to predict the consequences of voltage–gating of the calcium channels demonstrated in the previous chapter on the intracellular calcium concentration. Hence the requirement for measuring this directly. The results presented in this chapter demonstrate that the cell membrane calcium conductance has a significant effect on the intracellular calcium concentration and explore the variations in intracellular calcium concentration and the conditions required. In the 'resting' situation, i.e. when the isolated cell is in a high sodium/low potassium saline containing no depolarizing drugs, the intracellular calcium concentration was very low (a few tens of nanomolar). This is as would be expected for a cell with a relatively hyperpolarized membrane potential (as dictated by the $4mM$ extracellular potassium) as no calcium influx through voltage–gated calcium channels would occur and most intracellular calcium buffering mechanisms have a very high calcium affinity.

4.5.2.2 Voltage Dependence of Intracellular Calcium Concentration Increases

Tachibana (1981) showed that the resting potential of isolated goldfish horizontal cells was dependent on the extracellular potassium concentration in a Nernstian way. The inward (anomalous) potassium rectifier current (Sections 3.1.7 and 3.3.2) is thought to be responsible for the depolarization of the membrane potential on elevated extracellular potassium concentrations (Tachibana, 1983a,b). By using the intracellular potassium concentration calculated by Tachibana (1981) for goldfish horizontal cells (calculated on the basis of the membrane potentials measured in various extracellular potassium concentrations) the membrane potentials of horizontal cells exposed to extracellular potassium concentrations used in this study were calculated. In this way the voltage dependence of the intracellular calcium concentration increases observed could be estimated (Fig. 4.35).

The onset of changes in intracellular calcium concentration at extracellular potassium concentrations of $25mM$ corresponds to a membrane potential of about $-40mV$. This is in reasonably close agreement with the voltage dependence of the calcium current in these cells recorded with the whole cell patch clamp technique (Fig. 3.20) and in other horizontal cells (Table 3.3B). The relationship between the data from the patch clamp experiments and that from these fluorescence measurements is discussed further in Chapter 5.

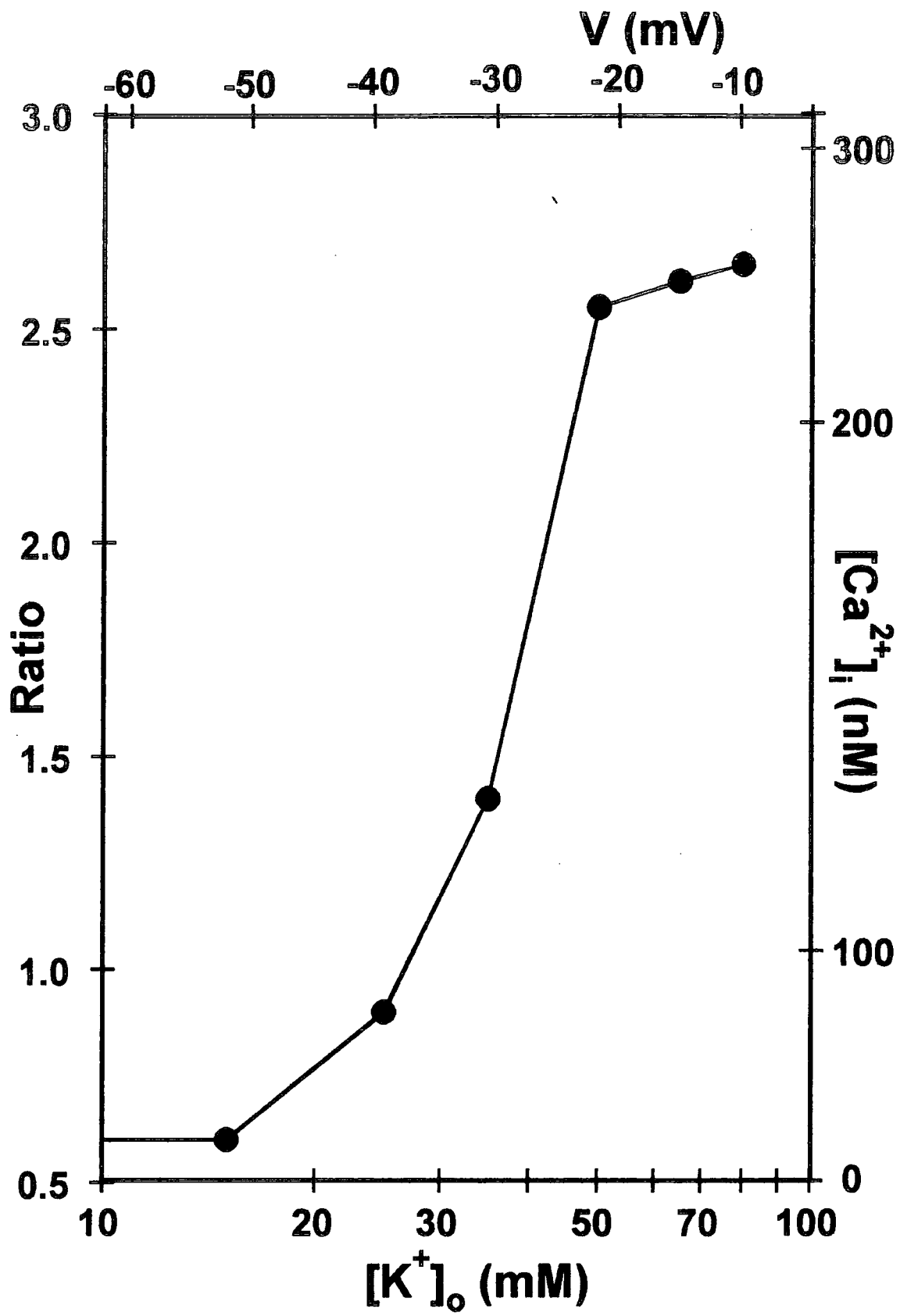
V (mV)
-60
-50
-40
-30
-20
-10
3.0
2.5
2.0
1.5
1.0
0.5
Ratio
300
200
100
0
$[Ca^{2+}]_i$ (nM)
10
20
30
50
70
100
$[K^+]_o$ (mM)

The all–or–nothing increase in intracellular calcium concentration on exposure to L–glutamate and its anologues can be explained as a calcium dependent action potential. In isolated horizontal cells which are not voltage clamped a calcium dependent action potential will be evoked when the cell is depolarized by either current injection (e.g. Johnston and Lam, 1981; Tachibana, 1981) or the application of L–glutamate (e.g. Lasater and Dowling, 1982; Dowling *et al.*, 1983; Ariel *et al.*, 1984). The time course of the action potentials recorded electrophysiologically is similar to the time course of the increase in intracellular calcium concentration seen on the application of L–glutamate — i.e. a rapid depolarization/increase in intracellular calcium concentration to a new level which is maintained for up to tens of seconds before a rapid repolarization/decrease in intracellular calcium concentration back to the 'resting' level. The timecourse of these responses probably depends not only on the membrane conductances of the individual cells but also on the speed of removal of the depolarizing stimulus, with higher concentrations of L–glutamate taking longer to be washed out of the experimental chamber (Fig. 4.12).

The response of the intracellular calcium concentration to exposure of the cells to L–aspartate, kainate, quisqualate and NMDA (Fig. 4.17) is consistent with previous results on the sensitivity of isolated horizontal cell membrane potentials to these compounds. Although L–aspartate depolarizes horizontal cells in the intact carp retina at similar or lower concentrations than L–glutamate (Kaneko and Shimazaki, 1976; Wu and Dowling, 1978; Ariel *et al.*, 1984) it has been consistently shown to have no depolarizing effect on the membrane potential of isolated cells, even at millimolar concentrations (Lasater and Dowling, 1982; Dowling *et al.*, 1983; Ariel *et al.*, 1984). This has been suggested as being due to an effect on the glutamate uptake mechanisms which results in an increase in glutamate concentration in the intact retina, but has no effect in an *in vitro* preparation (Norman *et al.*, 1986). In aggrement with the lack of an effect of L–aspartate on isolated horizontal cell membrane potentials there was no effect on the intracellular calcium concentration (Fig. 4.17 A). The glutamate analogues kainate and quisqualate, however, both depolarize isolated horizontal cells and generate action potentials, while NMDA does not (Lasater and Dowling, 1982; Dowling *et al.*, 1983; Ariel *et al.*, 1984) and the effects of exposure to these drugs, as would therefore be expected, produced

intracellular calcium concentration increases for the former two, but not the latter (Fig 4.17 B,C and D).

The application of L–glutamate to isolated horizontal cells at concentrations just below those required to generate an action potential caused small (5–30mV) depolarizations in the membrane potential (Lasater and Dowling, 1982; Dowling *et al.*, 1983). However no comparable changes in intracellular calcium concentration were observed using subthreshold L–glutamate concentrations since presumably the depolarizations were not large enough to open the voltage–gated calcium channels.

The depolarization caused by elevated extracellular potassium concentrations did not result in the generation of an action potential probably because of the properties of the anomalous rectifier. When the cells were depolarized by L–glutamate the opening of the voltage–gated calcium channels further depolarized the cell so the membrane potential 'broke free' from the anomalous rectifier to generate an action potential. In the case of elevated extracellular potassium concentrations, however, the high conductance region of the anomalous retifier voltage dependence 'follows' the depolarized membrane potential (Section 3.1.7), so even though the voltage–gated calcium conductance is increased the membrane potential is dominated by the potassium conductance.

Voltage clamp studies on goldfish axon terminals show that they have similar membrane currents to the horizontal cell soma, but at much lower membrane conductances (Yagi and Kaneko, 1988). These authors measured a calcium current with similar voltage characteristics to that in the soma but with an amplitude of $\sim$5% of that in the soma. The effects of elevated extracellular potassium on the intracellular calcium concentration of an axon terminal are shown in Fig. 4.18. The main conductance in the goldfish axon terminals is an anomalous rectifier, although like the calcium conductance at $\frac{\sim 1}{20}$ the magnitude in the cell soma (Yagi and Kaneko, 1988), so elevated extracellular potassium should depolarize the axon terminal in the same way as the cell soma. The very small intracellular calcium concentration changes resulting from the elevated extracellular potassium depolarization suggest that there is a similarly small calcium conductance in the carp horizontal cell axon terminals.

4.5.2.3 Origin of the Intracellular Calcium Concentration Increases

The results of the experiments in zero extracellular calcium and varying extracellular calcium concentrations (Figs. 4.14 to 4.16) demonstrate the dependence of the intracellular calcium concentration changes on presence and concentration of extracellular calcium. However, as described in Section 4.4.4, the potential contribution of intracellular calcium stores on the increase in intracellular calcium concentration was investigated. That an increase in intracellular calcium concentration independent of extracellular calcium could be induced by exposing cells to $20mM$ caffeine (Fig. 4.19) demonstrates the presence of intracellular calcium stores likely to release their stored calcium in a calcium dependent manner — calcium induced calcium release (Section 4.1.2; Neering and McBurney, 1984; Marrion and Adams, 1992).

Exposure to the caffeine for $\sim$40 seconds resulted in a transient increase in intracellular calcium concentration which, even in the continued presence of caffeine returned to the 'resting' concentration within $\sim$30 seconds of reaching a peak. The insensitivity of the cell to subsequent caffeine stimuli (Fig. 4.19) indicated that the intracellular calcium store was emptied by the caffeine and was refilled by subsequent influxes of extracellular calcium (Neering and McBurney, 1984). Consequently the total potential contribution of CICR is represented by the area under the transient rise in intracellular calcium concentration induced by the caffeine stimulus. This is small compared to the area under the depolarization–induced increases in intracellular calcium concentration (peak of $\sim 75nM$ compared to $\sim 400nM$ and a transient increase as opposed to sustained increase on prolonged depolarizing stimuli), so if the intracellular stores are contributing to the depolarization–induced increases then their contribution is a small proportion of the total increase.

4.5.2.4 Pharmacology

The current carried through the calcium conductance recorded using the whole cell patch clamp technique (Section 3.3.3) had current–voltage properties similar to those described in other horizontal cells (Table 3.3 B). These are usually referred to as having predominantly L–type calcium current characteristics. The sensitivity

of the depolarization–induced influx of calcium to various chemicals was examined to identify the voltage–gated channel responsible (Figs. 4.23 to 4.29). In all experiments the same depolarizing stimulus was used — $65mM$ extracellular potassium.

The supression of the intracellular calcium concentration increases by verapamil, with a half blocking concentration of $42\mu M$ (Figs. 4.23 and 4.24), is consistent with the properties of L–type calcium channels which are more sensitive to this drug than other calcium channels and typically show half blocking concentrations of 20–$50\mu M$ (Hille, 1992). Although L–type channels are usually more sensitive to dihydropyridines than other calcium channel types, the effects of nifedipine (Figs. 4.24 and 4.25) are at higher concentrations than are usually associated with L–type calcium channel block by this drug (e.g. Fox *et al.*, 1987). However Sullivan and Lasater (1992) found that the sustained calcium current in white bass isolated horizontal cells was not blocked by nifedipine at concentrations of up to $50\mu M$. Also Bean (1984) suggested that the gating state of the channel may be important for the binding of dihydropyridines. This explained the variations in sensitivity of currents to the drugs (over more than 3 log units) when different hold potentials were used in voltage clamp studies (Bean, 1984). The resting potential of the isolated horizontal cells was not measured but this may have influenced the sensitivity of the cells to the nifedipine although Sullivan and Lasater (1992) did not find any effect of varying the hold potential in their study.

The relative sensitivity of calcium currents to various divalent and polyvalent ions has been used as a method of distinguishing current types (e.g. Byerley *et al.*, 1985; Fox *et al.*, 1987; Narahashi *et al.*, 1987; Byerley and Hagiwara, 1988; Hille, 1992; Lentzner *et al.*, 1992; Mlinar and Enyeart, 1993) and may provide information on permeation mechanisms of the channel (Lester, 1991). In the case of calcium currents, L–type currents are more sensitive to block by Cd^{2+} than by Ni^{2+} and T–type currents have the inverse sensitivity (Fox *et al.*, 1987 and Section 3.1.8), although Sullivan and Lasater (1992) found that the two calcium currents they identified in isolated white bass horizontal cells which had predominantly L– and T–type characteristics were reduced by comparable amounts by 10–$50\mu M$ Cd^{2+} and Ni^{2+}.

The relative sensitivities to the ions tested in this study (Figs. 4.26 to 4.29; Table 4.2) are similar to the results for other calcium currents with L–type characteristics, i.e. the sensitivity sequence $La^{3+}>Cd^{2+}>Cu^{2+}>Co^{2+}\geq Ni^{2+}$ (e.g. Byerley *et al.*, 1985; Narahashi *et al.*, 1987; Hille, 1992). The calcium current in catfish isolated horizontal cells was reported as being blocked by metal ions with a similar order of effectiveness — $La^{3+}>Cd^{2+}>Co^{2+}\approx Ni^{2+}$, although inhibition curves were not constructed (Shingai and Christensen, 1986).

Usually the inhibition of calcium currents by metal ions is determined using voltage clamp techniques. The resulting inhibition curves, when they are construted, are often fitted with curves with Hill constants of one which suggest one to one binding (e.g. Byerley *et al.*, 1985; Narahashi *et al.*, 1987). The Hill constants calculated from the results of this study (Table 4.2) are not (with the exception of the Cd^{2+} results) numerically close to one. A possible explanation for this is that a degree of non–linearity is introduced by the calcium buffering mechanisms. The inhibition of the depolarization–induced increase in intracellular calcium concentration would not be expected to vary linearly with the inhibition of the calcium channels.

The variation in the Hill constants calculated cannot be explained as easily. Other studies which have measured the inhibition of elevated potassium induced calcium influx by metal ions have also appeared to generate inhibition curves with varying Hill constants for the different metal ions, although in these studies curves with Hill constants of one have been fitted to the data (Figure 1 in Nachshen, 1984; Figure 11 in Lentzner *et al.*, 1992). The curve fits for the patch clamp data, which show the direct effects of the metal ions on the calcium current and indicate the one to one binding, are more convincing (e.g. Figures 9 and 10 in Byerley *et al.*, 1985; Figure 6 in Narahashi *et al.*, 1987). Consequently the variation in Hill constants between these metal ions is not likely to be due to variations in the stochiometry between the metal ions and the calcium channels.

One possible explanation is that the metal ions are having some effect on other components contributing to the control of intracellular calcium concentration, as well as the calcium channels. For example Cd^{2+}, at nanomolar concentrations, has been shown to inhibit membrane transport of calcium in fish gill cells (Verbost

et al., 1988) and also interferes with calcium binding to calmodulin (Sutoo *et al.*, 1990). If Cd^{2+}, or other of the metal ions tested, interferes with the intracellular calcium concentration control mechanisms of horizontal cells then this would be expected to alter the dose response curve.

4.5.2.5 Prolonged Depolarizations

Horizontal cells in the unilluminated intact retina are depolarized by the continuous release of neurotransmitter from the photoreceptors (Trifinov, 1968). L–glutamate, the proposed transmitter released by the cones (see Chapter 1), depolarizes isolated horizontal cells as already described above. The normal method for investigating the pharmacological properties of isolated horizontal cells is to expose them to test substances for short (seconds at most) periods of time in an otherwise drug–free saline. However the situation in the intact retina is better mimicked *in vitro* by prolonged exposures to L–glutamate and its agonists (Perlman *et al.*, 1989). To investigate this the effects of such exposures and prolonged exposure to elevated extracellular potassium concentrations were recorded and are shown in Figs. 4.20 to 4.22.

The decrease in intracellular calcium concentration from an initial maximum to a lower sustained level (or a 'peak and plateau' increase) typically observed on long exposure to agonists or elevated extracellular potassium could be due to a number of mechanisms:

1 The calcium channels are inactivated. This could be in a calcium dependent manner as reported in goldfish horizontal cells (Tachibana, 1983a,b) or a voltage dependent manner as reported in a proportion of the white bass horizontal cells recorded from by Sullivan and Lasater (1992).

2 The intracellular calcium buffering mechanisms are upregulated by the increase in intracellular calcium concentration and consequently lower the intracellular calcium concentration, after the initial increase.

3 The membrane potential changes during the stimulus and the calcium current is reduced as a result.

The patch clamp results indicate that the voltage–gated calcium channels do not inactivate over the $500ms$ depolarizing stimuli used (Section 3.4.3). This does not preclude the possibility that the current inactivates over the much longer time scale studied in these experiments. The calcium currents in isolated horizontal cells from a number of other species show little inactivation over longer voltage clamp studies, although there are exceptions (see Table 3.3 B). One likely mechanism for inactivation is calcium dependent calcium channel inactivation which would not have been observed in the patch clamp experiments because of the use of Ba^{2+} as the charge carrier, which cannot replace calcium in this role (Section 3.4.3; Bean, 1985, 1992; Byerley and Hagiwara, 1988). This is one possible way in which the increase in intracellular calcium concentration could act to decrease the depolarization–induced increase in intracellular calcium concentration. Intracellular calcium buffering mechanisms (membrane bound calcium pumps, calcium binding compounds etc.) are also capable of upregulation in a calcium concentration dependent way (e.g. Carafoli, 1991; Kostyuk, 1992) and could cause a decline in intracellular calcium concentration as observed.

The possibility that the membrane potential is not constant during the prolonged exposure to L–glutamate and its agonists stems from the likelyhood that the L–glutamate receptors may become desensitized. O'Dell and Christensen (1989) showed that L–glutamate induced currents, but not kainate induced currents, in voltage clamped isolated stingray horizontal cells decreased rapidly (within $100ms$) from a maximum to a sustained (for at least 1.5 seconds) amplitude. Hals *et al.* (1986) and Murase *et al.* (1987) found that the amplitude and desensitization of a glutamate current in isolated catfish and goldfish horizontal cells respectively was dependent on the L–glutamate concentration. The current was at a maximum with L–glutamate concentrations of 50–$100\mu M$ and showed no desensitization over exposure times of up to minutes at this concentration. With L–glutamate concentrations of over 100–$200\mu M$ the maximum current amplitude decreased and desensitized to a new lower sustained amplitude over about one minute. However, the exposure of white perch horizontal cells to $200\mu M$ L–glutamate and $50\mu M$ kainate for periods of up to 25 minutes induced a current reversing at 0–$10mV$ which showed no sign of desensitization. Current clamp measurements of the membrane potential of these cells showed that the drugs induced a sustained depolarization

which was reversed on removal of the drug (Perlman *et al.*, 1989). Similar membrane potential changes, preceded by an action potential, were recorded by Ishida *et al.* (1984) in response to various concentrations of L–glutamate on isolated goldfish horizontal cells.

However, the exposure of horizontal cells to elevated extracellular potassium should depolarize them to a new and stable membrane potential. Tachibana (1981) found that in goldfish horizontal cells the membrane potential set by the extracellular potassium concentration was stable over long periods of time.

By comparing the timecourse of the change in intracellular calcium concentration from the peak to the plateau level in response to the three different depolarizing stimuli (Fig. 4.20) the possible effects of desensitization of the L–glutamate channels can be observed. Desensitization of the channels by L–glutamate, but not kainate, would be expected to result in a more rapid decline in the intracellular calcium concentration when depolarized by the L–glutamate. However no difference between the kainate and L–glutamate responses was observed. Morover the elevated extracellular potassium stimulus, which should have no effect on the glutamate channels, also demonstrated a similar timecourse during the 'peak to plateau' change. In fact rapid desensitization, of the type observed by O'Dell and Christensen (1989), might not have any effect on the intracellular calcium concentration which could be observed with the temporal resolution of the system used. The similarity of the decline in the intracellular calcium concentration during the prolonged depolarizing stimuli (Fig. 4.20) suggests that the same mechanism is responsible in all three cases. This is possibly some intracellular calcium concentration dependent mechanism(s) as described above. For example Ca–calmodulin dependent regulation of membrane bound calcium pumps or phosphorylation by Ca–calmodulin dependent protein kinases (Carafoli, 1991; Kostyuk, 1992).

4.5.2.6 The Effect of Dopamine

The effects on the depolarization–induced increase in intracellular calcium concentration of exposing horizontal cells to $200\mu M$ and $500\mu M$ dopamine and $50\mu M$ dibutyryl cAMP (Figs. 4.30 and 4.31) support the patch clamp results (Section 3.3.3.2). Although these patch clamp results indicated that the voltage–gated calcium current was not increased by dopamine, or dibutyryl cAMP, in contrast to

the results of Pfeiffer–Linn and Lasater (1993), the effect of these drugs on the depolarization induced increase in intracellular calcium concentration was examined for the reasons detailed in Section 4.4.8. This was primarily that the lack of an effect of the dopamine and dibutyryl cAMP on the current amplitudes recorded using the whole cell patch clamp technique could have been due to the washout of some intracellular factor (see Heidelberger and Matthews, 1994). The results presented in Figs. 4.30 and 4.31 indicate that this was not the case and that the calcium conductance in these cells is not affected by dopamine induced increases in cAMP.

The lack of an effect of dopamine on the response to glutamate is not surprising in view of the knowledge that it does not affect the calcium current amplitude. An increase in sensitivity of horizontal cells to L–glutamate and its analogues in response to intracellular cAMP concentration increases induced by dopamine (Knapp and Dowling, 1987) might be expected to increase the sensitivity of the horizontal cells to L–glutamate, but not the size of the resulting calcium action potential and therefore not the magnitude of the increase in intracellular calcium concentration. No attempt was made to investigate the sensitivity of the cells responses to glutamate in this study.

4.5.3 Relevance to the *In Vivo* situation.

As already mentioned (Section 4.5.2.5) the set of experiments which mimic the *in vivo* situation most closely were those involving prolonged depolarizations of the isolated horizontal cells. The sustained increase in intracellular calcium concentration on prolonged depolarization means that in the intact retina the intracellular calcium concentration will be higher in the dark (depolarized state) than when the retina is illuminated (hyperpolarized state). More importantly the graded changes in intracellular calcium concentration on depolarization of the isolated cells (Fig. 4.22) means that the graded changes in membrane potential in the horizontal cell in the intact retina should result in graded changes in the intracellular calcium concentration.

However the membrane potential range over which these changes in intracellular calcium concentration will occur is probably not as wide as the membrane

potential range of the horizontal cells in the intact retina. The current voltage relationship of the calcium current (Fig. 3.20) and the likely voltage dependence of the increases in intracellular calcium concentration (Section 4.5.2.2 and Fig. 4.35) suggest that the variations in intracellular calcium concentration will be effective only over the membrane potential range of about $-45mV$ to 0–$10mV$. The possible significance of this on the role of the calcium current in horizontal cells will be further discussed in Chapter 5.

Chapter V

Discussion

5.1 Temperature

The short and long term effects of temperature on the responses of horizontal cells to illumination were investigated in the intact retina (Sections 2.3.2 and 2.3.3 respectively). The dynamic range of these cells (i.e. the difference between the resting potential in the dark and V_{max}) was found to decrease on increasing and decreasing temperature away from an 'optimum'. For cells from fish acclimated to 16°C this optimum was ~18°C, but the dynamic range was reasonably stable over the temperature range 15–20°C (Fig.2.7). The kinetics of the response at $\frac{1}{2}V_{max}$ were found to be significantly affected by temperature, with the rates of change of membrane potential increasing with increasing temperature and the latency of the response decreasing with increasing temperature (Fig. 2.10). Acclimation to a high (26°C) and low (8°C) temperature shifted the thermal sensitivities of all these response characteristics in an adaptive manner (Figs. 2.11 to 2.14).

Possible mechanisms for both these short and long term effects of temperature were discussed (Section 2.4). However little information as to these mechanisms could be concluded from the microelectrode experiments. This is because many different processes are involved in the production of the horizontal cell response, e.g. phototransduction, the membrane properties of the photoreceptor, the pre– and post–synaptic mechanisms of the photoreceptor–horizontal cell synapse and the membrane properties of the horizontal cell. In order to understand further which of these components contribute to the plasticity of the horizontal cell responses observed on long term temperature changes they need to be studied individually.

However the effect of temperature on the length constant (Fig. 2.17) can be attributed to changes in the electrical conductance between the cells in the horizontal cell syncitium. The difference in both the mean length constant and in

the sensitivity to temperature shown by the 8°C acclimation group compared to the 16°C and the 26°C acclimation groups indicates that there is a considerably different affect of acclimation from 16°C to 8°C compared to 16°C to 26°C. This indicates changes in the gap junction density or conductance on acclimation to 8°C. This is discussed further in Section 5.2.2 where possible correlations with the temperature sensitivity of the rates of change of intracellular calcium concentration are considered.

The effects of temperature on the dynamics and amplitude of the horizontal response in the intact retina do not provide information on the specific mechanisms involved in either the short or long term changes (Section 2.4). Due to the flatness of the I–V relationship of the isolated horizontal cell over the membrane potentials observed in the intact retina (Fig. 3.10) the main membrane conductance in the depolarized horizontal cell is that produced by the photoreceptor neurotransmitter. The ligand gated channels of the horizontal cells need to be investigated using the whole cell and single channel patch clamp techniques to establish whether they demonstrate any temperature sensitivity, as acetylcholine receptor channels appear to (Dilger *et al.*, 1991). If a component of the thermal sensitivity of the horizontal cell response is due to temperature induced changes in the ligand gated channels then changes in the density or types of channels in the membrane would be a potential acclimatory mechanism. Lasater (1991) suggests that white bass horizontal cells express two types of glutamate sensitive channels with differing kinetics. A change in the relative ratio of such channels might have the potential to compensate for the effects of temperature changes on the whole cell glutamate induced currents.

Phototransduction mechanisms are also a possible site of thermal acclimation. To investigate this in detail photoreceptor responses would need to be seperately recorded. This could be done in a number of ways, such as using suction electrodes to measure the dark current and its changes on illumination (Baylor *et al.*, 1979). This was the technique used by Baylor *et al.* (1983), Lamb (1984) and Robinson *et al.* (1993) who investigated the temperature sensitivities of isolated photoreceptor responses. Alternatively whole cell patch clamp techniques could be used both to measure membrane potential changes on illumination and to investigate the voltage gated conductances which contribute to the photoreceptor response. A

comparison of the photoreceptor and horizontal cell responses at different experimental temperatures should reveal the component of the temperature sensitivity of the horizontal cell response which is due to the photoreceptor–horizontal cell synapse. Likewise the acclimation mechanisms responsible for the shifts in temperature dependence of the horizontal cell responses could be investigated.

The isolated horizontal cell patch clamp results were limited to comparing the amplitude and current–voltage relationship of the inward/anomalous rectifier current and the sustained calcium current from cells from fish acclimated to the three different temperatures, at the same experimental temperature (Sections 3.3.2.4 and 3.3.3.3 respectively). No experiments were carried out at different experimental temperatures, but the results suggest that no acclimatory process occured which could be correlated with the responses of the cells in the intact retina.

The anomalous rectifier is probably the dominant membrane conductance in the horizontal cell on bright illumination (when in the absence of photoreceptor neurotransmitter) and limits the hyperpolarization of the cell (see Section 3.4.2). Consequently acclimatory changes in the anomalous rectifier could have contributed to the shift in the temperature dependence of V_{max}. If temperature dependent changes of the anomalous rectifier were responsible for the changes in V_{max} shown in Fig 2.11 then the voltage dependence of this current might have been expected to be significantly different when acclimated to the different acclimation temperatures. However as this is not the case it can be concluded that the anomalous rectifier is not responsible for the long term changes in temperature sensitivity in V_{max}.

One of the most important aspects of the effects of temperature on V_{max} is the degree to which the dynamic range is conserved across the normal temperature range of the species. While the shift in the V_{max}–temperature curves (Fig. 2.11) demonstrate only 44% and 67% of complete acclimation (Table 2.2) for acclimation from 16°C to 8°C and 16°C to 26°C respectively the horizontal cell dynamic range can be completely maintained over the temperature range of 10°C to 25°C (Fig 2.11). This encompases most of the normal range of temperatures experienced by these fish, while they remain active. Moreover as the temperature sensitivity of the isolated retina may be greater than that in the intact fish (Schellart *et*

al., 1974) the temperatures over which the dynamic range remains greater than $40mV$ may be even wider than this. In conclusion this appears to demonstrate an exceptionally good example of a thermally sensitive cellular response which can function optimally over a much wider range of temperatures in the long term than in the short term, by gradually changing the thermal sensitivity of the response.

5.2 Calcium

5.2.1 Ca^{2+} Current and Intracellular Ca^{2+} Concentration Changes

The results presented in Chapters 3 and 4 demonstrate calcium currents and intracellular calcium concentrations. That extracellular calcium was required for depolarization–induced increases in intracellular calcium (Section 4.4.3) and that intracellular calcium stores were not likely to contribute greatly to the cytoplasmic free calcium concentration (Section 4.4.4) suggests that the voltage–gated calcium current demonstrated by the patch clamp experiments (Section 3.3.3) was the primary source of the changes in intracellular calcium concentration. One way of establishing this would be to show that the increase in intracellular calcium concentration has a similar voltage dependence as the calcium current, i.e. showing a maximum and approaching zero at the reversal potential. However this was not possible because the use of potassium to depolarize the cells limited the range of membrane potentials which could be used. Voltage clamp experiments with simultaneous measurements of the intracellular calcium concentration would be required (e.g. Mayer *et al.*, 1987, Figure 2; Thayer and Miller, 1990, Figure 3 A; Tse *et al.*, 1994, Figure 1).

The range of membrane potentials used to study the intracellular calcium concentration changes were estimated from the extracellular potassium concentrations used (see Fig. 4.35). These can be used to compare this response with the voltage dependence of the calcium current (cf. Fig. 3.20). The intracellular calcium concentration showed no detectable change at $\sim$–$50mV$ but a clear increase on depolarization to $-40mV$, while the calcium current was only slightly ($< 10\%$) activated at these potentials. Moreover the current showed a maximum at $10mV$ whereas the intracellular calcium concentration changes appeared to approach a peak at more

hyperpolarized levels. These results suggest considerable non–linearity between the calcium current and the intracellular calcium concentration changes.

Intracellular calcium buffering mechanisms would be expected to affect the linearity of the currrent–concentration change relationship. Ahmed and Conner (1988) and Tse *et al.* (1994) have shown that up to 99% of the calcium ions entering a cell can be buffered. However Ahmed and Miller (1988) suggested that the calcium buffering mechanisms were more effective at higher calcium concentrations. This is supported by the results of Thayer and Miller (1990) who found that the intracellular calcium concentration in rat dorsal ganglion cells reached an asymptope on continually increasing influxes of calcium. Intracellular calcium buffering mechanisms could therefore explain the apparent lack of correlation between the voltage sensivity of the calcium current and intracellular calcium concentration shown over this limited range of membrane potentials.

Another potential source of the apparent discrepancy between the results from these two techniques is the accuracy of the estimated membrane potential values ascribed to the various extracellular potassium concentrations used. They are based on the results of Tachibana (1981) on goldfish horizontal cells. A comparison of the current–voltage relationship of the potassium rectifier of the goldfish horizontal cell (Tachibana, 1983b, Figure 7 C) with that of the carp horizontal cell (Fig. 3.16) shows that they are very similar. However the variablity of the voltage–dependence of the potassium rectifier in the perfused experiments (see Section 3.4.2) means that the membrane potentials ascribed to the extracellular potassium concentrations in Fig. 4.35 may not be totally reliable. Furthermore the use of $10mM$ Ba^{2+} as the charge carrier in the patch clamp experiments means that the current–voltage relationship of the calcium current in Fig. 3.20 may not accurately reflect that of the calcium conductance under the conditions of the intracellular calcium measurements, which usually used $1mM$ Ca^{2+}.

These possible reasons for the apparent discrepencies between the measured calcium current and the intracellular calcium concentration changes illustrate the need to investigate the intracellular concentration as well as the calicum current simultaneously. What is clear from these results is that the intracellular calcium concentration is likely to fluctuate during membrane potential changes in the intact

retina, with the concentration being highest in the dark and being reduced on illumination.

5.2.2 Hypotheses on the Role of the Calcium Current

The presence of a voltage–gated calcium conductance in most neurones can readily be ascribed to a role in the control of neurotransmitter release (see Section 4.1.5). The apparent lack of calcium mediated neurotransmitter release from retinal horizontal cells (Schwartz, 1982, 1987; Section 1.3.3) has resulted in other roles for the current in these cells being suggested, although as pointed out by Sullivan and Lasater (1992), calcium–independent neurotransmitter release has been limited to H1 cells and other (as yet unidentified neurotransmitters) may be released in a calcium dependent manner.

Up to now one main role suggested for the calcium conductance in retinal horizontal cells has been in contributing to the very shallow sustained current–voltage relationship of the isolated cells over the normal range of membrane potentials observed in the intact retina (Sullivan and Lasater, 1992; Lasater, 1992). The benefit that this would convey is that the amount of photoreceptor neurotransmitter required to depolarize the cell would be reduced.

Nevertheless as the intracellular calcium concentration varies with membrane potential over a wide range of values and over long time periods (Sections 4.4.3 and 4.4.5) the calcium conductance could be mediating some membrane potential dependent intracellular second messenger effect by way of these changes. As mentioned above one of these could involve the release of an as yet unknown neurotransmiter in a calcium dependent manner. The main argument against this would be the relationship between the membrane potential and the intracellular calcium concentration changes. The lack of an effect on the intracellular calcium concentration of a depolarization to $\sim$–50mV shows that this mechanism would not be capable of transmitting information over part of the range of membrane potentials experienced by the cells in the intact retina.

However large changes in the membrane potential from the hyperpolarized dark state would result in large changes in the intracellular calcium concentration. Such changes might be expected to be capable of conveying information within the cell,

or, as in the horizontal cells case, within the syncitium. For example modulation of membrane conductances by the intracellular calcium concentration might be a mechanism which would utilise these changes. However horizontal cells from most species do not appear to demonstrate calcium modulated membrane channels, the only exception to date being those from *Xenopus* which appear to have a calcium dependent potassium conductance (Akopain and Witkovsky, 1994).

Intercellular gap–junctions between horizontal cells might be expected to be modified by changes in intracellular calcium concentration. Rose and Loewenstein (1975) demonstrated that in insect salivary gland cells an increse in intracellular calcium, monitored by aequorin, blocked the gap–junction channels between adjacent cells. Both Devries and Schwartz (1992) and Malchow *et al.* (1993) have shown that large dopamine and intracellular cAMP sensitive conductances, thought to be through hemi–gap–junctions in catfish and skate isolated horizontal cells respectively, are enhanced by reduced extracellular calcium concentrations. No attempt was made to estimate the intracellular calcium concentration in either of these experiments, presumably because of the presence of EGTA in the pipette which might have been expected to keep intracellular calcium concentration very low. Nevertheless a large influx of calcium through the channels might have caused a localized increase in concentration. The effect of acclimation to 8°C from 16°C appears to have an effect on both the length constant and the rates of change of intracellular calcium where as acclimation from 16°C to 26°C does not (Fig 2.17 and Figs 4.33 and 4.34 respectively). As the calcium current does not appear to be affected by acclimation to either 8°C or 26°C (Fig 3.23) the acclimation effect on the rates of change of intracellular calcium concentration would be due to changes in the intracellular calcium buffering mechanisms. This in turn might be expected to have an affect on the intracellular calcium concentration in the horizontal cell in the dark, when exposed to the maximum neurotransmitter concentration. If the gap junction density or conductivity is related to the intracellular calcium concentration then the differential effect of acclimation to low, as opposed to high, temperatures of the length constant and the rates of change on intracellular calcium concentration may demonstrate a relationship between these two variables.

However Spray *et al.* (1982) and Spray and Bennett (1985) suggest that the intracellular calcium concentration required to inactivate these channels is unphysiologically high. The inhibitory nature of normal extracellular calcium concentrations may be due to an action of the ion on the exposed region of the channel normally associated with another channel, on another cell, and therefore not normally exposed to the extracellular saline (Spray and Bennett, 1985).

A number of other processes might be expected to be modulated by changes in intracellular calcium concentration. Nitric oxide (NO) is one of a recently discovered group of neuronal messengers which have recently become the target of great interest (see Vincent and Hope, 1992 and Schuman and Madison, 1994 for recent reviews). One of the primary modes of action of NO is the activation of guanylate cyclase (Arnold *et al.*, 1977). A marker for nitric oxide synthase (NOS) has been shown to be present in carp H1 horizontal cells, but not in the cone inner segments (Weiler and Kewitz, 1993). The production of NO by NOS is calcium dependent (Knowles *et al.*, 1989) and consequently changes in the intracellular calcium concentration in these cells might be expected to alter the rate of production of NO. NO can act as an intercellular neuronal messenger, but due to its membrane permeable nature does not require specialized release structures. The location of NOS in the distal region of vertebrate retinae is variable, e.g. in a subset of the horizontal cells in the rat (Yamamoto *et al.*, 1993), in the ellipsoid region of cones and the pole region of Muller cells adjacent to the photoreceptors in tiger salamander (Kurenny *et al.*, 1994) and in the inner segments of bovine cones (Koch *et al.*, 1994). It has been suggested that NO modulates neurotransmitter release from the photoreceptors by modulating voltage gated calcium channels and cGMP gated channels in the inner segment (Koch *et al.*, 1994; Kurenny *et al.*, 1994). Both of these channel types are thought to be involved in controlling the photoreceptor inner segment calcium concenetration, and therefore neurotransmitter release, in cones (Rieke and Schwartz, 1994). NO released from the horizontal cell layer, in a calcium dependent manner, might diffuse to the cone inner segments and hence modulate the photoreceptor synapse.

An alternative more localized effect of NO in the horizontal cells might involve the activation of a guanylate cyclase in the horizontal cell syncitium. Petruv *et al.* (1993) found that the addition of sodium nitroprusside (SNP), a nitric oxide donor,

to carp retina affected the chromatic difference of the receptive field size of the H1 cells. However this effect was only present in the dark adapted retina when the NO concentration, if modulated by the intracellular calcium concentration, might be expected to be at its highest. This suggests that the action of the applied SNP observed was not a normal physiological action, unless the production of the NO is controlled by a mechanism other than the intracellular calcium concentration.

Intracellular calcium concentration changes in the horizontal cell might be expected to have a more direct modulatory role on the cells, rather than *via* the action of what is usually assumed to be an intercellular messenger. Horizontal cell spinule formation is an area of research in which considerable interest is attached due to the parallels it may have in memory in the rest of the CNS (Montague, 1993). Dopamine is known to influence the formation of spinules on light adaptation (Kirsch *et al.*, 1991; Wagner and Djamgoz, 1993) although it is not clear whether dopamine is the sole modulatory mechanism nor whether cAMP is involved in the mechanism (c.f. Kohler and Weiler, 1990 and Behrens *et al.*, 1992). Fluctations of intracellular calcium concentration in a light dependent way might be expected to have some role in the control of these spinules. One alternative to the dopamine–cAMP mechanism is that of the activation of a protein kinase–C being involved in the formation of the spinules (Weiler *et al.*, 1991). However as the intracellular calcium concentration is highest in the depolarized state (i.e. in the dark) and it was suggested that spinule formation was initiated by activation of the protein kinase–C on light adaptation the intracellular calcium concentration cannot be directly involved in activating the protein kinase–C. Also the possibility of calcium dependent fusion of plasmalemmal precursor vessicles (Lockerbie *et al.*, 1991) to increase the horizontal cell membrane during spinule formation (see Catsicas *et al.*, 1994) is unlikely for the same reason. The possibility that the intracelular calcium concentration changes shown to occur on depolarization of these cells act by way of some calcium modulated protein remains. For example it has been shown immunohistochemically that calmodulin is present in the horizontal cells of goldfish (Pochet *et al.*, 1991).

In conclusion the changes in intracellular calcium concentration measured in this study may be likely to have a modulatory effect, and while this might in-

volve control of the production of the retrograde messenger NO, or some calcium modulated protein, more information is required.

Bibliography

Abramson, J.J. and Salama, G. (1987). Regulation of the sarcoplasmic reticulum calcium permeability by sulphydril oxidation and reduction. *J. Memb. Biol.* **33**: 241–248.

Adams, M.E., Bindokas, V.P., Hasegawa, L. and Venema, V.J. (1990). ω–agatoxins: Novel calcium channel antagonists ot two subtypes from funnel web spider (*Agelenopsis aperta*) venom. *J. Biol. Chem.* **265**: 861–867.

Ahmed, Z and Conner, J.A. (1988). Calcium regulation by and buffer capacity of moluscan neurones during calcium transients. *Cell Calcium* **9**: 57–68.

Aho, A–C., Donner, K., Hyden, C., Larsen, L.O. and Reuter, T. (1988). Low retinal noise in animals with low body temperature allows high visual sensitivity. *Nature* **334**: 348–350.

Aho, A–C., Donner, K., Helenius, S., Larsen, L.O. and Reuter, T. (1993a). Visual performance of the toad (*Bufo bufo*) at low light levels: retinal ganglion cell responses and prey catching accuracy. *J. Comp. Physiol.* **172**: 671–682.

Aho, A–C., Donner, K. and Reuter,T. (1993b). Retinal origins of the temperature effects on absolute visual sensitivities in frogs. *J. Physiol.* **463**: 501–521.

Akopain, A and Witkovsky, P. (1994). Modulation of transient outward potassium current by GTP, calcium, and glutamate in horizontal cells of the *Xenopus* retina. *J. Neurophysiol.* **71**: 1661–1671.

Almers, W. (1994). How fast can you get? *Nature* **367**: 682–683.

Almers, W. and McCleskey, E.W. (1984). Non–selective conductance in calcium channels of frog muscle: calcium selectivity in a single–file pore. *J. Physiol.* **353**: 585–608.

Almers, W. and Neher, E. (1985). The Ca signal from Fura-2 loaded mast cells depends strongly on the method of dye loading. *FEBS Lett.* **192**: 13–18.

Ariel, M, Lasater, E.M., Mangle, S.C. and Dowling, J.E. (1984). On the sensitivity of H1 horizontal cells of the retina to glutamate, aspartate and their agonists. *Brain Res.* **295**: 179–183.

Armstrong, C.M. and Gilly, W.F. (1992). Access Resistance and Space Clamp Problems Associated with Whole–Cell Patch Clamping. *Meth. Enzymol.* **207**: 100–122.

Armstrong, C.M. and Neyton, J. (1992). Ion permeation through calcium channels: a one–site model. *Ann. N.Y. Acad. Sci.* **635**: 18–25.

Arnold, W.P., Mittal, C.K., Katsuki, S. and Murad, F. (1977). Nitric oxide activates gyuanylate cyclase and increases guanosine 3′:5′–cyclic monophosphate levels in various tissue preparations. *Proc. Natl. Acad. Sci. U.S.A.* **74**: 3202–3207.

Atkins, A.L. (1973). A simple didgital–computor program for estimating the parameters of the Hille Equation. *Eur. J. Biochem.* **33**: 175–180.

Ayoub, G.S. and Lam, D.M.K. (1984). The release of GABA from horizontal cells of the goldfish *Carassius auratus* retina. *J. Physiol.* **355**: 191–214.

Baldwin, J. and Hochachka, P.W. (1970). Functional Significance of isoenzymes in thermal acclimation. Acetylcholinesterase from trout brain. *Biochem. J.* **16**: 883–887.

Barlow, H. (1953). Summation and inhibition in the frog retina. *J. Physiol.* **119**: 69–88.

Barrett, E.F., Barrett, J.N., Bolz, D., Chang, D.B. and Mahaffee, D. (1978). Temperature–sensitive aspects of evoked and spontaneous transmitter release at the frog neuromuscular junction. *J. Physiol.* **279**: 253–273.

Barrett, J.N., Magleby, K.L. and Pallotta, B.S. (1982). Properties of single calcium–activated potassium channels in cultured rat muscle. *J. Physiol.* **331**: 211–230.

Barritt, G.J. (1992). Calcium. In *Communication Within Animal Cells* pp 193–229. Oxford Scientific Publications.

Baylor, D.A., Fuortes, M.G.F. and O'Bryan, P.M. (1971). Receptive fields of cones in the retina of the turtle. *J. Physiol.* **214**: 265–294.

Baylor, D.A., Lamb, D.A. and Yau, K.W. (1979). The membrane current of single rod outer segments. *J. Physiol.* **288**: 589–611.

Baylor, D.A., Matthews, G. and Yau, K–W. (1983). Temperature effects on the membrane current of retinal rod of the toad. *J. Physiol.* **337**: 723–734.

Bean, B.P. (1984). Nitrendipine block of cardiac calcium channels: High–affinity binding to the inactivated state. *Proc. Natn. Acad. Sci. U.S.A.* **81**: 6388–6392.

Bean, B.P. (1985). Two kinds of calcium channels in canine atrial cells. Differentces in kinetics, selectivity, and pharmacology. *J. Gen. Physiol.* **86**: 1–30.

Bean, B.P. (1989). Classes of calcium channels in vertebrate cells. *Annu. Rev. Physiol.* **57**: 367–384.

Bean, B.P. (1992). Whole–cell recording of calcium channel currents. *Meth. Enzymol.* **207**: 181–193.

Becker, P.L. and Fay, F.S. (1987). Photobleaching of Fura-2 and its effect on determination of calcium concentrations. *Am. J. Physiol.* **253**: C613–C618.

Behrens, U.D., Wagner, H–J. and Kirsh, M. (1992). cAMP–mediated second messenger mechanisms are involved in spinule formation in teleost cone horizontal cells. *Neurosci. Lett.* **147**: 93–96

Bernath, S. (1992). Calcium independent release of amino acid neurotransmitters: Fact of artifact? *Prog. Neurobiol.* **38**: 57–91.

Berridge, M.J. (1990). Calcium oscillations. *J. Biol. Chem.* **265**: 9583–9586.

Besharse, J.C. and Iuvone, P.M. (1992). Is dopamine a light or a dark adaptive modulator in retina. *Neurochem. Int.* **20**: 193–200.

Bisco, T.J., Evans, R.H., Headley, P.M., Martin, M. and Watkins J.C. (1975). Domoic and quisqualic acids as potent amino acid excitants of frog and rat spinal neurones. *Nature* **255**: 166–167.

Blatter, L.A. and Weir, W.G. (1990). Intracellular diffusion, binding and compartmentalization of the fluorescent calcium indicators Indo-1 and Fura-2. *Biophys. J.* **58**: 1491–1499.

Bohle, T. and Benndorf, K. (1994). Facilitated giga–seal formation with a just originated glass surface. *Pflugers Arch.* **427**: 487–491.

Bolsover, S.R., Silver, R.A. and Whitaker, M. (1993). Ratio imaging measurement of intracellular calcium and pH. In *Electronic Light Microscopy*, ed. David Shotton pp 181–210. Wiley–Liss, Inc.

Bowmaker, J.K. (1990). Visual pigmants of fishes. In *The Visual System of Fish*, ed. R.H. Douglas and M.B.A. Djamgoz pp 81–108. Chapman and Hall, London.

Bray, D. (1970). Surface movements during the growth of single explanted neurones. *Proc. Natl. Acad. Sci. U.S.A.* **65**: 905–910.

Burkhardt, D.A. (1993). Synaptic feedback, depolarization, and color opponency in cone photoreceptors. *Vis. Neurosci.* **10**: 981–989.

Byerly, L., Chase, P.B. and Stimers, J.R. (1985). Permeation and interaction of divalent cations channels of snail neurons. *J. Gen Physiol.* **85**: 491–518.

Byerly, L. and Hagiwara, S. (1988). Calcium channel diversity. In *Calcium and Ion channel Modulation* ed D. Armstrong and M.B. Jackson pp 3–18. Plenum New York.

Byerly, L. and Moody, W.J. (1984). Intracellular calcium ions and calcium currents in perfused neurones of the snail *Lymnea stagnalis*. *J. Physiol.* **352**: 637–652.

Byzov, A.L. and Trifinov, Y.A. (1968). The response to electrical stimululation of horizontal cells in the carp retina. *Vision Res.* **8**: 817–822.

Byzov, A.L., Trifinov, Y.A., Chailahian, L.M. and Golubtzov, K.W. (1977). Amplification of graded potentials in horizontal cells of the retina. *Vision Res.* **17**: 265–273.

Callam, D.A. and Hepler, P.K. (1991). Measurement of free calcium in plant cells. In *Cellular Calcium*, ed. McCormack, J.G. and Cobbold, P.H., pp 383–410 Oxford University Press.

Campbell, A.K. (1983). *Intracellular Calcium: its Universal Role as Regulator.* John Wiley and Sons Ltd. Chirenchester.

Carafoli, E. (1991). Calcium pump of the plasma membrane *Physiol.Rev* **71**: 129–153.

Catsicas, S., Grenningloh, G. and Pich, E.M. (1994). Nerve–terminal proteins to fuse to learn. *Trends Neurosci.* **17**: 368–373.

Cervetto, L. and MacNichol, E.F. (1972). Inactivation of horizontal cells in turtle retina by glutamate and aspartate. *Science* **178**: 767–768.

Chabre, M. and Vuong, T.M. (1992). Kinetics and energetics of the rodopsin–transducin–cGMP phosphodiesterase cascade of visual transduction. *Biochim. Biophys. Acta* **1101**: 260–263.

Chandra, S., Fewtrell, C., Millard, P.J., Sandison, D.R., Webb,, W.W. and Morrison, G.H. (1994). Imaging of total intracellular calcium and calcium influx and efflux in individual resting and stimulated tumor mast cells using ion microscopy. *J. Biol. Chem.* **269**: 15186–15194.

Chappelle, S., Meister, R., Brichon, G. and Zwingelstein, G. (1979). Influence of temperature on phospholipid metabolism of various tissues from the crab (*Carasius auratus*). *Comp. Biochem. Physiol.* **58**: 413-417.

Charlton, J.S. and Naka, K.I. (1970). Effects of temperature change on the catfish S–potential. *Vision Res.* **10**: 1119–1126.

Colburn, T.R. and Schwartz, E.A. (1972). Linear voltage control of current passed through a micropipette with a variable resistance. *Med. and Biol. Eng.* **10**: 504–509.

Cobbold, P.H. and Lee, J.A.C. (1991). Aequorin measurments of cytoplasmic free calcium. In *Cellular Calcium. A Practical Approach* ed J.G. McCormack and P.H. Cobbold pp 55–81. IRL Press, Oxford.

Connor, J.C. and Stevens, C.F. (1971a). Inward abd delayed outward membrane currents in isolated neural somata under voltage clamp. *J. Physiol.* **213**: 1–19.

Connor, J.C. and Stevens, C.F. (1971b). Voltage clamp studies of a transient outward membrane current in gastropod neural somata. *J. Physiol.* **213** : 21–30.

Connor, J.A., Tseng, H–Y. and Hockberger, P.E. (1987). Depolarization– and Transmitter–induced changes in intracellular Ca^{2+} of rat cerebellar granule cells in explant cultures. *J. Neurosci.* **1**: 1384–1400.

Copenhagen, D.R. and Jahr, C.E. (1989). Release of endogeneous excitatory amino acids from turtle photoreceptors. *Nature* **341**: 536–539.

Corey, D.P. and Stevens, C.F. (1983). Sience and Technology of Patch–Recording Electrodes. In *Single Channel Recording*, ed. Sakmann, B. and Neher, E., pp 53–68. New York: Plenum Press.

Cossins, A.R. (1977). Adaptation of biological membranes to temperature. Effect of seasonal acclimation of goldfish upon the viscosity of synaptosomal membranes. *Biochim. Biophys. Act* **470**: 395–411.

Cossins, A.R. (1983). The adaptation of membrane structure and function to changes in temperature. In *Temperature Acclimation to Environmental Change* ed. A.R. Cossins and P. Sheterline pp 3–32. Cambridge Uni. Press.

Cossins, A.R. and Bowler, K. (1987). *Temperature Biology of Animals* Chapman and Hall, London.

Cossins, A.R. and Prosser, C.L. (1982). Variable homeoviscous responses of different brain membranes of thermally–acclimated goldfish. *Biochimca et Biophysica Acta* **687**: 303–309.

Cowles, R.B. (1962). Semantics in biothermal studies. *Science* **135**: 670.

Deber, C.M., Tom–Kun. J., Mack, E. and Grinstein, S. (1985). Bromo-A23187: A non–fluorescent calcium ionopore for use with fluorescent probes. *Anal. Biochem.* **146**: 349–352.

DeVries, S.H. and Schwartz, E.A. (1989). Modulation of an electrical synapse between solitary pairs of catfish horizontal cells by dopamine and second messengers. *J. Physiol.* **414**: 351–375.

DeVries, S.H. and Schwartz, E.A. (1992). Hemi–gap junction channels in solitary horizontal cells of the catfish retina. *J. Physiol.* **445**: 201–230.

De Weille, J.R., Schweitz, H., Maes, P., Tartar, A. and Lazdunski, M. (1991). Calciseptine, a peptide isolated from black mamba venom, is a specific blocker of the L–type calcium channel. *Proc. Natl. Acad. Sci. U.S.A.* **88**: 2437–2440.

Dilger, J.P., Brett, R.S., Poppers, D.M. and Liu, Y. (1991). The temperature dependence of some kinetic and conductance properties of acetylcholine receptor channels. *Biocim. Biophys. Acta* **1063**: 253–258.

Dizhoor, A.M., Ray, S., Kumar, S., Niemi, G., Spenser, M., Brolly, D., Walsh, A., Philipov, P.P., Hurley, J.B. and Stryer, L. (1991). Recoverin: A calcium sensitive activator of retinal rod guanylate cyclase. *Science* **251**: 915–918.

Djamgoz, M.B.A. and Stell, W.K. (1984). Tetrodotoxin dos not block the axonal transmission of S–potentials in the goldfish retina. *Neurosci. Lett.* **49**: 233–238.

Djamgoz, M.B.A. and Wagner, H–J. (1992). Localisation and function of dopamine in the adult vertebrate retina. *Neurochem. Int.* **20**: 139–192.

Djamgoz, M.B.A. and Yamada, M. (1990). Electrophysiological characteristics of retinal neurones: synaptic interactions and functional outputs. In *The Visual System of Fish*, ed. R.H. Douglas and M.B.A. Djamgoz pp 159–210. Chapman and Hall, London.

Dowling, J. E. (1987). *The Retina. An Approachable Part of the Brain* The Belenkamp Press, Harvard University.

Dowling, J.E. and Ehinger, B. (1978). The interplexiform cell system. 1. Synapses of the dopamineergic neurones of the goldfish retina. *Proc. R. Soc. Lond. B* **201**: 7–26.

Dowling, J.E., Lasater, E.M., Van Buskirk, R. and Watling, K.J. (1983). Pharmacological properties of isolated fish horizontal cells. *Vision Res.* **23**: 421–432.

Dowling, J.E. and Werblin, F.S. (1969). Organisation of the retina of the mudpuppy *Necturus maculosus* I. Synaptic structure. *J. Neurophysiol* **32**: 315–338.

Downing, J.E.G., and Djamgoz, M.B.A. (1989). Quantitative analysis of cone photoreceptor–horizontal cell connectivity patterns in the retina of cyprinid fish: electron microscopy of functionally identified and HRP–labelled horizontal cells. *J. Comp. Neurol* **289**: 537–553.

Drujan, B.D. and Svaetichin, G. (1972). Characterization of different classes of isolated retinal cells. *Vision Res.* **12**: 1777-1784.

Duncan, C.J. and Statham, H.E. (1977). Interacting effects of temperature and extracellular calcium on the spontaneous relase of transmitter at the frog neuromuscular junction. *J. Physiol.* **268**: 319–333.

Edwards, C. (1983). Who invented the intracellular microelectrode? *Trends Neurosci.* **6**: 44.

Endo, M. (1977). Calcium release from the sarcoplasmic reticulum. *Physiol. Rev.* **57**: 71–108.

Fatt, P. and Katz, B. (1953). The electrical properties of crustacean muscle fibres. *J. Physiol.* **120**: 171–204.

Fatt, P. and Ginsborg, B.L. (1958). The ionic requirements for the production of action potentials in crustacean muscle fibres. *J. Physiol.* **142**: 516–543.

Fenwick, E.M., Marty, A. and Neher, E. (1982a). A patch–clamp stdy of bovine chromaffin cells and of their sensitivity to acetylchline. *J. Physiol.* **331**: 577–597.

Fenwick, E.M., Marty, A. and Neher, E. (1982b). Sodium and calcium channels in bovine chromaffin cells. *J. Physiol.* **331**: 599-635.

Fesenko, E.E., Kolesnikov, S.S. and Lyubarsky, A.L. (1985). Induction by cyclic GMP of cationic conductance in plasma membrane of retinal rod outer segments. *Nature* **313**: 310–313.

Finch, E.A., Turner, T.J. and Goldin, S.M. (1991). Calcium as a coagonist of inositol 1,4,5–triphosphate–induced calcium release. *Science* **252**: 443–446.

Forsyth, I.D. (1991). Microincubator for regulating temperature and superfusion of tissue cultured neurones during electrophysiological or optical studies. *Meth. Neurosci.* **4**: 301–318.

Fox, A.P., Nowycky, M.C. and Tsien, R.W. (1987). Kinetic and pharmacological properties distinguishing three types of calcium currents in chick sensory neurones. *J. Physiol.* **394**: 149–172.

Friedlander, M.J., Kotchabhakdi, N. and Prosser, C.L. (1976). Effect of cold and heat on behaviour and cerebellar function in goldfish. *J. Cmp. Physiol.* **112**: 19–45.

Fry, F.E.J. (1964). Animals in aquatic enviroments. In *Handbook of Physiology, Section 4. Adaptation to the Environment* ed. D.S. Dill pp 715–728. Waverley Press, Inc., Baltimore, Maryland.

Fuortes, M.G.F. and Simon, E.J. (1974). Interactions leading to horizontal cell responses in the turtle retina. *J. Physiol.* **240**: 177–198.

Gitter, A.H. and Theis, J. (1987). A low cost voltsge stepper devise for use in patch–clamp experiments. *Pflugers Arch.* **408**: 194–195.

Gollard, A., Witkovsky, P. and Tranchia, D. (1992). Membrane currents of horizontal cells isolated from turtle retina. *J. Neurophysiol.* **68**: 351–361.

Goolish, E.M. (1987). Cold–acclimation increases the ventrical size of carp, *Cyprinus carpio*. *J. Thermal Biol.* **12**: 203–206.

Grapengiesser, E. (1993). Cell photodamage, a potential hazard when measuring cytoplasmic Ca^{2+} with Fura-2. *Cell Structure and Function* **18**: 13–17.

Gray–Keller, M.P., Polans, A.S., Palczewski, K. and Detweiler, P.B. (1993). The effect of recoverin–like calcium–binding proteins on the photoresponse of retinal rods. *Neuron* **10**: 523–531.

Grynkiewicz, G., Poenie, M. and Tsien, R.Y. (1985). A new generation of Ca^{2+} indicators with greatly improved fluorescent properties. *J. Biol. Chem.* **260**: 3440–3450.

Gunter, T.E., Restrepo, D. and Gunter, K.K. (1988). Conversion of esterified Fura-2 and Indo–1 to Ca^{2+}–sensitive forms by mitochondria. *Am. J. Physiol.* **255**: c304–c310.

Gustafsson, B., Galvan, M., Grafe, P. and Wigstrom, H. (1982). A transient outward current in a mamalian central neurone blocked by 4–aminopyridine. *Nature* **299**: 252–254.

Hagins, W.A., Penn, R.D. and Yoshikami. S. (1970). Dark current and photocurrent in retinal rods. *Biophys. J.* **10**: 380–412.

Hagiwara, S., Miyazaki, S., Moody, W. and Patlak, J. (1978). Blocking effects of barium and hydrogen ions on the potassium current during anomalous rectification in the starfish egg. *J. Physiol.* **279**: 167–185.

Hagiwara, S., Miyazaki, S. and Rosenthal, N.P. (1976). Potassium current and the effect of cesium on this current during anomalous rectification of the egg cell membrane of a starfish. *J. Gen. Physiol.***67**: 621–638.

Hagiwara, S. and Yoshii, M. (1979). Effects of internal potassium and sodium on the anomalous retification of the starfish egg as examined by internal perfusion. *J. Physiol.***292**: 251–265.

Halliwell, J.V. and Whitaker, M.J. (1987). Using microelectrodes. In *Microelectrode Techniques. The Plymouth Workshop Handbook.* ed N.B. Standen, P.T.A. Gray and M.J. Whitaker pp 1–12. The company of Biologists.

Hals, G., Christensen, B.N., O'Dell, T., Christensen, M. and Shingai, R. (1986). Voltage clamp analysis of currents produced by glutamate and some glutamate analogues in horizontal cells isolated from the catfish retina. *J. Neurophysiol.* **56**: 19–31.

Hamill, O.P., Marty, A., Neher, E. Sakmann, B. and Sigworth, F.J. (1981). Improved Patch–Clamp Techniques for High–Resolution Current Recording from Cells and Cell–Free Membrane Patches. *Pflugers Arch.* **391**: 85–100.

Hanyu, I and Ali, M.A. (1963). Ficker fusion frequency of electroretinaogram in light adapted goldfish at various temperatures. *Science* **140**: 662–663.

Hanyu, I and Ali, M.A. (1964). Electroretinaogram and its flicker fusion frequency at different temperatures in light–adapted salmon. *J. Cell Comp. Physiol.* **63**: 309–321.

Harper, A.A., Shelton, J.R. and Watt, P.W. (1989). The temperature dependance of the time course of growth and decay of miniature end–plate currents in carp extraocular muscle following thermal acclimation. *J. Exp. Biol.* **147**: 237–248.

Harper, A.A., Watt, P.W., Hancock, N.A. and MacDonald, A.G. (1990). Temperature acclimation effects on carp nerve: A comparison of nerve conduction, membrane fluidity and lipid composition. *J. Exp. Biol.* **154**: 305–320.

Harrison, S.M. and Bers, D.M. (1987). The effect of temperature and ionic strength on the apparent Ca–affinity of EGTA and the analogous Ca–chelators BAPTA and dibromo–BAPTA. *Biochem. et Biophisica Acta.* **925**: 133–143.

Haugland, R. (1992). *Handbook of Fluorescent Probes and Research Chemicals.* Molecular Probes Inc. Eugene, Oregan.

Hauglang, R. (1993). Intracellular ion indicators. In *Fluorescent and Luminescent Probes for Biological Activity* ed. W.T. Mason pp 34–43 Academic Press London.

Hayashi, H. and Miyata, H. (1994). Fluorescence imaging of intracellular Ca^{2+} *J. Pharmacol. Toxicol. Meth.* **31**: 1–10.

Hazel, J.R. (1989). Cold adaptation in endotherms: Regulation of membrane function and cellular metabolism. In *Advances in Comparative and Environmental Physiology* 4 ed L.C.H. Wang. Springer–Verlag, Berlin, Heidelberg.

Hazel, J.R. and Williams, E.E. (1990). The role of alterations in membrane lipid composition in enabling physiological adaptation of organisms to their physical environment. *Prog. Lipid. Res.* **2**: 167–227.

Heap, S.P., Watt, P.W. and Goldspink, K.G. (1985). Consequences of temperature compensation in poikilotherms. *J. Fish Biol.* **26**: 733–738.

Hecht, S., Shlear, S. and Pirenne, M.H. (1942) Energy, quanta, and vision. *J. Gen. Physiol.* **25**: 819–840.

Heidelberger, R. and Matthews, G. (1992). Calcium influx and calcium current in single synaptic terminals of goldfish retinal bipolar neurons. *J. Physiol.* **447**: 235–256.

Heidelberger, R. and Matthews, G. (1994). Dopamine enhanses Ca^{2+} responses in terminals of retinal bipolar neurones. *Neuroreport* **5**: 729–732.

Heibrunn, L.V. (1943). *An Outline of General Physiology.* Saunders Philadelphia pp. 535–539.

Henzi, V. and MacDermott, A.B. (1992). Characteristics and function of Ca^{2+}– and inositol 1,4,5–triphosphate–releasable stores of Ca^{2+} in neurones. *Neurosci* **46**: 251–273.

Herve, J.C., Yamaoka, K., Twist, V.W. Powell, J.C., Ellory, J.C. and Wang, L.C.H. (1992). Temperature dependence of electrophysiological properties of guinea–pig and ground squirrel myocytes. *Am. J. Physiol.* **263**: R177–R184.

Hess, P. (1990). Calcium channels in vertebrate cells. *Annu. Rev. Neurosci.* **13**: 337–356.

Hess, P., Lansman, J.B. and Tsien, R.W. (1986). Calcium channel selectivity for divalent and monovalent cations. *J. Gen. Physiol.* **88**: 293–319.

Hess, P. and Tsien, R.W. (1984). Mechanism of ion permeation through calcium channels. *Nature* **309**: 453–456.

Hille, B. (1992). *Ionic Channels of Excitable Membranes.* 2^{nd} Edition. Sinuar Ass. Inc., Sunderland, Massachusetts.

Ho, K., Nichols, C.G., Lytton, J., Vassilev, P.M., Kanazirska, M.V. and Hebert, S.C. (1993). Cloning and expression of an inwardly rectifying ATP–regulated potassium channel. *Nature* **362**: 31–38.

Hochachka, P.W. (1988). Metabolic–, channel–, and pump–coupled functions: constraints and compromises of coadapation. *Can. J. Zool.* **66**: 1015–1027.

Hodgkin, A.L. and Huxley, A.L. (1952). A quantitative description of membrane current and its application to conduction and excitation in nerve. *J. Physiol.* **117**: 500–524.

Hoffman, F., Biel, M. and Flockerzi, V. (1994). Molecular basis for calcium channel diversity. *Trends Neurosci.* **17**: 399–418.

Horn, R. and Marty, A (1988). Muscarinic activation of ionic currents measured by a new whole–cell recording technique. *J. Gen. Physiol.* **92**: 145–159.

Hoyland, J. (1993). Fluorescent probes in practice – potential artifacts. In *Fluorescent and Luminescent Probes for Biological Activity* ed. W.T. Mason pp 223–228 Academic Press London.

Iino, M. (1987). Calcium dependent inositol trisphosphate–induced calcium release in the guinea–pig taenia caeci. *Biochem. Biophys. Res. Commun.* **142**: 47–52.

Inui, M., Saito, A. and Fleischer, S. (1987). Purification of the ryanodine receptor and identity with feet structures of junctional terminal cisternae of sarcoplasmic reticulum from fast skeletal muscle. *J. Biol. Chem.* **262**: 1740–1747.

Ishida, A.T., Kaneko, A. and Tachibana, M. (1984). Responses of solitary retinal horizontal cells from *Carassius auratus* to L–glutamate and related amino acids. *J. Physiol.* **348**: 255–270.

Ishihara, K., Takano, M., Mitsuiye, T. and Noma, A. (1989). The Mg^{2+} block and intrinsic gating underlying inward rectification of the K^+ current in guinea–pig cardiac muscle. *J. Physiol.* **419**: 297–320.

Ishii, I., Yamagishi, T. and Taira, N. (1994). Cloning and functional expression of a cardiac inward rectifier K^+ channel. *FEBS Lett.* **338**: 107–111.

Jahn, R. and Sudhof, T.C. (1994). Synaptic vesicles and exocytosis. *Trends Neurosci.* **17**: 219–246.

Johnston, I.A. (1983). Cellular responses to an altered body temperature: The role of alterations in the expression of protein isoforms. In *Cellular Acclimatization to Environmental Change* ed. A.R. Cossins and P. Sheterline pp 121–144. Cambridge Uni. Press.

Johnston, G.A.R., Curtis, D.R., Davies, J. and McCulloch, R.M. (1974). Spinal interneurone excitation by conformationally restricted analogues of L–glutamic acid. *Nature* **248**: 804–805.

Johnston, D. and Lam, D.M.K. (1981). Regenerative and passive membrane properties of isolated horizontal cells from a teleost retina. *Nature* **292**: 451–454.

Kaneko, A. (1970). Physiological and morphological identification of horizontal, bipolar and amicrine cells in the goldfish retina. *J. Physiol.* **207**: 623–633.

Kaneko, A. (1971). Electrical connexions between horizontal cells in the dogfish retina. *J. Physiol.* **213**: 95–105.

Kaneko, A. (1987). The functional role of retinal horizontal cells. *Jap. J. Physiol.* **37**: 341–358.

Kaneko, A. and Hashimoto, H. (1967). Recording site of single cone response determined by an electrode marking technique. *Vision Res.* **7**: 847–851.

Kaneko, A., Lam, D.M.K. and Wiesel, T.N. (1976). Isolated horizontal cells of elasmobranch retinae. *Brain Res.* **105**: 567–572.

Kaneko, A. and Shimazaki, A. (1976). Synaptic transmission from photoreceptors to the second order neurons in the carp retina. In *Neural Principles in Vision* ed F. Zetter and R. Weiler pp 143–151. Springer, Munich.

Kaneko, A and Stuart, A.E. (1984). Coupling between horizontal cells in the carp retina revealed by diffusion of Lucifer yellow. *Neurosci. Lett.* **47**: 1–7.

Kaneko, A. and Tachibana, M. (1983). Double color opponent receptive fields of carp bipolar cells. *Vision Res.* **23**: 381–388.

Kaneko, A. and Tachibana, M. (1985). Electrophysiological measurements of the spectral sensitivity of three types of cones in the carp retina. *Jap. J. Physiol.* **35**: 355–365.

Kaneko, A. and Tachibana, M. (1986). Effects of γ–aminobutyric acid on isolated cone photoreceptors of the turtle retina. *J. Physiol.* **373**: 443–461.

Kasai, H. and Neher, E. (1992). Dihydropropidine–sensitive and ω–conotoxin sensitive calcium channels in a mammalian neuroblastoma–glioma cell line. *J. Physiol.* **448**: 161–188.

Kato, S., Negishi, K., Teranishi, T. and Ishita, S. (1991). The use of the carp retina in neurobiology. Its uniqueness and application for neural network analysis of the inner retina. *Prog. Neurobiol.* **37**: 287–327.

Katz, B. (1946). Les constant electriques de la membrane du muscle. *Archs. Sci. Physiol.* **3**: 285–300.

Katz, B. (1969). *The Release of Neural Transmitter Substances.* Charles C. Thomas, Springfield, IL U.S.A.

Kaupp, U.B. and Koch, K–W. (1992). Role of cGMP and Ca^{2+} in vertebrate photoreceptor excitation and adaptation. *Annu. Rev. Physiol.* **54**: 153–175.

Kelly, R.B. (1993). Storage and release of neurotransmitters. *Cell* **72** *(Suppl.)*: 43–53.

Kirsh, M., Wagner, H–J. and Djamgoz, M.B.A. (1991). Dopamine and plasticity of horizontal cell function in the teleost retina: regulation of a spectral mechanism through D1 receptors. *Vision Res.* **31**: 401–412.

Kley, N., Loeffler, J–P., Pittus, C.W. and Hollt, V. (1987). Involvement of ion channels in the induction of proenkephalin A gene expression by nicotine and cAMP in bovine chromaffin cells. *J. Biol. Chem.* **262**: 4083–4089.

Knapp, A.G. and Dowling, J.E. (1987). Dopamine enhanses excitatory amino acid–gated conductances in retinal horizontal cells. *Nature* **325**: 437–439.

Knapp, A.G., Schmidt, K.F. and Dowling, J.E. (1990). Dopamine modulates the kinetics of ion channels gated by excitatory amino acids in retinal horizontal cells. *Proc. Natl. Acad. Sci. U.S.A.* **87**: 767–771.

Knowles, R.G., Palacirs, M., Palmer, R.M.J. and Monacada, S. (1989). Formation of nitric oxide from L–arginine in the central nervous system: A transduction mechanism for stimulation of the soluble guanylate cyclase. *Proc. Natl. Acad. Sci. U.S.A.* **86**: 5159–5162.

Koch, K–W., Lambrecht, H–G., Haberecht, M., Redburn, D. and Schmidt, H.H.W. (1994). Functional coupling of a Ca^{2+}/calmodulin–dependent nitric oxide synthase and a soluble guanylate cyclase in vertebrate photoreceptor cells. *EMBO J.* **13**: 3312–3320.

Kohler, K. and Weiler, R. (1990). Dopaminergic modulation of transient neurite outgrowth from horizontal cells in the fish retina is not mediated by cAMP. *Eur. J. Neurosci.* **2**: 788–794.

Kolb, H. and Lipetz, L.E. (1991). The anatomical basis for colour vision in the vertebrate retina. In *The perception of Colour* ed P. Gouras pp 128–145 MacMillen Press London.

Kostyuk, P.G. (1992). *Calcium Ions in Nerve Cell Function.* Oxford Scientific Publications.

Koyama, H., Morishige, K., Takahasi, N., Zanelli, J.S., Fass, D.N. and Kurachi, Y. (1994). Molecular cloning, functional expression and localization of a novel inward rectifier potassium channel in the rat–brain. *FEBS Lett.* **341**: 303–307.

Kubo, Y., Baldwin, T.J., Jan, Y.N. and Jan, L.Y. (1993). Primary structure and functional expression of a mouse inward rectifier potassium channel. *Nature* **362**: 127–133.

Kuffler, S.W., Nicholls, J.G. and Martin, A.R. (1984). *From Neurone to Brain* Sinauer Ass. Inc. Sunderland Massachusetts.

Kuo, C–C. and Hess, P. (1993). Ion permeation through the L–type Ca^{2+} channel in rat phaeochromocytoma cells: two sets of ion binding sites in the pore. *J. Physiol.* **466**: 629–655.

Kurenny, D.E., Moroz, L.L., Turner, R.W., Sharkey, K.A. and Barnes, S. (1994). Modulation of ion channels in rod photoreceptors by nitric oxide. *Neuron* **13**: 315–324.

Lagerspetz, K.Y.H. (1974). Temperarture acclimation and the nervous system. *Biol. Rev.* **49**: 477–514.

Lam, D.M–K., Lasater, E.M. and Naka, K–I. (1978). GABA: A neurotransmitter candidate for cone horizontal cells of the catfish retina. *Proc. Natl. Acad. Sci. U.S.A.* **75**: 6310–6313.

Lamb, T.D. (1976). Spatial properties of horizontal cell responses in the turtle retina. *J. Physiol.* **263**: 239–255.

Lamb, T.D. (1984). Effects of temperature changes on toad rod photocurrents *J. Physiol.* **346**: 557–578.

Lambrecht, H.G. and Koch, K.W. (1991). A 26Kd calcium binding protein from bovine rod outer segments as modulator of photoreceptor guanylate cyclase. *EMBO J.* **10**: 793–798.

Lasater, E.M. (1986). Ionic currents of cultured horizontal cells from white perch retina. *J. Neurophysiol.* **55**: 499–513.

Lasater, E.M. (1991). Characteristics of single–channels activated by quisqualate and kainate in teleost retinal horizontal cells. *Vision Res.* **31**: 413–424.

Lasater, E.M. (1992). Membrane properties of distal retinal neurons. *Prog. Retinal Res.* **11**: 215–246.

Lasater, E.M. and Dowling, J.E. (1982). Carp horizontal cells in culture respond selectively to L–glutamate and its agonists. *Proc. Natl. Acad. Sci. U.S.A.* **79**: 936–940.

Lasater, E.M. and Dowling, J.E. (1985). Electrical coupling between pairs of isolated fish horizontal cells is modulated by dopamine and cAMP. In *Gap Junctions* ed M.V.L. Bennett and D.C. Spray pp 393–404 Cold Spring Harbour, New York.

Laufer, M., Svaetichin, G., Matarai, G., Fatechand, R., Vallecalle, E. and Villegas, J. (1961). The effect of temperature, carbon dioxide and ammonia on the neurone–glia unit. In *The Visual System: Neurophysiology and Psychophysics.* ed E. Jung and H Kornhuber pp 457–463. Springer, Berlin.

Lee, J.A.C. (1987). Temperature acclimation of carp intestinal morphology. In *Temperature and Animal Cells* ed K. Bowler and Fuller, B.J. p 453 The Company of Biologists Limited, Cambridge.

Lee, K.S. and Tsien, R.W. (1984). Reversal of current through calcium channels in dialysed single heart cells. *Nature* **297**: 498–501.

Leech, C.A. and Stanfield, P.R. (1981). Inward rectification in frog skeletal muscle and its dependence on membrane potential and external potassium. *J. Physiol.* **319**: 295–309.

Lentzner, A., Bykov, V. and Bartschat, D.K. (1992). Time–resolved changes in intracellular calcium following depolarization of rat synaptosomes. *J. Physiol.* **450**: 613–628.

Leroi, A.M., Bennett, A.F. and Lenski, R.E (1994). Temperature acclimation and competitive fitness: an experimental test of the beneficial acclimation assumption. *Proc. Natl. Acad. Sci. U.S.A.* **91**: 1917–1921.

Lester, H.A. (1991). Strategies for studying permeation at voltage–gated ion channels. *Annu. Rev. Physiol.* **53**: 477–496.

Levi, G. and Raiteri, M. (1993). Carrier–mediated release of neurotransmitters *Trends Neurosci.* **16**: 415–419.

Liebman, P.A., Weiner, H.L. and Dryzmala, R.D. (1982). Lateral diffusion of visual pigment in rod disk membranes. *Meth. Enzymol.* **81**: 660–668.

Ling. G. and Gerard, R.W. (1949). The normal membrane potential of frog sartorious muscle. *J. Cell Comp. Physiol.* **34**: 383–396.

Lipscombe, D., Madison, D.V., Poenie, M., Reuter, H., Tsien, R.W. and Tsien, R.W. (1988). Imaging of cytosolic Ca^{2+} transients arising from Ca^{2+} stores and Ca^{2+} channels in sympathetic neurones. *Neurone* **1**: 355–365.

Llinás, R. and Nicholson, C. (1975). Calcium role in depolarization–secretion coupling: An aequorin study in squid giant axon. *Proc. Natl. Acad. Sci.* **72**: 187–190.

Llinás, R. and Sugimori, M. (1980). Electrophysiological properties of *in vitro* purkinje cell dendrites in mammalian cerebellar slices. *J. Physiol.* **305**: 197–213.

Llinás, R., Sugimori, M., Lin, J–W. and Cherksey, B. (1989). Blocking and isolation of a calcium channel from neurones in mammals and cephalopods utilizing a toxin fraction (FTX) from funnel–web spider poision. *Proc. Natl. Acad. Sci. U.S.A.* **86**: 1689–1693.

Liu, C. and Hermann, T.E. (1978). Characterisation of ionomycin as a calcium ionopore. *J. Biol. Chem.* **253**: 5892–5904.

Lockerbie, R.O., Miller, V.E. and Pfenninger, K.H. (1991). Regulated plasmalemmal expansion in nerve growth cones. *J. Cell Biol.* **112**: 1215–1227.

Low, C.L., Yamada, M. and Djamgoz, M.B.A. (1991). Voltage clamp study of electrophysiologically–identified horizontal cells in carp retina. *Vision Res.* **31**: 437–449.

MacDonald, A.G. (1988). Application of the theory of homeoviscous adaptation to excitable membranes: pre–synaptic processes. *Biochem. J.* **256**: 313–327.

MacDonald, A.G. (1990). The homeoviscous theory of adaptation applied to excitable membranes: A critical evaluation. *Biocimica et Biophysica Acta* **1031**: 291–310.

Madison, D.V., Malenka, R.C and Nicoll, R.A. (1991). Mechanisms underlying long–term potentiation of synaptic transmission. *Annu Rev. Neurosci.* **14**: 379–398.

Malchow, R.P., Qian, H., Ripps, H. and Dowling, J.E. (1990). Structural and functional properties of types of horizontal cells in the skate retina. *J. Gen. Physiol.* **95**: 177–198.

Malchow, R.P., Qian, H. and Ripps, H. (1993). Evidence for hemi–gap–junctional channels in isolated horizontal cells of the skate retina. *J. Neurosci. Res.* **35**: 237–245.

Malgaroli, A., Milani, D., Meldolesi, J. and Pozzan, T. (1987). Fura–2 measurement of cytosolic free Ca^{2+} in monolayers and suspensions of various types of animal cells. *J. Biol. Chem.* **105**: 2145–2155.

Marc, R., Stell, W.K., Bok, D. and Lam, D. M–K. (1978). GABA–ergic pathways in the goldfish retina. *J. Comp. Neurol.* **182**: 221–246.

Marks, W.B. (1965). Visual pigments of single goldfish cones. *J. Physiol.* **178**: 14–32.

Marrion, N.V. and Adams, P.R. (1992). Release of intracellular calcium and modulation of membrane currents by caffeine in bull–frog sympathetic neurones. *J. Physiol.* **445**: 515–535.

Marty, A. and Neher, E. (1983). Tight Seal Whole Cell Recording. In *Single Channel Recording*, ed. Sakmann, B. and Neher, E., pp 107–122. New York: Plenum Press.

Mason, W.T., Hoyland, J., Davidson, I., Carew, H., Somasundaram, B., Tregear, R., Zorec, R., Lledo, P.M., Shankar, G. and Horton, M. (1993). Quantitative real–time imaging of optival probes in living cells. In *Fluorescent and Luminescent Probes for Biological Activity* ed. W.T. Mason pp 161–195 Academic Press London.

Mayer, M.L., MacDermot, A.B., Westbrook, G.L., Smith, S.J. and Barker, J.L. (1987) Agonist– and voltage–gated calcium entry in cultured mouse spinal cord neurons under voltage clamp measured using Arsenazo III. *J. Neurosci.* **7**: 3230–3244.

McBurney, R.N. and Neering, I.R. (1987). Neuronal calcium homeostasis. *Trends Neurosci.* **10**: 164–169.

McCleskey, E.W. (1994). Calcium channels: cellular roles and molecular mechanisms. *Curr. Opin. Neurobiol.* 4: 304–312.

McMahon, D.G. (1994). Modulation of electrical synaptic transmission in Zebrafish retinal neurones. *J. Neurosci.* **14**: 1722–1734.

McNaughton, P.A. (1990). Light response of vertebrate photoreceptors. *Physiol. Rev.* **70**: 847–883.

Meissner, G. (1994). Ryanodine receptor / Ca^{2+} release channels and their regulation by endogenous effectors. *Annu. Rev. Physiol.* **56**: 485–508.

Meldolesi, J., Volpe, P. and Pozzan, T. (1988). The intracellular distribution of calcium. *Trends Neurosci.* **11**: 449–452.

Milani, D., Malgaroli, A., Guiddin, D., Fasolato, C., Skaper, S.D., Meldolesi, J. and Pozzan T. (1990). Ca^{2+} channels and intracellular Ca^{2+} stores in neuronal and endocrine cells. *Cell Calcium* **11**: 191–199.

Mintz, I.M., Venema, V.J., Swiderek, K.M., Lee, T.D., Bean, B.P. and Adams, M.E. (1992). P–type calcium channels blocked by the spider toxin ω–Aga–IVA. *Nature* **355**: 827–829.

Mitra, R.L. and Morad, M. (1991). Permeance of Cs^+ and Rb^+ through the inwardly rectifying K^+ channel in guinea pig ventricular myocytes. *J. Memb. Biol.* **122**: 33–42.

Mittmann, F., Flaming, D.G., Copenhagen, D.R. and Belgum, J.H. (1987). Bubble Pressure Measurement of Micropipette Tip Outer Diameter. *J. Neurosci. Meth.* **22** 161–166.

Miyachi, E–I. and Murakami, M. (1989). Decoupling of horizontal cells in carp and turtle by intracellular injection of cyclic AMP. *J. Physiol.* **419**: 213–224.

Miyazaki, S–I., Takahashi, K., Tsuda, K. and Yoshii, M. (1974). Analysis of non–linearity observed in the current–voltage relation of the tunicate embryo. *J. Physiol.* **238**: 55–77.

Miyazaki, S., Shirakawa, H., Nakada, K., Honda, Y., Yazaki, M., Nakade S. and Mikoshiba K. (1992). Antibody to the inositol trisphosphate receptor blocks thimerosal–enhansed Ca^{2+}–induced Ca^{2+} release and Ca^{2+} oscillations in hamster egg. *FEBS Lett.* **309**: 180–184.

Mlinar, B. and Enyert, J.J. (1993). Block of current through T–type calcium channels by trivalent metal cations and nickel in neural rat and human cells. *J. Physiol.* **469**: 639–652.

Mogul, D.J. and Fox, A.P. (1991). Evidence for multiple types of Ca^{2+} channels in acutely isolated hippocampal CA3 neurones of the guinea–pig. *J. Physiol.* **433**: 259–281.

Montague, P.R. (1993). Transforming sensory experiance into structuralchange. *Proc. Natl. Acad. Sci. U.S.A.* **90**: 6379–6380.

Montgomery J.C. and MacDonald J.A. (1990). Effects of temperature on nervous system: Implications for behavioural performance. *Am. J. Physiol.* **259**: R191–R196.

Moore, E.D.W., Becker, P.L., Fogarty, K.E., Williams, D.A. and Fay, F.S. (1990). Ca^{2+} imaging in single living cells: Theoretical and practical issues. *Cell Calcium* **11**: 157–179.

Morishige, K.E., Takahashi, N., Jahangir, A., Yamada, M., Koyama, H., Zanelli, J.S. and Kurachi, Y. (1994). Molecular cloning and functional expression of a novel brain–specific inward rectifier potassium channel. *FEBS Lett.* **346**: 251–256.

Murakami, M., Shimoda, Y., Nakatani, K., Miyachi, E. and Watanabe, S. (1982). GABA–mediated negative feedback from horizontal cells to cones on carp retina. *Jap. J. Physiol.* **32**: 911–926.

Murakami, M. and Takahashi, K.I. (1987). Calcium action potential and its use for measurement of reversal potentails of horizontal cell responses in carp retina. *J. Physiol.* **386**: 165–180.

Murase, K., Usui, S. and Kaneko, A. (1987). Properties of glutamate channels in solitary horizontal cells of the goldfish retina. *Neurosci. Res. Suppl.* **6**: S175–S190.

Nachshen, D.A. (1984). Selectivity of the Ca binding site in synaptosome Ca channels. Inhibition of Ca influx by multivalent metal cations. *J. Gen. Physiol.* **83**: 941–967.

Naka, K–I. and Rushton, W.A.H. (1967). The generation and spread of S–potential in fish (*Cyprinidae*). *J. Physiol.* **192**: 437–461.

Narahashi, T., Moore, J.W. and Scott, W.R. (1963). Tetrodotoxin blockage of sodium conductance in lobster giant axons. *J. Gen. Physiol.* **47**: 965–974.

Narahashi, T., Tsunoo, A. and Yoshii, M. (1987). Characterization of two types of calcium channels in mouse neuroblastoma cells. *J. Physiol.* **383**: 231–249.

Neering, I.R. and McBurney, R.N. (1984). Role for microsomal Ca storage in mammalian neurones? *Nature* **309**: 158–160.

Negishi, K. amd Drujan, B. (1979). Reciprocal changes in centre and surrounding S–potentials of fish retina in response to dopamine. *Neurochem. Res.* **4**: 313–318.

Negishi, K. and Svaetichin, G. (1966). Effects of temperature on S–potential producing cells and on neurons. Pflugers Arch. **292**: 206–217.

Neher, E. (1988). The influence of intracellular calcium concentration on degranulation of dialysed mast cells from rat peritoneum. *J. Physiol.* **395**: 193–214.

Neher, E. and Sakmann, B. (1976). Single–Channel Currents Recorded From Membrane of Denervated Frog Muscle Fibers. *Nature* **260**: 799–802.

Neher, E. and Sakmann, B. (1992). The Patch Clamp Technique. *Sci. American* **266**: 28–35.

Neill, W.H., Magnuson, J.J. and Chipman, G.G. (1972). Behavioural thermoregulation by fishes: A new experimental approach. *Science* **176**: 1443–1445.

Neumeyer, C. and Arnold, K. (1987). Tetrachromatic colour vision in goldfish and turtle. In *Seeing Contour and Colour* ed C. Dickenson and I. Murray pp 617–631. Permagon Press, Oxford.

Newman, E.A., Frambach, D.A. and Odette, L.L. (1984). Control of extracellular potassium levels by retinal glial cell K^+ syphoning. *Science* **225**: 1174–1175.

Norman, R.A., Perlman, I. and Daly, S.J. (1986). The effects of continuous superfusion of L–aspartate and L–glutamate on horizontal cells of the turtle retina. *Vision Res.* **26**: 259–268.

Nowycky, M.C., Fox, A.P. and Tsien, R.W. (1985a). Three types of neuronal calcium channel with different calcium agonist sensitivity. *Nature* **316**: 440–443.

Nowycky, M.C., Fox, A.P. and Tsien, R.W. (1985b). Long–opening mode of gating of neuronal calcium channels and its promotion by the dihydropyridine calcium agonist Bay K8644. *Proc. Natl. Acad. Sci. U.S.A.* **82**: 2178–2182.

Oakley, B and Green, D.G. (1976). Correlation of light–induced changes in retinal extracellular potassium conductance with c–wave of the electroretinogram. *J. Neurophysiol.* **39**: 1117–1133.

Oakley, B. and Steinberg, R.H. (1982). Effects of maintained illumination upon $[K^+]_o$ in the subretinal space of the frog retina. *Vision Res.* **22**: 767–773.

O'Dell, T.J. and Christensen, B.N. (1989). A voltage–clamp study of isolated stingray horizontal cell non–NMDA excitatory amino acid receptors. *J. Neurophysiol.* **61**: 162–171.

Olivera, B.M., Gray, W.R., Zeikus, R., McIntosh, J.M., Varga, J., Rivier, J., Santos, V. De and Cruz, L.J. (1985). Peptide neurotoxins from fish–hunting cone snails. *Science* **230**: 1338–1343.

Olivera, B.M., Miljanich, G.P., Ramachandran, J. and Adams, M.E. (1994). Calcium channel diversity and neurotransmitter release: The ω–conotoxins and ω–agatoxins. *Annu Rev. Biochem.* **63**: 823–867.

Perlman, I., Knapp, A.G. and Dowling, J.E. (1988). Local superfusion modifies the inward rectifying potassium conductance of isolated retinal horizontal

cells. *J. Neurophysiol.* **60**: 1322–1332.

Perlman, I., Knapp, A.G. and Dowling, J.E. (1989). Responses of isolated white perch horizontal cells to changes in the concentation of photoreceptor transmitter agonists. *Brain Res.* **487**: 16–25.

Perlman, I., Sullivan, J.M., and Norman, R.A. (1993). Voltage– and time–dependent potassium conductances enhance the frequency response of horizontal cells in the turtle retina. *Brain Res.* **619**: 89–97.

Petruv, R., Furukawa, T., Yasui, S. and Djamgoz, M.B.A. (1993). Sodium nitroprusside, a nitric oxide donor, generates chromatic difference in the receptive field size of H1 horizontal cells in isolated retinae of carp. *J. Physiol.* **473**: P163.

Pfeiffer–Linn, C. and Lasater, E.M. (1993). Dopamine Modulates in a different fashion T– and L–type calcium channels in Bass retinal horizontal cells. *J. Gen. Physiol.* **102**: 277–294.

Piccolino, M. (1986). Horizontal cells: Historical controversies and new interest. *Prog. Retinal Res.* **5**: 147–163.

Ploem, J.S. (1993). Fluorescent microscopy. In *Fluorescent and Luminescent Probes for Biological Activity* ed. W.T. Mason pp 1–11 Academic Press London.

Pochet, R., Pasteels, B., Seto–Ohshima, A., Bastianelli, E., Kitajima, S. and Van Eldik, L.J. (1991). Calmodulin and calbindin localization in retina from six vertebrate species. *J. Comp. Physiol.* **314**: 750–762.

Poenie, M. (1990). Alteration of Fura-2 fluorescence by viscosity: A simple correction. *Cell Calcium* **11**: 85–91.

Poenie, M., Alderton, J., Steinhardt, R. and Tsien, R. (1986). Calcium rises abruptly and briefly throughout the cell at the onset of anaphase. *Science* **233**: 886–889.

Pollack, P (1928). Micrurgical studies in cell physiology. VI. Calcium ions in living protoplasm. *J. Gen Physiol.* **11**: 539–545.

Pozzan, T., Rizzuto, R., Volpe, P. and Meldolesi, J. (1994). Molecular and cellular physiology of intracellular calcium stores. *Physiol. Rev.* **74**: 595–636.

Precht, H. (1958). Concepts of the temperature adaptation of unchanging reaction systems of cold–blooded animals. In *Physiological Adaptation* ed. C.L.Proser pp 50–78. American Association for the Advancement of Science, Washington D.C.

Prosser, C.L. (1973). *Comparative Animal Physiology.* Saunders, Philadelphia.

Prosser, C.L. and Heath, J.E. (1991). Temperature. In *Environmental and Metabolic Animal Physiology* ed C.L. Prosser pp 109–166. Wiley–Liss New York.

Prosser, C.L. and Nelson, D.O. (1981). The role of nervous systems in temperature adaptation of poikilotherms. Annu. Rev. Physiol. **43**: 281–300.

Pugh, E.N. and Lamb, T.D. (1990). Cyclic GMP and calcium: The internal messangers of excitation and adaptation in vertebrate photoreceptors. *Vision Res.* **30**: 1923–1948.

Pugh, E.N. and Lamb, T.D. (1993). Amplification and kinetics of the activation steps in phototransduction. *Biochimica et Biophysica Acta* **1141**: 111–149.

Rae, J.L. and Levis, R.A. (1992). Glass Tecnology for Patch Clamp Electrodes. *Meth. Enzymol.* **207** 66–92.

Randriamampita, C. and Trautmann, A. (1987). Ionic channels in murine macrophages. *J. Cell Biol.* **105**: 761–769.

Reichenbach, A., Henke, A., Eberhardt, W., Reichelt, W. and Dettmer, D. (1992). K^+ ion regulation in retina. *Can. J. Physiol. Pharmacol.* **70**: S239–S247.

Reuter, H. and Scholz, H. (1977). A study of the ionic selectivity and the kinetic properties of the calcium dependent slow inward current in mammalian cardiac muscle. *J. Physiol.* **264**: 17–47.

Reynolds, I.J., Wagner, J.A., Snyder, S.H., Thayer, S.A., Olivera, B.M. and Miller, R.J. (1986). Brain voltage–sensitive calcium channel subtypes differentiated by ω–conotoxin fraction GVIA. *Proc. NAtl. Acad. Sci. U.S.A.* **83**: 8804–8807.

Ridgeway, E.B. and Ashley, C.C. (1967). Calcium transients in single muscle fibres. *Biochem. Biophys. Res. Comm.* **29**: 229–234.

Rieke, F. and Schwartz, E.A. (1994). A cGMP–gated current can control exocytosis at cone synapses. *Neuron* **13**: 863–873.

Ringer, S. (1890). Concerning experiments to test the influence of small quantities of lime, sodium and potassium salts on the development of ova and the growth of tadpoles. *J. physiol.* **11**: 79–84.

Robertson, B. and Wann, K.T. (1984). The effect of temperature on the growth and decay of miniature end plate currents in the mouse diaphragm. *Brain Res.* **294**: 346–349.

Robinson, D.W., Ratto, G.M., Lagnado, L. and McNaughton, P.A. (1993). Temperature dependence of the light response in rat rods. *J. Physiol.* **462**: 465–481.

Roe, M.W., Lemasters, J.J. and Herman, B. (1990). Asessment of Fura-2 for mesurements of cytosolic free calcium. *Cell Calcium* **11**: 63–73.

Rome, C.L., Loughna, P.T. and Goldspink, G. (1985). Temperature acclimation: Improved sustained swimming performance in carp at low temperatures. *Science* **228**: 194-196.

Roots, B.I. and Prosser, C.L. (1962). Temperature acclimation and the nervous system in fish. *J. Exp Biol.* **39**: 617–629.

Rose, B. and Loewenstein, W.R. (1975). Permeability of cell junctions depends on local cytoplasmic calcium activity. *Nature* **254**: 250–252.

Rosseau, E. and Meissner, G. (1989). Single cardiac sarcoplasmic reticulum Ca^{2+}–release channel: activation by caffeine. *Am. J. Physiol.* **256**: H328–H333.

Rudy, B. (1988). Diversity and ubiquity of K channels. *Neurosci.* **25**: 729–749.

Saito, T. (1987). Physiological and morphological differences between on– and off–center bipolar cells in the vertebrate retina. Vision Res. **27**: 135–142.

Sakmann, B. and Neher, E. (1983). Geometric Parameters of Pipettes and Membrane Patches. In *Single Channel Recording*, ed. Sakmann, B. and Neher, E., pp 37–51. New York: Plenum Press.

Sakmann, B. and Trube, G. (1984). Conductance properties of single inwardly rectifying potassium channels in ventricular cells from guinea–pig heart. *J. Physiol.* **347**: 641–657.

Saran, S., Nakao, H., Tasaka, M., Iida, H., Tsuji, F.I., Nanjundiah, V and Takeuchi, I. (1994). Intracellular free calcium level and its response to cAMP stimulation in developing *Dictyostelium* cells transformed with jellyfish apoaquorin cDNA. *FEBS Lett.* **337**: 43–47.

Scanlon, M., Williams, D.W. and Fay, F.S. (1987). A Ca^{2+}–insensitive form of Fura-2 associated with polymorponuclear leukocytes. *J. Biol. Chem.* **262**: 6308–6312.

Schellart, N.A.M., Spekreijse, H. and Van Den Berg, T.J.T.P. (1974). Influence of temperature on retinal ganflion cell response and ERG of goldfish. *J. Physiol.* **238**: 251–267.

Schmidt, K–F., Kruse, M. and Hatt, H. (1994). Dopamine alters glutamate receptor desensitization in retinal horizontal cells of the perch (*Perca fluviatilis*). *Proc. Natl. Acad. Sci. U.S.A.* **91**: 8288–8291.

Schuman, E.M. and Madison, D.V. (1994). Nitric oxide and synaptic function. *Annu. Rev. Neurosci.* **17**: 153–183.

Schwartz, E.A. (1982). Calcium independent release of GABA from isolated horizontal cells of the toad retina. *J. Physiol.* **323**: 211–227.

Schwartz, E.A. (1987). Depolarization withiut calcium can release gamma–aminobutyric acid from a retinal neuron. *Science* **238**: 350–355.

Shimomura, O. and Johnson, F.H. (1976). Calcium triggered luminescence of the photoprotein aequorin. *Symp. Soc. Exp. Biol.* **30**: 41–54.

Shimomura, O., Johnson, F.H. and Saiga, Y. (1963). Microdetermination of calcium by aequorin luminescence. *Science* **140**: 1339–1340.

Shingai, R. and Christensen, B.N. (1983). Sodium and calcium currents measured in isolated catfish horizontal cells under voltage clamp. *Neurosci.* **10**: 893–897.

Shingai, R. and Christensen, B.N. (1986). Excitable properties and voltage–sensitive ion conductances of horizontal cells isolated from catfish (*Ictalurus punctatus*) retina. *J. Neurophysiol.* **56**: 32–49.

Sidel, B.D. (1983). Cellular acclimation to environmental change by quantitative alterations in enzymes and organelles. In *Cellular acclimation to Environmental Change* ed A.R. Cossins and P. Scheterline. pp 103–120. Cambridge Uni. Press.

Sigworth, F.J. (1983). Electronic design of the patch clamp. In *Single Channel Recording* ed B. Sakmann and E. Neher, pp 3–35. Plenum Press, New York.

Silver, M.R., Shapiro, M.S. and DeCoursay, T.E. (1994). Effects of external Rb^+ on the inward rectifier K^+ channels of bovine pulmonary artery endothelial cells. *J. Gen. Physiol.* **103**: 519–548.

Sinensky, M. (1974). Homeoviscous adaptation — A homeostatic process that regulates the viscosity of membrane lipids in *Escherichia coli. Proc Natl. Acad Sci. U.S.A.* **71**: 522–525.

Slaughter, M.M. and Millar, R.F. (1981). APB — a new pharmacological tool for retina research. *Science* **211**: 182–185.

Slaughter, M.M. and Millar, R.F. (1983). An excitatory amino acid antagonist blocks cone input to sign–conserving second–order retinal neurones. *Science* **219**: 1230–1232.

Snutch, T.P and Reiner, P.B. (1992). Ca^{2+} channels: diversity of form and function. *Current Opinion in Neurobiol.* **2**: 247–253.

Spray, D.C. and Bennett, M.V.L. (1985). Physiology and pharmacology of gap junctions. *Annu. Rev. Physiol.* **47**: 281–303.

Spray, D.C., Stern, H.C., Harris, A.L. and Bennett, M.V.L. (1982). Gap junctional conductance: comparison of sensitivities to H and Ca ions. *Proc. Natl. Acad. Sci. U.S.A.* **79**: 441-445.

Standen, N.B. and Stanfield, P.R. (1978). A potential– and time–dependent blockade of inward rectification in frog skeletal muscle fibres by barium and strontium ions. *J. Physiol.* **280**: 169–192).

Stanfield, P.R. (1983). Tetramethylammonium ions and the potassium permeability of excitable cells. *Rev. Physiol. Biochem. Pharmacol.* **97**: 1–67.

Steinberg, S.F., Bilezikian, J.P. Al–Awquati, Q. (1987). Fura–2 fluorescence is localised to mitochondria in endothelial cells. *Am. J. Physiol.* **253**: C744–C747.

Stell, W.K. (1975). Horizontal cell axons and axon terminals in goldfish retina. *J. Comp. Neurol.* **159**: 503–519.

Stell, W.K. and Lightfoot, D.O. (1975). Color–specific interconections of cones and horizontal cells in the retina of the goldfish. *J. Comp. Neurol.* **159**: 473–502.

Stephens, P.J. (1990). The effects of temperature on the physiology of crustacean nerves and muscle. *J. Therm. Biol.* **15**: 15–24.

Stephens, P.J. and Atwood, H.L. (1990). Thermal acclimation in a crustacean neuromuscular system. *J. Exp. Biol.* **98**: 39–47.

Stimson, A. (1974). *Photometry and Radiometry for Engineers.* John Wiley and Sons. New York.

Stryer, L. (1991). Visual excitation and recovery. *J. Biol. Chem.* **266**: 10711-10714.

Sullivan, J.M. and Lasater, E.M. (1990). Sustained and transient potassium currents of cultured horizontal cells from white bass retina. *J. Neurophysiol.* **64**: 1758–1766.

Sullivan, J.E. and Lasater, E.M. (1992). Sustained and transient calcium currents in horizontal cells of the white bass retina. *J. Gen Physiol.* **99**: 85–107.

Sutoo, D., Akiyama, K. and Imamiya, S. (1990). A mechanism of cadmium poisioning — the cross effect of calcium and cadmium in the calmodulin–dependent system. *Arch. Toxicol.* **64**: 161–164.

Svaetichin, G. (1953). The cone action potential. *Acta Physiol.Scand.* **29**: 565–600.

Svaetichin, G. and MacNichol, E.F. (1958). Retinal mechanisms for chromatic and achromatic vision. *Ann. N.Y. Acad. Sci.* **74**: 385–404.

Svaetichin, G., Negishi, K., Fatechand, R., Drujan, B.D., and Selvin, A. de T. (1965). Nervous function based on interactions between neuronal and non-neuronal elements. *Prog. Brain Res.* **15**: 243–266.

Swann, K. (1991). Thimerosal causes calcium oscillations and sensitizes calcium-induced calcium release in unfertilized hamster eggs. *FEBS Lett* **278**: 175–178.

Tabata, M., Meissl, H. and Martin, C. (1993). Thermal responses of achromatic ganglion cells in the photosensory pineal organ of the rainbow trout *Oncorhynchus mykiss*. *Comp. Biochem. Physiol.* **105A**: 453–457.

Tachibana, M. (1981). Membrane properties of solitary horizontal cells isolated from goldfish retina. *J. Physiol.* **321**: 141–161.

Tachibana, M. (1983a). Solitary horizontal cells in culture — I. Their electrical properties. *Vision Res.* **23**: 1209–1216.

Tachibana, M. (1983b). Ionic currents of solitary horizontal cells isolated from goldfish retina. *J. Physiol.***345**: 329–351.

Tachibana, M. (1985). Permeability changes induced by L–glutamate in solitary horizontal cells isolated from *Carassius auratus*. *J. Physiol.* **358**: 153–167.

Tachibana, M. and Kaneko, A. (1984). γ–aminobutyric acid acts at axon terminals of turtle photoreceptors: Difference in sensitivity among cell types. *Proc. Natl. Acad. Sci. U.S.A.* **81**: 7961–7964.

Tanabe, T., Takeshima, H., Mikami, A., Flockerzi, V., Takahishi, H., Kangawa, K., Kojima, M., Matsuo, H., Hirose, T and Numa, S. (1987). Primary structure of the receptor for calcium channel blockers from skeletal muscle. *Nature* **328**: 313–318.

Teranishi, T., Negishi, K. and Kato, S. (1983). Dopamine modulates S potential amplitude and dye coupling between external horizontal cells in the carp retina *Nature* **301**: 243–246.

Teranishi, T., Negishi, K. and Kato, S. (1984). Regulatory effect of dopamine on spatial properties of horizontal cells in carp retina. *J. Neurosci* **4**: 1271–1280.

Thayer, S.A. and Miller, R.J. (1990). Regulation of the intracellular free calcium concentration in single rat dorsal ganglion neurons *in vitro*. *J. Physiol.* **425**: 85–116.

Thomas, M.V. (1991). Metallochromic Indicators. In *Cellular Calcium*, ed. McCormack, J.G. and Cobbold, P.H., pp 115–122. Oxford University Press.

Thomas, A.P. and Delaville, F. (1991). The use of fluorescent indicators for measuremants of cytosolic free calcium in cell populations and single cells. In *Cellular Calcium*, ed. McCormack, J.G. and Cobbold, P.H., pp 1–54. Oxford University Press.

Thorpe, S.A. (1971). Behavioural measures of spectral sensitivity of the goldfish at different temperatures. *Vision Res.* **11**: 419–433.

Thorpe, S.A. (1973). The effects of temperature on the psychophysical and electroretinographic spectral sensitivity of the chromatically adapted goldfish. *Vision Res.* **13**: 59–72.

Tiiska, A.J. and Lagerspetz, K.Y.H. (1994). Thermal acclimation, neuromuscular synaptic delay and miniature end–plate current decay in the frog *Rana temporaria*. *J. Exp. Biol.* **187**: 131–142.

Tirri, R., Vornanen, M. and Cossins, A.R. (1978). The compensation of ATPase activities in brain and kidney microsomes from cold– and warm–acclimated carp (*Cyprinus carpio* L.). *J. Therm. Biol.* **3**: 131–135.

Tomita, T. (1970). Electrical activity of vertebrate photoreceptors *Q. Rev. Biophys.* **3**: 179–222.

Treistman, S.N. and Grant, A.J. (1993). Increase in cell size underlies neurone–specific temperature acclimation in *Aplysia*. *Am. J. Physiol.* **264**: C1061–C1065.

Trifinov, Y.A. (1968). Study of synaptic transmission between the photoreceptor and the horizontal cell using electrical stimulation of the retina. *Biofizika* **13**: 809–817.

Tse, A., Tse, F.W. and Hille, B. (1994). Calcium homeostasis in identified rat gonadotrophs. *J. Physiol.* **477**: 511–525.

Tsien, R.Y. (1980). New calcium indicators and buffers with high selectivity against magnesium and protons: design, synthesis and properties of prototype structures. *Biochem.* **19**: 2396–2404.

Tsien, R.Y. (1981). A non–disruptive technique for loading calcium buffers and indicators into cells. *Nature* **290**: 527–528.

Tsien, R.Y. (1988). Fluorescent measurement and photochemical manpulation of cytosolic free calcium *Trends Neurosci.* **11**: 419–424.

Tsien, R.W., Ellinor, P.T. and Horne, W.A. (1991). Molecular diversity of voltage–dependent Ca^{2+} channels. *Trends Pharmacol.* **12**: 349–354.

Tsien, R.W., Lipscombe, D., Madison, D.V., Bley, K.R. and Fox, A.R. (1988). Multiple types of neuronal calcium channels and their selective modulation. *Trends Neurosci.* **11**: 431–438.

Tsien, R.Y. and Pozzan, T. (1989). Measurement of cytosolic free Ca^{2+} with Quin2. *Meth. Enzymol.* **172**: 230–262.

Tsien, R.Y., Pozzan, T. and Rink, T.J. (1982). Calcium homeostasis in intact lymphocytes: cytoplasmic free calcium monitored with a new intracellularly trapped fluorescent indicator. *J. Cell Biol.* **94**: 325–334.

Tsien, R.W. and Tsien, R.Y. (1990). Calcium channels, stores and oscillations. *Annu. Rev. Cell Biol.* **6**: 715–760.

Ueda, Y., Kaneko, A. and Kaneda, M (1992). Voltage–dependent ionic currents in solitry horizontal cells isolated from cat retina. *J. Neurophysiol.* **68**: 1143–1150.

Uto, A., Arai, H. and Ogawa, Y. (1991). Reassessment of Fura-2 and the ratio method for determination of intracellular Ca^{2+} concentrations. *Cell Calcium* **12**: 29–37.

Van Buskirk and Dowling, J.E. (1981). Isolated horizontal cells from carp retina demonstrate dopamine dependent accumlation of cAMP. *Proc. Natl. Acad. Sci. U.S.A.* **78**: 7825–7829.

Vandenberg, C.A. (1987). Inward rectification of a potassium channel in cardiac ventricular cells depends on internal magnesium. *Proc. Natl. Acad. Sci. U.S.A.* **84**: 2560–2564.

Van Lunteren, E., Elmslie, K.S. and Jones, S.W. (1993). Effects of temperature on calcium current of bullfrog sympathetic neurons. *J. Physiol.* **466**: 81–93.

Verbost, P.M., Flick, G., Bonga, S.E.W. and Lock, R.A.C. (1988). Cadmium inhibits plasma–membrane calcium–transport. *J. Memb. Biol.* **102**: 97–104.

Vincent, S.R. and Hope, B.T. (1992). Neurons that say NO. *Trends Neurosci.* **15**: 108–113.

Von Gersdorff, H. and Matthews, G. (1994). Dynamics of synaptic vessicle fusion and membrane retrevial in synaptic terminals. *Nature* **367**: 735–739.

Wagner, H–J. and Djamgoz, M.B.A. (1993). Spinules: a case for retinal plasticity. *Trends Neurosci.* **16**: 201–206.

Wang, R., Karpinski, E and Pang, P.K.T. (1991). Temperature–dependence of L–type calcium–channel currents in isolated smooth–muscle cells from the rat tail artery. *J. Therm. Biol.* **16**: 83–87.

Watanabe, S–I. and Murakami, M. (1992). Phototransduction in cones as examined in excised membrane patch. *Jap. J. Physiol.* **42**: 309–320.

Watling, K.J. and Dowling, J.E. (1981). Dopamine mechanisms in the teleost retina. 1. Dopamine sensitive adenylate cyclase in homoginates of carp retina: effects of agonists, antagonists and ergots. *J. Neurchem.* **36**: 559–568.

Weight, F.F. and Erulkar, S.D. (1976). Synaptic transmission and effects of temperature at the squid giant synapse. *Science* **261**: 720–722.

Weiler, R. and Kewitz, B. (1993). The marker for nitric oxide synthase, NADPH–diaphorase, co–localizes with GABA in horizontal cells and cells of the inner retina in the carp retina. *Neurosci. Lett.* **158**: 151–154.

Weiler, R., Kohler, K. and Jansen, U. (1991). Protein kinase C mediates transient spinule outgrowth in the retina during light adaptation. *Proc. Natl. Acad. Sci. U.S.A.* **88**: 3603–3607.

Werblin, F.S. (1975). Anomalous rectification in horizontal cells. *J. Physiol.* **244**: 639–657.

Werblin, F.S. and Dowling, J.E. (1969). Organisation of the retina of the mudpuppy *Necturus maculosus*. II Intracellular recording. *J. Neurophysiol.***32**: 339–355.

Williams, D.A. and Fay, F.S. (1990). Intracellular calibration of the fluorescent indicator Fura-2. *Cell Calcium* **11**: 75–83.

Williams, D.A., Fogarty, K.E., Tsien, R.Y. and Fay, F.S. (1985). Calcium gradients in single smooth muscle cells revealed by the digital imaging microscope using Fura-2. *Nature* **318**: 558–561.

Wilkinson, G.N. (1961). Statistical estimations in enzyme kinetics. *Biochem. J.* **80**: 324–332.

Witkovsky, P. and Dearry, A. (1991). Functional roles of dopamine in the vertebrate retina. *Prog. Retinal Res.* **11**: 247–292.

Wu, S.M. (1991). Input–output relations of the feedback synapse between horizontal cells and cones in the tiger salamander retina. *J. Neurophysiol.* **65**: 1197–1206.

Wu, S.M. (1992). Feedback connections and operation of outer plexiform layer of the retina. *Current Opin. Neurobiol.* **2**: 462–468.

Wu, S.M. (1994). Synaptic transmission in the outer retina. *Annu. Rev. Physiol.* **56**: 141–168.

Wu, S.M. and Dowling, J.E. (1978). L–glutamate: evidence for a role in cone photoreceptor synaptic transmission in the carp retina. *Proc. Natl. Acad. Sci. U.S.A.* **75**: 5205–5209.

Wu, S.M. and Dowling, J.E. (1980). Effects of GABA and glycine on the distal cells of the cyprinid retina. *Brain Res.* **199**; 401–414.

Yager, D., Buck, S. and Duncan, I.A. (1971). Effects of temperature on the visually evoked tectal potential and brightness perception in goldfish. *Vision Res.* **11**: 849–860.

Yagi, T. (1986). Interaction between the soma and the axon termial of retinal horizontal cells in *Cyprinus carpio*. *J. Physiol.* **375**: 121–135.

Yagi, T. and Kaneko, A. (1988). The axon terminal of goldfish retinal horizontal cells: A low membrane conductance measured in solitary preparations, and its implication to the signal conduction from the soma. *J. Neurophysiol.* **59**: 482–494.

Yamada, E. and Ishikawa, T. (1965). The fine structure of horizontal cells in some vertebrate retinae. *Cold Spring Horbor Symp. Quant. Biol.* **30**: 383–392.

Yamamoto, R., Bredt, D.S., Snyder, S.H. and Stone, R.A. (1993). The localization of nitric oxide synthase in the rat eye and related cranial ganglia. *Neurosci.* **54**: 189–200.

Yang, J., Ellinor, P.T., Sather, W.A., Zhang, J–F., Tsien, R.W. (1993). Molecular determinants of Ca^{2+} selectivity and ion permeation in L–type Ca^{2+} channels. *Nature* **366**: 158–161.

Yau, K–W. (1994). Phototransduction mechanism in retinal rods and cones. *Invest. Opthalmol. Vis. Sci.* **35**: 9–32.

Yazulla, S. (1986). Evoked efflux of [^{3}H] GABA from goldfish retina in the dark. *Brain Res.* **325**: 171–180.

Yazulla, S. and Kleinschmidt, J. (1982). Dopamine blocks carier mediated release of GABA from retinal horizontal cells. *Brain Res.* **233**: 211–215.

Yazulla, S. and Kleinschmidt, J. (1983). Carrier mediated release of GABA from retinal horizontal cells. *Brain Res.* **263**: 63–75.

Zucker, R.S. (1989). Short term synaptic plasticity. *Annu. Rev. Neurosci.* **12**: 13–31.